VNIVERSITAT DE VALÈNCIA

Aspects of Physics beyond the Standard Model

Tesi Doctoral
Programa de Doctorat en Física

Mario Reig López

Director: Dr. José Wagner Furtado Valle

Tutora: Dra. Maria Amparo Tórtola Baixauli

IFIC - CSIC/Universitat de València
Department de Física Teòrica

València, juliol de 2021

Al meu germà i als meus pares

Dr. José Wagner Furtado Valle, Professor d'investigació del Consejo Superior de Investigaciones Científicas (CSIC), i Maria Amparo Tórtola Baixauli, professora contractada doctora de la Universitat de València, en títol de tutora

CERTIFIQUEN:

Que la present memòria "Aspects of physics beyond the Standard Model" ha sigut realitzada sota la seua direcció a l'Institut de Física Corpuscular, centre mixte del CSIC i de la Universitat de València, per Mario Reig López i constitueix la seua Tesi per a optar al grau de Doctor en Física.

I per a que així conste, en compliment de la legislació vigent, presenta al Departament de Física Teòrica de la Universitat de València la referida Tesi Doctoral, i firma el present certificat.

Paterna, a 7 de Juliol de 2021.

Dr. José Wagner Furtado Valle Dra. Maria Amparo Tórtola Baixauli

Preface

Physics thrives on crisis[1]. This is probably the most important lesson that a physicist learns during the first years of her/his career. During the last hundred years, from β-decay and the $\tau-\theta$ problem to the discovery of quarks and the birth of the Standard Model, we have witnessed how every apparent failure of the contemporaneous theory has lead to abrupt developments of our understanding of Nature. Despite experience forces me to be humble, this is the *raison d'être* of this Thesis. Using the loose ends of the Standard Model as lampposts I will consider models that, in my view, improve our understanding of Nature at the most fundamental level.

As a theoretical physicist, I am biased by simplicity and beauty. This is an aspect that I have developed since the early stages of my career and has part of its origin in the fantastic collaborations I have enjoyed. Perhaps, the most influential has been the principle of *Radical Conservatism*[2]: throughout the Thesis I will try to be loyal to well established physical laws, but I will push them into the extreme, exploring uncharted territories.

The contents of this Thesis are splitted in three different parts. In the first one, I will introduce to the reader our core theory of fundamental physics - the Standard Model - and enumerate the reasons why we need to go beyond. I will also review in some detail the different open questions that are studied in the second and third part of this Thesis.

Part two and three contain original research based on articles that I have completed during the last years. The former focuses on the interplay between the origin of neutrino mass and dark matter. In part three, I will tackle, in my opinion, one of the most perverse problems in physics: the origin of flavor and the quantum numbers of elementary particles.

I hope the reader enjoys as much as I do when learning and thinking about the topics included in this Thesis.

[1] I cannot resist starting my Thesis with this quote by S. Weinberg.

[2] Originally attributed to N. Bohr by J.A. Wheeler.

Acknowledgments

Aquesta és, molt probablement, la part més difícil d'escriure de tota la Tesi. És una tasca que he anat posposant i, per diferents motius, m'ha resultat quasi impossible escriure-la sense emocionar-me. És molt probable que algunes persones, que en major o menor mesura han contribuït a fer que açò siga possible, no apareguen. A vosaltres, vos done les gràcies i vos demane disculpes.

Vull començar per agrair a José, el meu tutor, el seu esforç i la confiança que sempre ha tingut en mi. Encara recorde els primers correus que vam intercanviar, ara fa més de 6 anys, quan jo era solament un estudiant de tercer de carrera fent un Erasmus a Mainz. *"Si te interesa la física, pásate por el despacho y hablamos"*. Amb eixes paraules va començar una relació de la qual estic enormement orgullós. Gràcies, José!

Una altra persona que durant els primers moments d'aquesta tesi va ser com un segon tutor és Carlos Vaquera. Amb una paciència infinita em va ajudar a entendre el model 331 i a aconseguir publicar un article abans d'acabar la carrera. Poques vegades m'he sentit tan nerviós com la nit d'abans que l'article apareguera en arXiv.

També vull agrair a tots els membres presents, passats i futurs de la *família* AHEP, sou increïbles! Gràcies especialment als membres més sènior del grup - Avelino, José, Mariam, Martin, Sergio i Valentina - que sempre heu tractat que els joves ens sentim com a casa des del primer moment. Crec que detalls com aquest marquen la diferència. Probablement sou allò que més trobaré a faltar del IFIC. Per sort, sempre ens quedarà Telegram.

En l'àmbit professional, vull donar les gràcies a totes les persones que heu compartit la vostra física i el vostre temps amb mi. Durant estos anys he tingut la sort de conéixer a gent com Andrea, Eduardo, Javi Castellano, Javi Fuentes i Rahul, gent que sempre estan disponibles per a discutir de física o simplement compartir qualsevol tipus de preocupació. Tots ells són particularment especials perquè aquesta tesi siga possible, ja que m'han ajudat en múltiples ocasions, des de consultes sobre física a llegir versions

preliminars d'aquest treball. Més que col·laboradors, vos considere amics i estic desitjant que ens tornem a veure.

També vull donar les gràcies a Frank qui, malgrat la seua ocupadíssima agenda, sempre ha tingut uns minuts per a mi. Treballar amb tu ha sigut de les coses més emocionants que he fet mai.

Durant la meua estada a Perimeter Institute, i en especial gràcies a Davide, vaig tindre la sort de coincidir amb Amalia, Daniel, Junwu, Mina i Savas. Va ser un període molt intens professionalment i, també, difícil per estar tan lluny de casa. Gràcies a vosaltres eixos mesos van ser increïbles.

No puc oblidar-me de Prateek i Junwu[3]. Vull agrair-vos la confiança que heu tingut en mi. Treballar amb vosaltres és sempre un repte i crec que no m'enganye si dic que m'heu canviat la forma de veure la física.

Aquest treball ha sigut possible, també, gràcies a gent lleugerament menys relacionada amb la física. Entre ells vull mencionar a tots els membres de *Radio Patio* - els meus amics de Muro -, i als meus amics ciclistes de *La Punxaeta*, que a pesar que mai llegiran aquesta tesi, sé que em donen i donaran suport cegament.

Una altra persona que ha sigut molt important per a aquesta tesi és Paula, qui em va acompanyar durant els meus primers passos com a físic i ha sigut una de les persones més influents per a mi. Pau, part d'açò és teu.

Un dels llocs més importants entre els agraïments l'ocupen els *pisiers*. No és per a menys, ja que a pesar de ens coneguem des de prou abans de ser físics, cada any heu sigut més importants per a mi. Ana, Andreu, Clara, Iker, Martí, Núria, Sílvia i Víctor, vos estime molt. Ens esperen uns anys diferents, en la distància, però açò no acaba ací.

No puc tancar aquesta secció sense donar les gràcies als meus pares, Aurelio i Elodia, i en especial al meu germà, Javi, qui sempre m'ha servit d'exemple i de referència en tot allò que he fet. A vosaltres vos vull agrair el vostre suport infinit. A pesar de no tindre ni idea del que faig[4], sempre heu sentit la mateixa il·lusió que jo. A vosaltres vos ho dec tot.

Per últim, n'hi ha altra persona a qui he tingut la sort de conéixer recentment i que per molts motius s'ha convertit en algú molt especial per a mi. A tu, Eli, també et done les gràcies.

[3]En realitat és la segona vegada que li done les gràcies, però ho mereix per la paciència que ha tingut amb mi.

[4]Últimament mon pare llig moltes notícies de física, però vos assegure que no té ni idea.

List of scientific publications

This thesis is based on the following publications:

I) Neutrinos and Dark Matter

1. ***Light majoron cold dark matter from topological defects and the formation of boson stars.***
   M. Reig, J.W.F. Valle, M. Yamada.
   JCAP09 (2019) 029.

2. ***Bound-state dark matter and Dirac neutrino mass.***
   M. Reig, D. Restrepo, J.W.F. Valle, O. Zapata.
   Phys.Rev. D97 (2018) no.11, 115032.

3. ***Bound-state dark matter with Majorana neutrinos.***
   M. Reig, D. Restrepo, J.W.F. Valle, O. Zapata. Phys.Lett. B790 (2019) 303-307.

II) The Flavor Puzzle

1. ***A Model of Comprehensive Unification.***
   M. Reig, J.W.F. Valle, C.A. Vaquera-Araujo, F. Wilczek.
   Phys.Lett. B774 (2017) 667-670.

2. ***SO(3) family symmetry and axions.***
   M. Reig, J.W.F. Valle, F. Wilczek.
   Phys.Rev. D97 (2018) no.9, 095008.

Other publications not included in the thesis:

1. ***Realistic*** $SU(3)_c \times SU(3)_L \times U(1)_X$ ***model with type-II Dirac neutrino seesaw mechanism.***
   M. Reig, J.W.F. Valle, C.A. Vaquera-Araujo.
   Phys.Rev. D94 (2016) no.3, 033012.

2. ***Unifying left-right symmetry and 331 electroweak theories.***
   M. Reig, J.W.F. Valle, C.A. Vaquera-Araujo.
   Phys.Lett. B766 (2017) 35-40.

3. ***Three-family left-right symmetry with low-scale seesaw mechanism.***
   M. Reig, J.W.F. Valle, C.A. Vaquera-Araujo.
   JHEP 1705 (2017) 100.

4. ***Towards gauge coupling unification in left-right symmetric*** $SU(3)_c \times SU(3)_L \times SU(3)_R \times U(1)_X$ ***theories.***
   C. Hati, S. Patra, M. Reig, J.W.F. Valle, C.A. Vaquera-Araujo.
   Phys.Rev. D96 (2017) no.1, 015004.

5. ***Spontaneous breaking of lepton number and cosmological domain wall problem.***
   G. Lazarides, M. Reig, Q. Shafi, R. Srivastava, J.W.F. Valle.
   Phys.Rev.Lett. 122 (2019) no.15, 151301.

6. ***Spontaneous proton decay and the origin of Peccei-Quinn symmetry.***
   M. Reig, R. Srivastava.
   Phys.Lett. B790 (2019) 134-139.

7. ***On the high-scale instanton interference effect: axion models without a domain wall problem.***
   M. Reig.
   JHEP 1908 (2019) 167.

8. ***Cosmic implications of a low-scale solution to the axion domain wall problem.***
   A. Caputo, M. Reig.
   Phys.Rev. D100 (2019) no.6, 063530.

9. ***Strong CP problem with low-energy emergent QCD: the 4321 case.***
   J. Fuentes-Martín, M. Reig, A. Vicente.
   Phys.Rev. D100 (2019) no.11, 115028.

10. ***Dirac neutrinos from Peccei-Quinn symmetry: a fresh look at the axion.***

E. Peinado, M. Reig, R. Srivastava, J.W.F. Valle.
Mod.Phys.Lett.A 35 (2020) 21, 2050176.

11. ***Generalizing the Scotogenic model.***
P. Escribano, M. Reig, A. Vicente.
JHEP 07 (2020) 097.

12. ***Maximal axion misalignment from a minimal model.***
J. Huang, A. Madden, D. Racco, M. Reig.
JHEP 10 (2020) 143.

13. ***The Stochastic Axiverse.***
M. Reig.
arXiv:2104.09923.

Contents

Part I

Introduction and Motivation

Chapter 1

The Standard Model in a Nutshell

1.1 The Standard Model

In the early '70s, some brilliant ideas were put together and resulted into a framework called the *Standard Model* (SM) of particle physics [1–3]. It is a humble name for such a successful theory. It predicted some phenomena, such as neutral currents, that were unknown by the time the theory was proposed and describes, with great accuracy, our microscopic world up to explored energies[1]. This lead to their *fathers*, S.L. Glashow, A. Salam and S. Weinberg to the 1979 Nobel prize.

The development of Quantum Electrodynamics (QED) [4–7] was very important for the growth of the SM. Its successful predictions told us how to do physics, that is in which principles we can rely. Among them, I would stress gauge invariance and Quantum Field Theory (QFT), as a theoretical and computational framework.

There are other theories that were crucial for the development and understanding of the SM. During the '30s, Enrico Fermi developed a theory for the description of β decay. The theory described this process with a 4-fermion point-like interaction. Nowadays, this process is naturally explained within the SM due to the exchange of $W^{\pm}$ bosons.

The work by Tsung-Dao Lee and Chen-Ning Yang [8] was also, in my view, a huge step forward in theoretical physics that *illuminated* the path for

[1]However, some other phenomena including neutrino masses, the matter-antimatter asymmetry, and dark matter cannot be described by this theory and suggest us the necessity of going beyond the SM.

future developments. They proposed that weak interactions could violate the parity symmetry, $\mathcal{P}$, solving the $\tau - \theta$ puzzle[2]. This was soon confirmed by Chien-Shiung Wu in 1956 by testing directional properties of Cobalt-60 beta decay [9], leading to the experimental verification of parity violation. The origin of parity violation is still unknown: we know that the SM is a chiral theory, but the fundamental reason for this fact is a mystery.

Another major advance, crucial for the construction of the SM is Yang-Mills (YM) theory [10]. In their work, Robert Mills and Chen-Ning Yang developed the theoretical framework of the SM gauge structure. They pointed out that, in the same way the electromagnetic field is linked to the electric charge, there are vector fields (spin 1) that appear when isospin symmetry is imposed locally and, moreover, these fields satisfy non-linear differential equations. YM theory is therefore the core of the SM, where one imposes local invariance under non-abelian symmetries.

In the early '60s, Gell-Mann and Zweig proposed the concept of quarks [11, 12]. This was a major advance in the understanding of the strong force (also known as *Quantum Chromodynamics*, QCD). Thanks to the quark model, they were able to explain the big number of baryons and mesons that were being discovered by that time. The main idea is that hadrons are not fundamental, but composed of other elementary particles, quarks, that bind together and form bound states which do not feel the strong force (at least not directly). Using symmetry principles and group theory, Gell-Mann and Zweig were able to explain the main hadron spectrum by combining three quark flavors: u, d and s. However, quark behaviour seemed weird. For instance, in order to explain the observed hadron spectrum quarks were forced to have fractional ($\frac{2}{3}$ and $-\frac{1}{3}$) charges. In addition, it was noticed that in some baryons quarks seemed not to obey the spin-statistics theorem. For example, this is the case for the Δ^{++} baryon which is composed of 3 up-type quarks and has spin 3/2 [13]. This baryon made people to doubt the existence of quarks since it seemed to have a total wave-function which is symmetric under interchanging quarks unless they violate the spin-statistics theorem. This puzzle was later solved with the introduction of a new quantum number for quarks: color charge.

Independently, at the end of the '60s, Feynman proposed the parton model to describe hadron collisions at high energies [14]. Soon after that, Bjorken and Paschos applied this model willing to understand electron-

[2]During the '50s physicists were intrigued about the decays of τ and θ mesons. Despite having the same mass and life-time, their decays (mediated by weak interaction) have opposite parities.

proton deep inelastic scattering [15]. It was later recognized that partons describe quarks and gluons. Despite in the early days quarks appeared to be very strange, today we know that quarks are not artifacts but real particles that form bound states and compose hadrons.

In 1964, in different works P. Higgs; F. Englert and R. Brout; and G. S. Guralnik, C. R. Hagen, and T. W. B. Kibble proved that the Goldstone theorem does not apply to gauge theories [16–18]. In the case of local symmetries, the would-be Goldstone bosons that arise after symmetry breaking can be *gauged away* and absorbed as longitudinal degrees of freedom of the gauge bosons. As a result, these gauge bosons get a non-zero mass and a particle associated with this mechanism appears. Nowadays this is known as the Higgs mechanism and the associated particle is known as the Higgs boson. The particle associated to the Higgs mechanism was discovered in 2012 and P. Higgs and F. Englert received the 2013 Nobel Prize in Physics.

In the '70s, the Glashow-Salam-Weinberg model for weak interactions had serious difficulties at high energies due to the vector boson mass term that was added to explain the weak interaction. M. Veltman, G. 't Hooft, C.G. Bollini and J.J. Giambiagi showed independently [19, 20] that one can have a renormalizable Yang-Mills theory for weak interactions. This was done using dimensional regularization to calculate renormalized higher loop diagrams, together with the Higgs mechanism as a way to consistently generate gauge boson masses.

In a QFT, coupling constants are not constant but they evolve with energy. This paradoxical behaviour was studied for non-abelian gauge theories by D.J. Gross, F. Wilczek and D. Politzer independently [21, 22]. They discovered that, if strong interactions are described by non-abelian symmetries, they will exhibit a fully reliable and perturbative behaviour at high energies even in the case they are non-perturbative at low energies. This is known as *asymptotic freedom*. They also pointed out that this non-perturbative regime at low energies might break symmetries dynamically. This breakthrough can be seen as the birth of modern Quantum Chromodynamics.

Symmetries and particle content

The SM is the QFT of the electromagnetic and weak interactions [1–3], also incorporating the strong interaction [21, 23, 24]. Being a gauge theory, it is invariant under the Lorentz group and under the gauge symmetry group:

$$SU(3)_C \times SU(2)_L \times U(1)_Y \,. \tag{1.1}$$

	l_L^i	e_R^i	q_L^i	u_R^i	d_R^i	H
$SU(3)_C$	**1**	**1**	**3**	**3**	**3**	**1**
$SU(2)_L$	**2**	**1**	**2**	**1**	**1**	**2**
$U(1)_Y$	$-\frac{1}{2}$	-1	$-\frac{1}{6}$	$\frac{2}{3}$	$-\frac{1}{3}$	$\frac{1}{2}$

Table 1.1: Particle content of the SM. The labels $i = 1, 2, 3$ correspond to the different SM families.

The SM contains the 8 bosons associated to the strong sector $SU(3)_C$, also known as gluons, and 4 electroweak gauge bosons corresponding to the $SU(2)_L \times U(1)_Y$ part. As we will see, the fermions are arranged in different representations of the SM group.

Depending on whether fermions are charged under QCD or not, we divide them into quarks and leptons. An important feature of the SM is that it is a chiral theory, i.e. left and right-handed fields transform differently under the gauge group. While left-handed fields are arranged in $SU(2)_L$ doublets, right-handed fields are $SU(2)_L$ singlets:

$$\begin{pmatrix} \nu_l \\ e \end{pmatrix}_L \,, \quad \begin{pmatrix} u \\ d \end{pmatrix}_L \,, \quad e_R \,, \quad u_R \,, \quad d_R \,. \tag{1.2}$$

This structure is replicated three times, resulting in the family structure of the SM. It is a mystery why the building-blocks of Nature, i.e. the elementary particles, are replicated. An obvious feature is the explicit violation of parity by the weak interaction. The last piece of the SM is the Higgs boson, H, a scalar field that transforms as a $SU(2)_L$ doublet which is the responsible of giving masses to the fundamental fermions as a result of the spontaneous symmetry breaking (SSB) mechanism. The quantum numbers of the particles in the SM are given in table 1.1.

Altogether, we can write the most general Lagrangian that respects SM gauge symmetry:

$$\mathcal{L}_{SM} = \mathcal{L}_{gauge} + \mathcal{L}_F + \mathcal{L}_H + \mathcal{L}_{Yuk} \,. \tag{1.3}$$

The first two pieces, $\mathcal{L}_{gauge}$ and $\mathcal{L}_F$, involve the kinetic terms of both, gauge bosons and fermions. We will see how the derivatives, when promoted to covariant derivatives, turn on the fundamental interactions of the strong and electroweak sectors. The second part involves interactions related to the

Higgs boson. We will see that $\mathcal{L}_H$ is responsible of the electroweak symmetry breaking (EWSB) mechanism and $\mathcal{L}_{Yuk}$ describes the interaction of fermions with the Higgs boson. Finally, we will also review how elementary fermions gain a mass due to the interaction with the Higgs condensate.

1.1.0.1 Quantum Chromodynamics

As we mentioned before, the SM also includes the strong interaction which corresponds to the $SU(3)_C$ sector, and is only felt by quarks. We start with the quark Lagrangian:

$$\mathcal{L}_0^{\text{quark}} = \sum_{quarks} \bar{q}_i \left(i\gamma^\mu \partial_\mu - m_f\right) q_i \,. \tag{1.4}$$

This Lagrangian is invariant under global $SU(3)_C$ transformations $q' = Uq$, where

$$U = \exp\{i\frac{\lambda^a \theta_a}{2}\} \,. \tag{1.5}$$

In the equation above λ^a are the Gell-Mann matrices and θ_a the transformation parameters. Promoting $SU(3)_C$ to be a local symmetry requires that the parameters vary locally, $\theta_a = \theta_a(x)$, and also requires the introduction of the covariant derivaties to preserve gauge invariance

$$D^\mu q_i = \left(\partial_\mu + i g_s \frac{\lambda^a}{2} G_a^\mu(x)\right) q_i \,. \tag{1.6}$$

Here $G_a^\mu(x)$ is the gluon field and $a = 1, ..., 8$ is the $SU(3)_C$ index. One immediately notices that the strong interaction is mediated by the 8 gluons, each corresponding to a $SU(3)_C$ generator. Finally, adding the gauge-invariant kinetic term we obtain the QCD Lagrangian:

$$\mathcal{L}_{QCD} = \mathcal{L}_{gauge} + \mathcal{L}_0^{\text{quark}} = -\frac{1}{4} G^a_{\mu\nu} G_a^{\mu\nu} + \sum_{quarks} \bar{q}_i \left(i\gamma^\mu D_\mu - m_f\right) q_i \,. \tag{1.7}$$

The field strength tensor for the gluon fields, responsible of gluon self-interactions, reads:

$$G^a_{\mu\nu} = \partial_\mu G^a_\nu - \partial_\nu G^a_\mu - g_s f_{abc} G^b_\nu G^c_\mu \,. \tag{1.8}$$

The symbol f_{abc} stands for the structure constants of the $SU(3)$ group. One easily appreciates how the non-abelian behaviour of YM theories gives rise to gauge boson self-interactions.

1.1.0.2 Electroweak interaction

As mentioned before, the group $SU(2)_L \times U(1)_Y$ describes the electroweak interaction. The kinetic Lagrangian of the corresponding gauge bosons reads

$$\mathcal{L}_{gauge} = -\frac{1}{4} W^a_{\mu\nu} W^{\mu\nu}_a - \frac{1}{4} B_{\mu\nu} B^{\mu\nu} \,, \tag{1.9}$$

where the field strength tensor are given by:

$$\begin{aligned} W^a_{\mu\nu} &= \partial_\mu W^a_\nu - \partial_\nu W^a_\mu - g \epsilon_{abc} W^b_\nu W^c_\mu \,, \\ B_{\mu\nu} &= \partial_\mu B_\nu - \partial_\nu B_\mu \,. \end{aligned} \tag{1.10}$$

An important feature of the gauge Lagrangian is that it contains gauge boson self-couplings (see Eq. (1.10)) as expected from the non-Abelian nature of the $SU(2)_L$ part of the group. As it occurs for QCD, promoting $SU(2)_L \times U(1)_Y$ to a local symmetry requires the introduction of the associated covariant derivatives. These derivatives will now be different for left-handed and right-handed fermions due to their different transformation under the gauge group:

$$\begin{aligned} D_\mu \psi_L &= \Big(\partial_\mu + i g \frac{\sigma_a}{2} W^a_\mu + i g' Y B_\mu \Big) \psi_L \,, \\ D_\mu \psi_R &= \Big(\partial_\mu + i g' Y B_\mu \Big) \psi_R \,, \end{aligned} \tag{1.11}$$

where g and g' are the coupling constants of the $SU(2)_L$ and $U(1)_Y$ interactions, W^a_μ and B_μ are the associated gauge fields, and σ_a and Y are the group generators. At this point it is easy to see that, within the SM, left-handed and right-handed fields transform differently. In other words, the SM is a chiral theory.

All in all, we have achieved a good and consistent microscopic theory of the EW interaction. However, this is not the end of the story. From radioactive decays we know that $W^\pm$ bosons are massive and also that the only neutral massless gauge boson is the photon. The Z boson, responsible of the weak neutral current, must also get a mass. In few words, we need to recover the electromagnetic (EM) interaction as an effective theory. As we will see in the next section, the Higgs mechanism describes the sponta-

neous breaking of the EW group by the Higgs condensate down to $U(1)_{EM}$. Therefore, in the SM, the photon is actually a linear combination of the gauge bosons of $SU(2)_L$ and $U(1)_Y$.

Symmetry breaking

The Standard Model is a chiral gauge theory. This is actually an interesting and non-trivial property. First of all, chiral gauge theories are challenged by gauge anomalies, implying that the fermion quantum numbers somehow *conspire* so that the resulting theory is anomaly free. On the other hand, in a chiral theory, bare mass terms are forbidden by symmetry. This is actually a desirable feature since, in general, bare mass terms are not under control and can be arbitrarily large. In the SM, left and right-handed fermions transform differently and invariant bare mass terms, $m\bar{f}f = m(\bar{f}_L f_R + \bar{f}_R f_L)$, are forbidden by the gauge symmetry of the theory.

Another important feature of gauge theories is that unbroken symmetries describe massless gauge bosons. A mass term for gauge bosons is forbidden by gauge invariance and terms like

$$M^2 \mathbf{B}^\mu \mathbf{B}_\mu \,, \tag{1.12}$$

are not allowed at the renormalizable level.

A world with an exact $SU(2)_L \times U(1)_Y$ symmetry would look very different from ours. In such a world, fermions would be massless and all the gauge bosons - including the EW gauge bosons - would be massless[3]. If we want to describe our world with a QFT based on the SM gauge group, the EW symmetry must be broken.

1.1.0.3 Spontaneous symmetry breaking. The Higgs mechanism

There are different ways to break symmetries. If the breaking is explicit at the Lagrangian level but is sufficiently small, they may look as approximate symmetries. An observer will only notice the breaking, and the possible violation of a conservation law, if sufficient experimental precision is achieved. However, by definition, the breaking of gauge symmetries cannot be explicit. One is challenged to find another way consistent with the gauge principle. Fortunately, a mechanism was known in condensed matter

[3]This neglects the possibility of chiral symmetry breaking in QCD as the origin of EW symmetry breaking. See [25] for an interesting *gedanken experiment* of a world without the Higgs boson.

systems such as the Bardeen-Cooper-Schrieffer (BCS) theory of superconductivity [26], where Cooper pairing of electrons spontaneously breaks the electromagnetic gauge symmetry, giving mass to the photon and producing the Meissner effect.

In the context of the EW theory, the Higgs mechanism, proposed independently by R. Brout and F. Englert; by Peter Higgs; and by G. Guralnik, C.R. Hagen, and T. Kibble [16–18], can be viewed as a type of superconductivity that occurs in the vacuum and permeates all the space. The main idea of spontaneously broken symmetries is that the Lagrangian preserves the symmetry while the ground state of the theory breaks it. This simple and beautiful idea is carried out by a complex scalar field, transforming as $H \sim (1, 2, 1/2)$ under the SM gauge group, that we introduce in the theory. Specifically, the scalar doublet is:

$$H = \begin{pmatrix} H^+ \\ H^0 \end{pmatrix} . \tag{1.13}$$

The introduction of this field to the SM has enormous consequences. The following interactions will now be allowed by gauge symmetries (at dimension $d \leq 4$):

$$\mathcal{L}_H = \left(D^\mu H\right)^\dagger \left(D_\mu H\right) - V_H \, , \tag{1.14}$$

where the Higgs potential, V_H, reads:

$$V_H = \mu^2 |H|^2 + \lambda |H|^4 \, . \tag{1.15}$$

This potential has a non-unique minimum for $H^\dagger H = |H|^2 = -\frac{1}{2}\mu^2/\lambda$. These minima correspond to a classical ground state that, in the quantized theory, corresponds to a non-zero vacuum expectation value (VEV) for the scalar doublet H[4]:

$$\langle H \rangle = \frac{1}{\sqrt{2}} \begin{pmatrix} 0 \\ v \end{pmatrix} . \tag{1.16}$$

We can always parametrize the scalar field as

$$H = e^{i \frac{\theta^a(x)\sigma_a}{v}} \begin{pmatrix} 0 \\ \frac{v+h(x)}{\sqrt{2}} \end{pmatrix} , \tag{1.17}$$

[4]The SM Higgs VEV is known to be $v = 246$ GeV [13].

where $\theta^a(x)$ and $h(x)$ are real scalar fields. The three θ^a fields can be *gauged away* by a $SU(2)_L$ transformation with parameter $\alpha^a = -\frac{2\theta^a}{v}$

$$H' = e^{-i\frac{2\theta^a(x)}{v}\frac{\sigma^a}{2}} H = \begin{pmatrix} 0 \\ \frac{v+h(x)}{\sqrt{2}} \end{pmatrix} . \tag{1.18}$$

In this gauge (unitary gauge), the θ^a degrees of freedom become the longitudinal components of $SU(2)_L$ bosons, which become massive. This is how the Higgs mechanism evades Goldstone's theorem and allows us to give masses to the gauge bosons without spoiling the quantum consistency of the theory.

Gauge boson masses arise from the kinetic terms of the Higgs Lagrangian, $\left(D^\mu H\right)^\dagger \left(D_\mu H\right)$, when H develops a VEV. This VEV (see Eq. (1.17)) leaves the part of the gauge group $SU(3)_C \times U(1)_{EM}$ unbroken. Therefore, the photon and the gluon remain massless. The photon, A_μ, and Z-boson, Z_μ, will be given by linear combinations of the neutral components of the original EW gauge bosons, W^3_μ and B_μ:

$$\begin{aligned} W^3_\mu &= \sin\theta_w A_\mu + \cos\theta_w Z_\mu \,, \\ B_\mu &= \cos\theta_w A_\mu - \sin\theta_w Z_\mu \,. \end{aligned} \tag{1.19}$$

The weak mixing angle, θ_w, is determined by the relation:

$$\frac{g'}{g} = \tan\theta_w \,. \tag{1.20}$$

By introducing Eq. (1.18) into the Higgs Lagrangian and rotating the gauge bosons, we get

$$\begin{aligned} \mathcal{L}_h = &\frac{1}{2}(\partial_\mu h)^2 - \frac{1}{2}M_h^2 h^2 - \frac{1}{4}\lambda h^4 - \lambda v h^3 + \frac{1}{2}v g^2 W^+_\mu W^{-\mu} h \\ &+ \frac{1}{4}v\frac{g^2}{\cos\theta_w} Z_\mu Z^\mu h + \frac{1}{4}g^2 W^+_\mu W^{-\mu} h^2 + \frac{1}{8}\frac{g^2}{\cos\theta_w} Z_\mu Z^\mu h^2 \\ &+ \frac{1}{2}M_Z^2 Z_\mu Z^\mu + M_W^2 W^+_\mu W^{-\mu} + \lambda\frac{v^4}{4} \,, \end{aligned} \tag{1.21}$$

with the gauge and Higgs boson masses given by

$$M_W = \frac{1}{2}gv \,, \;\; M_Z = \frac{1}{2}g_Z v = \frac{M_W}{\cos\theta_W} \,, \;\; M_h = \sqrt{2\lambda}v \,. \tag{1.22}$$

Another important relation between weak boson masses and weak mixing angle arises

$$\cos^2\theta_w = \frac{M_W^2}{M_Z^2}\,, \tag{1.23}$$

and allows us to define the electroweak parameter

$$\rho := \frac{M_W^2}{M_Z^2\cos^2\theta_w}\,. \tag{1.24}$$

In the SM, at tree-level, the electroweak parameter is predicted to be $\rho = 1$, while the experimental value is given by $\rho^{exp} = 1.00037 \pm 0.0023$ [27]. It can be easily shown that the addition of an arbitrary number of Higgs singlets and doublets (with non-vanishing VEV) does not change the value of ρ. However, the value of ρ changes if we add higher $SU(2)_L$ representations, such as triplets, with non-vanishing VEVs. For example, in the case of an additional Higgs triplet (important for the type-II seesaw, which will be studied later in Chapter 2) the ρ parameter is changed by

$$\rho = \frac{v^2 + 2v_\Delta^2}{v^2 + 4v_\Delta^2}\,, \tag{1.25}$$

constraining the VEV of the Higgs triplet to be $v_\Delta \leq 3$ GeV.

1.1.0.4 Yukawa interaction and fermion masses

The introduction of an elementary scalar in the model has several implications. Among them, some interactions will be allowed by the symmetries and must be taken into account. One of the most important are the so-called Yukawa interactions

$$\mathcal{L}_{Yuk} = -\sum_{ij}\left[Y^l_{ij}\bar{l}_{iL}He_{jR} + Y^u_{ij}\bar{q}_{iL}\tilde{H}u_{jR} + Y^d_{ij}\bar{q}_{iL}Hd_{jR} + \text{h.c.}\right], \tag{1.26}$$

where $\tilde{H} = i\sigma_2 H^*$. It is important to notice that l_L, q_L, u_R and d_R are the weak or interaction eigenstates and not the mass eigenstates. Here we stress that, due to the absence of a right-handed neutrino in the Standard Model, neutrinos are predicted to be massless if we restrict ourselves to operators with dimension $d \leq 4$. Later in this thesis, we will study in some detail several mechanisms beyond the SM to generate naturally small neutrino masses, both in Dirac and Majorana fashion.

Fermion masses and mixing are also generated at tree level due to the Higgs mechanism. Fermions that interact with the Higgs condensate, $\langle H \rangle$, get a non-zero mass. As stated before, in the unitary gauge we have:

$$H = \begin{pmatrix} 0 \\ \frac{v+h(x)}{\sqrt{2}} \end{pmatrix}, \quad \tilde{H} = \begin{pmatrix} \frac{v+h(x)}{\sqrt{2}} \\ 0 \end{pmatrix}. \tag{1.27}$$

Introducing them in the Yukawa Lagrangian, Eq. (1.26), we get the fermion masses and their interaction with the physical Higgs boson, h:

$$\begin{aligned} \mathcal{L}_{Yuk} = -\sum_{ij} \Big[& \bar{l'}_{iL} M^l_{ij} l'_{jR} + \bar{u'}_{iL} M^u_{ij} u'_{jR} + \bar{d'}_{iL} M^d_{ij} d'_{jR} \\ & + \frac{h}{\sqrt{2}} \bar{l'}_{iL} Y^l_{ij} l'_{jR} + \frac{h}{\sqrt{2}} \bar{u'}_{iL} Y^u_{ij} u'_{jR} + \frac{h}{\sqrt{2}} \bar{d'}_{iL} Y^d_{ij} d'_{jR} \Big], \end{aligned} \tag{1.28}$$

where

$$M^l_{ij} = Y^l_{ij} \frac{v}{\sqrt{2}}, \quad M^u_{ij} = Y^u_{ij} \frac{v}{\sqrt{2}}, \quad M^d_{ij} = Y^d_{ij} \frac{v}{\sqrt{2}}, \tag{1.29}$$

are the Dirac mass matrices for the charged leptons, up-type and down-type quarks, respectively.

If we denote by l,u and d the mass eigenstates of charged leptons, up-type and down-type quarks, respectively, we get that these are obtained by rotating the flavor or interaction eigenstates (l',u' and d'):

$$\begin{aligned} l_{iL} &= \mathcal{U}^l_{L\,ij} l'_{jL}, \quad u_{iL} = \mathcal{U}^u_{L\,ij} u'_{jL}, \quad d_{iL} = \mathcal{U}^d_{L\,ij} d'_{jL}, \\ l_{iR} &= \mathcal{U}^l_{R\,ij} l'_{jR}, \quad u_{iR} = \mathcal{U}^u_{R\,ij} u'_{jR}, \quad d_{iR} = \mathcal{U}^d_{R\,ij} d'_{jR}. \end{aligned} \tag{1.30}$$

These unitary matrices correspond to rotations that diagonalize the mass matrices given in Eq. (1.29), resulting in the rotated Lagrangian:

$$\begin{aligned} \mathcal{L}_{Yuk} = -\sum_{i} \Big[& \bar{l}_i m^l_i l_i + \bar{u}_i m^u_i u_i + \bar{d}_i m^d_i d_i \\ & + \frac{m^l_i}{v} h \bar{l}_i l_i + \frac{m^u_i}{v} h \bar{u}_i u_i + \frac{m^d_i}{v} h \bar{d}_i d_i \Big]. \end{aligned} \tag{1.31}$$

It follows automatically that the physical Higgs that results after EWSB couples to fermions with strength proportional to the fermion mass. This has phenomenological importance since it follows that the coupling to heavy fermions is larger and easier to test.

1.2 Flavor in the Standard Model

Fundamental fermions are replicated in the SM. For each elementary fermion we have 3 copies, only differing in their mass, known by the name of *flavors*. For example, the 3 different flavors of charged leptons are called *electron*, *muon* and *tau* and present an interesting mass hierarchy:

$$m_e \ll m_\mu \ll m_\tau \,. \tag{1.32}$$

Similar hierarchies are also present for up-type and down-type quarks. It is a deep mystery why families are replicated and also why their mass scales are hierarchically distributed. Flavor physics involves any process in which a given SM fermion participates in an *inter-family transition* (see [28–30] for comprehensive reviews). For example, in the quark sector, this process of flavor conversion is driven by the quark mixing angles that arise since interaction and mass eigenstates of fermions do not coincide. Another interesting feature of these processes of flavor dynamics is that at leading order, they involve only left-handed fermions and are exclusively determined by the dynamics of the charged-currend of the weak interaction. All these features render the flavor sector in the SM testable.

Finally, it is a rather remarkable fact that thanks to this rich flavor structure with three families, CP symmetry is violated by the weak interaction in the SM. Indeed, it is well known that the violation of CP symmetry can only occur if there are at least three families and also that any CP violating process involves necessarily all of the quark families [31]. Of course, introducing new ingredients (for example new vector-like fermions and scalar fields) to the SM implies the introduction of new couplings, some of which may be complex, leading to new sources of CP violation (CPV). Probes of CP violation such as the searches for electric dipole moments (EDM) offer interesting constraints to BSM models [32].

In this section we start by reviewing the parameter counting that systematically allows us to determine, for a given theory, the number of physical parameters. After that, we will briefly review flavor dynamics mediated by the charged current and CP violation in the SM.

Parameter counting in the Standard Model

A precise determination of the number of physically relevant parameters is crucial prior to the study of any theory. In particular, the Yukawa interaction we described in Eq. (1.26), has many complex parameters when

the 3 families are taken into account. However, many of the parameters are unphysical and can be *rotated away* with an appropriate basis transformation.

Let us focus on the Yukawa interaction to illustrate the parameter counting. If one turns off the Yukawa couplings, the kinetic Lagrangian enjoys a large flavor symmetry given by:

$$G_{flavor} = U(3)_{q_L} \times U(3)_{u_R} \times U(3)_{d_R} \times U(3)_{l_L} \times U(3)_{e_R} \,. \tag{1.33}$$

In the SM, there is no vertex connecting quarks and leptons, allowing us to study their case separately.

Let us start with the leptonic case. In this case, we have a flavor symmetry given by $U(3)_{l_L} \times U(3)_{e_R}$, resulting in 18 generators. This flavor symmetry is broken down to $U(1)_e \times U(1)_\mu \times U(1)_\tau$ by the lepton Yukawa matrix:

$$Y^l_{ij} \bar{l}_L H e_R \,. \tag{1.34}$$

This 3×3 matrix is complex in general, resulting in 18 parameters. Using a symmetry transformation, one can rotate away as many parameters as broken generators of the flavor symmetry, resulting in: $18 - (18 - 3) = 3$ physical parameters. These physical parameters correspond to the charged lepton masses. This is a general result: in breaking the global symmetry, there is an extra freedom to eliminate as many parameters as broken generators.

Let us now turn to the quark sector. In this case the flavor symmetry in the limit of vanishing Yukawa couplings is $U(3)_{q_L} \times U(3)_{u_R} \times U(3)_{d_R}$, resulting in 27 generators. Since now we have two complex 3×3 Yukawa matrices, Y^u_{ij} and Y^d_{ij} (see Eq. (1.26)), the number of free parameters is 36. These couplings break the large flavor symmetry down to baryon number, $U(1)_B$, which is the only exact symmetry in this case. Applying the general rule gives us a total of $36 - (27 - 1) = 10$ physical parameters. These parameters correspond to the 6 quark masses, 3 mixing angles and the CPV phase of the Cabibbo-Kobayashi-Maskawa (CKM) matrix.

Flavor dynamics and CP violation in the Standard Model

As stated above in Eq. (1.26), in the SM, the fermions obtain their masses through their Yukawa interaction with the Higgs condensate. With 3 generations, the Yukawa matrices of different fermion types are 3×3 complex matrices. In order to go from the flavor or interaction basis to

the mass basis we need to diagonalize these matrices, rotating the flavor eigenstates (see Eq. (1.30)):

$$q_{iL} = \mathcal{U}^{q}_{L\,ij} q'_{jL}\,, \tag{1.35}$$

where q' denotes the flavor eigenstates. With this rotation we obtain the so-called mass eigenstates. The matrices $\mathcal{U}^{q}_{L\,ij}$ are 3×3 unitary matrices:

$$\mathcal{U}^{q}_{L} \mathcal{U}^{q\,\dagger}_{L} = 1\,, \text{ with } q = u, d\,. \tag{1.36}$$

However, in general, the product $\mathcal{U}_{u\,L}\mathcal{U}^{\dagger}_{d\,L}$ differs from the identity. This leads to flavor-changing processes mediated by the weak charged current.

The Lagrangian describing these processes is given by:

$$-\mathcal{L}_W = \frac{g}{\sqrt{2}} \bar{u}_{L\,i} \gamma^{\mu} \left(V_{CKM}\right)_{ij} d_{L\,j} W^{+}_{\mu} + h.c. \tag{1.37}$$

where we have defined the CKM matrix as:

$$V_{CKM} = \mathcal{U}_{u\,L}\mathcal{U}^{\dagger}_{d\,L} = \begin{pmatrix} V_{ud} & V_{us} & V_{ub} \\ V_{cd} & V_{cs} & V_{cs} \\ V_{td} & V_{ts} & V_{tb} \end{pmatrix}, \tag{1.38}$$

This matrix, describing the quark mixing and flavor-changing processes, is a 3×3 unitary matrix. Although very hierarchical, it is non-diagonal and can be parametrized as [13]:

$$V_{CKM} = \begin{pmatrix} c_{12}c_{13} & s_{12}c_{13} & s_{13}e^{-i\delta} \\ -c_{12}s_{23}s_{13}e^{i\delta} - s_{12}c_{23} & c_{12}c_{13} - s_{12}s_{23}s_{13}e^{i\delta} & s_{23}c_{13} \\ s_{12}s_{23} - c_{12}c_{23}s_{13}e^{i\delta} & -c_{12}s_{23} - s_{12}c_{23}s_{13}e^{i\delta} & c_{23}c_{13} \end{pmatrix} \tag{1.39}$$

where we have defined $s_{ij} = \sin\theta_{ij}$ and $c_{ij} = \cos\theta_{ij}$. Here θ_{ij} denotes the mixing angle between i and j families and δ is the CPV phase. Notice that in the SM, with massless neutrinos, there is no analogous to the CKM matrix for leptons because of the freedom to redefine the neutrino fields so that the charged leptons are rotated to the diagonal mass-basis. Later, in Chapter 2, we will consider the situation with massive neutrinos that leads to the lepton mixing matrix and the phenomenon of neutrino oscillations.

As shown before, the quark sector with 3 families contains a physical CPV phase, contained in Eq. (1.39), the CKM phase δ. The explicit expression depends on the parametrization of the CKM matrix. Fortunately, one

can define a CPV quantity that contains all the relevant information and is a basis-independent quantity. This is the so-called Jarlskog invariant [31] and is defined as:

$$\mathrm{Im}(V_{ij}V_{kl}V_{il}^{*}V_{kj}^{*}) = J_{CKM}\sum_{m,n=1}^{3}\epsilon_{ikm}\epsilon_{jln}\,. \tag{1.40}$$

In terms of the Particle Data Group (PDG) parametrization introduced above (see Eq. (1.39)) the Jarlskog invariant is given by:

$$J_{CKM} = c_{12}c_{23}c_{13}^{2}s_{12}s_{23}s_{13}\sin\delta\,. \tag{1.41}$$

One immediately observes that CPV can only be present if all mixing angles are different from zero and, therefore, all quarks are massive.

The global fit of different experimental results is (see [13] and references therein):

$$V_{CKM} = \begin{pmatrix} 0.97401 \pm 0.00011 & 0.22650 \pm 0.00048 & 0.00361^{+0.00011}_{-0.00009} \\ 0.22636 \pm 0.00048 & 0.97320 \pm 0.00011 & 0.04053^{+0.00083}_{-0.00061} \\ 0.00854^{+0.00023}_{-0.00016} & 0.03978^{+0.00082}_{-0.00060} & 0.999172^{+0.000024}_{-0.000035} \end{pmatrix}. \tag{1.42}$$

On other hand, the value of the Jarlskog invariant is given by:

$$J = 3.00^{+0.15}_{-0.09}\times 10^{-5}\,. \tag{1.43}$$

1.3 Beyond the Standard Model

The previous sections contain a brief overview of the most precise microscopic theory of Nature, the SM. This theory accurately describes the elementary particles and their fundamental interactions. It leaves, however, several phenomena unexplained. These open questions include theoretical and purely phenomenological issues. Among them we can mention:

- **Neutrino Masses.** Due to its particle content, neutrinos are massless within the SM at the renormalizable level. However, since the discovery of neutrino oscillations we know that they have a small but non-zero mass. Despite the fact that the exact mass scale value is unknown, their lightness points to a mass-generation mechanism beyond the standard Higgs mechanism.

- **Flavor puzzle.** It is a striking fact that each SM family/generation is replicated 3 times. In some sense, Rabi's famous question "*Who ordered that?*" has been rescaled to "*Why does Nature repeat herself?*"[5]. Additionally, the very particular pattern of fermion masses and mixing is unexplained in the SM.

- **Dark Matter.** Observations reveal that around one quarter of the total energy density of the Universe corresponds to some sort of non-luminous matter called *dark matter*. Today we know that without this form of non-relativistic matter galaxies would look very different. However, the nature and interactions of dark matter are a deep mystery. With many different proposals and experimental efforts, it is currently a very active field of research.

- **Grand Unified Theories.** Charge quantization has remained an open question since the early days of quantum mechanics. With the advent of the SM, this question has escalated to explain the particular quantum numbers of known elementary particles and the relative strength of their interactions. With great elegance and simplicity, Grand Unified Theories (GUT) postulate that the plethora of different charges and interactions is just a low-energy manifestation of a deeper underlying unity. Therefore, in the ultraviolet (UV), the separate parts of the SM gauge group are merged into a unique gauge symmetry. One of the most interesting phenomenological predictions is the instability of the proton.

- **Strong CP problem.** In principle, QCD could violate CP invariance. However, from non-observation of the neutron EDM, we now that either CP is conserved by the strong force or its violation is extremelly small. Given that CP is largely violated in the quark sector by the weak interaction, explaining the non-observation of strong CPV is very challenging.

- **Matter-antimatter asymmetry.** A Universe full of matter is hard to accommodate in the standard picture of the hot Big Bang theory, where one expects the same amount of particles and antiparticles. Matter seems to be the preferred building block of Nature, from living beings to the largest known structures in the Universe. Explaining this asymmetry is a long-standing open question.

[5]Quote extracted from [33].

- **Hierarchy problem.** The root of the problem is the huge hierarchy between the weak scale and the Planck scale, where gravity becomes relevant. Since scalar fields usually receive large quantum corrections, it is a mystery why the SM Higgs remains light. The hierarchy problem is one of the open questions that has received more attention in the last decades and has lead to the development of frameworks such as weak-scale supersymmetry, technicolor and large extra-dimensions.

- **Inflation.** Originally proposed as a solution to the horizon and flatness problems of the original hot Big Bang theory, the inflationary Universe [34] is the theory that offers the best understanding of the standard cosmology's peculiar initial conditions. The key idea behind inflation is an early epoch of accelerated expansion that lead to an exponential growth of physical scales. Therefore, all the presently observable Universe corresponds to a tiny initial region. To explain the observed correlations in the cosmic microwave background (CMB), we need at least 60 e-foldings of exponential expansion. However, the duration of the inflationary period and its characteristic scale, i.e. the inflationary Hubble parameter H_I, are unknown. Also unknown are the nature and interactions of the inflaton field.

- **Cosmological constant problem and Dark Energy.** Most of the energy density content of the Universe remains a mystery. At the end of the last century it was experimentally confirmed that our Universe is currently dominated by vacuum energy, leading to an accelerated expansion [35,36]. The problem in this case is to understand why this contribution to the total energy density budget of the Universe is so small, that is why $\rho_{vac} \sim (3 \text{ meV})^4$ is much smaller than any other scale in the theory such as the weak or the Planck scale. Indeed, a QFT estimation reveals that the contribution from Standard Model fields is at least 60 orders of magnitude larger than the observed value [37]. Currently, we lack a fully satisfactory answer to the smallness of ρ_{vac}. There exist several possibilities ranging from dynamical dark energy or *quintessence*, to anthropic selection. Different proposals can be distinguished by measuring the equation of state parameter $w \equiv p/\rho$. While the pure cosmological constant predicts $w = -1$, a quintessence scenario would imply a $w > -1$ which, in addition, increases with time. Planck data currently suggests: $w \lesssim -0.95$ at 95% C.L. [38].

- **Towards a quantum theory of gravity.** While electromagnetism, the nuclear force and Fermi's theory of radioactivity are successfully quantized and described by spin-1 bosons, gravity is simply different. Indeed, as shown by Feynman [39], perturbation theory, when applied to Einstein gravity, leads to the appearance of a massless spin-2 particle: the graviton. However, a fully consistent formulation is not yet available. To this end, one of the most promising avenues, string theory, consists of replacing the usual picture of point-like particles by extended objects such as strings and branes. Unfortunately, the effects associated to this new paradigm are expected to be extremely challenging to detect, if possible at all. A general feature of string theories is the presence of compact dimensions in addition to our usual 4 non-compact dimensions. Other feature which is quite common in string-theoretic frameworks is the presence of additional dark gauge sectors and the proliferation of light scalar fields; axions and moduli [40].

This thesis is based on several articles where the author attains the first 5 open questions.

Chapter 2

Neutrino Masses

The discovery of neutrino oscillations led to the Nobel Prize in Physics to Takaaki Kajita [41] and Arthur McDonald [42], and established the existence of small neutrino masses as one of the leading hints for new physics beyond the SM. In this chapter, after reviewing the phenomenon of neutrino oscillations in vacuum, we will briefly overview the simplest SM extensions that account for naturally light neutrinos. By *natural* we mean that the smallness of neutrino mass will be connected to either a heavy scale or a loop suppression. This occurs when we UV-complete the Weinberg operator [43] at the tree-level or at the loop-level, respectively. As particular examples, we will study in more detail the case of the type-I seesaw [44–48] and the Scotogenic model [49].

2.1 The Lepton Mixing Matrix

In this section we summarize the properties of the lepton mixing matrix, V_{LEP}. To this end, we follow closely the procedure detailed in [50]. Similarly to the quark sector, the lepton mixing matrix describes the charged current weak interaction between neutrinos and charged leptons. It is well known that a theory with massless neutrinos would imply a trivial lepton mixing matrix. However, the observation of neutrino oscillations demonstrates that neutrinos are massive. In this case, a non-trivial lepton mixing matrix is generated when the new Yukawa-like matrix of neutrinos does not commute with the charged lepton Yukawa matrix. Depending on whether neutrinos are Dirac or Majorana particles, the situation changes qualitatively. For example, a theory with 3 light Dirac neutrinos resembles the quark case,

with a lepton mixing matrix given by:

$$V_{LEP} = \mathcal{U}_L^{e\,\dagger}\mathcal{U}_L^{\nu}\,. \tag{2.1}$$

This mixing matrix is qualitatively similar to the CKM matrix and is fully determined by $n(n-1)/2$ mixing angles, θ_{ij}, and $n(n-1)/2-(n-1)$ independent CP phases.

If neutrinos turn out to be Majorana particles, the situation is expected to be richer. The reason is that in a theory with Majorana fermions one has less freedom to remove some of the CP phases. This occurs because the mass terms are not invariant under Majorana field redefinitions and some of the phases that would be unphysical in a theory with Dirac fermions become physical. As a result, in a theory with n light Majorana neutrinos one has $n(n-1)/2$ CP phases in addition to the $n(n-1)/2$ mixing angles. It is interesting to see that a simple theory with 2 Majorana fermions already accounts for a CP violating phase [51].

If one takes into account a fully general (n, m) scenario, with n isodoublet neutrinos and m isosinglets, the total number of parameters is [44]:

$$\begin{aligned} &n(n+2m-1)/2 \;\; \text{mixing angles.} \\ &n(n+2m-1)/2 \;\; \text{CP phases.} \end{aligned} \tag{2.2}$$

Once the heavy states are integrated out, the ligh neutrinos are described by a non-unitary mixing matrix. It is not implausible that the number of heavy isosinglets is smaller than the number of SM neutrinos, $m < n$. In this case, there exist $n-m$ massless neutrinos at leading order. These massless neutrinos will acquire a non-zero mass through higher-order corrections.

2.2 Neutrino Oscillations

The phenomenon of neutrino oscillations has a quantum mechanical origin. This process occurs whenever the mass eigenstates, which determine their temporal evolution, and the flavor eigenstates do not coincide. Therefore, if neutrinos are massive their flavor changes throughout their propagation. These oscillations explain the deficit found in solar neutrino experiments and were confirmed later by Super-Kamiokande [52] and SNO [53]. The discovery of neutrino oscillations led to the Nobel Prize in Physics to Takaaki Kajita [41] and Arthur McDonald [42].

The flavor and mass eigenstates are related through the lepton mixing matrix:

$$|\nu_\alpha\rangle = \sum_{i=1}^{3} U^{\nu\,*}_{\alpha\,i} \, |\nu_i\rangle \ . \tag{2.3}$$

Where the greek (latin) indices denote the flavor (mass) eigenstates and we assumed $U^\nu \equiv V^{LEP}$, that is we assumed that the mixing comes exclusively from the neutrino sector. These neutrino eigenstates form a basis of a Hilbert space and satisfy the usual orthonormality relation:

$$\langle \nu_\alpha | \nu_\beta \rangle = \delta_{\alpha\beta} \text{ and } \langle \nu_i | \nu_j \rangle = \delta_{ij} \, . \tag{2.4}$$

As stated above, the mass eigenstates correspond to the eigenstates of the Hamiltonian and determine the temporal evolution of neutrinos in vacuum:

$$|\nu_i(t)\rangle = e^{i(t-t_0)H} \, |\nu_i(t_0)\rangle = e^{iE_i(t-t_0)} \, |\nu_i(t_0)\rangle \ , \tag{2.5}$$

with $E_i^2 = p^2 + m_i^2$. Being part of the $SU(2)_L$ doublets, neutrinos are always produced and detected as flavor eigenstates. Then, if a neutrino is produced as ν_α, the probability of detecting it as ν_β is given by the square of the transition amplitude:

$$\begin{aligned} P_{\alpha\beta} &= |\langle \nu_\alpha | \nu_\beta(t) \rangle|^2 = \left| \sum_j U^*_{\alpha j} U_{\beta j} e^{-i \frac{m_j^2}{2E} L} \right| \\ &= \delta_{\alpha\beta} - 4 \sum_{i>j} \Re \left(U^*_{\alpha i} U_{\alpha j} U_{\beta i} U^*_{\beta j} \right) \sin^2 \left(\frac{\Delta m^2_{ij} L}{4E} \right) \\ &- 2 \sum_{i>j} \Im \left(U^*_{\alpha i} U_{\alpha j} U_{\beta i} U^*_{\beta j} \right) \sin \left(\frac{\Delta m^2_{ij} L}{2E} \right) \ . \end{aligned} \tag{2.6}$$

In the equation above, $\Re$ and $\Im$ denote the real and imaginary parts, respectively. We have assumed the ultrarelativistic limit, that is $E = p$ and $L = t - t_0$, and $\Delta m^2_{kj} = m^2_k - m^2_j$. In the next section we will summarize the current values for the neutrino oscillation parameters, which are determined by performing global fits to neutrino oscillation data from different experiments.

Global fits to oscillation parameters

In the standard picture of 3 light neutrinos, the phenomenon of neutrino oscillations is determined by 3 mixing angles, θ_{12}, θ_{13} and θ_{23}; 2 mass differences, Δm^2_{21} and Δm^2_{31}, and a CPV phase δ. Depending on the origin of the measured neutrinos, we can classify them in solar neutrinos, reactor neutrinos, atmospheric neutrinos and accelerator neutrinos. As we will see now, different types of neutrinos will provide information about different oscillation parameters. In this section we briefly review these types and summarize the current status of the global fits to neutrino oscillation parameters.

- **Solar neutrinos.** Solar neutrinos are produced in the solar interior due to hydrogen burning and different thermonuclear reactions. These neutrinos have energies ranging from 0.1 MeV to 20 MeV. Solar neutrino experiments include Borexino, SNO and Super-Kamiokande and are sensitive to θ_{12} and Δm^2_{21}.

- **Reactor neutrinos.** Neutrino detectors placed relatively close to a nuclear power plant can be used to detect the anti-neutrino flux produced in nuclear reactions. These experiments, including KamLAND, RENO and Daya Bay are generically more sensitive to θ_{13} and Δm^2_{31}.

- **Atmospheric neutrinos.** These neutrinos are produced when a cosmic ray collides with the atmosphere, producing a particle shower. These particle showers lead to highly energetic neutrinos with energies up to 10^9 GeV. However, for oscillation parameters only energies from 0.1 GeV to 100 GeV are relevant. The most relevant atmospheric neutrino experiments are Super-Kamiokande and IceCube Deep Core, which are sensitive to θ_{23} and Δm^2_{31}.

- **Accelerator neutrinos.** Neutrinos are produced in the decay of mesons. When a meson beam is focused, one can get a relatively pure neutrino beam after a filtering process by a beam dump. In long-baseline experiments, the initial flux is measured thanks to a near detector, placed at the accelerator complex. These neutrino beams are produced and detected in experiments including NOVA, T2K, MINOS and K2K to study some oscillation parameters: Δm^2_{31}, θ_{23}, θ_{13} and δ. These long-baseline experiments are, in principle, also sensitive to the neutrino mass ordering. However, this ordering is not yet fully resolved and is one of the goals of future neutrino facilities like DUNE.

parameter	best fit $\pm 1\sigma$	2σ range	3σ range
$\Delta m^2_{21}[10^{-5}\text{eV}^2]$	$7.50^{+0.22}_{-0.20}$	7.12–7.93	6.94–8.14
$\lvert\Delta m^2_{31}\rvert[10^{-3}\text{eV}^2]$ (NO)	$2.55^{+0.02}_{-0.03}$	2.49–2.60	2.47–2.63
$\lvert\Delta m^2_{31}\rvert[10^{-3}\text{eV}^2]$ (IO)	$2.45^{+0.02}_{-0.03}$	2.39–2.50	2.37–2.53
$\sin^2\theta_{12}/10^{-1}$	3.18 ± 0.16	2.86–3.52	2.71–3.69
$\theta_{12}/^\text{o}$	34.3 ± 1.0	32.3–36.4	31.4–37.4
$\sin^2\theta_{23}/10^{-1}$ (NO)	5.74 ± 0.14	5.41–5.99	4.34–6.10
$\theta_{23}/^\text{o}$ (NO)	49.26 ± 0.79	47.37–50.71	41.20–51.33
$\sin^2\theta_{23}/10^{-1}$ (IO)	$5.78^{+0.10}_{-0.17}$	5.41–5.98	4.33–6.08
$\theta_{23}/^\text{o}$ (IO)	$49.46^{+0.60}_{-0.97}$	47.35–50.67	41.16–51.25
$\sin^2\theta_{13}/10^{-2}$ (NO)	$2.200^{+0.069}_{-0.062}$	2.069–2.337	2.000–2.405
$\theta_{13}/^\text{o}$ (NO)	$8.53^{+0.13}_{-0.12}$	8.27–8.79	8.13–8.92
$\sin^2\theta_{13}/10^{-2}$ (IO)	$2.225^{+0.064}_{-0.070}$	2.086–2.356	2.018–2.424
$\theta_{13}/^\text{o}$ (IO)	$8.58^{+0.12}_{-0.14}$	8.30–8.83	8.17–8.96
δ/π (NO)	$1.08^{+0.13}_{-0.12}$	0.84–1.42	0.71–1.99
$\delta/^\text{o}$ (NO)	194^{+24}_{-22}	152–255	128–359
δ/π (IO)	$1.58^{+0.15}_{-0.16}$	1.26–1.85	1.11–1.96
$\delta/^\text{o}$ (IO)	284^{+26}_{-28}	226–332	200–353

Table 2.1: Global fit to neutrino oscillation parameters, adapted from [54].

As we have seen, some of the oscillation parameters are measured by more than one experiment. In addition, due to the weak nature of neutrino

interactions with matter, measuring precisely these parameters is a tremendously hard experimental task. This motivates to combine data from different experiments to achieve a result which is more precise than any single experimental measurement. There are several groups [54–56] performing these global fits to oscillation parameters. In table 2.1 we summarize the results of [54].

Neutrino's known unknowns

The field of neutrino physics has received a lot of experimental and theoretical attention in recent years. Thanks to the experimental verification of neutrino oscillations we know that neutrinos are massive[1]. This opens a plethora of experimental possibilities to determine currently unknown fundamental parameters of our theory of Nature. Some of these parameters are currently unknown and others are not very precisely measured. In this section I briefly overview the current open questions of the field of neutrino physics that, hopefully, will be answered in a near future.

- **Absolute mass scale.** Neutrino oscillations are only sensitive to mass diferences and, therefore, give no information about the mass of the lightest neutrino. Cosmological bounds can currently provide an upper bound to the sum of the neutrino masses: $\sum m_\nu \lesssim 0.12$ eV at 95% C.L. [38]. However, this limit has some dependence on the details of the cosmological model. A model independent way to measure the absolute scale of neutrino masses is the study of the kinematics of β decays. The current bound has already reached the sub-eV sensitivity: $m_\nu < 0.8$ eV at 90% C.L. [57].

- **Dirac or Majorana nature.** Oscillations do not depend on the nature of neutrino mass. Indeed, probing that neutrinos are Dirac particles may be extraordinarily challenging [58]. On the other hand, according to the *Black box* theorem, the observation of neutrinoless double-beta decay would automatically imply that at least one of the SM neutrinos is a Majorana particle [59]. Such a discovery would have an unprecedented impact on our understanding of Nature at the most fundamental level. Among many other possibilities, if neutrinos turn out to be Majorana particles, they could play a relevant role in the inception of the Universe's matter-antimatter asymmetry.

[1] From oscillations we know that at least two of them have non-zero masses. There is still the possibility that the lightest neutrino is massless.

- **Mass ordering.** The sign of the atmospheric mass splitting Δm^2_{31} is currently unknown. The reason is that this parameter is measured in atmospheric neutrino oscillations in vacuum, which only depend on the absolute value. The possibilities are *normal ordering*, which corresponds to $\Delta m^2_{31} > 0$, and *inverse ordering* if $\Delta m^2_{31} < 0$. Currently, the global analysis of neutrino data prefers normal ordering over the inverse ordering with a significance of 2.5σ [54].

- **CPV in the lepton sector.** So far, CP violation has only been observed in the quark sector. The measurement of $\delta \neq 0$ would be an exciting discovery for several reasons, including the possible connection to the generation of the matter-antimatter asymmetry. The phase δ induces opposite sign shifts to the oscillation processes $\nu_\mu \to \nu_e$ and $\bar{\nu}_\mu \to \bar{\nu}_e$. Therefore, δ can be determined by analyzing oscillation data in the associated appearance channels. Despite currently these channels do not offer precise measurements of δ, long-baseline experiments such as T2K and NOνA can in principle measure the CPV phase δ [54]. Additionally, if neutrinos are Majorana particles one expects additional CPV phases. These Majorana phases are not observable in conventional neutrino oscillation experiments but can have an impact in neutrinoless double-beta decay processes [60] and neutrino to anti-neutrino oscillations [51].

- **Cosmic Neutrino Background (CNB)**: In similarity to the CMB, the Cosmic Neutrino Background (CNB) is a robust prediction of the hot Big Bang model. Detecting these relic neutrinos would be one of the biggest discoveries in cosmology, as it provides a new window to observe the early Universe. In addition, the CNB offers precise information about the absolute mass scale of neutrinos. Currently, the best experimental strategy to detect the CNB is the neutrino capture by β-unstable nuclei [61]. Despite being extremely challenging, there are proposals to detect the CNB using a large amount of tritium [62].

These *known unknowns* make neutrino physics one of the most exciting fields in particle physics and is expected to be very prolific in the next few years.

2.3 Neutrino masses and physics beyond the SM

In sharp contrast to charged fermions, neutrinos are massless in the SM at the renormalizable level, that considering operators with dimension $d \leq 4$. This can be easily seen by looking at the SM particle content (see table 1.1). Since there are no right-handed neutrinos within the SM, we cannot build a Dirac mass term for neutrinos.

If one takes the SM as the effective field theory (EFT) of a more complete fundamental theory, in addition to the operators with $d \leq 4$, one adds an infinite tower of effective operators:

$$\mathcal{L} = \mathcal{L}_{SM}^{(4)} + \sum_{i=4}^{\infty} \frac{C_i}{\Lambda^{i-4}} O_i \,. \tag{2.7}$$

The operators O_i are gauge invariant under the SM gauge group but do not need to conserve baryon and lepton number symmetries. The expectation is that the coefficients in this expansion are $C_i \sim O(1)$ and the UV scale Λ suppresses their contribution as the dimension of the operator increases. As noted by Weinberg [43], one can easily see that at dimension-5 there is a gauge invariant effective operator that after EWSB generates a Majorana mass term for neutrinos:

$$\mathcal{O}_5 \sim l_L l_L \phi \phi \,. \tag{2.8}$$

In this scenario, neutrino masses are given by $m_\nu \sim \frac{\langle\phi\rangle^2}{\Lambda}$, and we can explain their smallness due to a suppression by the large scale, Λ. Since lepton number is violated in two units by this operator, neutrinos have necessarily Majorana nature [59]. Unfortunately the EFT language gives no clue about the particular mechanism responsible for neutrino mass generation. Several possibilities arise to UV-complete the Weinberg operator. We classify these UV mechanisms in two main categories, depending on whether neutrino masses are generated at tree-level or at the quantum level through loop corrections.

At tree-level, one can UV-complete the Weinberg operator as follows:

- **Type-I seesaw.** We add (at least two) right-handed neutrinos, $\nu_R \sim (1, 1, 0)$, singlets under the SM [44–48].
- **Type-II seesaw.** We add a Higgs triplet with the appropriate hypercharge: $\Delta \sim (1, 3, 1)$ [44, 63].

- **Type-III seesaw.** We add a fermion triplet with the appropriate hypercharge: $\Sigma \sim (1, 3, 0)$ [64].

We can also UV complete the Weinberg operator at the loop level (see [65] and [66] for comprehensive reviews). Some of the simplest mechanisms, at one loop, are:

- **Zee model.** In addition to the SM particles 2 new scalar fields are introduced: a $SU(2)_L$ singlet with hypercharge equal to 1, $\chi \sim (1, 1, 1)$, and a new weak doublet, transforming as $\Phi_2 = (1, 2, 1/2)$. [67]. This is the simplest SM extension that leads to loop-induced neutrino masses but, unfortunately, is experimentally ruled out [68].

- **Ma model**. Also known as the scotogenic model, is an attractive framework that also accounts for DM [49]. The SM is extended with an inert Higgs doublet, $\eta \sim (1, 2, 1/2)$, and 3 SM singlets $N \sim (1, 1, 0)$. The SM symmetry is extended with a discrete Z_2 symmetry under which only these new particles transform non-trivially. See also [69] for an alternative formulation.

Despite the theoretical prejudice that neutrinos are of Majorana nature, the mechanisms mentioned above can also be used to generate small Dirac neutrino masses in a natural way. Indeed, there has been a recent surge in interest in the field of Dirac neutrinos [70, 71]. The idea is that to achieve small Dirac neutrino masses one has to forbid the Weinberg operator in Eq.(2.8) to all orders in perturbation theory. To this end, one is forced to introduce additional symmetries beyond the gauge symmetry of the SM. Note, however, that the symmetry does not necessarily have to be related to the SM lepton number symmetry. Different examples have been recently proposed, ranging from gauge symmetries [72, 73] to discrete symmetries ensuring the *Diracness* of the neutrino mass [74, 75]. Of particular interest is the attractive connection to the stability of DM [71, 75, 76].

In the following section we will briefly review the most minimal mechanism to generate Majorana neutrino masses, the type-I seesaw mechanism. The rest of the chapter is devoted to the most general version of the Scotogenic model [49], recently studied in full detail in [77].

Seesaw type-I

As we have seen before, the simplest way to generate neutrino masses is adding the right-handed component of neutrino field [44–48], $\nu_R \sim (\mathbf{1}, \mathbf{1}, 0)$,

to the SM. This field is a SM singlet and, therefore, does not contribute to the gauge anomalies. In principle we can add an arbitrary number of ν_R. However, for simplicity, we will introduce 3 right-handed neutrinos to match the number of SM generations[2]. The relevant Lagrangian for neutrino mass generation reads:

$$-\mathcal{L}_{type-I} = y_D \bar{l}_L \tilde{H} \nu_R + \frac{1}{2} M_R \bar{\nu}_R^c \nu_R + \text{h.c.} \tag{2.9}$$

In the equation above, y_D and M_R are 3×3 matrices. Additionally, the Majorana mass matrix is symmetric. Note that since the right-handed neutrinos are SM singlets, the second term, a bare Majorana mass term, does not come from the Higgs mechanism and can be arbitrarily large. Despite it violates lepton number conservation in two units, it is allowed by gauge invariance and, thus, there is no reason to forbid such a term. This is an example of how an accidental symmetry of the Standard Model (lepton number conservation) is violated when adding new ingredients to the theory.

In more detail, after EWSB, the neutrino mass matrix is given by

$$M_\nu = \begin{pmatrix} 0 & m_D \\ m_D^T & M_R \end{pmatrix} . \tag{2.10}$$

The entries m_D and M_R correspond to the 3×3 Dirac and Majorana mass matrices, respectively. This matrix can be block-diagonalized perturbatively [78], giving us the light and heavy neutrino mass matrices:

$$m_{\text{light}} \sim -m_D M_R^{-1} m_D \,, \;\; m_{\text{heavy}} \sim M_R \,. \tag{2.11}$$

Here we note that, in order to have light neutrino masses of order $m_\nu \sim \mathcal{O}(10^{-1})$ eV and keeping $m_D \sim 10^2$GeV, the scale of the Majorana mass of the right-handed neutrino has to be $M_R \sim 10^{14-15}$ GeV, i.e. close to the GUT scale ($M_{GUT} \sim 10^{15-16}$ GeV). This is the key point of the seesaw mechanism and, also, the origin of its name: the heavier is ν_R, the lighter will be the active neutrino. Despite the seesaw mechanism is not necessarily connected to unified theories and is well-motivated by itself, the apparent coincidence of scales of the right-handed neutrino mass and the GUT scale has added further motivation for GUTs such as $SO(10)$, where these representations arise automatically. Indeed, in some of the simplest $SO(10)$

[2]Strictly speaking, to reproduce the observed oscillation parameters, only 2 right-handed neutrinos are necessary.

constructions (see Chapter 5), right-handed neutrinos acquire a mass after the spontaneous breaking of the $SO(10)$ symmetry. This constitutes a deep, interesting connection between light neutrino masses and the gauge structure of the SM.

In theories where the right-handed neutrino mass is generated spontaneously, that is generated by the VEV of a scalar field, a new particle appears: the majoron [78, 79], which is the Nambu-Goldstone boson associated to lepton number symmetry. The phenomenology associated to this particle can be very rich. We will consider this possibility in full detail, with special attention to its role as DM, in Chapter 6.

The general Scotogenic Model

The Scotogenic model, originally proposed in [49], is a simple extension of the SM where neutrinos get a non-zero mass radiatively. Another attractive feature of the model is that it provides a dark matter candidate, stabilized by the same symmetry that prevents the tree-level mass term (see [80, 81] for different realisations, where dark matter plays a crucial role in the neutrino mass generation). The typical new physics scales in the scotogenic model can be substantially lower than those appearing in the minimal type-I seesaw that we considered in the previous section. This renders the scotogenic framework a compelling possibility of neutrino mass mechanisms with signals that may be observable at colliders (see [82] and [83] for recent studies).

In this section, based on [77], we will consider a generalization of the scotogenic model. The SM particle content is extended by an arbitrary number, n_N, of singlet fermions N[3], and an arbitrary number, n_η, of inert scalar doublets η. In addition to the gauge symmetry of the SM, we add a *dark* Z_2 parity, under which only the new fields are odd, while the SM particles are even. The particle content of the model, is given in Tab. 2.2.

The relevant interactions for neutrino mass generation are:

$$\mathcal{L}_N \supset y_{na\alpha}\, \overline{N}_n\, \eta_a\, \ell_L^\alpha + \frac{1}{2}\, M_{N_n}\, \overline{N^c}_n\, N_n + \text{h.c.}\,, \tag{2.12}$$

where $n = 1, \ldots, n_N$, $a = 1, \ldots, n_\eta$ and $\alpha = 1, 2, 3$ are generation indices and y is a general complex $n_N \times n_\eta \times 3$ object. The quantity M_N is a symmetric

[3]This field has the quantum numbers of a right-handed neutrino, denoted with ν_R for the type-I seesaw mechanism. In the context of scotogenic neutrino masses we use the notation N to refer to the SM singlet.

Field	Generations	$\mathrm{SU(3)_C}$	$\mathrm{SU(2)_L}$	$\mathrm{U(1)_Y}$	Z_2
ℓ_L	3	**1**	**2**	$-1/2$	$+$
e_R	3	**1**	**1**	-1	$+$
H	1	**1**	**2**	$1/2$	$+$
η	n_η	**1**	**2**	$1/2$	$-$
N	n_N	**1**	**1**	0	$-$

Table 2.2: Particle content of the general Scotogenic model.

$n_N \times n_N$ Majorana mass matrix that can be chosen diagonal without any loss of generality. Additionally, the most general scalar potential, also including the terms with the inert doublets is given by:

$$\begin{aligned}\mathcal{V} = & m_H^2 H^\dagger H + \left(m_\eta^2\right)_{ab} \eta_a^\dagger \eta_b + \frac{1}{2}\lambda_1 \left(H^\dagger H\right)^2 + \frac{1}{2}\lambda_2^{abcd}\left(\eta_a^\dagger \eta_b\right)\left(\eta_c^\dagger \eta_d\right) \\ & + \lambda_3^{ab}\left(H^\dagger H\right)\left(\eta_a^\dagger \eta_b\right) + \lambda_4^{ab}\left(H^\dagger \eta_a\right)\left(\eta_b^\dagger H\right) \\ & + \frac{1}{2}\left[\lambda_5^{ab}\left(H^\dagger \eta_a\right)\left(H^\dagger \eta_b\right) + \text{h.c.}\right] .\end{aligned} \tag{2.13}$$

Here all the indices are η generation indices. Therefore, the quantities m_η^2 and $\lambda_{3,4,5}$ are $n_\eta \times n_\eta$ matrices, while λ_2 is an $n_\eta \times n_\eta \times n_\eta \times n_\eta$ object. Note also that the matrix λ_5 must be symmetric and the matrices $\lambda_{3,4}$ must be Hermitian. Again, we will assume m_η^2 to be diagonal without any loss of generality. As we will show later, the quartic couplings λ_5^{ab}, are of fundamental importance for the neutrino mass generation mechanism.

We will assume that the minimization of the scalar potential in Eq. (2.13) leads to the vacuum configuration:

$$\left\langle H^0 \right\rangle = \frac{v}{\sqrt{2}} \quad , \quad \left\langle \eta_a^0 \right\rangle = 0\,, \tag{2.14}$$

with $a = 1, \ldots, n_\eta$. This means that the inert doublets have zero VEVs, ensuring that the Z_2 symmetry remains unbroken. This fact guarantees the stability of the lightest Z_2-charged particle. In this thesis we do not consider the possibility of Z_2 breaking due to Renormalization Group Equations

(RGEs) effects. This phenomenon has been recently studied in detail in [77] by the author of this thesis and collaborators.

As usual, we decompose the neutral component of the η_a multiplets, η_a^0, as:

$$\eta_a^0 = \frac{1}{\sqrt{2}} \left(\eta_{R_a} + i\, \eta_{I_a}\right) . \tag{2.15}$$

We will make the assumption that all the parameters in the scalar potential are real, which implies the conservation of CP symmetry in the scalar sector. This precludes the mixing of the real and imaginary components of η_a^0. After EWSB, the mass matrices for the real and imaginary components are given by:

$$(\mathcal{M}_R^2)_{ab} = (m_\eta)_{aa}^2\, \delta_{ab} + \left(\lambda_3^{ab} + \lambda_4^{ab} + \lambda_5^{ab}\right) \frac{v^2}{2} \tag{2.16}$$

and

$$(\mathcal{M}_I^2)_{ab} = (m_\eta)_{aa}^2\, \delta_{ab} + \left(\lambda_3^{ab} + \lambda_4^{ab} - \lambda_5^{ab}\right) \frac{v^2}{2} . \tag{2.17}$$

One easily notes that in the limit $\lambda_5 \to 0$ the mass matrices coincide, $\mathcal{M}_R^2 = \mathcal{M}_I^2$. This will be of fundamental importance in the calculation of neutrino masses, in the next section. Both mass matrices can be rotated into a diagonal form with a change of basis. The gauge eigenstates, η_{A_a}, are as usual related to the mass eigenstates by:

$$\eta_A = V_A\, \hat{\eta}_A \,, \tag{2.18}$$

where $A = R, I$. In general, the $n_\eta \times n_\eta$ matrices V_A are unitary. However, when CP symmetry is conserved in the scalar sector, $\mathcal{M}_R^2$ and $\mathcal{M}_I^2$ are real symmetric matrices and, therefore, V_A are orthogonal matrices. Taking this into account, the diagonal mass matrices for the scalar fields are given by:

$$\widehat{\mathcal{M}}_A^2 = \begin{pmatrix} m_{A_1}^2 & & 0 \\ & \ddots & \\ 0 & & m_{A_{n_\eta}}^2 \end{pmatrix} = V_A^T \mathcal{M}_A^2 V_A \,. \tag{2.19}$$

Explicit expressions for the mass eigenvalues $m_{A_a}^2$ and mixing matrices V_A will be rather complicated, since they involve combinations of the scalar

potencial parameters. However, with the assumptions[4]:

$$\lambda_{3,4}^{aa}\,\frac{v^2}{2} \ll \left(m_\eta^2\right)_{aa} \quad \text{and} \quad \lambda_5^{ab} \ll \lambda_{3,4}^{ab} \ll 1\,, \tag{2.20}$$

one can find simple expressions. For example, the mass eigenvalues for the real and imaginary parts of the neutral components are given by:

$$m_{R_a}^2 = \left(m_\eta^2\right)_{aa} + \left(\lambda_3^{aa} + \lambda_4^{aa} + \lambda_5^{aa}\right)\,\frac{v^2}{2}\,, \tag{2.21}$$

$$m_{I_a}^2 = \left(m_\eta^2\right)_{aa} + \left(\lambda_3^{aa} + \lambda_4^{aa} - \lambda_5^{aa}\right)\,\frac{v^2}{2}\,. \tag{2.22}$$

As expected, the mass splitting $m_{R_a}^2 - m_{I_a}^2 = \lambda_5^{aa}\,v^2$ vanishes in the limit $\lambda_5 \to 0$. Regarding the orthogonal matrices V_A, we can write them as a product of $n_\eta(n_\eta - 1)/2$ rotation matrices, where the mixing angles are given by:

$$\tan 2\,\theta_A^{ab} = \frac{2\,(\mathcal{M}_A^2)_{ab}}{(\mathcal{M}_A^2)_{bb} - (\mathcal{M}_A^2)_{aa}} = \left(\lambda_3^{ab} + \lambda_4^{ab} + \kappa_A^2\,\lambda_5^{ab}\right)\,\frac{v^2}{m_{A_b}^2 - m_{A_a}^2}\,, \tag{2.23}$$

To achieve a compact expression we have introduced the sign κ_A^2 ($\kappa_R^2 = +1$ and $\kappa_I^2 = -1$).

2.3.0.1 Scotogenic neutrino masses

In this section we study in detail neutrino mass generation at the 1-loop level *à la* scotogenic [49]. Due to the simultaneous presence of the terms given in Eqs. (2.12) and (2.13), lepton number is explicitly broken in two units, and neutrinos have Majorana masses. Since the scalars η_a do not develop a VEV, see Eq. (2.14), neutrino masses are forbidden at tree-level. However, they are induced at the quantum level, as shown in Fig. 2.1. There are different diagrams contributing to to the neutrino mass matrix:

$$(m_\nu)_{\alpha\beta} = \sum_{A,a,n} \left(m_\nu^A\right)_{\alpha\beta}^{an}\,. \tag{2.24}$$

[4]Note that this assumption is technically natural [84]: the smallness of λ_5 is not dynamically explained but is stable against RGE flow. This is due to the fact that the limit $\lambda_5 \to 0$ increases the symmetry of the model by restoring lepton number conservation. Therefore, if λ_5 is set small at one scale it will remain small at all scales.

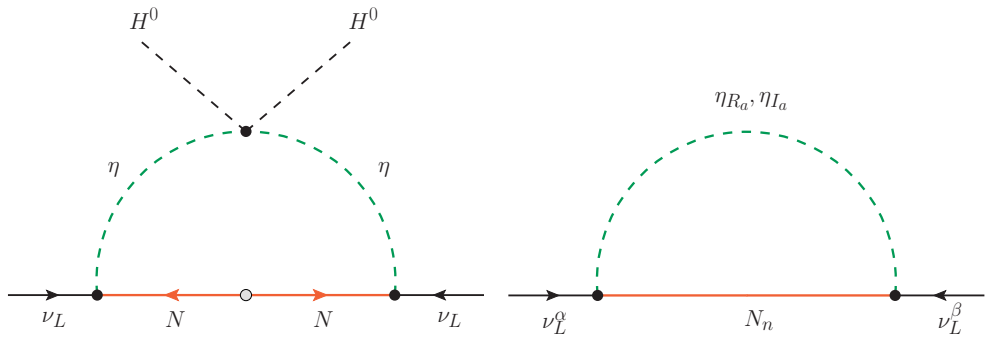

Figure 2.1: Neutrino mass generation diagrams with the gauge eigenstates (left) and the physical mass eigenstates (right) that propagate in the loop.

In the equation above, $\left(m_\nu^A\right)_{\alpha\beta}^{an}$ is the contribution to $(m_\nu)_{\alpha\beta}$ generated by the $N_n - \eta_{A_a}$ loop. This loop is given by the integral:

$$-i\left(m_\nu^A\right)_{\alpha\beta}^{an} = C_{na\alpha}^A \int \frac{\mathrm{d}^D k}{(2\pi)^D} \frac{i}{k^2 - m_{A_a}^2} \frac{i\left(\not{k} + M_{N_n}\right)}{k^2 - M_{N_n}^2} C_{na\beta}^A \,, \tag{2.25}$$

where $D = 4 - \varepsilon$ is the number of space-time dimensions, the external neutrinos are taken at rest and k is the momentum running in the loop. Note that, being odd in the loop momentum, terms proportional to $\not{k}$ do not contribute to the integral. The constant $C_{na\alpha}^A$ corresponds to the $N_n - \eta_{A_a} - \nu_L^\alpha$ coupling, given by:

$$C_{na\alpha}^A = i\,\frac{\kappa_A}{\sqrt{2}} \sum_b \left(V_A\right)_{ba}^* \, y_{nb\alpha} \,, \tag{2.26}$$

with $\kappa_R = 1$ and $\kappa_I = i$. Due to CP conservation, the parameters in the scalar sector are real and complex conjugation in V_A can be dropped. We now substitute Eq. (2.26) into Eq. (2.25) and make use of the Passarino-Veltman loop function B_0 [85]:

$$B_0\left(0, m_{A_a}^2, M_{N_n}^2\right) = \Delta_\varepsilon + 1 - \frac{m_{A_a}^2 \log m_{A_a}^2 - M_{N_n}^2 \log M_{N_n}^2}{m_{A_a}^2 - M_{N_n}^2}, \tag{2.27}$$

where Δ_ε diverges in the limit $\varepsilon \to 0$. Finally, the light neutrino mass matrix becomes:

$$(m_\nu)_{\alpha\beta} = -\frac{1}{32\pi^2} \sum_{A,a,b,c,n} M_{N_n}\, \kappa_A^2\, (V_A)_{ba}\ (V_A)_{ca}\ y_{nb\alpha}\, y_{nc\beta}\, B_0(0, m^2_{A_a}, M_{N_n})\,. \tag{2.28}$$

We remark here that the divergent parts cancel exactly due to the orthogonality of the matrices V_A. The equation above, Eq. (2.28), provides a simple analytical expression for the neutrino mass matrix. However, the dependence on the fundamental parameters of the model is not explicit. Working under the assumptions in Eq. (2.20) we now derive approximate forms of the neutrino mass matrix valid in the limit of small λ_5^{ab} and small mixing angles in the scalar sector. Using $\lambda_5^{ab} \ll 1$ as the expansion parameter, one can write:

$$\begin{aligned}(m_\nu)_{\alpha\beta} = -\frac{1}{32\pi^2} \sum_n M_{N_n} \sum_{a,b,c} y_{nb\alpha}\ y_{nc\beta} \\ \Big\{ [(V)_{ba}\ (V)_{ca}]^{(0)}\ \left[B_0^{(1)}(0, m^2_{R_a}, M_{N_n}) - B_0^{(1)}(0, m^2_{I_a}, M_{N_n})\right] \\ + [(V_R)_{ba}\ (V_R)_{ca} - (V_I)_{ba}\ (V_I)_{ca}]^{(1)}\ B_0^{(0)}(0, m^2_a, M_{N_n})\Big\} + \mathcal{O}\left(\lambda_5^2\right)\,.\end{aligned} \tag{2.29}$$

The superindex $^{(i)}$, with $i = 0, 1$, denotes the order in the perturbation parameter λ_5^{ab}. Note that the limit $\lambda_5 = 0$ would imply the restoration of lepton number and massless neutrinos, explaining why the expansion begins at the first order in λ_5. With this in mind, the origin of the two terms in Eq. (2.29) is easy to understand.

One can easily see that in the first term, the λ_5^{ab} couplings are kept at leading order in the difference of B_0 functions. The mass matrices for the real and imaginary components of η^0 are equal at 0th order in λ_5, $\widehat{\mathcal{M}}_R^{2\,(0)} = \widehat{\mathcal{M}}_I^{2\,(0)}$, and then we can define $V \equiv V_R^{(0)} = V_I^{(0)}$. On the other hand, in the second term, λ_5^{ab} are neglected in the B_0 loop functions and kept at first order in the mixing matrices, V_A. At 0th order in λ_5 we have $m_{R_a}^{(0)} = m_{I_a}^{(0)} \equiv m_a$ and, then, the argument of the loop function reads:

$$m_a^2 = \left(m_\eta^2\right)_{aa} + (\lambda_3^{aa} + \lambda_4^{aa})\ \frac{v^2}{2}\,. \tag{2.30}$$

We require that the λ_5 matrix contains non-vanishing off-diagonal entries, since $[(V_R)_{ba}\ (V_R)_{ca} - (V_I)_{ba}\ (V_I)_{ca}]$ would vanish otherwise.

We now proceed to find approximate expressions for the V_A mixing matrices. Approximate expressions for V_A require small scalar mixing angles, in agreement with the assumptions in Eq. (2.20). In this case one can expand the matrix V in powers of the small parameter:

$$s_{ab} = \frac{1}{2}\left(\lambda_3^{ab} + \lambda_4^{ab}\right)\frac{v^2}{m_b^2 - m_a^2} \ll 1\,. \tag{2.31}$$

This parameter is defined for $a \neq b$ and corresponds to $\sin\theta_{R,I}^{ab}$ at 0th order in λ_5, see Eq. (2.23). One finds the expression for the mixing matrix as a funcion of the small parameter: $(V)_{ab} = \delta_{ab} + (1-\delta_{ab})\, s_{ab} + \mathcal{O}\left(s^2\right)$. Perturbative expansions for V_R and V_I can be obtained by replacing s with $\sin\theta_R$ and $\sin\theta_I$, respectively. Finally, the neutrino mass matrix Eq. (2.29) can be given in closed form as:

$$(m_\nu)_{\alpha\beta} = \frac{v^2}{32\pi^2}\sum_{n,a,b}\frac{y_{na\alpha}\, y_{nb\beta}}{M_{N_n}}\,\Gamma_{abn} + \mathcal{O}\left(\lambda_5^2\right) + \mathcal{O}\left(\lambda_5\, s^2\right) \tag{2.32}$$

In the equation above we have defined the dimensionless quantity:

$$\Gamma_{abn} = \delta_{ab}\,\lambda_5^{aa}\, f_{an} - (1-\delta_{ab})\left[\left(\lambda_5^{aa}\, f_{an} - \lambda_5^{bb}\, f_{bn}\right)\, s_{ab} - \frac{M_{N_n}^2}{m_b^2 - m_a^2}\,\lambda_5^{ab}\; g_{abn}\right] \tag{2.33}$$

and the loop functions:

$$f_{an} = \frac{M_{N_n}^2}{m_a^2 - M_{N_n}^2} + \frac{M_{N_n}^4}{\left(m_a^2 - M_{N_n}^2\right)^2}\log\frac{M_{N_n}^2}{m_a^2}\,, \tag{2.34}$$

$$g_{abn} = \frac{m_a^2}{m_a^2 - M_{N_n}^2}\log\frac{M_{N_n}^2}{m_a^2} - \frac{m_b^2}{m_b^2 - M_{N_n}^2}\log\frac{M_{N_n}^2}{m_b^2}\,. \tag{2.35}$$

The first term in Eq.(2.33) contributes only for $a = b$, involving only diagonal elements of λ_5. On the other hand, the second term, involves diagonal as well as off-diagonal elements of λ_5, only contributes for $a \neq b$. Note also that $g_{abn} = -g_{ban}$.

The expression in Eq.(2.32) is valid for any value n_N and n_η. We now show how for the particular case $\boldsymbol{(n_N, n_\eta) = (3,1)}$, the formula above reduces to a well-known expression in the literature.

Original Ma's model: $(n_N, n_\eta) = (3, 1)$

The scotogenic model was originally introduced in [49] for $(n_N, n_\eta) = (3, 1)$. In this case, there is a single inert doublet η and three singlet fermions. One easily realizes that all the matrices in the scalar sector are now scalar parameters: $V_A = 1$, $\lambda_5^{ab} \equiv \lambda_5^{11} \equiv \lambda_5$ and $(m_\eta^2)_{aa} \equiv (m_\eta^2)_{11} \equiv m_\eta^2$. Additionally, the Yukawa couplings become 3×3 matrices: $y_{na\alpha} \equiv y_{n1\alpha} \equiv y_{n\alpha}$. Regarding the loop functions we have $f_{an} \equiv f_{1n} \equiv f_n$, and the second term in Eq. (2.33) is of course not present.

In this simple scenario, the quantity Γ_{abn} reduces to $\Gamma_n^{(3,1)}$, simply given by:

$$\Gamma_{abn}^{(3,1)} \equiv \Gamma_{11n}^{(3,1)} \equiv \Gamma_n^{(3,1)} = \lambda_5 \, f_n \, . \tag{2.36}$$

Replacing this last expression into Eq. (2.32), we obtain the well-known scotogenic neutrino mass matrix:

$$(m_\nu)_{\alpha\beta}^{(3,1)} = \frac{\lambda_5 \, v^2}{32\pi^2} \sum_n \frac{y_{n\alpha} \, y_{n\beta}}{M_{N_n}} \left[\frac{M_{N_n}^2}{m_0^2 - M_{N_n}^2} + \frac{M_{N_n}^4}{\left(m_0^2 - M_{N_n}^2\right)^2} \log \frac{M_{N_n}^2}{m_0^2} \right] , \tag{2.37}$$

with $m_0^2 = m_\eta^2 + (\lambda_3 + \lambda_4) \, v^2/2$.

Later, in Chapter 7, we will consider a colored version of the scotogenic model where both, the scalars and the new fermions responsible of neutrino mass generation, transform non-trivially under the $SU(3)_C$ group.

Chapter 3

The strong CP problem and axions

An important issue related to the QCD interaction within the SM is the strong CP problem. Indeed, one can add to the QCD Lagrangian (1.7) the following term:

$$\mathcal{L}_\theta = \theta \frac{\alpha_s}{8\pi} G^a_{\mu\nu} \tilde{G}^{\mu\nu}_a \,, \;\; \tilde{G}^{\mu\nu}_a = \frac{1}{2} \epsilon^{\mu\nu\rho\sigma} G_{a\rho\sigma} \,. \tag{3.1}$$

This term, known as the θ-term, does violate CP symmetry. Since QCD is vector-like, acting equally on right and left-handed quarks, the phase θ cannot be rotated away and becomes physical once the quark fields have been rotated to a basis in which their masses are real, that is:

$$\bar{\theta} = \theta + \mathrm{Arg}[\det Y_u Y_d] \,. \tag{3.2}$$

Experimentally, from the non-observation of neutron EDM, we know that $\bar{\theta} \leq 10^{-10}$ [86,87]. The smallness of $\bar{\theta}$ is the origin of the *strong CP problem*. The solution to this problem - that is, explaining such an unnatural value for $\bar{\theta}$ - requires a dynamical mechanism[1]. Currently, the most attractive solution to the strong CP problem is the Peccei-Quinn mechanism [90]. The presence of a light pseudo-scalar particle, the *axion*, is the smoking gun of this solution [91, 92].

In this chapter we overview the Peccei-Quinn solution to the strong CP problem and how the axion appears in such a theory. After studying the

[1] It has been argued in [88,89] that anthropic reasoning does not explain the smallness of $\bar{\theta}$.

basic properties of the axion in a model-independent way, we introduce the most basic models of invisible axions, i.e. the DFSZ and KSVZ axion models, and summarize the associated experimental constraints.

3.1 The PQ mechanism

From an EFT perspective, the PQ mechanism (see [93, 94] for recent reviews) consists of adding a new pseudo-scalar particle, the axion [91, 92], coupled to the QCD sector as:

$$\mathcal{L} \supset \left(\frac{a}{f_a} + \bar{\theta}\right) \frac{g_s^2}{32\pi^2} G\tilde{G}\,. \tag{3.3}$$

We denote by $\bar{\theta}$ the theta-term in the basis in which all quarks have real masses. This new degree of freedom is usually visualized, from a UV point of view, as the Nambu-Goldstone boson associated to the PQ symmetry [90], which is anomalous under the QCD interaction. The crucial point is that QCD instanton effects induce a non-trivial potential which can be estimated by using chiral perturbation theory techniques [95]:

$$V(a) = -m_\pi^2 f_\pi^2 \sqrt{1 - \frac{4 m_u m_d}{(m_u + m_d)^2} \sin\left(\frac{a}{2f_a} + \frac{\bar{\theta}}{2}\right)}\,. \tag{3.4}$$

Being a dynamical field, the axion will relax down to its minimum at

$$\langle a \rangle = -f_a \bar{\theta}\,. \tag{3.5}$$

This minimum is CP-conserving by virtue of the Vafa-Witten theorem [96] and therefore leads to a vanishing neutron EDM:

$$d_n \propto \frac{a}{f_a} + \bar{\theta} = 0\,. \tag{3.6}$$

In this way, the PQ mechanism solves the strong CP problem and leads to the appearance of the axion [91, 92]. In addition to solving the strong CP problem, the QCD axion is an excellent DM candidate. This possibility will be considered in detail in Sec.4.1.0.2.

Two of the most important axion properties, that is the axion mass and its coupling to photons, automatically emerge from the coupling to gluons (3.3). Below the confinement scale, and due to the non-perturbative

potential above (see Eq.(3.4)), the axion acquires a mass [95]

$$m_a = 5.7\mu\text{eV}\left(\frac{10^{12}\text{ GeV}}{f_a}\right). \tag{3.7}$$

On the other hand the coupling to photons is given by:

$$\mathcal{L}_{a\gamma} = g_{a\gamma} a F_{\mu\nu}\tilde{F}^{\mu\nu}, \tag{3.8}$$

with the coupling constant given by:

$$g_{a\gamma} = (E/N - 1.92)\frac{\alpha_{em}}{8\pi}\frac{1}{f_a}. \tag{3.9}$$

The term E/N stands for the ratio of the QED and QCD anomaly coefficients and is model dependent. The second term comes exclusively from the axion-pion mixing and is a model-independent prediction of any axion that solves the strong CP problem through the coupling in Eq.(3.3).

Another important property of the axion, the coupling to SM fermions, is substantially model dependent and will be considered in the following section.

3.2 Minimal QCD axion models and experimental constraints

The original PQWW [90–92] axion model was rapidly ruled out [97]. The model included, in addition to the SM fermions, a duplicated Higgs sector: $H_u \sim (1, 2, -1/2)$, $H_d \sim (1, 2, 1/2)$, coupled respectively to up-type and down-type fermions. The relevant Lagrangian

$$\mathcal{L}_{PQWW} = Y^u_{ij}\bar{q}^i_L H_u u^j_R + Y^{ij}_d \bar{q}^i_L H_d d^j_R + Y^{ij}_e \bar{l}^i_L H_d e^j_R, \tag{3.10}$$

has an anomalous $U(1)$ symmetry, under which the scalars and fermions are charged, if the term $\sim \mu^2 H_u H_d$ is forbidden at the scalar potential. This anomalous symmetry plays the role of the PQ symmetry to solve the strong CP problem. Unfortunately, in this simple model, the PQ symmetry breaking scale coincides with the EW scale

$$f_a = \sqrt{v_u^2 + v_d^2} = 246\text{ GeV}, \tag{3.11}$$

leading to moderately unsuppressed axion interactions and was excluded soon [97].

As we will see now, with a minimal extension, the axion can be made *invisible* and compatible with experiments. There are two main frameworks depending on whether the SM quarks are charged under PQ symmetry, or not. These are the DFSZ and KSVZ models.

DFSZ axion model

In this scenario, a SM singlet scalar with PQ charge is added to the PQWW model [98, 99]

$$S = \frac{(v_s + \rho_s)}{\sqrt{2}} e^{i\theta_s} \,. \tag{3.12}$$

There exist two types of DFSZ axion models depending on how we *communicate* the anomalous PQ symmetry to S. This is done through a coupling to the Higgs doublets, at the scalar potential, proportional to the field operator:

$$O_{DFSZ} \sim H_u H_d S^\alpha \,, \text{ with } \alpha = 1, 2 \,. \tag{3.13}$$

Once this coupling is taken into account, the PQ breaking scale is mainly determined (up to small EW-scale corrections) by the scalar singlet VEV, $\langle S \rangle$. Since $\langle S \rangle$ is a free parameter, the axion can be made very light (see (3.7)) and weakly coupled to the SM if $\langle S \rangle \sim f_a \gg 246$ GeV.

Both DFSZ axion models, $\alpha = 1, 2$, have the same axion couplings to matter but differ in the number of degenerate vacua, given by $N_{DW} = 3\alpha$. This number is known as domain wall (DW) number and, as will be studied in detail later, is cosmologically relevant since situations with $N_{DW} \neq 1$ lead to the formation of stable DW when the PQ symmetry is broken after inflation [100] (for a comprehensive review on domain walls and other topological defects see [101]). Several mechanisms exist to solve the DW problem [100, 102, 103] including the ones studied by the author of this thesis [104, 105].

In these minimal DFSZ models, the anomaly coefficient ratio is predicted to be $E/N = 8/3$ and the axion couples to SM fermions at tree-level [106]. As we will see in the next section, interesting constraints arise from the coupling to electrons at tree-level.

KSVZ axion model

In the KSVZ model [107, 108], a new colored fermion Q is added to the SM. In this case, the SM quarks carry no PQ charge but the new fermion transforms chirally under it:

$$Q_L \to e^{i\beta/2} Q_L \,, \; Q_R \to e^{-i\beta/2} Q_R \,. \tag{3.14}$$

The colored fermion Q implements the PQ mechanism and receives a mass from a SM scalar singlet which transforms as $S \to e^{i\beta} S$.

Therefore, omitting the kinetic terms, the relevant Lagrangian in the KSVZ model is just

$$\mathcal{L}_{KSVZ} = (y S \bar{Q}_L Q_R + \text{h.c.}) - \lambda \left(|S|^2 - v_S^2 \right)^2 \,. \tag{3.15}$$

In this case, writing $S = (v_S + \rho_s) e^{i\theta_s}$, the QCD axion coincides exactly with the phase θ_s.

The anomaly coefficient ratio depends on the hypercharge of Q, $E/N = 2Y_Q^2$. The hypercharge also determines the possible mixing with SM quarks. In the most minimal model, $Y_Q = 0$, there is no mixing and the axion couples to the SM fermions via loop-induced couplings [106]. On the other hand, the axion-photon coupling has only the model-independent contribution which comes from the mixing with pions (see (3.9)).

Summary of experimental constraints

Here we briefly summarize different searches for axions. For a detailed review with a full set of references on axion searches, see [109]. There exist different ways to classify these searches. For example, one can separate them as DM-independent and DM-dependent searches depending on whether axions constitute, or not, the dominant part of the cosmological DM (see Chapter 4).

Conversely, one can classify axion searches depending on their couplings to the SM sector. For example, if the coupling to fermions is non-diagonal in flavor space, very stringent bounds to the strength of this interaction comes from rare meson decays [110] (see also section 6.5 of [94] for a recent review). Another example is the axion coupling to photons (see Eq.(3.9)) which is a promising avenue to test axion models in both DM-dependent and independent searches. The current constraints to this coupling are summarized in Fig.(3.1). For example, helioscopes look for axions that are

produced in the Sun. The fundamental principle used in these helioscope experiments is axion-photon conversion due to an external, large magnetic field. These experiments are sensitive to masses below 1 eV and constrain the axion-photon coupling $g_{a\gamma} \lesssim 10^{-10}$ GeV^{-1}. The strongest bounds come from CAST [111]. In a near future, IAXO [112] will continue with the search of solar axions, substantially improving the current bounds.

On the other hand, haloscopes are experiments that look for axions which compose the DM halo. These experiments search for axion DM converting into photons under the influence of a strong magnetic field. If we are looking for conversions inside a cavity, the size of the experiment has to be about the Compton wavelength of the axion, $L \sim m_a^{-1}$. Haloscopes look for the energy deposited by the axion field into the cavity. One of the leading experiments of this kind is ADMX [113].

Let us also mention that there exist laboratory searches such as the *light shining through the wall* experiments that are sensitive to the axion-photon coupling for axion masses below 10^{-3} eV [114–116]. As stated above, a large magnetic field generates a non-zero axion-photon mixing. Let's assume that in a region where we have a strong magnetic field we have a wall. At one side, we put a laser that hits the wall and, at the other side, we put a photon detector. When the laser hits the wall, because of the magnetic field, there is a non-zero probability that a photon oscillates into an axion and goes through the wall. Again, this axion can oscillate back into a photon and be detected at the other side of the wall. Despite this process is suppressed by $g_{a\gamma}^2$, it offers interesting and competitive constraints that do not depend on the DM abundance nor the production of axions in the Sun. The model independence renders this kind of searches very attractive and has excellent future prospects [117, 118].

Regarding the couplings to fermions, the most relevant for axions with flavor-conserving couplings are the couplings to electrons and nucleons. The current constraints to the former are summarized in Fig.(3.2). The most stringent bound to the latter, that is the axion-nucleon coupling, comes from the supernova SN1987 and reads: $f_a \geq 4 \times 10^8$ GeV [119].

Finally, black hole (BH) superradiance offers an interesting opportunity to test axions without any assumption on their couplings to matter or DM abundance [120, 121]. The idea is that the superradiant instability of Kerr BH efficiently extracts angular momentum from the BH, populating an axion cloud around it. Measuring the properties of fast-spinning BH allows to constrain axions with a Compton wavelength of the order of the size of the BH, $R_{BH} \sim m_a^{-1}$. These constraints from BH superradiance become

weaker for axion decay constants below $f_a \sim 10^{14-16}$ GeV, depending on the axion mass, where the self-interaction effect becomes relevant and can suppress the BH superradiance spin-down. See [122–124] for recent studies.

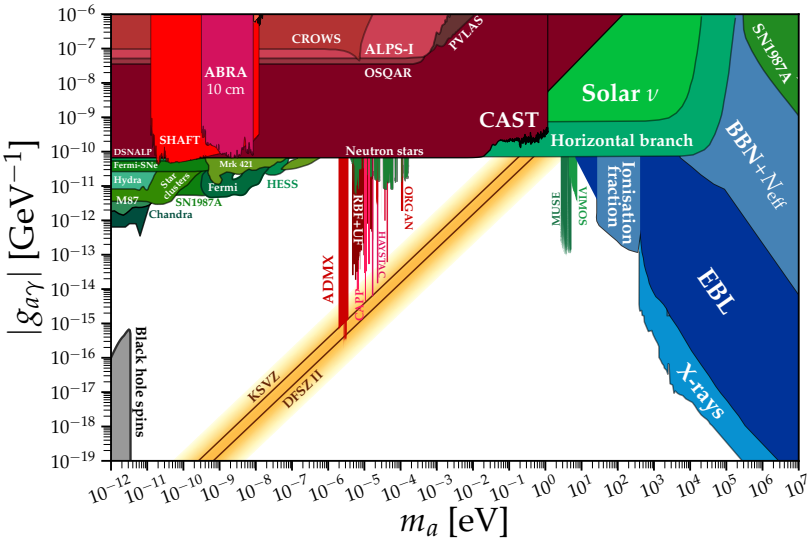

Figure 3.1: Review of experimental contraints in the $(m_a, g_{a\gamma})$ plane (from [125]). The KSVZ and DFSZ-II lines correspond to the model predictions. In red we have laboratory searches and haloscopes, the greenish regions correspond to different bounds from astrophysics while the blueish regions stand for cosmological constraints. The dark gray stand for the superradiant constraints.

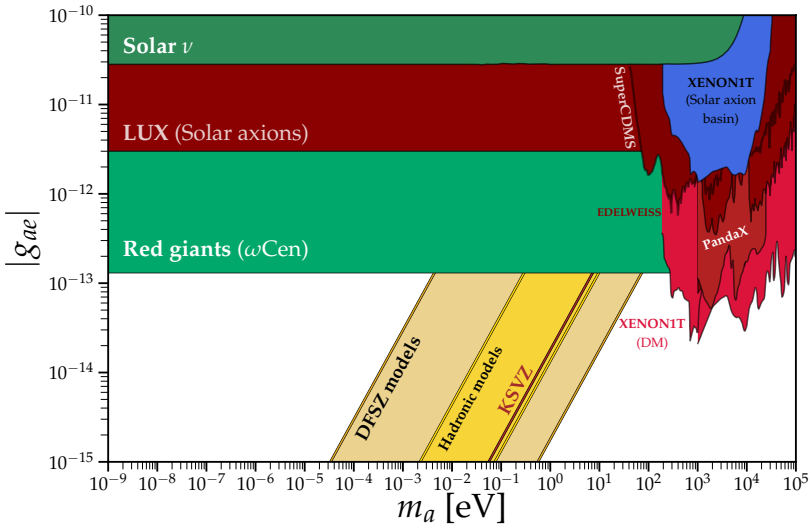

Figure 3.2: Review of experimental contraints in the (m_a, g_{ae}) plane (from [125]). In this case we have different constraints from searches at underground detectors and from astrophysics.

Chapter 4

Dark Matter

The nature of dark matter (DM) is one of the most urgent questions in fundamental physics. Thanks to a number of different observations, ranging from galaxy rotation curves and structure formation to the observation of the Bullet Cluster, we do know that there is more matter than what we see. This extra amount of non-relativistic matter, which constitutes around 5 more times than baryonic matter and does not interact with light, is what we call dark matter and its nature remains a mystery. Different pieces of evidence for the existence of DM can be classified according to the scale (see [126] for a detailed historical review and a complete list of references):

- **Galaxy rotation curves**: several results during the first part of the 20th century, culminated with the pioneer work by Vera Rubin and others in the '70s, showed that for a distance larger than the main disk of spiral galaxies, the rotational velocity (rotation curves) of stars has an approximately flat profile. This result suggests the existence of non-luminous matter outside of the main disk of these galaxy.

- **Galaxy clusters**: In the '30s, Zwicky estimated the Coma cluster mass by applying the virial theorem to the cluster. From that result, he was able to estimate the average kinetic energy and velocity dispersion. This estimation turned out to be much smaller than the observed velocities by Hubble and Humason (see [126] for a detailed historical review). From this comparison, he concluded that there should be much more matter than what we *see* in galaxy clusters. Despite the fact that his results clearly overestimated the abundance of non-luminous matter, this was one of the first times that the concept of dark matter was proposed in the literature to explain the mystery

of the *missing mass*. In the next decades, there were several other proposals to explain this phenomenon that were eventually ruled out by measurements of the primordial light element abundances. Finally, gravitational lensing has also confirmed that massive clusters are indeed DM dominated. Last but not least, there is one important observation of the collision of two clusters that offers interesting constraints to DM self-interaction and constitutes a solid argument against proposals of modified gravity theories. This is the so-called Bullet Cluster, a pair of merging clusters that collided long ago. Despite the fact that individual stars do not collide, we can observe the distribution of hot gas and compare with the bulk mass distribution. This points to a barycentre of the hot gas displaced with respect to the centre of mass of the distribution. In other words, the dominant source of mass in this system does not follow the distribution of baryonic matter. This result is extremely hard to explain if one gives up the (very) weakly interacting DM hypothesis.

- **CMB anisotropies and the power spectrum**: One of the strongest hints in favour of the existence of DM is the CMB and its properties. Measurements of CMB anisotropies provide us information of our Universe at the recombination epoch. The power spectrum of these anisotropies has confirmed the standard ΛCDM model and favors the existence of DM over MOND (MOdified Newtonian Dynamics) theories. From the properties of the power spectrum, according to the last release of data by the Planck collaboration [38], we get a DM relic density: $\Omega_{DM}h^2 = 0.120 \pm 001$.

In order to accommodate this evidence, there are two main avenues. The first possibility consists of the modification of General Relativity at galactic scales, the so-called MOND theories. However these theories are in conflict with several observations such as the Bullet Cluster and the spectrum of the CMB anisotropies. In this thesis we will not consider this type of theories further. The other possibility is to add extra matter to the energy density budget of the Universe. This matter is presumably non-luminous, although it can interact with light if the interaction strength is sufficiently feeble. Depending on its nature, there exists a plethora of different candidates ranging from massive compact objects (MACHOs) or primordial black holes (PBH) to weakly interacting massive particles (WIMPS) and axions. This means that different DM candidates span over more than 80 orders of magnitude,

from PBH of $O(10)$ solar masses down to bosonic DM with mass $m \sim 10^{-22}$ eV.

4.1 Dark Matter candidates

In this section we will briefly overview the different DM candidates that we consider later in this thesis. Among the many possibilities, we will focus on WIMPs and light bosonic DM[1]. The most important properties of any DM candidate, independently of its mass, are the following:

- Production mechanism.
- Stability or longevity mechanism.
- Detectability: direct and indirect detection.

Any property of a given DM candidate follows automatically from the ones above. The first one tells us, for example, if a given candidate is produced thermally, that is from the interaction with the SM thermal bath in the early Universe, or non-thermally. Dark matter has to be stable on cosmological time scales, but not necessarily absolutely stable. Many candidates have a symmetry that prevents their decay, while others are just very long-lived because of their feeble interactions with the SM or due to kinematical reasons. Finally, whenever a new candidate is proposed, it is important to estimate detectability prospects. To this end, one has to specify the interactions with the visible sector. In many cases, this interaction will be much weaker than the EW interactions and in some scenarios DM only interacts gravitationally with the SM. Obviously, depending on these interactions, some experiments will be more sensitive than others for each DM candidate.

Basic thermodynamics in the early Universe

In this section we review basic concepts of thermodynamics in the early Universe that will be useful to compute observables such as the relic abundance of any DM candidate. We will work with an expanding Universe that obeys the Friedmann–Robertson–Walker (FRW) metric:

$$ds^2 = dt^2 - a(t)^2 dx^2 \,. \tag{4.1}$$

[1]With this generic name we include axions, majorons and other axion-like particles.

In the equation above $a(t)$ is the scale factor, defined as $a(t_0) = 1$. From now on, we denote present quantities with the subindex "0". The Hubble rate is defined as:

$$H = a^{-1}\frac{da}{dt} \equiv \frac{\dot{a}}{a}\,. \tag{4.2}$$

The expansion rate of the Universe is determined by the energy density:

$$H^2 = \left(\frac{\dot{a}}{a}\right)^2 = \frac{8\pi}{3M_P^2}\rho\,, \tag{4.3}$$

where ρ includes all types of energy density: matter, radiation and dark energy. In an expanding Universe, the energy density is not conserved and its time dependence is given by:

$$\dot{\rho} + 3H(p+\rho) = 0\,. \tag{4.4}$$

One immediately notices that the Hubble parameter acts as a friction term. For example, in matter domination epoch we have $p = 0$, while during radiation domination: $\rho = 3p$. The interesting case of constant vacuum energy, or cosmological constant, leads to $p = -\rho$. This *negative pressure* term has an interesting effect in the cosmic expansion: the expansion rate *accelerates* with time.

To see why this case leads to an accelerated expansion of the Universe one combines 4.3 and 4.4 to get:

$$\frac{\ddot{a}}{a} = -\frac{4\pi}{3M_P^2}(\rho + 3p)\,. \tag{4.5}$$

From this equation one has that for matter and radiation dominated universes the cosmic expansion decelerates, while for the vacuum energy or cosmological constant case the Universe experiments an accelerated expansion. We believe that there have been at least two epochs during which the Universe has expanded in an accelerated way. The first one is the era of cosmic inflation [34, 127, 128] which is believed to be the responsible for the peculiar initial conditions of our flat, homogeneous and isotropic Universe. The second is happening at this very moment. From Planck data [38], we know with great accuracy that our Universe is currently dominated by dark energy with an equation of state very close to that of a cosmological constant, $w_\Lambda = p/\rho = -1$. Both, inflation and dark energy, are currently very active and interesting topics of research. In table (4.1) we summarize the evolution of the basic forms of energy density.

Let us now turn to the radiation dominated epoch. In this case, the number density of relativistic fermionic particles in thermal equilibrium is given by[2]:

$$n = \frac{3}{4}\frac{\zeta(3)}{\pi^2} g T^3 \,, \tag{4.6}$$

with g the number of degrees of freedom of a given particle. On the other hand, the total energy density is given by:

$$\rho = \frac{\pi^2}{30} g_*(T) T^4 \,, \tag{4.7}$$

where $g_*(T)$ is the total number of relativistic degrees of freedom which is, as we will see, temperature dependent (see Fig.4.1). These quantities are obtained by integrating over momentum the phase space distributions for particles in thermodynamic equilibrium (for example, see [129] for details). The formula above applies at temperatures exceeding the masses of the particles in the thermal bath. For the SM, when all particles are relativistic, we have $g_*(T > m_t) = 106.75$.

From Eq.(4.7), we can write the Hubble parameter as a function of temperature:

$$H(T) = 1.66\sqrt{g_*(T)}\,\frac{T^2}{M_P} \,. \tag{4.8}$$

Let us also mention another important quantity, the entropy density:

$$s = \frac{p+\rho}{T} = \frac{2\pi^2}{45} T^3 \left[\left(\frac{7}{8}\right)\sum_i g_i \frac{T_i^3}{T^3}\right] = \frac{2\pi^2}{45} g_{*,S}(T) T^3 \,. \tag{4.9}$$

This allows us to define the comoving entropy density, $sa(T)^3$, which is conserved for particles in thermal equilibrium. Provided the number of relativistic degrees of freedom $g_{*,S}(T)$ is conserved, the temperature redshifts as:

$$T \sim 1/a(T) \,. \tag{4.10}$$

However, the quantity $g_{*,S}(T)$ is not constant and decreases with temperature (see Fig. 4.1). This decreasing of the number of relativistic degrees of freedom is particularly important during the QCD phase transition due to the fact that the confinement scale, and therefore the typical mass of hadrons, is substantially larger than the light quark masses.

[2]For bosons the formula reads: $n = \frac{\zeta(3)}{\pi^2} g T^3$.

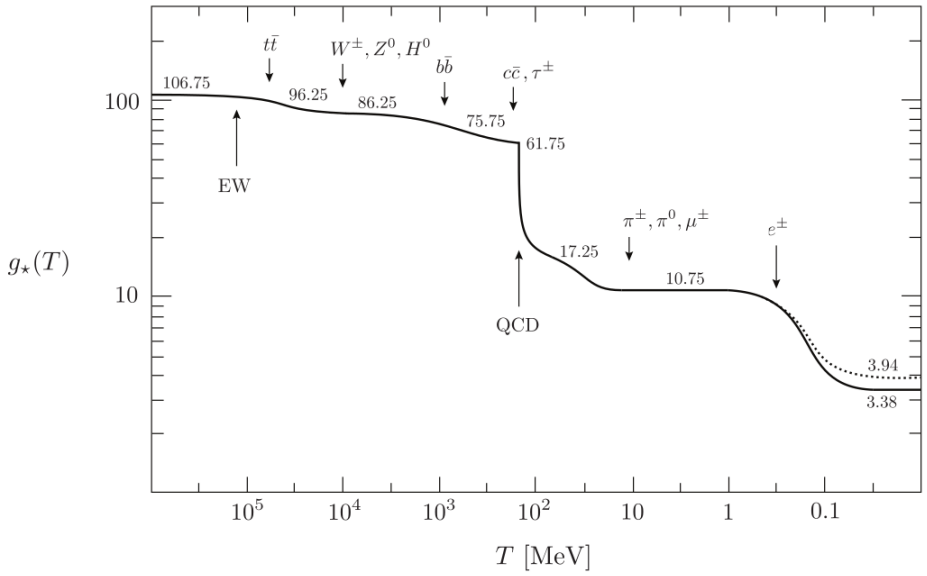

Figure 4.1: Evolution of the effective degrees of freedom $g_\star$ throughout the cosmic evolution assuming the SM particle content. The dotted line stands for the entropy relativistic degrees of freedom $g_{\star s}$. Extracted from [130].

Given a particle with mass m, since the temperature decreases with the cosmic expansion, at some point one reaches $T \sim m$. Below this temperature, in addition to the change in $g_*(T)$, the number density of particles will follow the non-relativistic equilibrium Boltzmann distribution:

$$n \propto e^{-m/T}\,, \tag{4.11}$$

and, therefore, the number density will decrease exponentially fast. The fact that cosmic expansion can bring some species out of equilibrium, avoiding the final Boltzmann suppression, is the key point to understand basic production mechanisms such as the freeze-out that we will consider in the following section.

Thermal DM candidates: the WIMP case

Weakly interacting massive particles (WIMPs) consitute one of the best motivated DM candidates. They easily appear in theories beyond the SM and a lot of experimental effort has been dedicated to them in the last years. In this section, after reviewing the freeze-out mechanism, we briefly study

	$\rho(a)$	$a(t)$	H	$1/Ha$
Matter	$1/a^3$	$t^{2/3}$	$2/3t$	$t^{1/3}$
Radiation	$1/a^4$	$t^{1/2}$	$1/2t$	$t^{2/3}$
Vacuum Energy	const.	e^{Ht}	const	e^{-Ht}

Table 4.1: Summary of cosmic evolution for different forms of energy density.

how such a weakly coupled particle at the weak scale can reproduce the observed DM abundance.

4.1.0.1 The freeze-out mechanism

Let us assume that we have two stable particles A and B in thermal equilibrium[3] in the early Universe at a temperature $T \gg m_{A,B}$. Let us also assume that B is heavier, $m_B > m_A$. The two species are relativistic and can annihilate into each other through the reaction:

$$AA \leftrightarrows BB\,, \tag{4.12}$$

mantaining chemical equilibrium. At some point, due to the cosmic expansion, the cosmic temperature, $T \sim 1/a(T)$, drops below the mass of B. Assuming that it remains in thermal equilibrium, its number density will be Boltzmann suppressed: $n_B \propto e^{-m_B/T}$. One can easily understand this suppression qualitatively since the process $BB \to AA$ is allowed, but $AA \to BB$ is thermodynamically very suppressed. If the equilibrium is mantained, this fact would bring the number density n_B to very small values, approaching zero density. However, one has to take into account the effect of cosmic expansion.

The key point of the freeze-out mechanism is that, in part due to Boltzmann suppression, the interactions between B particles become rare and at some point become less efficient than cosmic expansion. In other words, the interaction rate of the process $BB \to AA$, that we define as $\Gamma_{B\to A}$, becomes at some point smaller than the Hubble rate, H. This occurs at the

[3]Other scenarios such as the freeze-in mechanism [131] are qualitatively different. In this case, the DM particle never reaches thermal equilibrium and the initial relic abundance is negligible. Still, there is production of DM due to interactions with the thermal plasma, and the right relic abundance can be obtained. In this thesis we will not consider this case further.

freeze-out temperature, defined as:

$$\Gamma_{B\to A} \sim n_B \langle\sigma v\rangle = H(T_f)\,. \tag{4.13}$$

For temperatures $T < T_f$, B decouples from the thermal plasma and the quantity $n_B a^3$ remains constant or *frozen*. The conservation of this comoving number density,

$$n_{B,f} a_f^3 = n_{B,0} a_0^3\,, \tag{4.14}$$

allows us to estimate the relic density of B particles today as the energy density of B particles normalized to the critical energy density, ρ_c:

$$\Omega_B = \frac{m_B n_{B,0}}{\rho_c} = \frac{x_f T_0^3}{\rho_c M_P}\frac{1}{\langle\sigma v\rangle}\,. \tag{4.15}$$

In the equation above we have defined $x_f = m_B/T_f$ which, for moderately weak couplings, is approximately $x_f \sim 20$. Let us analyze the previous formula (4.15). While the first factor is approximately constant, the dependence on the cross section, $\langle\sigma v\rangle^{-1}$, completely fixes the relic abundance. In fact, as one can intuitively imagine, the larger is the cross section, the later the particle B will decouple from the plasma. This generates a larger Boltzmann suppression. A more detailed quantitative analysis of freeze-out dynamics requires solving numerically the so-called Boltzmann equations in an expanding Universe:

$$\frac{dn_B}{dt} = -3Hn_B - \langle\sigma v\rangle\left(n_B^2 - n_{B,eq}^2\right)\,. \tag{4.16}$$

Here, however, we will qualitatively study the situation to understand the parametric dependence on the DM mass and couplings.

4.1.0.2 The WIMP miracle and the Griest-Kamionkowski limit

From naive dimensional analysis one can estimate the cross section for the process $BB \to AA$ as:

$$\langle\sigma v\rangle \sim \pi\alpha_B^2/m_B^2\,. \tag{4.17}$$

From this cross section one can estimate the relic abundance as a function of the DM mass. First of all, one can get an upper bound to the mass of the DM candidate by assuming the coupling $\alpha_B \to 1$, that is at the limit of

perturbativity. Imposing $\Omega_B \leq \Omega_{DM}$ one gets the upper bound:

$$m_B \lesssim 50 - 100 \text{ TeV} . \tag{4.18}$$

This bound is known as the Griest-Kamionkowski limit or unitarity bound [132]. A stable particle that was in thermal equilibrium with the thermal bath would overclose the Universe if its mass is larger than the previous bound. More precise limits to the mass of B depend on the details of the model and the cosmological evolution.

It is also interesting to consider the case $\alpha_B \sim \alpha_{weak} \sim 0.03$. In this case, imposing $\Omega_B = \Omega_{DM}$ leads to a weakly coupled stable particle with a mass at around the TeV scale. The observation that:

$$\langle \sigma v \rangle \sim \frac{\alpha_{weak}^2}{\text{TeV}^2} , \tag{4.19}$$

reproduces the observed relic abundance for a particle that once was in thermal equilibrium is known as the WIMP miracle and has driven the experimental DM searches during the last years. Notice that this kind of candidates at the weak scale with $\alpha_B \sim \alpha_{weak}$ can naturally appear in well motivated extensions of the SM such as supersymmetric (SUSY) constructions and the scotogenic model.

Non-thermal DM candidates. The axion case

In this section we briefly review the non-thermal production of scalar particles in the early Universe. If scalars are sufficiently light and weakly coupled they can constitute good DM candidates even in the absence of a stabilizing symmetry. This is the case for axions and axion-like particles, including the QCD axion [90–92] (reviewed in chapter 3), the majoron [78, 79], familons [110] and other light scalar and pseudo-scalar fields. In this section we review a production mechanism of non-relativistic, light scalars in the early Universe: the misalignment mechanism.

4.1.0.3 The Misalignment Mechanism

The misalignment mechanism [133–135] is an efficient production mechanism of scalar fields in the early Universe. In some sense it is model independent as it does not need any interaction apart from a mass term, $V_{\text{mass}} \sim \frac{1}{2} m_\phi^2 \phi^2$. In an expanding Universe, the equation of motion (EOM)

for a scalar field reads:

$$\ddot{\phi} + 3H\dot{\phi} + V'(\phi) = 0\,. \tag{4.20}$$

For simplicity, we assume that the field is relatively close to a local minimum so that we can approximate the potential just as a quadratic potential and, therefore, the first derivative reads:

$$V'(\phi) \approx m_\phi^2 \phi\,. \tag{4.21}$$

In general, additional self-interactions of the scalar field such as quartic self-interactions will not largely modify our conclusions. However, it has been recently shown in [136] that in the case of *cosine* potentials, quite generic in the case of axions (see chapter 3), one can have situations that qualitatively differ from the standard misalignment scenario. This occurs when the axion field starts oscillating sufficiently close to the top of its potential. This situation is known as the large-misalignment mechanism and we refer the reader to [136–138] for further details. Throughout this section we will focus our discussion on the standard misalignment mechanism.

Coming back to the EOM in Eq.(4.20), we see that as the cosmic temperature decreases, we will reach a temperature at which the Hubble parameter becomes comparable to the scalar mass:

$$H(T_{osc}) \sim m_\phi\,. \tag{4.22}$$

At this point, the scalar field will start oscillating around the minimum, $\phi(t) \propto \cos(m_\phi t)$. The energy density stored in these oscillations can be estimated by assuming that the entropy remains conserved within the comoving volume:

$$\rho_\phi(T) = m_\phi n_\phi(T) = m_\phi n_\phi(T_{osc}) \frac{s(T)}{s(T_{osc})}\,. \tag{4.23}$$

One easily notices that the energy density scales as $\rho_\phi \sim a(t)^{-3}$, where $a(t)$ is the scale factor. This scaling corresponds to non-relativistic matter and shows that the energy density of the coherent oscillations of the scalar field behaves as cold DM.

So far we have assumed that the scalar mass is a constant parameter throughout the cosmological history. It turns out that, in well motivated situations, the mass of this particle depends on the cosmic temperature.

This is the case if the potential comes from instantons of some non-abelian interaction as for the QCD axion. In this case, for example, the axion potential is turned off for temperatures above Λ_{QCD} and turns on after QCD phase transition. The axion mass is therefore very sensitive the temperature and turns on fast after the QCD-induced potential appears. This temperature dependence generically delays the onset of oscillations with respect to the constant m_ϕ case, producing an enhancement of the relic density of the scalar field. For the sake of completeness, we now consider a couple of specific situations where the relic density of DM generated by these oscillations can be estimated as a function of the parameters of the theory.

In the first example, let us consider a QCD axion in a pre-inflation PQ symmetry breaking scenario (that is, a situation where the PQ symmetry was spontaneously broken before inflation and never restored afterwards.). The axion field can be written as $a = f_a\theta$, where f_a is the decay constant and θ is the misalignment angle. In the pre-inflation scenario, θ_i is a free parameter that ranges from 0 to π. Taking into account the temperature dependence of QCD instantons, and also the fact that m_a and the decay constant are related as $m_a^2 f_a^2 \sim (75.5 \text{ MeV})^4$ [95], the relic density of axions today can be estimated as [93]:

$$\Omega h^2 \sim 0.01\theta_i^2 \left(\frac{f_a}{10^{11} \text{ GeV}}\right)^{1.19} . \tag{4.24}$$

As a second example, let us now consider one of the typical axion-like fields that arise in string theory. This is the case of ultra-light axion (ULA) DM and has been extensively studied in [139]. Assuming that the mass does not depend on the temperature, which is also the case of the majoron as we will see later in Chapter 6, we estimate the relic density of ULA DM as:

$$\Omega_a h^2 \sim 0.05\, \theta_i^2 \left(\frac{f_a}{10^{17} \text{ GeV}}\right)^2 \left(\frac{m_a}{10^{-22} \text{ eV}}\right)^{1/2} . \tag{4.25}$$

In both situations one can easily see that, as the decay constant grows, the initial misalignment angle θ_i has to be tuned to small values so that the relic density does not exceed the value $\Omega_{DM} h^2 = 0.12$.

Later, in Chapter 6, we will consider in detail the case of the majoron as a DM candidate and the associated phenomenology of the most minimal model. In addition to coherent oscillations as a production mechanism of non-thermal majorons, we will also consider the production from the decay

of topological defects which constitutes a very efficient production mechanism. Finally, as we will see later, for a sufficiently large decay constant ($f_a > 10^8$ GeV) the thermal production of relativistic axions (which would contribute to hot DM) is expected to be small, albeit they might be detectable in future experiments.

4.2 Experimental strategies to detect DM

In this section we briefly summarize some techniques that have been developed to look for different DM candidates. The case of axion detection has been discussed previously in section 3.2.

4.2.0.1 Direct detection

Direct detection is a promising type of DM searches where one looks for the result of a DM particle scattering off a target material (see [140] for a review). The motion of the Solar System implies that the Earth encounters a DM *wind* along its cosmic propagation. Despite the cross section of the process is expected to be small, large detectors with high density target materials may have the chance to observe one of these rare collision events. DM detectors are usually built in mines, or below mountains, with the aim to reduce the background that comes for example from cosmic rays. The expected signal consists of a nuclear recoil generated by the elastic scattering of the DM particle. This type of DM detection was proposed long ago [141] and has received a large portion of the experimental effort in the last decade.

Let us analyze in more detail these scattering processes. When a DM particle kicks off the target material one can consider the process as a non-relativistic elastic collision of two particles. One of them, the nucleus, can be considered at rest and assuming the process is elastic one can estimate the maximum momentum transfer by the DM particle and the corresponding recoil energy. After basic kinematics, the maximum energy that can be transferred by the DM particle to the nucleus reads:

$$E_R^{max} = \frac{2\,\mu_{DM,N}^2 v^2}{m_N} \simeq 20 - 200\,\mathrm{keV}\,. \tag{4.26}$$

In the above equation $\mu_{DM,N} = \frac{m_{DM} m_N}{m_{DM}+m_N}$ is the reduced mass of the DM-nucleus system and v is the typical DM velocity. One expects the recoil energy to grow fast with the DM velocity. However, the number of DM

particles with a large velocity is exponentially suppressed. One sees that the reduced mass saturates to $\mu_{DM,N} \approx m_N$ for large DM masses. Since the flux is proportional to the number density, $n_{DM} = \rho_{DM}/m_{DM}$ the interaction rate becomes smaller as m_{DM} grows. Finally, let us comment that precise evaluation of the DM-nucleus scattering cross section usually requires the use of EFT methods and determination of nuclear matrix elements. This renders direct detection an active research topic both in theory and experiment. See Fig.(4.2) for a summary of current constraints for the spin-independent cross section.

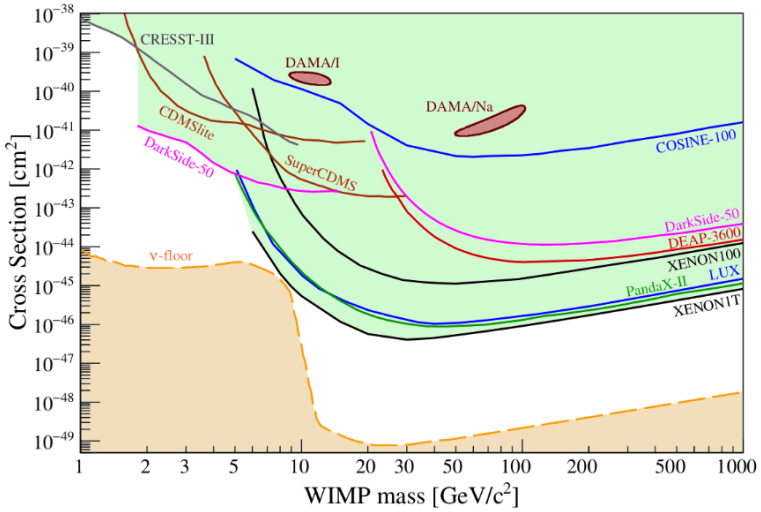

Figure 4.2: Current experimental parameter space for spin-independent WIMP-nucleon nucleon cross sections. Not all published results are shown. The space above the lines is excluded at a 90% confidence level. Image extracted from Ref. [140].

4.2.0.2 Indirect detection

Indirect searches of DM constitute a very active topic of research. The idea is that we look for the radiation associated to DM annihilation or decay. For example, the annihilation of dark matter particles can lead to the production of a variety of SM states such as photons, proton-antiproton pais, or $e^{\pm}$ pairs regardless the primary annihilation channel. One of the most stringent constraints comes from searches of γ rays associated to these annihilations. The most promising directions to look for these processes

are places where DM accumulates. This includes, for example, the Galactic Center and dwarf galaxies.

Another possibility is that DM is not completely stable but has some finite lifetime, τ_{DM}. Of course, τ_{DM} has to be substantially larger than the age of the Universe, $t_0 \sim 10^{10}$ yr $\sim$ few $\times\, 10^{17}$ s, to explain the current abundance. This metastability of DM particles can be explained if, for example, the decay occurs through an effective operator with dimensionality larger than 4 or if the coupling is suppressed for some other reason. An example of the latter is the majoron-neutrino coupling, which is proportional to the neutrino mass [78].

To illustrate how powerful are these searches, let us consider a simple example. Let us assume a pseudoscalar particle with mass m_a is coupled to photons through a dimension-5 operator:

$$O_5 \sim \alpha_{EM} \frac{a}{F_a} F_{\mu\nu} \tilde{F}^{\mu\nu} \,. \tag{4.27}$$

This is in fact the case of an axion-like particle decaying into photons. From dimensional analysis, the lifetime is given by:

$$\tau_a \sim \alpha_{EM}^{-2} F_a^2 / m_a^3 \,. \tag{4.28}$$

If $m_a \sim 0.1$ MeV and $F_a \sim 10^{16}$ GeV, we obtain a lifetime:

$$\tau_a \sim 10^{48}\ \text{GeV}^{-1} \sim 10^{24} s \gg t_0 \,. \tag{4.29}$$

Although it seems that such a weakly coupled and long-lived particle could be a good DM candidate, searches for the associated γ-lines at around the MeV scale at INTEGRAL exclude lifetimes below $\tau \sim 10^{28}$ s. See Fig.(4.3) for a summary of constraints of the lifetime of a DM particle decaying into photons in the mass regime 0.01 MeV $\lesssim m_a \lesssim 10^4$ MeV. This simple example provides further evidence on the potential of indirect DM searches. We refer the reader to [142] for a detailed review on indirect detection and a comprehensive list of references.

4.2.0.3 Collider searches

A third possibility consists in producing DM at collider experiments. This in principle seems challenging since the coupling of DM to the visible sector is weak and also DM is expected to leave the detector without any imprint.

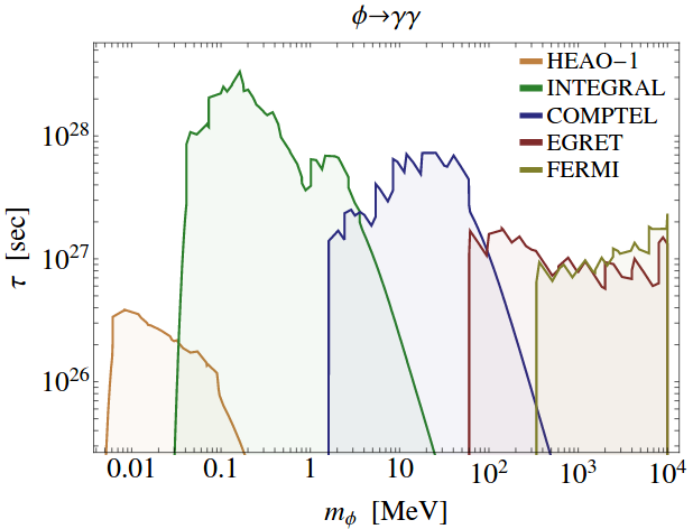

Figure 4.3: Lower bounds on τ_{DM} for a DM candidate decaying into photons. Image extracted from Ref. [142].

However, if DM is produced at colliders it is expected to appear together with SM states. ATLAS and CMS collaborations look for processes such as dilepton, dijet and mono-jet that come together with missing energy (see Fig. (4.4) for a summary of current contraints). So far there is no evidence for these processes, but it remains a promising avenue to look for DM candidates that appear, for example, in SUSY constructions.

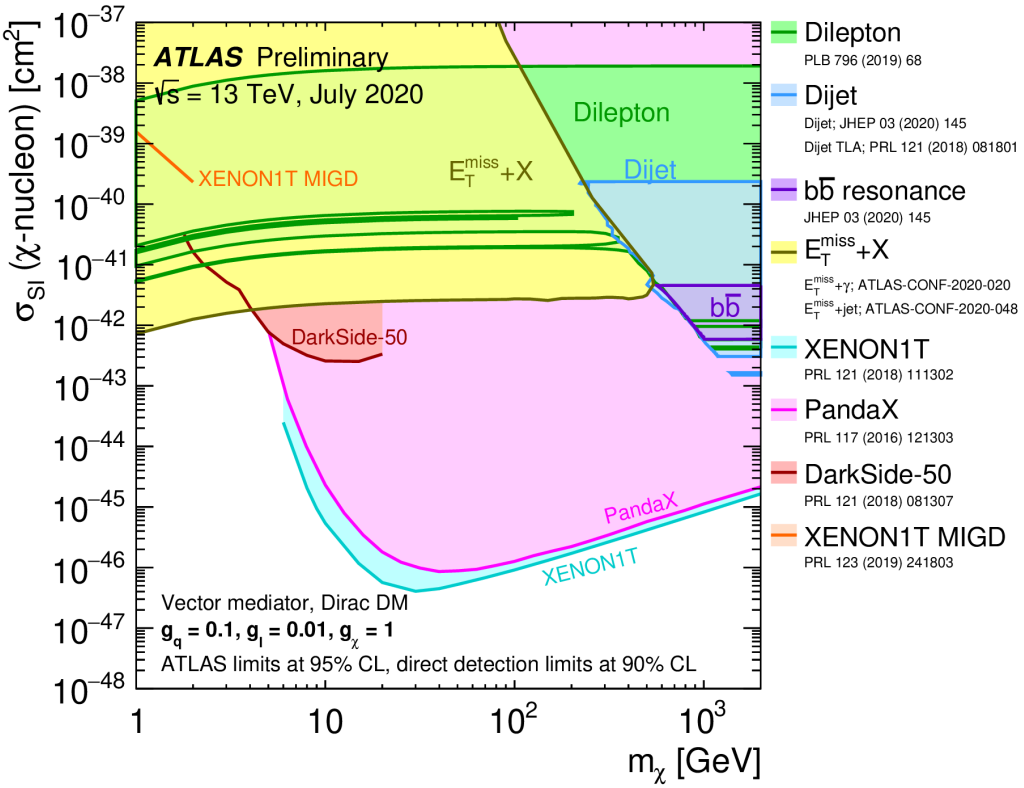

Figure 4.4: Comparison of several collider limits (from monojet, dilepton and dijet channels) with the constraints from direct-detection experiments on the spin-independent WIMP-nucleon scattering cross-section in the context of the Z'-like simplified model with leptophilic vector couplings. Several assumptions are made: a mediator width fixed by the dark matter mass, a DM coupling $g_{DM} = 1$, quark coupling $g_q = 0.1$, and lepton coupling $g_l = 0.01$. Image from [143].

Chapter 5

Grand Unified Theories

Since the early days of Quantum Mechanics, physicists have argued that the electric charge of particles should be a discrete property, automatically implying the existence of a fundamental unit of charge. Paul Dirac went a step further, showing how the existence of magnetic monopoles necessarily implies that the electric charge must be quantized. For almost a hundred years, a huge experimental effort has been dedicated to look for this exotic *particle* without success. Today, more than 80 years after Dirac's work and thanks to the discovery of gauge theories to describe fundamental interactions, most physicists are convinced that there is a deeper unity underlying the plethora of charges and quantum numbers of the SM particles. In modern language, a Grand Unified Theory (GUT) based on simple gauge groups may explain not only why electric charge is quantized but also the mere existence of the different fundamental interactions and their relative strength.

In addition to charge quantization, GUTs are usually simple theories. The meaning of *simple* here is two-fold. On the one hand, in GUTs all SM gauge couplings are unified in the UV and there exists a single interaction based on a simple gauge group that at some energy scale, M_{GUT}, breaks down to the SM gauge group. The breaking occurs through a process of spontaneous symmetry breaking (SSB) by Higgs condensates. Depending on the model, this SSB process may have intermediate steps, with intermediate gauge symmetry groups, before obtaining the SM. On the other hand, GUTs usually have less parameters than the SM, offering powerful predictions. Depending on the model we can have connections among Yukawa couplings and similar relations. These connections translate into some degree of predictivity that has usually to be corrected with a notorious model building effort to make the theory consistent with the experiment.

After reviewing gauge coupling unification in the Standard Model, in this chapter we will briefly introduce the basics of GUTs. We will discuss the basic features of the Georgi-Glashow model and also motivate theories based on spinor unification as compelling candidates for GUTs.

5.1 Running couplings

In QFT, couplings are not fixed quantities but usually depend on the energy scale. In this section we review the energy scale dependence of the gauge couplings and how, when applied to the SM, this interesting quantum mechanical effect suggests the existence of an underlying unified theory. For the sake of simplicity, let us start considering the case of QED vacuum polarization induced by a charged fermion. We represent this phenomenon by the Feynman diagram in Fig.5.1.

The QED vacuum polarization reduces to the calculation of an integral that goes as:

$$I \sim \int d^4k \frac{1}{k^2} \,. \tag{5.1}$$

This integral is clearly divergent but can be regularized, for example, using

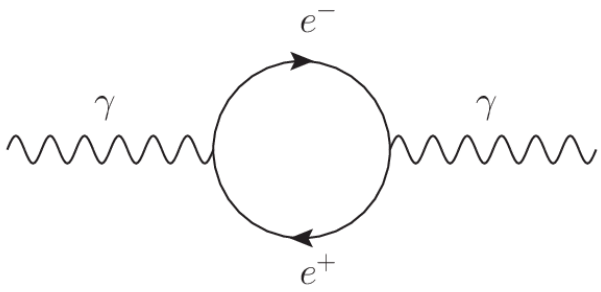

Figure 5.1: QED vacuum polarization.

dimensional regularization. The main idea is that we can split the self-energy into a non-physical divergent part and a finite quantity that includes the dependence on the physical momentum q^2:

$$\Pi(q^2) = \Delta\Pi_{div}(\mu^2) + \Pi_R(q^2/\mu^2) \,. \tag{5.2}$$

This separation is ambiguous and, depending on the q^2-independent part, we have the different renormalization schemes. The crucial part is that, thanks to the regularization procedure, we can split $\Pi(q^2)$ in two parts and

the divergent corrections generated by the quantum loops can be reabsorbed by a redefinition of the QED coupling:

$$\alpha_B \left(1 - \Delta\Pi_{div}(\mu^2) - \Pi_R(q^2/\mu^2)\right) \equiv \alpha_R(\mu^2) \left(1 - \Pi_R(q^2/\mu^2)\right) . \tag{5.3}$$

The quantity we measure in experiments is $\alpha_R(\mu^2)$ and is of course finite. We call $\alpha_R \equiv \alpha$ the *running coupling* and its scale dependence is determined by the β-function:

$$\mu \frac{d\alpha}{d\mu} = \alpha\beta(\alpha) , \ \beta(\alpha) = \beta^{\text{1-loop}} \frac{\alpha}{\pi} + \beta^{\text{2-loop}} \left(\frac{\alpha}{\pi}\right)^2 + O(\alpha^3) . \tag{5.4}$$

If we truncate at one loop, which is reasonable for small couplings, we get the well-known formula relating the gauge coupling at 2 different scales:

$$\alpha^{-1}(Q^2) = \alpha^{-1}(\mu^2) + \frac{\beta^{\text{1-loop}}}{2\pi} \log\left(Q^2/\mu^2\right) . \tag{5.5}$$

The beta function coefficients, $\beta^{i\text{-loop}}$, depend on the particle content and, therefore, are model dependent. For QED with a charged fermion with charge q_f we get: $\beta^{\text{1-loop}}_{QED} = \frac{2}{3} q_f^2$. Since the coefficient is positive, the running coupling increases with the energy scale. This is equivalent to a screening effect of the electric charge, i.e. the electric charge appears to be smaller at larger distances.

Renormalization of the gauge coupling in QCD and in other YM theories proceeds in a similar way. Interestingly, the non-abelian nature of YM theories implies an additional self-interaction between gauge bosons that, at the end of the day, results in a negative contribution to the $\beta^{\text{1-loop}}$ coefficient [21, 22]. In full generality, $\beta^{\text{1-loop}}$ is given by:

$$\beta^{\text{1-loop}} = \frac{2}{3} T_f d_f + \frac{1}{3} T_s d_s - \frac{11}{3} C_2(G) . \tag{5.6}$$

The above expression contains the contributions of fermions, scalars and gauge bosons respectively. The quantities $T_{f/s}$ are the Dynkin indices of each fermion and scalar representation, $d_{f/s}$ is the dimension of the representation with respect to other groups and $C_2(G)$ is the quadratic Casimir operator for the gauge group G. As an example, for QCD with the particle

content of the SM with 6 quark flavors we get the well-known[1]:

$$\beta_{QCD} = \frac{2}{3} \times \frac{1}{2}(2 \times 1 + 1 + 1) \times N_{fam.} - \frac{11}{3} \times 3 = -7\,. \tag{5.7}$$

Since $\beta_{QCD} < 0$ the coupling decreases with increasing energy. This is equivalent to an anti-screening effect of the effective color charge and is known as *asymptotic freedom* [21, 22].

Running of gauge couplings in the SM and beyond

Having introduced the running of gauge couplings, let us now study the case of the SM. As explained in Chapter 1, the SM is a gauge theory of the strong and EW interactions. The particle content is given by 3 families of quarks and leptons, and a Higgs doublet. We can easily compute the coefficients of the beta function which, for energies $E > m_t$, are given by:

$$\beta_1 = \frac{41}{10}\,,\ \beta_2 = -\frac{19}{6}\,,\ \beta_3 = -7\,. \tag{5.8}$$

In the following, the subindices $1, 2, 3$ will refer to the $U(1)_Y$, $SU(2)_L$ and $SU(3)_C$ groups, respectively. The couplings seem to converge to a common value at high energies but they do not unify exactly. New physics is needed to change slightly the β-functions and have precise unification of the gauge couplings. A prototype example of this kind of new physics is supersymmetry. In addition to solving the hierarchy problem and giving a DM candidate under certain circumstances, supersymmetric models usually have the particles with the right quantum numbers so that the running of the gauge coupling unify at large energies. This was first noted in [144] and is one of the main motivations for low-scale supersymmetry. For example, in the Minimal Supersymmetric Standard Model (MSSM), the coefficients of the beta function change to:

$$\beta_1 = \frac{33}{5}\,,\ \beta_2 = 1\,,\ \beta_3 = -3\,. \tag{5.9}$$

In Fig. 5.2 we compare the gauge coupling running for the SM and MSSM with low-scale SUSY. Precise unification is achieved in the latter case at a

[1] We will consider only the running at one-loop and therefore, from now on, we will omit the label "i-loop" which indicated the number of loops in Eq. (5.4).

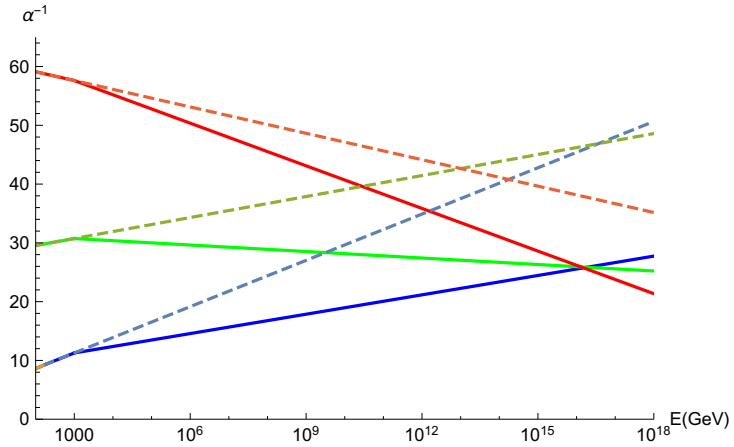

Figure 5.2: Gauge coupling running for the SM (dashed lines) and MSSM (solid lines). The red, green and blue colors stand for the $U(1)_Y$, $SU(2)_L$ and $SU(3)_C$ gauge couplings, respectively. Precise unification is achieved in the MSSM case at around $M_{GUT} \sim 2 \times 10^{16}$ GeV for a SUSY scale $m_{susy} \sim O(TeV)$. This value for the GUT scale is compatible with the bounds coming from proton decay searches.

scale $M_{GUT} \sim 2 \times 10^{16}$ GeV. This scale is compatible with proton decay experiments as we discuss below.

5.2 The Georgi-Glashow model

In this section we overview the first, and one of the prototype examples of grand unified theories: the pioneer Georgi-Glashow model [145]. The model is based on a $SU(5)$ gauge symmetry that after a SSB process gives the SM gauge group. Incidentally, $SU(5)$ is the smallest simple group that contains the SM. In addition, it has representations with the appropriate quantum numbers to accomodate the fermion quantum numbers of a given SM family. In particular, the anti-fundamental $\bar{\mathbf{5}}_F$ and the $\mathbf{10}_F$ representation is the smallest, chiral set of fermions that is anomaly-free and reproduces the quantum numbers of SM families. In more detail, after SSB down to the SM, they split as:

$$\begin{aligned} \bar{\mathbf{5}}_F &\to (1,2,-1/2) + (\bar{3},1,1/3)\,, \\ \mathbf{10}_F &\to (1,1,1) + (\bar{3},1,-2/3) + (3,2,1/6)\,. \end{aligned} \tag{5.10}$$

The generators of the $SU(3)$ and $SU(2)$ groups of the SM are trivially embedded into traceless 5×5 matrices as:

$$SU(3): \begin{bmatrix} \frac{\lambda^a}{2} & 0 \\ 0 & 0 \end{bmatrix}, \quad SU(2): \begin{bmatrix} 0 & 0 \\ 0 & \frac{\sigma^i}{2} \end{bmatrix}. \tag{5.11}$$

On the other hand, the hypercharge generator is given by a diagonal matrix:

$$Y = \mathrm{diag}(-1/3, -1/3, -1/3, 1/2, 1/2)\,, \tag{5.12}$$

which obviously commutes with $SU(3)$ and $SU(2)$. Relating Y to the generators of the $SU(5)$ group, one obtains the normalization factor: $T = \sqrt{3/5}Y$.

The Higgs sector

As a simple parameter counting, one easily sees that, while the 12 SM gauge bosons remain massless, the rest of the initial $SU(5)$ gauge bosons acquire a mass after SSB. In general, a $SU(N)$ group has $N^2 - 1$ generators and therefore 12 of the $SU(5)$ bosons will get a mass. The simplest way to break $SU(5)$ down to the SM while providing the 12 Goldstone bosons that we need is to use the $SU(5)$ adjoint representation, $\mathbf{24}_H$. The adjoint field can be regarded as a traceless 5×5 matrix. The most general renormalizable potential for this field is given by:

$$V(\Phi) = -\frac{\mu^2}{2}\mathrm{Tr}\,\mathbf{24}_H^2 + \frac{\lambda}{4}\mathrm{Tr}\,\mathbf{24}_H^4 + \frac{\lambda_2}{4}\left(\mathrm{Tr}\,\mathbf{24}_H^2\right)^2. \tag{5.13}$$

Once $\mathbf{24}_H$ acquires a VEV, $\langle\mathbf{24}_H\rangle$, the $SU(5)$ group will be broken down to the SM. The simplest way to see this is by using a gauge transformation to bring all the non-zero components to the diagonal. Due to the traceless property, the diagonal entries will satisfy:

$$\sum_i N_i v_i = 0\,, \tag{5.14}$$

where N_i is the multiplicity of any non-zero VEV in the diagonal. This condensate, $\langle\mathbf{24}_H\rangle$, leaves a $SU(N_1)\times SU(N_2)\times ...\times U(1)$ subgroup unbroken. In the case of the potential in Eq.(5.13), it can be shown that a global minimum corresponds to the VEV:

$$\langle\mathbf{24}_H\rangle = \frac{v_{GUT}}{\sqrt{30}}\mathrm{diag}(2,2,2,-3,-3)\,. \tag{5.15}$$

This condensate leaves an unbroken subgroup $SU(3)\times SU(2)\times U(1)$, which is precisely the gauge group of the SM.

The adjoint Higgs, $\mathbf{24}_H$, decomposes upon SSB as:

$$\begin{aligned}\mathbf{24}_H \rightarrow &(1,1,0)+(1,3,0)+(8,1,0)\\ &+(3,2,-5/6)+(\bar{3},2,5/6)\,.\end{aligned} \tag{5.16}$$

A detailed analysis of the scalar boson mass matrix reveals that the scalar states $(3,2,-5/6)$ and $(\bar{3},2,5/6)$ have zero mass and correspond to the 12 massless Goldstone bosons that are eaten by the massive gauge bosons, the so-called vector or gauge leptoquarks.

As usual, the mass of these gauge bosons comes from the kinetic term of the Higgs field once we promote the derivative to a covariant derivative:

$$\mathrm{Tr}\left[(D_\mu \mathbf{24}_H)^\dagger (D^\mu \mathbf{24}_H)\right]\,. \tag{5.17}$$

After some algebra, one finds that the gauge bosons $X_\mu \sim (3,2,-5/6)$ and $\bar{X}_\mu \sim (\bar{3},2,5/6)$ gain a mass

$$M_X \sim g^2 v_{GUT}^2\,. \tag{5.18}$$

These fields mediate quark-lepton transitions that induce baryon number violation processes such as the dangerous proton decay. We will see later that this process offers an interesting way to test GUTs.

Yukawa sector

We have reviewed in the previous section how the initial $SU(5)$ gauge symmetry is broken down to the SM. However, the EWSB still proceeds by a Higgs doublet as in the SM. This Higgs doublet cannot come from the adjoint $\mathbf{24}_H$ and therefore we need to extend the scalar sector. The simplest extension is to add a scalar field in the fundamental representation $\mathbf{5}_H$ (we use the subindex H to remark that this corresponds to a scalar field) that, in addition to the EW Higgs doublet, comes with a color triplet:

$$\mathbf{5}_H = \begin{bmatrix} T \\ H \end{bmatrix}\,. \tag{5.19}$$

Let us focus now on the Yukawa interactions and charged fermion mass generation. The most general renormalizable Yukawa Lagrangian is given

by:

$$\mathcal{L}_Y = Y_5 \bar{\mathbf{5}}_F \mathbf{10}_F \mathbf{5}_H^* + Y_{10} \mathbf{10}_F \mathbf{10}_F \mathbf{5}_H + \text{h.c.} \tag{5.20}$$

In the equation above, Y_5 and Y_{10} are 3×3 matrices in family space and offer an interesting prediction that relates the charged lepton and down quark mass matrices:

$$Y_E = Y_D^T \,. \tag{5.21}$$

This prediction is unfortunately not realized in Nature and forces us to extend the minimal $SU(5)$ model by introducing extra scalar fields. Finally we also note that, within the minimal $SU(5)$ model, neutrinos are massless and one has to introduce additional ingredients to generate their masses.

Proton Decay

One of the most exciting predictions of GUTs is the presence of states that mediate proton decay. It is well known that renormalizability and gauge invariance render the proton absolutely stable in the SM at the perturbative level. However, since the representations in GUT bring together quarks and leptons, $B + L$ is not a good symmetry of the theory. This allows $\Delta(B + L) = 2$ processes that unavoidably lead to the desintegration of protons. Fortunately, as we will see now, the large mass of these states together with the high-dimensionality of the effective operators lead to an adequate suppression of the process. Just by using dimensional analysis one can estimate the decay width of, for example, the process:

$$p \to e^+ \pi^0 \,. \tag{5.22}$$

If the process is mediated by one of the X_μ gauge bosons we mentioned before, the amplitude will be proportional to $|\mathcal{A}|^2 \propto 1/M_{GUT}^4$. Since the other relevant scale in the problem is the proton mass, m_p, it is straightforward to estimate the decay width of the process:

$$\Gamma_{p\to e^+\pi^0} \sim \frac{m_p^5}{M_{GUT}^4} \,. \tag{5.23}$$

Experimentally, from proton decay searches at Super Kamiokande experiment, we obtain $\tau > 1.6 \times 10^{34}$y [146] that corresponds to a GUT scale around $M_{GUT} \geq 10^{16}$ GeV. This is precisely the scale predicted by SUSY scenarios! This interesting coincidence constitutes an additional motiva-

tion for experimental searches of both, supersymmetry and Grand Unified Theories.

5.3 Beyond minimal GUTs: spinor unification

It is a well known fact that fermions in real representations have invariant bare-mass terms. This is known with the name of *survival hypothesis* [147]. It is therefore a subtle task of model building to have theories with a chiral fermion content without running into troubles with gauge anomalies. Interestingly enough, there is a class of groups that are always anomaly-free and still have chiral representations. These are the celebrated spinor representations of the $SO(4N+2)$ family[2]. In this section, closely following Wilczek and Zee [148], we briefly review why unified theories using spinors are an attractive framework to have successful unification with a chiral fermion content.

Spinors exist because Clifford algebras exist [148]. Also, the properties of spinor representations are easily understood once the construction of Cliffors algebra is understood. The Clifford algebra of the $SO(2n)$ group are $2n$ hermitian matrices, γ_i, that satisfy:

$$\{\gamma_i, \gamma_j\} = 2\delta_{ij}\,, \tag{5.24}$$

One defines the spinor representation of $SO(2n)$ as an object that transforms as:

$$\psi \to e^{i\omega^{ij}\sigma_{ij}}\psi\,, \tag{5.25}$$

where σ_{ij} is the generalization of rotations in the $i-j$ plane of the $SO(2n)$ space:

$$\sigma_{ij} = \frac{i}{2}[\gamma_i, \gamma_j]\,. \tag{5.26}$$

As it is done in the case of the Lorentz group, one can define the generalization of the γ_5 matrix:

$$\gamma_{FIVE} = (-i)^n\,(\gamma_1\gamma_2...\gamma_{2n})\ . \tag{5.27}$$

[2]The exceptional group E_6 is also anomaly-free and supports chiral representations. We will not consider this kind of theories in this thesis.

This allows to define the two spinor representations of $SO(2n)$ group:

$$\psi_{\pm} = \frac{1}{2}(1 \pm \gamma_{FIVE})\psi\,, \tag{5.28}$$

which transform irreducibly and are of course 2^{n-1} dimensional objects. Two important properties of spinors emerge automatically from their construction:

- All the $SO(N)$ groups (with the exception of $SO(6)$, which is isomorphic to $SU(4)$) are anomaly-free. In the case of the $SO(4N+2)$ family, as we anticipated, the spinors $\psi_{\pm}$, defined as in Eq.(5.28), are complex and conjugates of each other. This striking fact suggests the complex spinors of $SO(4N+2)$ as compelling candidates to have anomaly-free GUTs with chiral fermion content.

- Spinors decompose repetitively into copies of spinors of the orthogonal subgroups. As an example, the 2^{n+m-1} dimensional spinor of the group $SO(2n+2m)$ decomposes as 2^m copies of the spinor representation of the $SO(2n)$ subgroup. This feature suggests spinor unification as an interesting mechanism to accomodate the repetitive family structure of the SM. This fact is the central idea of Chapter 8.

SO(10) unification

The group SO(10) [149, 150] is the smallest in the $SO(4N+2)$ family that allows a constistent unification of SM interactions. Additionally, the **16** spinor successfully accounts for the quantum numbers of an entire SM family plus a SM singlet with the quantum numbers of a right-handed neutrino. This is easily understood from the SU(5) subgroup point of view, since the SO(10) spinor decomposes as:

$$\mathbf{16} \to \mathbf{10} + \bar{\mathbf{5}} + \mathbf{1}\,. \tag{5.29}$$

Therefore, SO(10) GUT is a theory of gauge and *intra*-family unification.

The SO(10) group has a richer structure than $SU(5)$. Since it has rank 5 we can obtain the SM (rank 4) through different SSB chains. One of them includes an intermediate stage where SO(10) breakes down to the group $SU(5)\times U(1)$ or the well-known Pati-Salam group $SU(4)\times SU(2)\times SU(2)$.

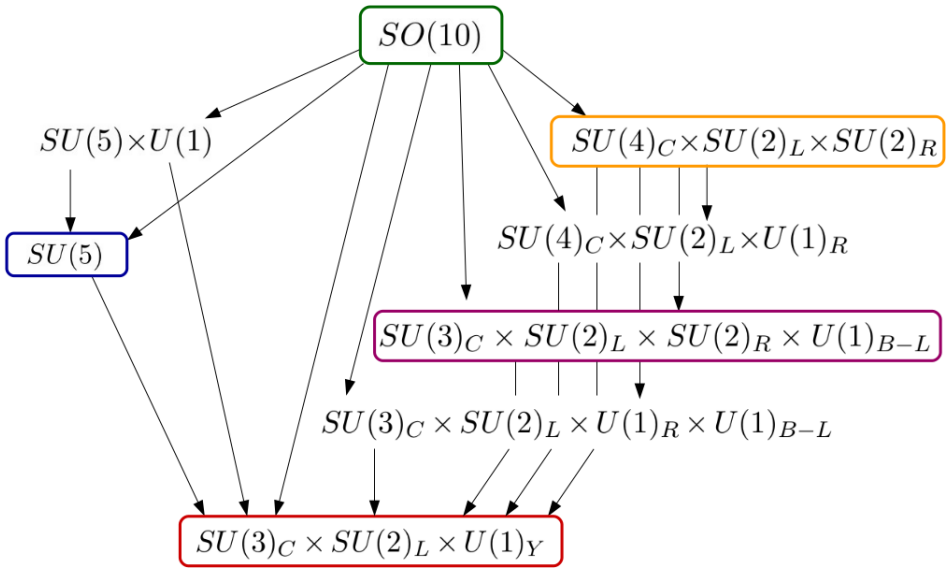

Figure 5.3: Patterns of symmetry breaking from $SO(10)$ (green) to the SM group (red). Well-motivated intermediate symmetries include the $SU(5)$ group (blue), the Pati-Salam group (orange) and the left-right symmetric (purple) gauge symmetries. Adapted from [151, 152].

Being a member of the $SO(4N+2)$ family, the SO(10) spinor is a chiral spinor:

$$\mathbf{16} \times \mathbf{16} = \mathbf{10} + \mathbf{120} + \mathbf{126}\,. \tag{5.30}$$

Therefore, we can have 3 different types of Yukawa interactions for the fermions in the $\mathbf{16}_F$ with scalar fields in the $\mathbf{10}_H$, $\mathbf{120}_H$, $\mathbf{126}_H$ representations which, after SSB, give masses to the fermions contained in $\mathbf{16}_F$.

The SM Higgs is usually given by a linear combination of the EW doublets contained in the $\mathbf{10}_H$ and $\mathbf{126}_H$ representations. In addition, the $\mathbf{126}_H$ has a SM singlet that can be used to break $SO(10)$ and, at the same time, generate a large mass for the right-handed neutrino. Therefore, in $SO(10)$, it is a simple task to relate the seesaw scale to the GUT scale with a minimal particle content. Together with the $\mathbf{10}_H$ and $\mathbf{126}_H$, one usually requires the presence of additional scalars in the $\mathbf{45}_H$, $\mathbf{54}_H$ or $\mathbf{210}_H$ representation to have a consistent SSB mechanism of the $SO(10)$ group down to the SM. All these possibilities, and the rich phenomenology of the associated fields, make $SO(10)$ model building an interesting and active subject of research.

Part II

Neutrinos and Dark Matter

Chapter 6

Light majoron cold DM

In this chapter, based on [153], we consider the possibility that the lepton number symmetry is spontaneously broken in two units by the VEV of a scalar singlet, therefore leading to Majorana neutrinos. In this case, a new state appears in the theory: the majoron, a Nambu-Goldstone boson associated to the breaking of lepton number [78, 79][1]. We will see that despite its simplicity, the minimal majoron model provides an interesting connection between dark matter and the generation of small neutrino masses.

The typical expectation is that the majoron behaves as a good DM candidate in the case it is thermally produced with a mass at the keV scale [155–159]. In this chapter we will focus on the case where the $U(1)_L$ symmetry is broken after inflation and the majoron mass is relatively small ($\ll$ eV). This is the case when the $U(1)_L$ symmetry is restored by the thermal effect at a high temperature after reheating. We will see how non-relativistic Majorons are efficiently produced from coherent oscillations and the decay of topological defects, obtaining the right relic DM abundance, $\Omega h^2 = 0.12$, for majorons with mass $m_J \ll O(1)$ keV.

Before going into details, let us summarize the cosmological evolution of the majoron model (see Fig.(6.1)) and the main results of the present chapter. As the temperature decreases due to the cosmic expansion, the thermal effect is weakened and the $U(1)_L$ symmetry becomes spontaneously broken at a critical temperature. Since the phase of the $U(1)_L$ Higgs boson is randomly distributed at the phase transition time, and since causality

[1] Here we focus on the case of Majorana neutrinos, however Nambu-Goldstone bosons can also appear in the Dirac case [154].

does not hold beyond the horizon, cosmic strings form at the time of the $U(1)_L$ symmetry breaking. This is the well-known Kibble mechanism [160].

In order for the majoron to be a good DM candidate, lepton number symmetry has to be explicitly broken by some non-perturbative effect, generating a small but non-zero majoron mass, m_J. This explicit breaking is expected to arise naturally in string theoretical constructions where several types of non-perturbative effects, including gravitational instantons, break all the non-gauged symmetries. Nevertheless, the particular origin of the explicit breaking is not important at this point.

When the Hubble parameter decreases below the majoron mass scale, the $U(1)_L$ symmetry-breaking effect becomes relevant and the majoron starts to oscillate coherently around a minimum of the potential. Due to the explicit breaking of $U(1)_L$ symmetry, domain walls form in such a way that their boundaries are the cosmic strings (see [101] for a comprehensive review on topological defects). These defects disappear due to the tension of the domain wall. Their energy is mainly released as non-relativistic majorons. We expect these majorons to be the dominant component of the cosmological dark matter. Later in this chapter, we will estimate the abundance of non-thermal majorons produced from the topological defects and determine the parameter region where we can explain the observed amount of dark matter. As usual, if kinematically allowed, the majoron will decay to neutrinos [155], though its lifetime is much longer than the present age of the Universe in most parameter regions of interest[2]. We find that the majoron can make up all of the dark matter even in this case. This is a particularly interesting case since the neutrinos produced from the decay of majorons with mass $\mathcal{O}(0.1-1)$ eV are a promising target for direct detection experiments of cosmic neutrinos, such as PTOLEMY [162, 163].

As a separate issue, we will argue that the DM majoron density fluctuations grow after the matter-radiation equality and boson stars may form because of the gravitational attractive interaction. Unlike typical axion scenarios, an interesting feature of the majoron model is that it can have either attractive or repulsive interactions, depending on the higher-dimensional operators. We will estimate the size and mass of a typical boson star and study how the sign of the leading self-interaction leads to qualitatively different situations.

[2]The effect of decaying majoron dark matter on the CMB was discussed in [161]. The impact of decaying warm dark matter on structure formation and comparison with the ΛCDM paradigm was treated in [159].

6.1 The minimal majoron model

We adopt the simplest type-I seesaw model (see Chapter 2) with spontaneous lepton number violation [78,79]. The Yukawa Lagrangian responsible for the generation of neutrino mass generation reads:

$$\mathcal{L}_\nu = y^D_{ij}\bar{l}^i_L H^\dagger \nu^j_R + \frac{y_{ij}}{2}\bar{\nu}^{ic}_R \sigma \nu^j_R + \text{h.c.} \tag{6.1}$$

In the equation above, $H \sim (1,2,1/2)_0$ and $\sigma \sim (1,1,0)_2$ are the SM Higgs doublet responsible for EW breaking and the singlet giving mass to right-handed neutrinos, respectively. The subscript indicates the lepton number charge.

The scalar potential is chosen to respect the $U(1)_L$ lepton number global symmetry:

$$V = \mu_H^2|H|^2 + \lambda_H|H|^4 + \mu_\sigma^2|\sigma|^2 + \lambda_\sigma|\sigma|^4 + \lambda_{H\sigma}|\sigma|^2|H|^2\,, \tag{6.2}$$

where $\mu_\sigma^2 < 0$. We assume that $\lambda_{H\sigma}$ is so small that the last term does not strongly affect the Higgs potential. One can write the majoron field in polar form as:

$$\sigma = \frac{(v_\sigma + \rho)e^{iJ/v_\sigma}}{\sqrt{2}}\ . \tag{6.3}$$

Majoron potential

As we discussed at the beginning of the chapter, as the Universe cools down, the σ field will develop a non-zero vacuum expectation value $\langle\sigma\rangle = v_\sigma/\sqrt{2}$. So far, the majoron is massless to all orders in perturbation theory. Therefore, in addition to the spontaneous breaking of the $U(1)_L$ global symmetry, one needs to assume some source of explicit symmetry breaking. This breaking may arise from higher-dimensional terms of the scalar potential, which could be induced by gravitational instanton effects [164]. The exact dynamics of the physics triggering such breaking is not important at this point. This in general gives a mass to the majoron, which in our minimal picture corresponds to the angular part of the σ field: J. The most important parameter, required to be non-zero, is:

$$\left(\frac{d^2 V_{\text{eff}}}{dJ^2}\right)_{\langle\sigma\rangle}\ ,$$

where V_{eff} is the effective operator for higher-dimensional terms.

This means that, for simplicity, we can just assume that some underlying theory generates an effective potential violating lepton number. Such potential is assumed to be a combination of d-dimensional operators,

$$\begin{aligned} V_{\text{eff}}^{d} =& \frac{c_1}{M_{\text{Pl}}^{d-4}}\sigma^d + \frac{c_2}{M_{\text{Pl}}^{d-4}}|\sigma|^2\sigma^{d-2} + ... + \frac{c_{d-2}}{M_{\text{Pl}}^{d-4}}|\sigma|^{d-2}\sigma^2 \quad (d\text{=even}) \\ & \text{or } + \frac{c_{d-1}}{M_{\text{Pl}}^{d-4}}|\sigma|^{d-1}\sigma \quad (d\text{=odd}) \\ & + \frac{b_1}{M_{\text{Pl}}^{d-4}}|H|^2\sigma^{d-2} + ... + \frac{b_{d-2}}{M_{\text{Pl}}^{d-4}}|H|^{d-2}\sigma^2 \quad (d\text{=even}) \\ & \text{or } + \frac{b_{d-1}}{M_{\text{Pl}}^{d-4}}|H|^{d-1}\sigma \quad (d\text{=odd}) + \text{h.c.} \end{aligned} \tag{6.4}$$

where c_i and b_i are $\mathcal{O}(1)$ coefficients. Since we are interested in the case where $\langle H\rangle \ll \langle\sigma\rangle$, the terms involving $\langle H\rangle$ are subdominant and can be neglected. The full effective potential (up to order d_{max}) will contain a sum over odd and even d's:

$$V_{\text{eff}}(\sigma) = \sum_{d\geq 5}^{d_{max}} V_{\text{eff}}^{d}. \tag{6.5}$$

This potential explicitly breaks the lepton number $U(1)_L$ symmetry. However, a discrete subgroup may remain unbroken depending on which of the coefficients c_i are non-zero. This unbroken subgroup corresponds to the periodicity of the vacuum and can be the responsible for dangerous domain wall formation. To see this, we write the pseudo-Nambu-Goldstone part of the potential (forgetting about the radial excitation) using the polar form in (6.3). The effective potential for the pseudo-Nambu-Goldstone field, ignoring the contributions of the terms proportional to $\langle H\rangle$, is given by

$$\begin{aligned} V_{\text{eff}}^{d\,(\text{even})}(J) &= \sum_{k=1}^{d/2} c_k \frac{v_\sigma^d}{2^{d/2-1}M_{\text{Pl}}^{d-4}}\cos(2kJ/v_\sigma)\,, \\ V_{\text{eff}}^{d\,(\text{odd})}(J) &= \sum_{k=0}^{(d-1)/2} \tilde{c}_k \frac{v_\sigma^d}{2^{d/2-1}M_{\text{Pl}}^{d-4}}\cos((2k+1)J/v_\sigma)\,, \end{aligned} \tag{6.6}$$

where we have separated even and odd d parts. These clearly show that the vacuum has a periodicity $2\pi/2k$ and $2\pi/(2k+1)$, respectively, and may be smaller than 2π.

The spontaneous breaking of discrete symmetries in general implies a cosmological catastrophe since it predicts the formation of stable domain walls [165], which lead to a highly inhomogeneous Universe. In addition, their energy density evolves slower than radiation or matter, and is bound to dominate the energy density of the Universe [166], contradicting observation. Although domain-wall-free constructions can be envisaged [167], the existence of domain walls is a generic problem. One possible solution is to rely on either inflation (effectively pushing the walls beyond the horizon) or on removing the physical degeneracy of the associated vacua via the Lazarides-Shafi mechanism [102]. A last possibility is to have explicit breaking of the residual discrete symmetry. This explicit breaking can be associated to new physics in many forms, such as the Witten effect [168] or instantons of a new confining interaction [103, 104].

In our framework, however, we assume that spontaneous symmetry breaking takes place after inflation, and the same gravitational physics generating the majoron mass is responsible of lifting the degeneracy of the associated vacua. Noting that a combination of co-prime powers of σ drives the explicit breaking $U(1)_L \to Z_1$, we need at least two terms at the potential involving co-prime powers of σ so as to avoid undesirable, stable domain walls. Note that this mild requirement cannot always be satisfied. For example, let us assume d is even. If the potential contains all possible powers on σ

$$\sigma^2|\sigma|^{d-2}, \sigma^4|\sigma|^{d-4}, ..., \sigma^{d-2}|\sigma|^2, \sigma^d\,, \tag{6.7}$$

one notices that the $U(1)_L$ is not completely broken. Instead, in the model under consideration, it is broken down to a Z_2 discrete symmetry. In such a situation, when the scalar field σ develops a non-zero vacuum expectation value, domain walls are formed leading to a cosmological disaster.

In contrast, if d is an odd number, the requirement of co-prime powers in σ in the effective potential can be easily achieved, since the possible powers on σ in the chain

$$\sigma|\sigma|^{d-1}, \sigma^3|\sigma|^{d-3}, ..., \sigma^{d-2}|\sigma|^2, \sigma^d\,, \tag{6.8}$$

always contain, at least two co-prime powers in σ. Thus, avoiding domain walls requires that at least one d is odd. For example one can imagine a situation where we have d-dimensional and $(d+1)$-dimensional operators. These situations are always safe from domain walls, if the relative suppression of the operators is not extremely large. If one of the operators is

suppressed with respect to the other, then one has the interesting situation where the domain walls survive for a short period and decay. This case is expected to happen in a potential with a combination of terms like

$$V = \frac{c_1}{M_P}\sigma^5 + \frac{c_2}{M_P^2}\sigma^6 + \text{h.c.}\,, \tag{6.9}$$

which generate an effective potential for the majoron field:

$$V = c_1 \frac{v_\sigma^5}{2^{3/2} M_P} \cos\left(5J/v_\sigma\right) + c_2 \frac{v_\sigma^6}{2^2 M_P^2} \cos\left(6J/v_\sigma\right)\,. \tag{6.10}$$

Since one naturally expects $\frac{c_1}{M_P} \gg \frac{c_2}{M_P^2} v_\sigma$, domain walls may survive for a period of time before they disappear. One must make sure that the hierarchy between operators is such that the walls never dominate the Universe energy density. This puts constraints on the parameters, as we will discuss in Sec. 6.2.

The terms in (6.4) clearly break lepton number symmetry and, therefore, generate an effective potential for the majoron (this is, the angular part of σ),

$$V_{\text{eff}}(J) = \left(\frac{d^2 V_{\text{eff}}}{dJ^2}\right)_{J=0} J^2 + \left(\frac{d^3 V_{\text{eff}}}{dJ^3}\right)_{J=0} J^3 + \left(\frac{d^4 V_{\text{eff}}}{dJ^4}\right)_{J=0} J^4 + \text{higher orders}\,. \tag{6.11}$$

From the first term we get the majoron mass. The trilinear and quartic couplings are self-interactions that may be relevant for the formation of astrophysical objects such as boson stars, as we will see later. If we focus in the high-scale seesaw model, the scale of lepton number breaking is much larger than the EW scale. This means that the contributions coming from d-dimensional operators involving Higgs doublets (see (6.4)) are suppressed by a factor $\frac{v_{EW}^2}{v_\sigma^2} << 1$ [3] and can be neglected when computing the effective potential for the majoron in Eq. (6.11).

[3] In previous chapters we refered to the SM Higgs VEV as v. To avoid confusion with the majoron VEV, we will use here v_{EW}.

From Eq. (6.6), the majoron mass and quartic self-coupling can be written as

$$\begin{aligned} m_J^2 &= -\sum_d^{d_{max}} \left[\sum_{k=1}^{d/2} c_k \frac{(2k)^2}{2^{d/2-1}} \left(\frac{v_\sigma^{d-2}}{M_P^{d-4}} \right) + \sum_{k=0}^{(d-1)/2} \tilde{c}_k \frac{(2k+1)^2}{2^{d/2-1}} \left(\frac{v_\sigma^{d-2}}{M_P^{d-4}} \right) \right] \\ \lambda_4 &= \sum_d^{d_{max}} \left[\sum_{k=1}^{d/2} c_k \frac{(2k)^4}{2^{d/2-1}} \left(\frac{v_\sigma^{d-4}}{M_P^{d-4}} \right) + \sum_{k=0}^{(d-1)/2} \tilde{c}_k \frac{(2k+1)^4}{2^{d/2-1}} \left(\frac{v_\sigma^{d-4}}{M_P^{d-4}} \right) \right]. \end{aligned} \tag{6.12}$$

In contrast to the axion case, where the quartic self-interaction is known to be attractive, the potential in Eq. (6.4) can lead to an effective quartic self-interaction between majorons ((6.11)) that is either attractive or repulsive. The reason is that, while in the axion case the coefficients are all related following the Taylor expansion of a $\cos(x)$ function, in the majoron case the coefficients $c_k, \tilde{c}_k$ in (6.12) are free parameters. For example, if we take the operators $d = 5$ and $d = 6$, as in Eq. (6.10),

$$\begin{aligned} m_J^2 &= v_\sigma^2 \left[-c_5 \frac{5^2}{2^{3/2}} \frac{v_\sigma}{M_P} - c_6 \frac{6^2}{2^2} \frac{v_\sigma^2}{M_P^2} \right] = -v_\sigma^2 \left[c_5 \frac{5^2}{2^{3/2}} + \tilde{c_6} \frac{6^2}{2^2} \right] \frac{v_\sigma}{M_P} \\ \lambda_4 &= c_5 \frac{5^4}{2^{3/2}} \frac{v_\sigma}{M_P} + c_6 \frac{6^4}{2^2} \frac{v_\sigma^2}{M_P^2} = \left[c_5 \frac{5^4}{2^{3/2}} + \tilde{c_6} \frac{6^4}{2^2} \right] \frac{v_\sigma}{M_P}, \end{aligned} \tag{6.13}$$

with $\tilde{c_6} = \frac{v_\sigma}{M_P} c_6$. Depending on their relative value, the sign of m_J^2 and λ_4 can be the same, or not. When both come with the same sign, the interaction is repulsive. On the other hand, if $m_J^2 > 0$ and $\lambda_4 < 0$, the interaction is attractive. We conclude that the majoron can have both attractive and repulsive self-interactions. As we will see later, this opens interesting possibilities for the formation of astrophysical size bound states made of majorons: majoron stars.

Constraints on parameters

A viable dark matter candidate must have a lifetime about ten times longer than the age of the Universe t_0 ($\simeq 14\,\mathrm{Gyr} \simeq 1/(1.5{\times}10^{-42}\,\mathrm{GeV})$) [169]. For the case of the majoron the main decay mode is expected to be to two

neutrinos [78]. The decay width, when kinematically allowed, is given as

$$\Gamma = \frac{m_J}{16\pi}\frac{\sum_i m_{\nu_i}^2}{v_\sigma^2} \simeq 4.8\times 10^{-56}\,\mathrm{GeV}\left(\frac{m_J}{1\mathrm{eV}}\right)\left(\frac{v_\sigma}{10^{12}\,\mathrm{GeV}}\right)^{-2}, \tag{6.14}$$

where m_{ν_i} $(i = 1, 2, 3)$ denote the neutrino masses. We take $\sum_i m_{\nu_i}^2 = \Delta m_{12}^2 + \Delta m_{32}^2 \simeq (0.049\,\mathrm{eV})^2$ for a reference parameter. Here we assumed that the majoron is heavier than all the SM neutrinos. Otherwise the constraint is weaker or absent. For the majoron to be a viable DM candidate it must obey limits that follow from the CMB and structure formation [156–159,161]. These are quite relevant for the case of keV majorons and depend on whether the majorons are thermally produced or not (see [159] for a recent analysis). Since we will be considering light majorons with $m_J \ll O(1)$keV, these constraints are satisfied in most of the parameter regions.

Another restriction to majorons and their couplings follows from astrophysics. The predicted energy released in supernovae is consistent with the Standard Model, hence any additional particle that contributes significantly can be constrained by the SN1987A observations. From the process $\nu_\alpha\nu_\beta \to J$ one can place constraints on the coupling to neutrinos $g_{\nu_\alpha\nu_\beta}$ [170, 171], excluding a considerable part of the ($g_{\nu_\alpha\nu_\beta}$,m_J) plane [172],

$$2.1\times 10^{-10}\,\mathrm{MeV} \leq |g_{\nu_e\nu_e}| \times\ m_J \leq 10^{-7}\,\mathrm{MeV}\,. \tag{6.15}$$

However, this constraint does not apply for the strong coupling regime $10^{-6} \leq |g_{\nu_e\nu_e}|$, where the mean free path of the majoron is smaller than the radius of the core of the supernova and majorons cannot escape. Moreover, for the region of interest, $m_J \ll 10^2$ eV, the luminosity constraints are almost irrelevant for our model. As an example, taking $m_J = 1$ eV, the supernova constraint applies if: $2.1\times 10^{-4} \leq |g_{\nu_e\nu_e}| \leq 10^{-1}$. Note, however, that in the model we are considering the coupling is $|g_{\nu_e\nu_e}| \sim \frac{m_\nu}{v_\sigma}$ and, therefore, for the scales we consider for v_σ the constraint does not apply.

Turning to the coupling of the majoron to charged fermions, in our minimal type-I seesaw majoron model [78, 79] it arises at one-loop order and can be written as [173]

$$g_{Jll} \approx \frac{m_l}{8\pi^2 v_{EW}}\left[-\frac{1}{2}\mathrm{Tr}\left[\frac{m_D m_D^\dagger}{v_{EW}v_\sigma}\right] + \frac{(m_D m_D^\dagger)_{ll}}{v_{EW}v_\sigma}\right], \tag{6.16}$$

where $m_D \equiv y^\nu v_{EW}/\sqrt{2}$ is the Dirac mass matrix for neutrinos. Focusing on the case of electrons, one can show, after a bit of trivial algebra, that this reduces to

$$g_{Jee} \approx \frac{1}{8\pi^2} \frac{m_e}{v_{EW}} \frac{m_\nu}{v_{EW}} y_{\nu_R} \,. \tag{6.17}$$

For reasonable Yukawa couplings this leads to a tiny coupling well below the limits from stellar cooling.

In summary, the majoron couples to the SM particles only weakly and its lifetime is many orders of magnitude larger than the age of the Universe. Therefore, it provides a good dark matter candidate. As we will see shortly, the majorons can be produced non-thermally with small kinetic energy, and hence can be cold DM.

6.2 Primordial density of majorons

In this section, we give a quantitative estimate of the abundance of majorons produced either thermally or non-thermally in the early Universe. The cosmological history of our model, which was summarized at the beginning of this chapter, is given in Fig. 6.1. We will also discuss the signatures of the light, cold majoron and its possible detectability.

Thermal production

Before spontaneous breaking of the lepton symmetry, the scalar field σ interacts with the right-handed neutrinos and these interact with the SM leptons via the Yukawa interactions. The interaction brings all particles to thermal equilibrium until the scalar field obtains a VEV at the time of the lepton number violation phase transition.

After the spontaneous symmetry breaking of lepton number, the right-handed neutrinos obtain the effective masses via the Yukawa interaction. Their abundance becomes exponentially suppressed in the non-relativistic regime, where the temperature drops below their mass. Then the right-handed neutrinos decouple from the SM sector. The thermal energy density of majorons is given by

$$\rho_{\rm th} = \frac{\zeta(3)}{2\pi^2} T_J^3 m_J \,, \tag{6.18}$$

where T_J is the temperature of majorons. Since the majorons decouple from the SM sector at the time of spontaneous lepton number symmetry

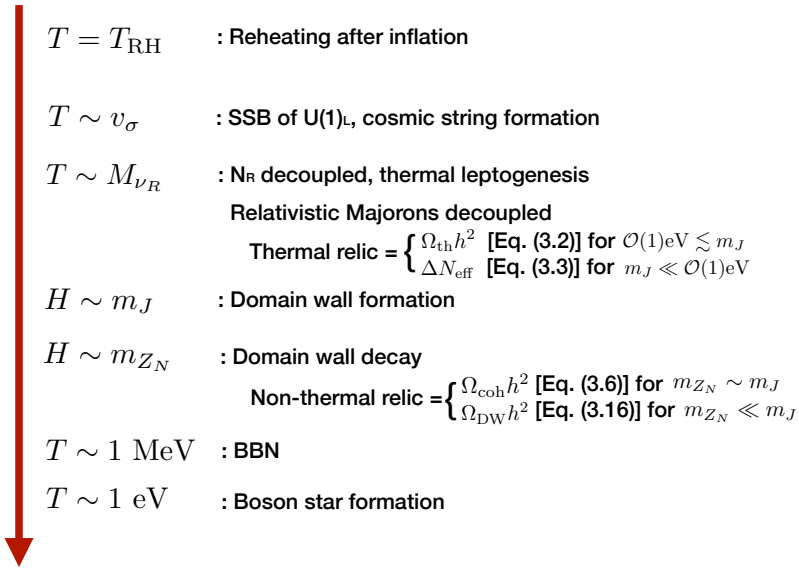

Figure 6.1: Cosmological history of our simple type-I seesaw majoron model. See text for details.

breaking, their relic abundance at present is calculated as

$$\Omega_{J,\rm th}h^2 \simeq g_*^{-1}\left(\frac{m_J}{12\,\rm eV}\right)e^{-t_0/\tau_J}, \tag{6.19}$$

where g_* ($= 106.75$) is the number of effective degrees of freedom at the time of decoupling, t_0 the age of the Universe and τ_J the majoron lifetime. Here we assumed that the majoron becomes non-relativistic before the matter-radiation equality, which is the case for $m_J \gtrsim \mathcal{O}(1)\,\rm eV$. Since we require $\Omega_{J,\rm th}h^2 \leq (\Omega_{J,\rm th}h^2)^{(\rm obs)} \simeq 0.12$, the majoron should be much lighter than $\mathcal{O}(100)\,\rm eV$.

If the majoron mass is of order the keV scale, its thermal velocity is not negligible during the matter-dominated epoch. The free-streaming of thermal relic majorons erases density perturbations on the small scales, which may be in contradiction with observations of large-scale structure [159][4]. A stringent constraint on the free-streaming length comes from the observa-

[4]Under certain circumstances, cold keV dark matter may also arise from decays and scatterings, see [174].

tion of the Lyman-α forest by the 21 cm line. This requires that the majoron mass is larger than about 5.3 KeV (see, e.g., Ref. [175] and references therein). This in principle excludes a thermally produced majoron with a mass $m_J \sim O(100)$ eV. Fortunately, ultralight majorons with $m_J \ll 1$ eV can be efficiently produced with the non-thermal production mechanisms that we will present in the next section. In this regime, the thermal production of majorons is negligible[5].

Notice that when the majoron mass is smaller than $\mathcal{O}(1)$ eV, its thermal relic behaves like dark radiation[6]. The energy density of dark radiation is conveniently parametrized by the "effective" number of neutrino species $N_{\rm eff}$. The deviation from the SM prediction is given by

$$\Delta N_{\rm eff} = \frac{4}{7}\left(\frac{g_*}{43/4}\right)^{-4/3} \simeq 0.027. \tag{6.20}$$

Bounds from primordial ^{4}He abundance constrain $\Delta N_{eff} \leq 0.33$ at 95% C.L [178, 179] if the majoron is relativistic during BBN. On the other hand, the cosmic microwave background (CMB) anisotropies are also sensitive to the energy density of the Universe and can put a constraint on $N_{\rm eff}$. The Planck collaboration reported the constraint as $N_{\rm eff} = 2.99 \pm 0.17$ [38], which is consistent with the SM prediction of $N_{\rm eff}^{\rm (SM)} \simeq 3.046$ [180]. The CMB-S4 experiment will improve the sensitivity as $\Delta N_{\rm eff} = 0.0156$ [181, 182]. We expect that a deviation from the SM prediction may be observed in the near future.

Non-thermal production

Majorons are produced non-thermally around the time when the Hubble parameter becomes comparable to the majoron mass, which we denote as $H_{\rm osc}$. Although it is technically difficult to distinguish them, there are three contributions for the non-thermal production of majorons: coherent oscillation of majorons, decay of cosmic strings and decay of domain walls. As we will see below, these contributions give comparable amounts of primordial majorons. The discussion below is analagous to the misalignment mecha-

[5] We will not consider the possibility of freeze-in production of majorons, which might require extensions beyond the minimal type-I seesaw model.

[6] See, e.g., Refs. [176, 177] for other models of dark radiation.

nism reviewed in section 4.1.0.2 but we will also consider non-relativistic majorons coming from the decay of the topological defects.

Since we consider the case where lepton number symmetry breaking occurs after inflation, the phase direction of σ, that is the majoron field direction, is randomly distributed with a correlation length of the order of the Hubble radius at the time of the phase transition. When the initial state angle is not aligned with the explicit symmetry breaking minimum, the majoron starts to oscillate coherently at the time when $H_{\rm osc} \simeq m_J/3$. The temperature of the thermal plasma at this time is given by

$$T_{\rm osc} \simeq 5 \times 10^2\,{\rm GeV} \left(\frac{m_J}{1\,{\rm meV}}\right)^{1/2}, \tag{6.21}$$

where we used $g_* = 106.75$ as the effective number of relativistic degrees of freedom. The energy density of coherent oscillation of majorons can therefore be estimated by taking an average over the flat distribution as

$$\rho_{\rm coh} \simeq \frac{1}{2\pi} \int m_J^2 v_\sigma^2 (1-\cos\theta) d\theta = m_J^2 v_\sigma^2, \tag{6.22}$$

where we assumed a majoron potential, $V \sim m_J^2 v_\sigma^2 (1-\cos\theta)$, with $\theta = J/v_\sigma$, and neglected the anharmonic effect around the top of the potential. The energy fraction from this contribution is given by[7]

$$\Omega_{\rm coh} h^2 \simeq 0.05 \left(\frac{m_J}{1\,{\rm meV}}\right)^{1/2} \left(\frac{v_\sigma}{10^{12}\,{\rm GeV}}\right)^2 e^{-t_0/\tau_J}. \tag{6.23}$$

Because of the hierarchy of energy scales between the lepton number violation scale and the majoron mass, there are two kinds of phase transitions associated to the majoron. The first one is the phase transition associated to the σ VEV, $\langle\sigma\rangle = v_\sigma/\sqrt{2}$, around the time when $T \sim v_\sigma$. We denote the temperature and the Hubble parameter at this time as T_1 and H_1, respectively. We consider the case where $m_J \ll H_1$ so that the explicit $U(1)_L$ symmetry breaking term is negligible at the time of the first phase transition.

[7]Note that when the majoron lifetime is of the same order as the age of the Universe its decay is relevant in computing the relic density today. On the other hand, for lifetimes $\tau \geq O(10)\,t_0$, the effects of majoron decay become negligible and the e^{-t_0/τ_J} factor is close to 1.

Since the phase of the σ field is distributed randomly, cosmic strings form after the first phase transition. The tension of the string is determined by the lepton number breaking VEV as

$$\mu_{\rm string} \simeq \pi v_\sigma^2 \ln \frac{L}{d}, \tag{6.24}$$

where $d \sim 1/m_\rho$ is the core width of cosmic strings and L is an infrared cutoff determined below. The dynamics of comic strings is complicated but can be qualitatively understood by causality. When a cosmic string collides with another cosmic string, they are connected to form longer cosmic strings. Since the typical velocity of cosmic strings does not exceed order unity, the number of cosmic string within one Hubble volume is also of order one. The infrared cutoff L is taken to be $\sim 1/H$ because the typical distance between cosmic strings is of order $1/H$.

When the Hubble parameter decreases down to m_J, the explicit $U(1)_L$ symmetry breaking term becomes relevant and the second phase transition with domain wall formation occurs. Because of the explicit symmetry breaking term, each cosmic string becomes attached by domain walls. The tension of the domain wall is determined by the $U(1)_L$ symmetry breaking term and the σ field VEV as

$$\sigma_{\rm wall} \simeq \frac{8}{N^2} m_J v_\sigma^2 \,. \tag{6.25}$$

We also introduce the domain wall number N_{DW} for later convenience, which is equal to unity when high-dimensional operators break $U(1)_L$ completely.

The cosmic strings start to shrink to a point due to the tension of the domain wall after the second phase transition. They disappear when the tension of the domain wall exceeds that of the cosmic string

$$\sigma_{\rm wall} = H_{\rm decay} \mu_{\rm string}, \tag{6.26}$$

which corresponds to a Hubble parameter $H = H_{\rm decay}$, given by

$$H_{\rm decay} \simeq \frac{8}{\pi} \left(\ln \frac{m_\rho}{H_{\rm decay}} \right)^{-1} m_J \quad (\sim H_{\rm osc}), \tag{6.27}$$

where we used $N_{DW} = 1$. Majorons are produced from the decay of these topological defects. Noting that the number of cosmic strings within one

Hubble volume is of order unity before they disappear, the energy density of cosmic strings can be estimated by

$$\rho_{\rm string} \sim \frac{2H_{\rm decay}^{-1}\mu_{\rm string}}{4\pi/3H_{\rm decay}^{-3}} \simeq \frac{96}{\pi^2}\left(\ln\frac{m_\sigma}{H_{\rm decay}}\right)^{-1} m_J^2 v_\sigma^2. \tag{6.28}$$

In a similar way, the energy density of domain walls can be estimated by

$$\rho_{\rm DW} \sim \frac{4\pi H_{\rm decay}^{-2}\sigma_{\rm wall}}{4\pi/3H_{\rm decay}^{-3}} \simeq \frac{192}{\pi}\left(\ln\frac{m_\sigma}{H_{\rm decay}}\right)^{-1} m_J^2 v_\sigma^2. \tag{6.29}$$

The typical energy of majorons produced from this process is of order $H_{\rm decay}$, which is the only parameter determining the dynamical time scale of topological defects. Since $H_{\rm decay} \sim m_J$, the majorons become non-relativistic soon after they are produced [183]. Note that the energy densities (6.28) and (6.29) are comparable to (6.22) and hence we can use (6.23) for an order of magnitude estimate of the majoron relic density. The result is shown in Fig. 6.2. Notice that, along the red line one can explain the observed amount of dark matter as cold majorons arising from these three processes. In the shaded regions, majorons are overproduced by the thermal (right region) or the non-thermal (upper region) processes.

We now turn to the case where the energy scale where all discrete symmetries are broken by higher dimensional operators is much smaller than the majoron mass. This is possible if the $U(1)_L$ symmetry is broken to Z_N at the energy scale of m_J and then the residual Z_N symmetry is broken explicitly by another operator. This is related to the fact that we need at least two higher-dimensional operators with coprime powers in σ to break completely the $U(1)_L$ symmetry at the energy scale of m_{Z_N} ($\ll m_J$). In this case, each cosmic string is attached by N domain walls after the phase transition of $U(1)_L$ to Z_N. Although the cosmic string is pulled by the domain walls, the collective effect of N domain walls does not make the cosmic string to shrink to a point. Therefore the cosmic string and domain wall network will survive until the effect of explicit Z_N breaking becomes efficient.

We now proceed to estimate the effect of these *long-lived* majoron domain walls. Suppose that the explicit Z_N breaking generates a typical difference of vacuum energies among the N vacua given by $V_{\rm dif}$. The energy differences lead to vacuum pressure on the domain walls. When the vacuum pressure becomes stronger than the tension of the domain walls, the lowest

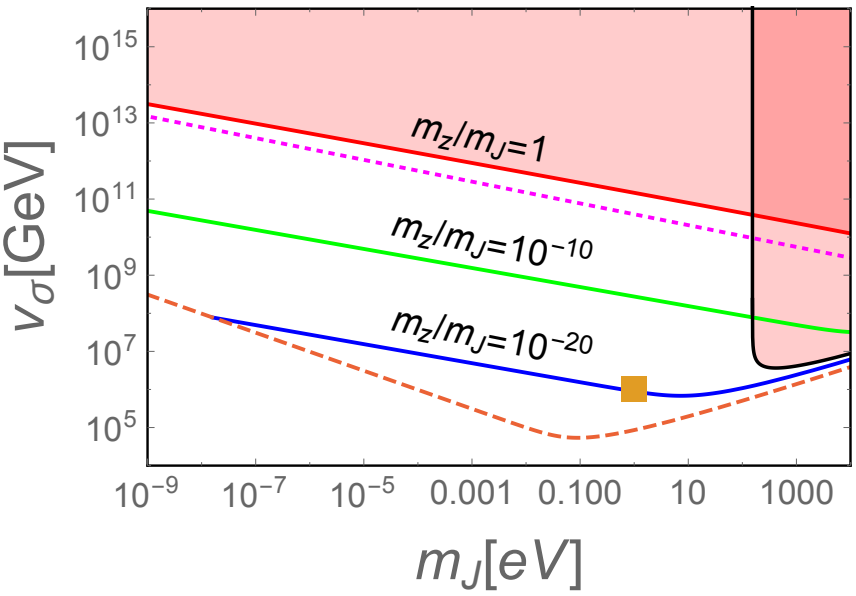

Figure 6.2: Constraints on the majoron dark matter scenario. Within the shaded regions, thermal (right vertical band) and non-thermal (upper region) majorons are overproduced. By changing the ratio $m_J/m_{Z_N} = 1$, 10^{10}, and 10^{20}, one can account for the observed amount of dark matter along the red, green, and blue lines, respectively. The region below the orange dashed line cannot explain the observed dark matter due to the requirements in Eqs. (6.34) and (6.35). The square dot at $m_J = 1\,\mathrm{eV}$ and $v_\sigma = 10^6\,\mathrm{GeV}$ represents the parameter region in which neutrino signals from majoron decay would be observable by the PTOLEMY experiment. Above the magenta dotted line the majoron may form dilute boson stars, see Sec. 6.4, while in the region below that line it would form dense boson stars, provided it has a repulsive quartic interaction.

vacuum state will dominate the entire Universe and the string-wall system will disappear. Noting that a typical length scale of the network is given by H^{-1}, the condition that the vacuum pressure exceeds the domain wall tension is given by

$$V_{\rm dif} > H\sigma_{\rm wall}. \tag{6.30}$$

The network disappears at the threshold of the above condition:

$$H_{\rm decay}(\equiv m_{Z_N}) \simeq \frac{V_{\rm dif}}{\sigma_{\rm wall}}. \tag{6.31}$$

The energy density of majorons produced by the domain-wall decay is given by

$$\rho_{\rm DW} \sim \frac{4\pi H_{\rm decay}^{-2} N_{DW} \sigma_{\rm wall}}{4\pi/3 H_{\rm decay}^{-3}} \simeq \frac{24}{N_{DW}} \left(\frac{m_{Z_N}}{m_J}\right) m_J^2 v_\sigma^2, \tag{6.32}$$

at $H = H_{\rm decay}$ ($\equiv m_{Z_N}$). It follows that the relic density at present is:

$$\Omega_{\rm DW} h^2 \sim N_{DW}^{-1} \left(\frac{m_J}{m_{Z_N}}\right)^{1/2} \left(\frac{m_J}{1\,{\rm meV}}\right)^{1/2} \left(\frac{v_\sigma}{10^{12}\,{\rm GeV}}\right)^2 e^{-t_0/\tau_J}. \tag{6.33}$$

The relation between m_J and v_σ for a fixed $\Omega_{\rm DW} h^2$ can be changed by choosing a different m_{Z_N} (or $V_{\rm dif}$). This is shown in Fig. 6.2, where the red, green, and blue lines represent $\Omega_{\rm DW} h^2 = 0.12$ for $m_J/m_{Z_N} = 1$, 10^{10}, and 10^{20}, respectively. While these may seem unnaturally large values for the ratio, one must keep in mind that their relative size is controlled by a power of (M_P/v_σ), since m_J and m_{Z_N} can come from different high-dimensional operators and is expected to be large.

Since we are interested in the case where the majorons produced from these topological defects constitute the dark matter, they must be produced before the matter-radiation equality. The reason is that since this majoron domain walls are topological defects in the phase direction of σ, they can decay only into majorons and gravitational waves (gravitons). These particles do not interact with the SM particles efficiently and, as a result, they do not spoil Big-Bang Nucleosynthesis (BBN). This requirement constrains $H_{\rm decay} \equiv m_{Z_N}$ to be

$$m_{Z_N} \gg 1.6 \times 10^{-37}\,{\rm GeV}. \tag{6.34}$$

Combining with $\Omega_{\rm DW} h^2 \lesssim 1$, this ensures that the domain walls disappear before dominating the energy density of the Universe [166]:

$$\rho_{\rm DW}(H_{\rm decay}) \ll 3 M_{\rm Pl}^2 H_{\rm decay}^2 \quad \leftrightarrow \quad \frac{m_{Z_N}}{m_J} \gg \frac{8}{N_{DW}} \left(\frac{v_\sigma}{M_{\rm Pl}}\right)^2. \tag{6.35}$$

From these constraints, we cannot take arbitrary small m_J or v_σ to explain the observed amount of dark matter. This is shown as the orange dashed line in Fig. 6.2, below which $\Omega_{\rm DW} h^2$ cannot reproduce the observed amount of dark matter ($\simeq 0.12$) consistently with (6.34) and (6.35). Note that for larger majoron masses its decay becomes relevant. This is due to the e^{-t_0/τ_J} factor in the relic densities (see Eqs.(6.19), (6.23) and (6.33)) and explains why larger values for m_J are allowed by thermal production constraints

provided v_σ is not larger than $\mathcal{O}(10^7)$ GeV. This is the case of the well-known keV majoron [155–159, 161, 184] which would lie in the region between the boundary of the shaded region and the dashed orange line. This majoron behaves as decaying warm dark matter when it is thermally produced.

6.3 Possible signatures

Apart from generic signatures associated to neutrino masses and mixing, such as neutrino oscillations [185] and neutrinoless double beta decay [186], the majoron scenario can lead to more specific processes involving majoron emission. For example, majoron emission in neutrinoless double beta decay has been suggested long ago [187]. In our simplest singlet majoron setup, the coupling of the majoron to matter is too weak for an observable impact on neutrinoless double beta decay experiments.

However, as we will see now, this light and cold majoron may induce interesting signatures that might perhaps lie within the capabilities of upcoming cosmological observations.

PTOLEMY

We now comment on the possibility that the majoron can be observed by direct detection experiments for cosmic neutrinos, like PTOLEMY. If the lifetime of the majoron is of order $10-100$ times longer than the age of the Universe and its mass is $\mathcal{O}(1)\,\text{eV}$, one expects that PTOLEMY experiment will observe signals of neutrinos produced from the majoron decay [162,163]. From (6.14), we require $v_\sigma = \mathcal{O}(10^6)\,\text{GeV}$ to make the $\mathcal{O}(1)\,\text{eV}$ majoron decay at around $(10-100)t_0$. This is plotted as a square dot in Fig. 6.2. We note that such light and relatively short-lived majorons cannot be efficiently produced from the coherent oscillation (see (6.23)). However, they can be produced appreciably via the domain-wall decay if there remains a residual Z_N symmetry below the energy scale of m_J. From (6.33), we can see that the majoron can make up all of the dark matter if $m_J/m_{Z_N} \sim 10^{20}$. This is consistent with the constraints (6.34) and (6.35).

6.4 Majoron stars

Before closing this chapter we will study the possibility that DM majorons form a very particular astrophysical object: boson stars. Indeed, this will be particularly relevant if the bulk of majoron DM comes from the decay of the string-wall network.

It is known that an oscillating real scalar field may form a quasi-stable localized clump under certain conditions[8]. When the second derivative of the potential for the scalar field is smaller for a larger field value, one can find such a localized solution, called an oscillon. There is also a solution stabilized by the gravitational interaction, in which case the solution is called a boson star. There are several formalisms to calculate the configuration of these objects [189–194]. In the following qualitative discussion we follow the formalism developed in Ref. [193], which is accurate enough for our purpose.

The configuration is determined by the balance amongst the gradient energy, the potential energy, and the gravitational potential energy. For the case of the majoron, the leading self-interaction (the four-point interaction) can be either an attractive or a repulsive force. When the self-interaction is attractive, a smaller configuration is preferred to minimize the potential energy and the gravitational potential energy, while a smooth and broader configuration is favoured to minimize the gradient energy. On the other hand, when the self-interaction is a repulsive force, it prefers a larger configuration. The size of the stable configuration is therefore determined by the balance of these effects.

We can estimate the typical values of the gradient energy, potential energy, and the gravitational potential energy normalized to $m_J^2\phi^2$ as:

$$\begin{aligned} \delta_x &\sim \frac{(\nabla\phi)^2}{m_J^2\phi^2} \sim (m_J R)^{-2}, \\ \delta_V &\sim \frac{|\lambda_4|\phi^4}{m_J^2\phi^2}, \\ \delta_g &\sim \Psi \sim \frac{1}{M_{\rm Pl}^2}\int \frac{m_J^2\phi^2}{r} d^3r \sim \frac{m_J^2\phi^2}{M_{\rm Pl}^2} R^2, \end{aligned} \tag{6.36}$$

In the above equation R is the radius of the boson star and ϕ is a field value at the center of the boson star. In our case, the majoron J will play

[8] See, e.g., Ref. [188] in the context of the QCD axion. Boson star formation may also occur in the context of axion-like particle models.

the role of ϕ. We generically denote the quartic interaction coupling of the majoron as λ_4. Being a pseudo-Nambu-Goldstone boson, in absolute value, this self-interaction is given by $|\lambda_4| \sim m_J^2/v_\sigma^2$. The mass of the boson star is roughly given by $M \sim m_J^2 \phi^2 R^3$. When the potential energy is negligible, the configuration is determined by the balance $\delta_x \sim \delta_g$, which gives:

$$M \sim \left(\frac{M_{\rm Pl}}{m_J}\right)^2 \frac{1}{R}. \tag{6.37}$$

This kind of configuration is known as a dilute boson star. The critical radius R_c below which the self-interaction is relevant can be estimated by the condition $\delta_V \sim \delta_x \sim \delta_g$. This leads to:

$$\begin{aligned} R_c &\sim \frac{\sqrt{|\lambda_4|}M_{\rm Pl}}{m_J^2} \simeq 5 \times 10^2\,{\rm m} \left(\frac{m_J}{1\,{\rm meV}}\right)^{-1} \left(\frac{v_\sigma}{10^{12}\,{\rm GeV}}\right)^{-1}, \\ M_c &\sim \frac{M_{\rm Pl}}{\sqrt{|\lambda_4|}} \simeq 4 \times 10^{18}\,{\rm g} \left(\frac{m_J}{1\,{\rm meV}}\right)^{-1} \left(\frac{v_\sigma}{10^{12}\,{\rm GeV}}\right), \end{aligned} \tag{6.38}$$

where M_c is the critical mass.

When the self-interaction is an attractive force, the dilute boson star branch, (6.37), is connected to a dense boson star branch around $R = R_c$. The configuration is then determined by the attractive self-interaction and the gradient energy. The dense boson star branch has two types of solutions: an unstable solution and a stable one. The dilute boson star branch is connected to the unstable branch, which is shown as a dashed blue curve in Fig. 6.3.

When the self-interaction is a repulsive one, the boson star is stabilized by the attractive gravitational force and the repulsive self-interaction when its mass is larger than the critical mass. The solution (6.37) is therefore connected to a branch that is determined by the balance $\delta_V \sim \delta_g$. Since this condition gives a constant radius $R \sim R_c$, the branch is asymptotic to R_c as we can see from Fig. 6.3.

Now we shall consider the formation of boson stars. Since the initial field value of the majoron is random and since the dynamics of the topological defects is complicated, majorons produced from these mechanisms have $\mathcal{O}(1)$ fluctuations at the time of their production. Due to causality, maintained within the Hubble volume, the wavelength of the fluctuations is of order $1/H_{\rm decay}$. The non-thermally produced majorons inside the comov-

ing volume of this scale result in the formation of a compact object due to the gravitational instability during the matter dominated era. We also note that the relaxation time scale via the self-interactions is much shorter than the Hubble expansion rate [195]. All in all, the typical mass of the object is then given by [196]:

$$\begin{aligned} M &\sim \frac{4\pi}{3} H_{\rm decay}^{-3} \rho_J(T_{\rm decay}) \\ &\simeq 2\times 10^{14}\,{\rm g}\times N_{DW}^{-1}\left(\frac{m_J}{m_{Z_N}}\right)^2\left(\frac{m_J}{1\,{\rm meV}}\right)^{-1}\left(\frac{v_\sigma}{10^{12}\,{\rm GeV}}\right)^2, \end{aligned} \tag{6.39}$$

where we used (6.32) for ρ_J and $H_{\rm decay} \equiv m_{Z_N}$. The ratio between M and the critical mass, M_c, is given by

$$\frac{M}{M_c} \sim 3\times 10^{-5}\times N_{DW}^{-1/2}\left(\frac{m_{Z_N}}{m_J}\right)^{-7/4}\left(\frac{m_J}{1\,{\rm meV}}\right)^{-1/4}, \tag{6.40}$$

where we assumed $\Omega_{\rm DW}h^2 = 0.12$ and used Eq.(6.33) to eliminate v_σ dependence. Note that the kinetic energy of majorons is extremely small and their typical de Broglie wavelength is of order $1/H_{\rm decay}$ at the time of their production. Then a typical occupancy number of majorons is given by

$$\mathcal{N} \sim \frac{4\pi}{3} H_{\rm decay}^{-3}\frac{\rho_J(T_{\rm decay})}{m_J} \sim 10^{50}\times N_{DW}^{-1}\left(\frac{m_J}{m_{Z_N}}\right)^2\left(\frac{m_J}{1\,{\rm meV}}\right)^{-2}\left(\frac{v_\sigma}{10^{12}\,{\rm GeV}}\right)^2. \tag{6.41}$$

This extremely large occupancy number implies that majorons form a Bose-Einstein condensate. As the perturbations grow, a gravitationally bound object, called a boson star, forms for each condensation. When $M \lesssim M_c$, the size of the boson star is determined by the offset between the kinetic energy and the gravitational potential energy as in Eq.(6.37). We then obtain

$$R \sim \frac{1}{M}\left(\frac{M_{\rm Pl}}{m_J}\right)^2 \sim 10^7\,{\rm m}\ \times N_{DW}\left(\frac{m_J}{m_{Z_N}}\right)^{-2}\left(\frac{m_J}{1\,{\rm meV}}\right)^{-1}\left(\frac{v_\sigma}{10^{12}\,{\rm GeV}}\right)^{-2}, \tag{6.42}$$

where we use Eq.(6.39) in the last equality. Note that (6.42) can be rewritten as

$$R \sim H_{\rm decay}^{-1}\left(\frac{a(T_{\rm eq})}{a(T_{\rm decay})}\right)\left(\frac{m_J}{m_{Z_N}}\right)^{-2}, \tag{6.43}$$

where $T_{\rm eq}$ is the temperature at the matter-radiation equality. This means that the typical size of boson stars is of the same order with the wavelength of the perturbations at the matter-radiation equality for the case of $m_{Z_N} \sim m_J$.

On the other hand, when $M \gtrsim M_c$, the potential energy becomes relevant. If the interaction is attractive, a boson star, called a dense boson star, may or may not form. If it forms, the typical lifetime of this kind of boson star is relatively short and may not survive on a cosmological time scale. Therefore we do not consider this case further. In contrast, if the interaction is repulsive, the size of boson star is given by the critical radius, R_c, which is determined by the offset between the repulsive potential energy and the gravitational potential energy. The threshold at which $M = M_c$ is shown as a magenta dotted line in Fig. 6.2, where we assume that the total amount of non-relativistic majorons is equal to the observed amount of dark matter. Above the line, dilute (gravitational) boson stars form after the matter-radiation equality. We can see that this is the case when the $U(1)_L$ is completely broken at $H = m_J$. It is known that the lifetime of the dilute boson star is exponentially long, so that it is stable on cosmological time scales [190, 193, 197, 198]. On the other hand, below the magenta dotted line, where $M > M_c$, boson stars may or may not form depending on the sign of the quartic interaction. One expects a stable boson star to form for the repulsive case.

Next, we comment on the effect of boson stars on the neutrino production rate from majoron decay. The neutrino production rate from a boson star may be saturated by the Pauli statistics near its surface if the density of majorons is high enough in the boson star [199, 200]. We can check if this is the case by calculating the total neutrino production rate from the majorons inside a boson star and comparing it with the upper bound of the flux from the boson star with radius R. The former quantity is given by the number of majorons inside a boson star, $\mathcal{N}$, times the decay rate of individual majorons Γ, while the latter one is [199]

$$\left(\frac{dN}{dt}\right)_{\rm sat} \simeq \frac{m_J^3 R^2}{24\pi}. \tag{6.44}$$

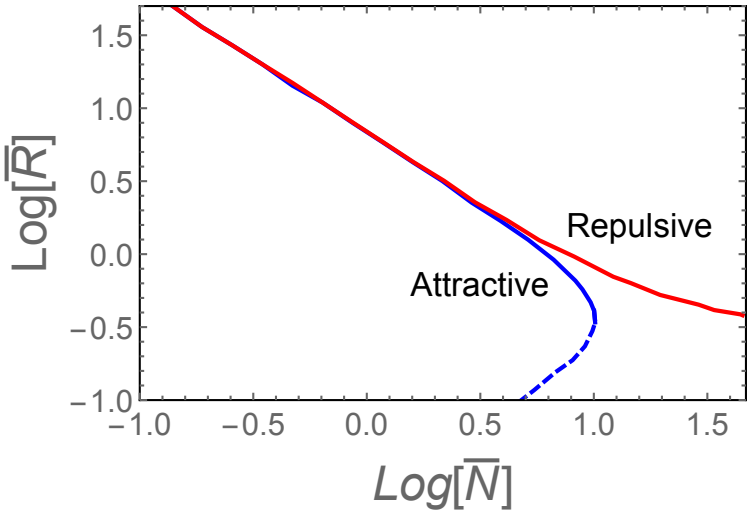

Figure 6.3: Phase diagram of boson stars for the majoron with either an attractive (blue line) or a repulsive (red line) interaction. The dashed blue line represents an unstable branch. The vertical axis is normalized by the critical radius R_c and the horizontal axis is normalized by the occupancy number at the critical radius.

The ratio is given by

$$\mathcal{N}\Gamma\left(\frac{dN}{dt}\right)^{-1}_{\rm sat} \simeq \left\{ \begin{array}{c} 3\times 10^{-17}\left(\dfrac{m_{Z_N}}{m_J}\right)^{-5}\left(\dfrac{m_J}{\rm mev}\right)^{-3} \text{ for } M<M_c \\ 3\times 10^{-8}\left(\dfrac{m_{Z_N}}{m_J}\right)^{-3/2}\left(\dfrac{m_J}{\rm mev}\right)^{-5/2} \text{ for } M>M_c \end{array} \right\} \quad (6.45)$$

where we assumed $\Omega_{\rm DW}h^2 = 0.12$. If this is larger than unity, the neutrino production rate is saturated by the Pauli exclusion principle and is given by (6.44). This is the case for a small m_{Z_N}/m_J.

In fact, for example, the ratio is of order 10^{15} for $m_J = 1\,\text{eV}$, $m_{Z_N}/m_J = 10^{-20}$, and $v_\sigma = 10^6\,\text{GeV}$. Since the neutrino production rate is many orders of magnitude suppressed by Pauli statistics, the neutrino signal may not be observable in this scenario. However, the efficiency of boson star formation may not be so high that all of non-relativistic majorons go into boson stars. We should note that a typical boson star size R is many orders of magnitude smaller than the initial size of density perturbations for a small m_{Z_N}/m_J. Since the initial density perturbations are not completely spherical, a significant energy density of majorons may not be absorbed by

the boson star. Therefore it could happen that most of the non-relativistic majorons exist in the Universe without forming a boson star. If this is the case, the prediction of the neutrino signal does not change qualitatively. In any case, it would be interesting to extend the present work and perform a quantitative estimation of the amount of majorons that form dense boson stars.

Summary

In this chapter, based on reference [153], we have studied in detail a situation where the cosmological DM is composed of majorons, the Nambu-Goldstone boson associated to the spontaneous breaking of the lepton number symmetry. We have challenged the standard picture where the majoron is a thermal DM candidate and studied in detail the different non-thermal contributions to the majoron abundance: coherent oscillations around the potential minimum and the decay of topological defects. In particular, we have found that a $O(0.1-1)$ eV majoron is a viable dark matter candidate with lifetime a few orders of magnitude longer than the age of the Universe. The decay of such a light and short lived majoron might be observed in direct detection experiments of cosmic neutrinos, such as PTOLEMY (see Fig.(6.2)).

These non-relativistic light majorons have large density perturbations because they are produced from the decay of topological defects. We have considered for the first time in the context of the majoron that these over-dense regions may condense forming boson stars after the matter-radiation equality. We have qualitatively discussed the properties of these boson stars, including their size and mass. Interestingly enough - and unlike other light bosons such as axions - the majoron can have an attractive or repulsive leading self-interaction. We have shown that depending on this self-interaction the properties of majoron stars differ substantially. While for the attractive self-interaction case we only have stable dilute boson stars, dense boson stars may form for the repulsive case.

Chapter 7

Colored Scotogenic

As we have seen in Chapter 4, due to the requirement of feeble interactions with the visible sector, the DM candidates are usually asssumed to be electrically neutral and without color charge. However, in recent years there has been a surge in interest in DM candidates that challenge these assumptions. In this chapter we will consider the case of composite DM, studied in detail in [201]. In this reference, the authors suggest that DM may be in the form of an hadron composed of two stable color octet Dirac fermions, $\mathcal{Q}$, with mass around 12.5 TeV. Of course, the interest of this idea may go well beyond QCD since, as we will see later in Chapter 8, analogous bound-state DM candidates emerge in models with a new confining hypercolor interaction [202].

In this chapter, based in [203, 204], after reviewing the basics of the bound-state DM scenario, we propose the possibility that these new particles are also involved in the generation of neutrino masses *à la* scotogenic [49]. We will consider the possibility of having Majorana neutrinos and also a Dirac version of the colored scotogenic model. In the case of Dirac neutrinos, their Dirac nature is tightly connected to the DM stability. We also study the basic phenomenological implications of the model, such as lepton flavor violation (LFV) processes, which occurs for the Dirac and Majorana versions, and neutrinoless double-beta decay for the case of Majorana neutrinos. Finally, we will also discuss how this scenario can be tested with future hadron colliders.

7.1 Bound-state Dark Matter

When a new heavy colored state is introduced in the theory, new QCD bound-states can form. Since we will consider a fermion transforming under the SM gauge symmetry as

$$\mathcal{Q} \sim (8, 1, 0)\,, \tag{7.1}$$

two different possibilities arise. The first bound-state that we can form, which we denote as $\mathcal{Q}\mathcal{Q}$, involves only the new fermion and is characterized by a small Bohr-like radius, $a_B \sim M_{\mathcal{Q}}^{-1}$, and a large binding energy, $E_B \sim \alpha_s^2 M_{\mathcal{Q}}$. On the other hand, hybrid configurations such as $\mathcal{Q}g$ and $\mathcal{Q}q\bar{q}$ can form when the new colored fermion hadronizes together with a gluon or a SM quark, respectively. These *hybrids* have a larger size, $\sim \Lambda_{QCD}^{-1}$, and smaller binding energy, comparable to the QCD scale. Their larger size leads to large cross-sections and, therefore, these configurations are severly constrained [205].

Fortunately, due to their large binding energy, the *pure* configuration, $\mathcal{Q}\mathcal{Q}$, constitutes the ground state and is the one that will populate the Universe after these particles thermalize. Indeed, after solving the Boltzmann equations, the authors of [201] find that $\mathcal{Q}\mathcal{Q}$ states can reproduce the observed DM abundance, $\Omega_{DM}h^2 \approx 0.12$, when their mass is:

$$M_{\mathcal{Q}} = 12.5 \pm 1 \text{ TeV}\,. \tag{7.2}$$

This mass scale is close to the one which is naively expected after a rescaling of the WIMP miracle result (see Chapter 4). Dangerous hybrids, on the other hand, are found to be subdominant by a factor 10^4.

Bound-state dark matter will impart nuclear recoil in underground dark matter search experiments. By using EFT techniques, the spin-independent direct detection cross-section can be estimated as [201]:

$$\sigma_{\text{SI}} \approx 2 \times 10^{-45} \text{ cm}^2 \left(\frac{20 \text{ TeV}}{M_{\mathcal{Q}\mathcal{Q}}}\right)^6 \frac{\Omega_{\mathcal{Q}\mathcal{Q}}}{\Omega_{\text{Planck}}}\,, \tag{7.3}$$

strongly correlated to the dark matter mass, $M_{\mathcal{Q}\mathcal{Q}} = 2M_{\mathcal{Q}}$, as shown in the red line in Fig. 7.1. In this figure the star corresponds to the case where our bound-state DM makes up 100% of the cosmological dark matter. In the presence of an additional dark matter particle, such as the axion, bound-

state dark matter masses below 25 TeV can be envisaged, as indicated by the red line. In this case their contribution to the relic density will be correspondingly smaller, while the spin-independent cross section would be correspondingly larger. The blue line denotes the current Xenon1T limit after 1.0 t×yr exposure [206]. This should be compared with the future sensitivities expected at XENON1T (2 t×yr) [207], LZ [208] and DARWIN [209] indicated by the black (dashed, dot-dashed and dotted) lines. We also note that, within the standard thermal cosmological scenario, DM masses above 25 TeV are ruled out by current observations of the Planck collaboration [38] (gray band). Notice also that the current LHC limit of 2 TeV [210, 211], implies that the cross section is always small enough so as to have the bound-state dark matter candidate reaching underground detectors.

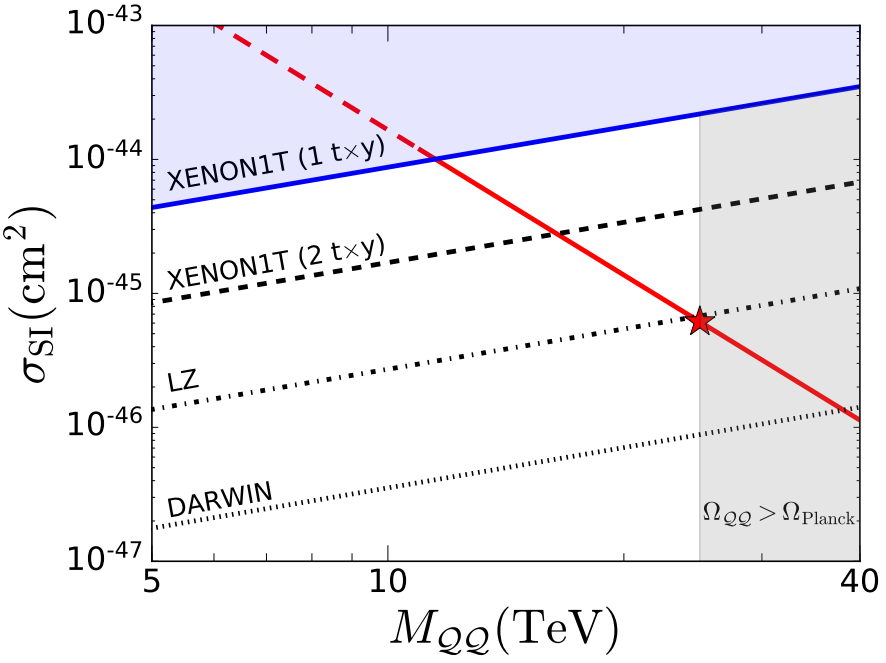

Figure 7.1: Spin-independent cross section as a function of $M_{\mathcal{Q}\mathcal{Q}} = 2M_{\mathcal{Q}}$ (red line). The star represents the mass required for a thermal bound-state 25 TeV dark matter. Lower values can be probed by direct searches, the current bound is indicated in blue, while the black lines (dashed, dotted and dot-dashed) correspond to future sensitivities. See text for details.

7.2 The Dirac case

The Dirac nature of neutrinos may ensure dark matter stability [212]. Here we present a variant realization of this idea where dark matter is present today in the form of stable neutral hadronic thermal relics. For definiteness we assume DM is a neutral bound-state of colored constituents, such as $\mathcal{Q}\mathcal{Q}$, where $\mathcal{Q}$ is the vector-like color octet isosinglet fermion. A necessary and sufficient condition for dark matter stability in this case is the presence of a global $U(1)$ symmetry, under which the $\mathcal{Q}$ is charged. In this section we present a model where the role of such apparently *ad-hoc* symmetry is played by the usual $B-L$ symmetry present in the SM. In fact, in our model, dark matter stability and the Dirac nature of the exotic fermion $\mathcal{Q}$ and of the neutrinos are all equivalent, and result from $B-L$ conservation.

In addition to the heavy Dirac fermion, our model introduces extra scalars. These states ensure that at least two neutrino masses are nonzero as required by the neutrino oscillation data in order to account both for solar and atmospheric mass scales [54, 185]. This simple picture can account for current neutrino oscillation and dark matter phenomena, and can be falsified relatively soon in nuclear recoil experiments (see Fig. 7.1). Moreover, the extra colored states, including scalar bosons, may lead to new phenomena at a next generation hadron collider [213].

As a theory preliminary, we recall that, within the type-I seesaw mechanism with a single right-handed neutrino, two neutrinos remain massless after the seesaw [44]. This degeneracy is lifted by calculable loop corrections. Here we propose a variant radiative seesaw scheme, in which a single colored fermion Dirac messenger $\mathcal{Q}$ is introduced, charged under the $\mathrm{U}(1)_{B-L}$ symmetry, plus two sets of colored scalars (see table 7.1). This situation resembles a $(n_N, n_\eta) = (1, 2)$ case of the general scotogenic model, studied in Sec.2.3.

Apart from the right-handed neutrinos, which are introduced to account for small Dirac neutrino masses, all of the new particles are colored. For definiteness, we assign them to the octet $\mathrm{SU}(3)_c$ representation [1]. We also impose that the $B-L$ symmetry holds, together with a Z_2 symmetry. The former ensures that $\mathcal{Q}$ has only a Dirac-type mass term, while the latter forbids the tree-level Dirac neutrino mass terms from $\overline{\nu_{Ri}}\widetilde{H}^\dagger L_j$. The relevant Lagrangian for neutrino masses contains the following new terms

[1] Notice, however, that our neutrino mass discussion also holds if they had different $\mathrm{SU}(3)_c$ transformation properties.

Particles	$\mathrm{U}(1)_{B-L}$	$(\mathrm{SU}(3)_c, \mathrm{SU}(2)_L)_Y$	Z_2
$Q_i = \begin{pmatrix} u_L & d_L \end{pmatrix}_i^{\mathrm{T}}$	$+1/3$	$(\mathbf{3},\mathbf{2})_{1/6}$	$+$
$\overline{u_{Ri}}$	$-1/3$	$(\overline{\mathbf{3}},\mathbf{1})_{-2/3}$	$+$
$\overline{d_{Ri}}$	$-1/3$	$(\overline{\mathbf{3}},\mathbf{1})_{1/3}$	$+$
$L_i = \begin{pmatrix} \nu_L & e_L \end{pmatrix}_i^{\mathrm{T}}$	-1	$(\mathbf{1},\mathbf{2})_{-1/2}$	$+$
$\overline{e_{Ri}}$	$+1$	$(\mathbf{1},\mathbf{1})_{1}$	$+$
$\overline{\nu_{Ri}}$	$+1$	$(\mathbf{1},\mathbf{1})_{0}$	$-$
$\mathcal{Q}_L$	$-r$	$(\mathbf{N}_c,\mathbf{1})_0$	$+$
$\overline{\mathcal{Q}_R}$	r	$(\mathbf{N}_c,\mathbf{1})_0$	$+$
H	0	$(\mathbf{1},\mathbf{2})_{1/2}$	$+$
σ_a	$1-r$	$(\mathbf{N}_c,\mathbf{1})_0$	$-$
η_a	$1-r$	$(\mathbf{N}_c,\mathbf{2})_{1/2}$	$+$

Table 7.1: Left-handed fermions and scalar fields (with $a = 1, 2$). The $B - L$ charge ensures that the vector-like quark $\mathcal{Q}$, taken as a color octet, composes cosmologically stable bound-states.

(summation is implied over repeated indices, and trace over $\mathbf{N}_c = \mathbf{8}$ is implicit.)

$$\begin{aligned}\mathcal{L} \supset & -\left[h_i^a \overline{\mathcal{Q}_R}\widetilde{\eta}_a^\dagger L_i + M_{\mathcal{Q}}\,\overline{\mathcal{Q}_R}\mathcal{Q}_L + y_i^a \overline{\nu_{Ri}}\;\sigma_a^* \mathcal{Q}_L + \mathrm{h.c}\right] \\ & - \mathcal{V}(H, \eta_a, \sigma_a)\,. \end{aligned} \tag{7.4}$$

The condition $r \neq 1$ forbids Higgs-like Yukawa couplings of η^α to the Standard Model fermions (for $r = 1$ one would need an additional Z_2 symmetry, as in [214]). Hence, by construction, the new Yukawa interactions in Eq. (7.4) do not affect the stability of our bound-state dark matter, since the colored scalars are assumed to be heavier than $\mathcal{Q}$, and $\mathcal{Q}\mathcal{Q}$ annihilation processes mediated by η, σ, are all forbidden by the conserved $B - L$ symmetry. The set of scalars η^a, σ^a in Fig. 7.2 can be either neutral or charged under $B - L$, depending on the baryon number assignment. If $B - L$ neutral, both η^a and σ^a are expected to be unstable, decaying to quarks [215] and two gluons respectively [216, 217].

The new part of the scalar potential can be cast as

$$\begin{aligned}\mathcal{V}(H,\eta_a,\sigma_a) &= \mathcal{V}(\eta_a)+\mathcal{V}(\sigma_a)+\mathcal{V}(\eta_a,\sigma_a)\\ &\quad+\mathcal{V}(H,\eta_a)+\mathcal{V}(H,\sigma_a),\end{aligned} \tag{7.5}$$

where the various terms in the Higgs potential are

$$\mathcal{V}(\eta_a,\sigma_a) = \kappa^{ab}\ \mathrm{Tr}\left(\sigma_a\eta_b^\dagger\right)H + \lambda_{\sigma\eta}^{abcd}\,\mathrm{Tr}\left(\sigma_a^*\sigma_b\right)\mathrm{Tr}\left(\eta_c^\dagger\eta_d\right) \tag{7.6}$$

$$+\,\tilde{\lambda}_{\sigma\eta}^{abcd}\,\mathrm{Tr}\left(\sigma_a^*\eta_b\right)\mathrm{Tr}\left(\sigma_c\eta_d^\dagger\right)+\mathrm{h.c.}, \tag{7.7}$$

$$\mathcal{V}(H,\eta_a) = \lambda_{3\eta H}^{ab}\left(H^\dagger H\right)\mathrm{Tr}\left(\eta_a^\dagger\eta_b\right)+\lambda_{4\eta H}^{ab}\,\mathrm{Tr}\left[\left(\eta_a^\dagger H\right)\left(H^\dagger\eta_b\right)\right]+\mathrm{h.c.}, \tag{7.8}$$

$$\mathcal{V}(H,\sigma_a) = \lambda_{\sigma H}^{ab}\,\mathrm{Tr}\left(\sigma_a^*\sigma_b\right)H^\dagger H+\mathrm{h.c.}. \tag{7.9}$$

Since CP conservation is assumed, the CP-even and CP-odd scalars do not mix. Moreover, terms like $\left(\eta^\dagger H\right)^2$ are also forbidden and, as a consequence, the real and imaginary parts of the scalars with nonzero $B-L$ charges are degenerate. Note, however, that the cubic scalar coupling terms κ^{ab} breaking the Z_2 symmetry softly allow for the mixing between the σ_a and η_a. At the end the 4×4 mass matrices for the CP-odd and CP-even scalars are equal, since the κ^{ab} terms do not break such a degeneracy.

In order to illustrate the neutrino mass generation mechanism we consider the following block-diagonal mass matrix for the CP-even scalars (in the basis $S_R=(\eta_{1R}^0,\sigma_{1R}^0,\eta_{2R}^0,\sigma_{2R}^0)^T$):

$$\mathcal{M}_R^2 = \begin{pmatrix} (\mu_\eta^{11})^2 & \frac{\kappa_{11}v}{\sqrt{2}} & 0 & 0\\ \frac{\kappa_{11}v}{\sqrt{2}} & (\mu_\sigma^{11})^2 & 0 & 0\\ 0 & 0 & (\mu_\eta^{22})^2 & \frac{\kappa_{22}v}{\sqrt{2}}\\ 0 & 0 & \kappa_{22}\frac{v}{\sqrt{2}} & (\mu_\sigma^{22})^2 \end{pmatrix}. \tag{7.10}$$

Here we have used the parametrization $\eta_a=(\eta_a^+,(\eta_{aR}^0+i\eta_{aI}^0)/\sqrt{2})^T$, $\sigma_a=(\sigma_{aR}^0+i\sigma_{aI}^0)/\sqrt{2}$ and $H=(0,(h+v)/\sqrt{2})^T$, with h denoting the SM Higgs boson, and $v=246$ GeV. The parameters $\mu_{\eta(\sigma)}^{ab}$ are the quadratic mass terms after electroweak symmetry breaking in $\mathcal{V}(\eta_a)$ and $\mathcal{V}(\sigma_a)$.

Since the tree-level Dirac mass term is forbidden by symmetry, calculable Dirac neutrino masses are generated at one–loop order, by the Feynman diagram displayed in Fig. 7.2. One finds the following effective mass matrix

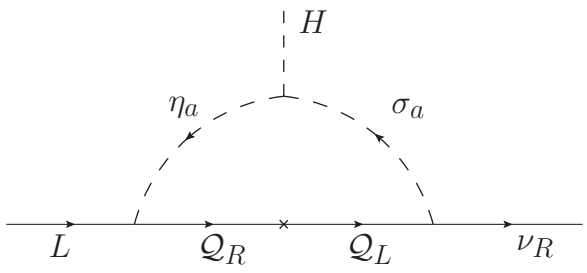

Figure 7.2: $B - L$ flux in the one-loop Dirac neutrino mass.

$$(\mathcal{M}_\nu)_{ij} = N_c \frac{M_\mathcal{Q}}{64\pi^2} \sum_{a=1}^{2} h_i^a y_j^a \frac{\sqrt{2}\kappa_{aa} v}{m^2_{S^a_{2R}} - m^2_{S^a_{1R}}} \left[F\left(\frac{m^2_{S^a_{2R}}}{M^2_\mathcal{Q}}\right) - F\left(\frac{m^2_{S^a_{1R}}}{M^2_\mathcal{Q}}\right) \right] + (R \to I) \tag{7.11}$$

where $F(m^2_{S_\beta}/M^2_\mathcal{Q}) = m^2_{S_\beta} \log(m^2_{S_\beta}/M^2_\mathcal{Q})/(m^2_{S_\beta} - M^2_\mathcal{Q})$ and the $\mathrm{SU}(3)_c$ color factor N_c is assumed to be 8, since the new particles running in the loop transform as octets. The four CP-even mass eigenstates are denoted as $S^1_{1R}, S^1_{2R}, S^2_{1R}, S^2_{2R}$, with a similar notation for the CP-odd ones.

Here the effective one-loop induced neutrino mass matrix has in general rank two, as in [218], implying two non-vanishing Dirac neutrino masses. As a simple numerical estimate, let us consider the case $\mu^{aa}_\eta = \mu^{aa}_\sigma \gg \sqrt{2}\kappa^{aa} v$. Taking $m^2_{S^a_{2R}} - m^2_{S^a_{1R}} = \sqrt{2}\kappa^{aa} v$ and $m^2_{S^a_{2R}} + m^2_{S^a_{1R}} = 2(\mu^{aa}_\eta)^2$ one finds

$$(\mathcal{M}_\nu)_{ij} = N_c \frac{M_\mathcal{Q}}{32\pi^2} \sqrt{2}\kappa^{aa} v \sum_{a=1}^{2} \frac{h_i^a y_j^a}{(\mu^{aa}_\eta)^2 - M^2_\mathcal{Q}} \left[1 - \frac{M^2_\mathcal{Q}}{(\mu^{aa}_\eta)^2 - M^2_\mathcal{Q}} \log\left(\frac{(\mu^{aa}_\eta)^2}{M^2_\mathcal{Q}}\right) \right],$$

so that if $(\mu^{aa}_\eta)^2 \gg M^2_\mathcal{Q}$ one has

$$(\mathcal{M}_\nu)_{ij} = N_c \frac{M_\mathcal{Q}}{32\pi^2} \sqrt{2} v \sum_{a=1}^{2} \kappa^{aa} \frac{h_i^a y_j^a}{(\mu^{aa}_\eta)^2} \tag{7.12}$$

$$\sim 0.03\,\mathrm{eV} \left(\frac{M_\mathcal{Q}}{12.5\,\mathrm{TeV}}\right) \left(\frac{\kappa^{aa}}{1\,\mathrm{GeV}}\right) \left(\frac{50\,\mathrm{TeV}}{\mu^{aa}_\eta}\right)^2 \left(\frac{h_i^a y_j^a}{10^{-6}}\right).$$

One sees that, indeed, small neutrino masses arise naturally by taking reasonable values for the Yukawa couplings, small value for the soft breaking parameter κ^{ab}, as well as sufficiently large values for the scalar masses. Notice that the smallness of κ^{ab} is natural in t'Hooft's sense [84], as the theory attains a larger symmetry when $\kappa^{ab} \to 0$, i.e. the smallness of neutrino mass is symmetry-protected.

7.3 The Majorana case

In this section we present a model where the symmetry responsible of the bound-state stability also gives rise to radiative Majorana neutrino masses. To ensure the stability of the bound-state, the heavy messenger $\mathcal{Q}$ is charged under a dark $U(1)_D$ symmetry. In fact, both dark matter stability and the Dirac nature of the exotic fermion $\mathcal{Q}$ are equivalent, resulting from dark charge conservation. We will see that neutrinos being Majorana particles does not imply the violation of the $U(1)_D$ symmetry, responsible of DM stability.

As shown in table 7.2, we consider a simple realization of the radiative seesaw neutrino mass generation picture, in which a single colored fermion $\mathcal{Q}$ is introduced along with two colored SU(2) doublet scalars η_a $(a = 1, 2)$.

Particles	$\mathrm{U}(1)_D$	$(\mathrm{SU}(3)_c, \mathrm{SU}(2)_L)_Y$
$Q_i = \begin{pmatrix} u_L & d_L \end{pmatrix}_i^{\mathrm{T}}$	0	$(\mathbf{3}, \mathbf{2})_{1/6}$
$\overline{u_{Ri}}$	0	$(\overline{\mathbf{3}}, \mathbf{1})_{-2/3}$
$\overline{d_{Ri}}$	0	$(\overline{\mathbf{3}}, \mathbf{1})_{1/3}$
$L_i = \begin{pmatrix} \nu_L & e_L \end{pmatrix}_i^{\mathrm{T}}$	0	$(\mathbf{1}, \mathbf{2})_{-1/2}$
$\overline{e_{Ri}}$	0	$(\mathbf{1}, \mathbf{1})_{1}$
$\mathcal{Q}_L$	-1	$(\mathbf{N}_c, \mathbf{1})_0$
$\overline{\mathcal{Q}_R}$	1	$(\mathbf{N}_c, \mathbf{1})_0$
H	0	$(\mathbf{1}, \mathbf{2})_{1/2}$
η_a	$(-1)^a$	$(\mathbf{N}_c, \mathbf{2})_{1/2}$

Table 7.2: Particle content of the Majorana version of the colored scotogenic model. The fermion $\mathcal{Q}$ forms the bound-state which composes the cosmological DM.

Note that, as in previous sections, all dark sector particles carry color charge. For definiteness, we assign them to the octet $\mathrm{SU}(3)_c$ representation.

Notice, however, that our neutrino mass discussion also holds if they had different $\mathrm{SU}(3)_c$ transformation properties. The $\mathrm{U}(1)_D$ symmetry implies that $\mathcal{Q}$ has only a Dirac-type mass term, which is required to ensure the stability of the bound state, $\mathcal{Q}\mathcal{Q}$. Hence the relevant terms in the Lagragian are the following

$$\mathcal{L} \supset -\left[h_i \overline{\mathcal{Q}_R}\widetilde{\eta}_1^\dagger L_i + y_i \overline{\mathcal{Q}_L^c}\widetilde{\eta}_2^\dagger L_i + M_{\mathcal{Q}}\, \overline{\mathcal{Q}_R}\mathcal{Q}_L + \mathrm{h.c}\right] - \mathcal{V}(H,\eta_a)\ , \qquad (7.13)$$

where summation is implied over repeated indices, and trace over $\mathbf{N}_c = \mathbf{8}$ is implicit. The Higgs potential contains the following terms

$$\begin{aligned}\mathcal{V}(H,\eta_a) =\ & V(H) + V(\eta_a) \\ & + \left(\lambda^{ab}_{3\eta H}\left(H^\dagger H\right)\mathrm{Tr}\left(\eta_a^\dagger\eta_b\right) + \lambda^{ab}_{4\eta H}\,\mathrm{Tr}\left[\left(\eta_a^\dagger H\right)\left(H^\dagger\eta_b\right)\right]\right)\delta_{ab} + \mathrm{h.c.} \\ & +\ \mathrm{Tr}\left[\lambda_{\eta_1\eta_2}\left(\eta_1^\dagger\eta_2\right)\left(\eta_2^\dagger\eta_1\right)\right] + \left\{\mathrm{Tr}\left[\lambda_{\eta_1\eta_2 H}\left(H^\dagger\eta_1\right)\left(H^\dagger\eta_2\right)\right] + \mathrm{h.c.}\right\} \qquad (7.14)\end{aligned}$$

Note that terms like $\left(\eta_a^\dagger H\right)^2$ are forbidden by symmetry reasons.

The Higgs boson triggering EWSB is the same as that in the SM. The neutral scalar components η_a^0 of the dark charge carrying scalars, η^a, with quadratic mass coefficients μ_a mix into two complex mass eigenstates S_a. Since the tree-level mass term is forbidden by symmetry, neutrino masses are calculable at one–loop order, by the Feynman diagram displayed in Fig. 7.3.

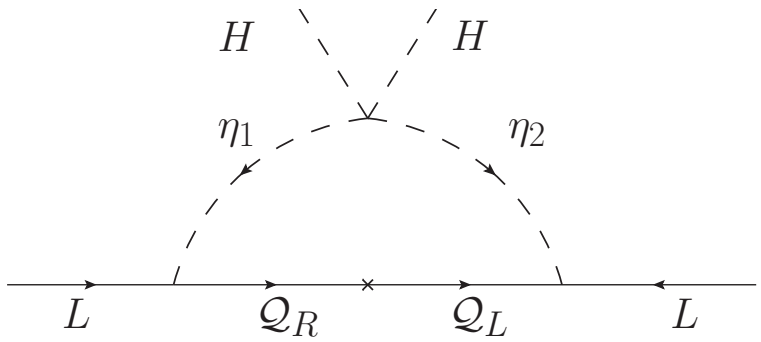

Figure 7.3: Feynman diagram representing the neutrino mass mechanism. Despite the Majorana nature of neutrinos, the $U(1)_D$ symmetry remains exact. See text for details.

One finds the following effective mass matrix

$$(\mathcal{M}_\nu)_{ij} = N_c \frac{M_{\mathcal{Q}}}{32\pi^2} (h_i y_j + h_i y_j) \frac{\lambda_{\eta_1\eta_2 H} v^2}{m^2_{S^0_2} - m^2_{S^0_1}} \left[F\left(\frac{m^2_{S^0_2}}{M^2_{\mathcal{Q}}}\right) - F\left(\frac{m^2_{S^0_1}}{M^2_{\mathcal{Q}}}\right) \right]. \tag{7.15}$$

As in the previous section, the loop function reads

$$F(m^2_{S_\beta}/M^2_Q) = m^2_{S_\beta} \log(m^2_{S_\beta}/M^2_Q)/(m^2_{S_\beta} - M^2_Q)\,, \tag{7.16}$$

and the $\mathrm{SU}(3)_c$ color factor N_c is assumed to be 8, since the new particles running in the loop transform as octets. Note that the effective one-loop induced neutrino mass matrix has in general rank two, implying two non-vanishing neutrino masses, as required to account for neutrino oscillation data.

As a simple numerical estimate, assuming $\mu^2_{\eta_1} \gg M^2_{\mathcal{Q}}$, we consider the case $\mu^2_{\eta_1} = \mu^2_{\eta_2} \gg \lambda_{\eta_1\eta_2 H} v^2$ and $\lambda_{3\eta H}, \lambda_{4\eta H} \ll 1$. Taking $m^2_{S_2} - m^2_{S_1} = \lambda_{\eta_1\eta_2 H} v^2$ and $m^2_{S^a_{2R}} + m^2_{S^a_{1R}} = 2\mu^2_{\eta_1}$, we find

$$(\mathcal{M}_\nu)_{ij} \sim 0.04\,\mathrm{eV} \left(\frac{M_{\mathcal{Q}}}{12.5\,\mathrm{TeV}}\right) \left(\frac{\lambda_{\eta_1\eta_2 H} v^2}{0.1\,\mathrm{GeV}^2}\right) \left(\frac{15\,\mathrm{TeV}}{\mu_{\eta_1}}\right)^2 \left(\frac{h_i y_j}{10^{-6}}\right). \tag{7.17}$$

As in the Dirac case, small neutrino masses are protected by the parameter $\lambda_{\eta_1\eta_2 H}$ in whose absence the theory acquires a larger symmetry. As a result, adequate neutrino masses arise naturally for reasonable values of the Yukawa couplings and scalar potential parameters.

Neutrinoless double beta decay

In contrast to the proposal in the previous section, here total lepton number is a broken symmetry, hence we expect neutrinoless double beta decay to occur. The effective mass parameter characterizing the amplitude for neutrinoless double beta decay is given by [60]

$$\langle m_{ee} \rangle = \left| \sum_j U^2_{ej} m_j \right| = \left| c^2_{12} c^2_{13} m_1 + s^2_{12} c^2_{13} m_2 e^{2i\phi_{12}} + s^2_{13} m_3 e^{2i\phi_{13}} \right|, \tag{7.18}$$

where m_i are the neutrino masses, c_{12} and s_{13} correspond to the angles measured from oscillations and ϕ_{12}, ϕ_{13} are the Majorana phases (here we use the symmetrical parametrization of the lepton mixing matrix [44]).

As discussed in Sec. 2.1, since our model predicts the lightest neutrino to be massless, $m_1 = 0$, it follows that there is one single physical (relative) Majorana phase $\phi \equiv \phi_{12} - \phi_{13}$. Furthermore, one can also write the physical masses directly in terms of the squared mass splittings measured in neutrino oscillation experiments. Depending on the ordering, these masses read

$$\begin{aligned} &\text{NO}: \ m_2 = \sqrt{\Delta m^2_{21}}\,, \ m_3 = \sqrt{\Delta m^2_{31}}\,, \\ &\text{IO}: \ m_1 = \sqrt{\Delta m^2_{13}}\,, \ m_2 = \sqrt{\Delta m^2_{13} + \Delta m^2_{12}}\,. \end{aligned} \tag{7.19}$$

Given that the lightest neutrino is massless, one can plot the effective Majorana mass parameter $\langle m_{ee} \rangle$ as a function of the unknown Majorana phase ϕ without loss of generality, see Fig. 7.4. The results are given for the cases of normal (yellow band) and inverted (green band) mass orderings, varying the neutrino oscillation parameters within 3σ [185, 219] of their best fit values. One sees that, in contrast to the general three-neutrino scenario, here the $0\nu\beta\beta$ amplitude never vanishes, even when the neutrino mass ordering is of the normal type (models with this feature typically require the existence of specific flavor symmetries [220–222]). The top four horizontal bands represent the 90% C.L. upper limits from CUORE [223], EXO-200 Phase II [224], GERDA Phase II [225] and KamLAND-Zen [226] experiments. The sensitivity bands for the upcoming nEXO experiment after 10 years of data taking [227] as well as for the SNO+ Phase II [228] and LEGEND [229] experiments are indicated by the horizontal red bands.

7.4 Lepton Flavor Violation

The models presented in previous sections may also lead to indirect virtual effects, such as charged lepton flavor violation. For example, the Yukawa interactions in Eqs. (7.4) and (7.13) lead to radiative lepton flavor violation processes such as $\mu \to e\gamma$, as seen in Fig. 7.5, mediated by the charged scalar η_a^+.

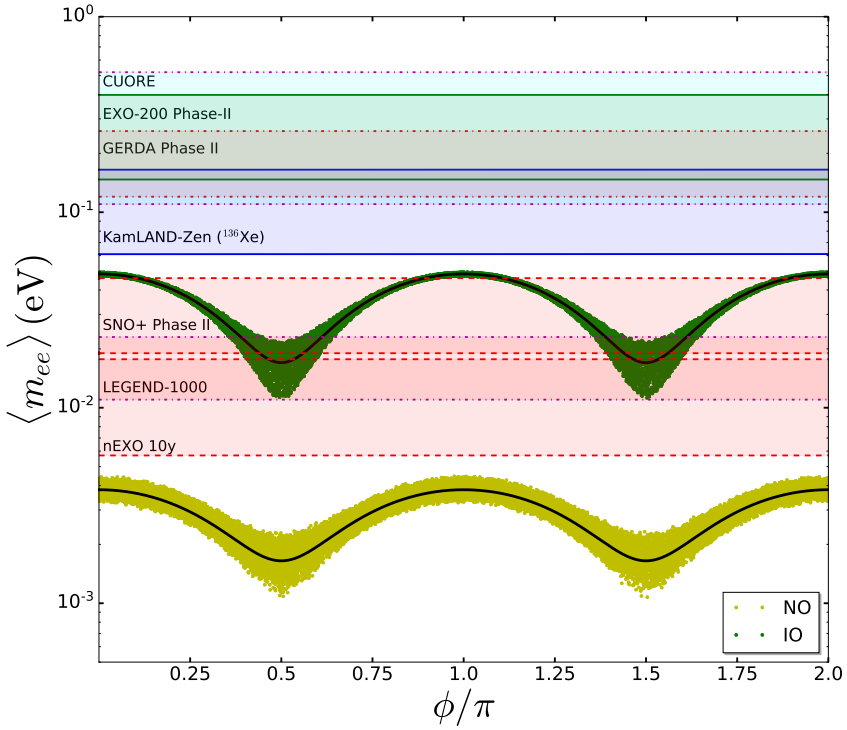

Figure 7.4: Effective Majorana mass as a function of the Majorana phase for normal (yellow band) and inverted (green band) mass orderings. The bands represent the 3σ uncertainties in the neutrino oscillation parameters [185, 219]. The solid black lines represent their best fit values. The horizontal bands are the experimental limits and sensitivities.

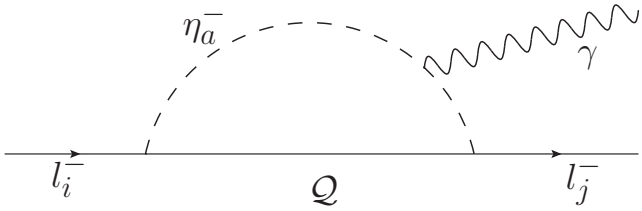

Figure 7.5: Feynman diagram for the process $l_i \to l_j \gamma$.

The corresponding decay rate is given as [230],

$$\Gamma(l_i \to l_j \gamma) = \frac{e^2 m_i^5}{16\pi} \Big[\sum_a N_c h_i^a h_j^{a*} \frac{i}{16\pi^2 M_{\eta_a^+}^2} \left[\frac{-t^2 \log t}{2(t-1)^4} + \frac{2t^2+5t-1}{12(t-1)^3} \right] \Big]^2 , \tag{7.20}$$

with $t = M_{\mathcal{Q}}^2/M_{\eta^+}^2$ and $N_c = 8$. In the limit of heavy scalars, $t \to 0$, the decay width reads

$$\Gamma(l_i \to l_j\gamma) = \frac{e^2 m_i^5}{16\pi}\Big[\sum_a N_c h_i^a h_j^{a*} \frac{i}{16\pi^2 M_{\eta_a^+}^2}\left[-\frac{1}{12}\right]\Big]^2.$$

As an example, focusing on the process $\mu \to e\gamma$, one sees that the current experimental constraint [231]:

$$\mathrm{BR}(\mu \to e\gamma) = \frac{\Gamma(\mu \to e\gamma)}{\Gamma_{\mathrm{total}}} < 4.2 \times 10^{-13}\,, \text{ at } 90\% \text{ C.L.} \tag{7.21}$$

can be fullfilled provided

$$\left(\sum_a \frac{h_\mu^a h_e^{a*}}{M_{\eta_a^+}^2}\right)^2 \leq 4.2 \times 10^{-13} \frac{G_F^2}{\alpha_{\mathrm{EM}}} \frac{768\pi}{N_c^2}\,. \tag{7.22}$$

This leads to a relatively mild requirement for the new scalar masses,

$$\left|\sum_a h_\mu^a h_e^{a*} \left(\frac{50\,\mathrm{TeV}}{M_{\eta_a^+}}\right)^2\right| \lesssim 1.5. \tag{7.23}$$

7.5 Color octets at hadron colliders

In our model the messengers of neutrino mass generation (both, for the Dirac and Majorana cases) are the colored constituents of the bound-state dark matter candidate. Given enough energy, the $\mathcal{Q}$'s are copiously pair produced at hadron colliders through the processes $q_i\bar{q}_i \to \mathcal{Q}\bar{\mathcal{Q}}$ and $gg \to \mathcal{Q}\bar{\mathcal{Q}}$, and are expected to hadronize. In contrast to standard WIMP dark matter scenarios, which engender only missing-energy signals, the bound-state dark matter scenario gives rise to very visible signals at hadron colliders, as they can form either neutral or charged bound-states, e.g. neutral hybrid states $\mathcal{Q}g$ (detected as neutral hadrons, presumably stable) or charged $\mathcal{Q}q\bar{q}'$ states, or even more exotic $\mathcal{Q}qqq$ states, expected to be long-lived on collider time-scales.

Current LHC data place a limit to the fermion color octet mass, $M_{\mathcal{Q}} > 2$ TeV [210]. Since the cosmological relic abundance requires $M_{\mathcal{Q}} \approx 12.5$ TeV, this scenario offers an attractive benchmark for future collider experiments

beyond the energies attainable at the LHC. In fact, from the estimate in Ref. [232] one finds that a hadron collider of at least 65 TeV center-of-mass energy would be required to probe the full cosmologically allowed range of masses of our bound-state DM model. A future hadron collider with a center of mass energy of 100 TeV, would probe masses up to $M_{\mathcal{Q}} \lesssim 15$ TeV [232]. This will allow a cross-check of the DM search results of direct detection experiments and fully test the colored dark matter hypothesis.

The scalar sector, as we have seen, depends on whether the neutrino is a Dirac or a Majorana particle. Concerning the Dirac case (see section 7.2), we have two pairs of scalars, the $\sigma_a \sim (\mathbf{8}, 1, 0)$, which are singlets under $\mathrm{SU}(2)_L$, and the η_a, which transform as weak doublets, $\eta_a \sim (\mathbf{8}, \mathbf{2}, 1/2)$. As color octets, they would also be copiously produced at a hadron collider of sufficient energy [233, 234]. However, their masses are expected to lie well above the reach of the LHC. Moreover, in our model these scalars carry non-trivial $B - L$ charges, see Table 7.1. This makes them relatively *inert* with respect to the SM fermions. This, in addition to their heavy masses, makes them very difficult to probe directly.

In the Majorana case, there is a single pair of color octet scalars. If the lightest color octet scalar, η_1, transforming as a weak doublet, has a mass close to that of $\mathcal{Q}$, they could be pair-produced with similar cross sections. The pair produced scalars further decay into a $\mathcal{Q}\bar{\mathcal{Q}}$ pair and charged leptons or neutrinos. This gives rise to similar signals with long-lived bound-states but with extra charged leptons or missing transverse energy.

7.6 Summary

In this chapter, based on [203, 204], we have considered a simple and viable model in which dark matter emerges as a stable neutral hadronic thermal relic. Following [201], we employ an exotic color octet Dirac fermion, $\mathcal{Q}$, with mass around $M_{\mathcal{Q}} \sim 12.5$ TeV as the DM constituent.

The novel part of this construction - and the central idea of the present chapter - is that the colored DM candidate is the neutrino mass messenger. We have considered a minimum particle content leading to two non-zero neutrino masses (associated to the solar and atmospheric scales) both for Dirac and Majorana neutrinos. As shown in Fig.(7.1), these models can be falsified relatively soon by dark matter searches, and could also be cross-checked later by a next generation hadron collider.

Part III

The Flavor Puzzle

Chapter 8

Comprehensive Unification

In previous chapters we have studied how our core theory of fundamental physics, based on promoting $SU(3) \times SU(2) \times U(1)$ to a local symmetry, describes a vast range of phenomena precisely and very accurately. In that sense, it is close to Nature's last word. On the other hand, it contains a diversity of interactions and, when we come to the fermions, a plethora of independent elements. It is attractive to imagine that a deeper unity underlies this observed multiplicity. Gauge unification, studied in Chapter 5, perhaps most elegantly realized using the group $SO(10)$ and the spinor **16** representation of fermions [145], goes a long way toward that goal. It leaves us with a single interaction (i.e., a simple gauge group) but three fermion families, each embodying in a chiral spinor **16** representation. It is then natural to ask, whether one can take that success further, to unite the separate families.

As we briefly reviewed in section 5.3, the mathematical properties of spinor representations are suggestive in this regard [148]. Specifically, for example, the irreducible spinor **256** representation of $SO(18)$ reduces, upon breaking $SO(18) \to SO(10) \times SO(8)$, according to [235]

$$\mathbf{256} \to (\mathbf{16}, \mathbf{8}) \; + \; (\overline{\mathbf{16}}, \mathbf{8}') \,, \tag{8.1}$$

involving spinor representations of the smaller groups (including conjugate and alternate spinors). From the standpoint of $SO(10)$, then, we have eight families and eight mirror families. Notably, there are no problematic exotic color or charge quantum numbers: we get basically the sorts of representations we want, and no others. Still, there are too many families, and also mirror families with the "wrong" chirality for low-energy phenomenol-

ogy. Confinement of some $SO(8)$ quantum numbers, or interaction with condensates, can effectively remove an equal number of families and mirror families, but it seems difficult to change their net balance by those means.

The idea of comprehensive unification has continued to attract attention over the years, both in context of $SO(18)$ and in variant forms [236–240], but the issue of chirality has remained problematic.

In this Chapter, based on [202], we explore a different direction. After reviewing the orbifold symmetry breaking mechanism we will see how it can be applied to break $SO(18)$ down to $SO(10) \times SO(8)$. The orbifold mechanism will allow us to obtain a chiral fermion spectrum with zero modes in the $(\mathbf{16}, \mathbf{8})$ representation. In addition, we postulate condensates that break $SO(8) \to SO(5)$ and decompose $\mathbf{8} \to 3 \times \mathbf{1} + \mathbf{5}$. The $SO(5)$ interaction then becomes strongly coupled and confining at a scale $\mathcal{O}(\text{TeV})$, effectively leaving only three chiral spinors of $SO(10)$ at low energies. These unconfined families correspond to the three SM families. When one includes contributions from the required Higgs fields, an acceptable fit to gauge coupling unification emerges. An interesting consequence of this scheme is the existence of stable $SO(5)$ hyperbaryons, protected by a Z_2 symmetry. Although they annihilate in pairs, a significant relic density emerges from big bang cosmology. Similarly to the Griest-Kamionkowski bound [132], hyperbaryons will be required to have a mass $M \lesssim O(10)$ TeV in order to have an acceptable abundance.

8.1 Orbifold symmetry breaking in a nutshell

In this section we briefly review the orbifold symmetry breaking mechanism, closely following [241]. We will exploit the possibility to obtain chiral fields by imposing appropriate boundary conditions on orbifolds. Additionally, we overview how orbifolding can also reduce an initial extra-dimensional gauge symmetry down to a smaller symmetry in 4 dimensions. This mechanism has been used in the past in different contexts, from the hierarchy problem and EWSB [242, 243] to GUTs [241, 244–246], flavor [247, 248] and neutrino mass generation [248, 249].

Let's assume, for simplicity, a 5-dimensional space where the extra dimension is compactified on a circle S_1. In addition, we impose a Z_2 trans-

formation acting on the extra dimension:

$$y \to -y\,. \tag{8.2}$$

This symmetry transformation divides the circle in two intervals of length πR, with R the radius of the extra dimension. In this way we obtain the simplest, one-dimensional orbifold S_1/Z_2. Additionally, there are a couple of 3-branes (4D *walls*) at the fixed points: $y = 0, \pi R$.

In our toy model, any 5D bulk field will transform under the orbifold *parity*:

$$\phi(x^\mu, y) \to \phi(x^\mu, -y) = P\phi(x^\mu, y)\,. \tag{8.3}$$

The parity eigenvalue, P, determines the 4D behavior of the field. In the 5D space under consideration, $M_4 \times S_1/Z_2$, any field can be written as a KK expansion, which in a flat space-time is just a Fourier expansion:

$$\begin{aligned} \phi_+(x^\mu, y) &= \frac{1}{\sqrt{\pi R}} \sum_{n=0}^{\infty} \phi_+^{(n)}(x) \cos\left(\frac{ny}{R}\right)\,, \\ \phi_-(x^\mu, y) &= \frac{1}{\sqrt{\pi R}} \sum_{n=0}^{\infty} \phi_-^{(n)}(x) \sin\left(\frac{ny}{R}\right)\,. \end{aligned} \tag{8.4}$$

In the equation above, the sign $\pm$ refers to the orbifold parity of the 5D field and n corresponds to the integer that labels the n-th KK mode, $\phi_\pm^{(n)}(x)$.

For the sake of simplicity, let us consider the case of a scalar field. From the 5D free-field Lagrangian

$$\mathcal{L}_\phi^{(5)} = |\partial_M \phi|^2\,, \tag{8.5}$$

one can see that these KK modes get a mass given by $m_n \sim n/R$ due to the derivatives with respect to the extra dimension. An immediate consequence is that only bulk fields with positive parity have zero modes that, from a low-energy 4D perspective, correspond to massless fields.

In the case we have a set of scalars which transform non-trivially under a certain symmetry group, G, the orbifold parity does not necessarily commute with the generators of G. This mismatch generates a symmetry breaking process that reduces the initial group G due to the lack of zero modes. As an example, if we have N_f complex scalar fields forming a vector with N_f components, $\Phi(x^\mu, y)$, the symmetry group is some sort of flavor group given by $G = U(N_f)$. In this case P is a $N_f \times N_f$ matrix that determines the transformation of the multiplet under the orbifold parity.

Whenever P is not proportional to the identity matrix, it does not commute with the generators of $U(N_f)$ and, then, the group is broken. For example, if the orbifold symmetry is

$$P = \begin{pmatrix} \mathbb{I}_{n_f} & \\ & -\mathbb{I}_{N_f - n_f} \end{pmatrix} , \tag{8.6}$$

with $\mathbb{I}_{n_f}$ the $n_f \times n_f$ identity matrix, the initial $U(N_f)$ symmetry is broken down to $U(n_f)$ due to the orbifold boundary conditions. As a result, from the low energy point of view - that is, at energies $E \ll R^{-1}$ - a 4D observer will notice a set of n_f massless complex scalars with a $U(n_f)$ flavor symmetry.

Chiral fermions and orbifolds

5-dimensional Lorentz invariance requires that fermions come in Dirac pairs

$$\Psi = (\psi_L \, , \psi_R)^T \, . \tag{8.7}$$

This seems to preclude the possibility to obtain the SM fermion content from a theory with one extra dimension. However, as we have seen, the orbifold parity allows us to *select* which bulk fields have zero modes. Fortunately, this mechanism can be applied to fermions to obtain a chiral 4D spectrum.

Let's consider the 5D Dirac Lagrangian for a free, massless fermion,

$$\mathcal{L}_D^{(5)} = i\bar{\Psi}\gamma^M \partial_M \Psi \, . \tag{8.8}$$

Since $\partial/\partial y$ is odd under the orbifold parity transformation, the Lagrangian above can only be invariant under the orbifold symmetry if ψ_L and ψ_R transform differently

$$\begin{aligned} \psi_L(x^\mu, -y) &= P\psi_L(x^\mu, y) \\ \psi_R(x^\mu, -y) &= -P\psi_R(x^\mu, y) \end{aligned} \tag{8.9}$$

For example, if $P = +1$, then only the LH component

$$\psi_L(x^\mu, y) \sim \sum_{n=0}^{\infty} \psi_L^{(n)}(x) \cos\left(\frac{ny}{R}\right) \tag{8.10}$$

has a zero mode. The RH component, involving only $\sin\left(\frac{ny}{R}\right)$ functions, has only non-zero KK modes at the 4D walls. We have obtained a 4D chiral spectrum from a non-chiral 5D theory! In addition, a Dirac mass term $m\bar{\Psi}\Psi$ is forbidden due to the orbifold parity[1].

Fermion flavor symmetry reduction works in close analogy to the scalar case. If the orbifold symmetry is

$$P = \begin{pmatrix} \mathbb{I}_{n_f} & \\ & -\mathbb{I}_{N_f - n_f} \end{pmatrix} , \tag{8.11}$$

then the initial 5D symmetry, $U(N_f) \equiv SU(N_f) \times U(1)_V$, is broken down to

$$SU(n_f)_L \times SU(N_f - n_f)_R \times U(1)_V \times U(1)_A \tag{8.12}$$

As in the scalar case, this symmetry breaking process occurs due to the lack of fermion zero modes. The resulting symmetry group is larger due to the presence of LH and RH fermions.

Gauge symmetry breaking by orbifolding

Gauge symmetry can also be reduced due to the orbifold boundary conditions. This occurs when some of the would-be zero modes of the 5D gauge field, $A_M(x^\mu, y)$, are removed from the spectrum. Being in the adjoint representation, the transformation properties of $A_M(x^\mu, y) = (A_\mu(x^\mu, y), A_5(x^\mu, y))$ slightly differ from the previously studied cases:

$$\begin{aligned} A_\mu(x, y) &\to A_\mu(x^\mu, -y) = P A_\mu(x^\mu, y) P^{-1} , \\ A_5(x, y) &\to A_5(x^\mu, -y) = -P A_5(x^\mu, y) P^{-1} . \end{aligned} \tag{8.13}$$

Let's assume that the gauge symmetry is given by $G = SU(N)$ and the orbifold transformation matrix is:

$$P = \begin{pmatrix} \mathbb{I}_n & \\ & -\mathbb{I}_{N-n} \end{pmatrix} , \tag{8.14}$$

The boundary conditions do not respect the full gauge symmetry and the generators, T^a, that transform as $PT^aP^{-1} = -T^a$ are broken after orbifold-

[1] Although we will not consider this case further, bulk fermion masses can be dynamically generated through the coupling to a scalar field, see [250] for a recent discussion.

ing. Because of the transformation properties of the adjoint representation, the unbroken group is larger than the case of a scalar in the fundamental representation. In this case, the symmetry breaking reads:

$$SU(N) \to SU(n) \times SU(N-n) \times U(1)\,. \tag{8.15}$$

The case $N = 5$, $n = 3$ has been studied in the original reference [241] as a candidate to obtain the SM gauge group from a fundamental $SU(5)$ GUT in 5 dimensions, using the simplest orbifold S_1/Z_2.

An interesting consequence is that the fifth component of the 5D gauge field, $A_5(x^\mu, y)$, has the opposite transformation properties. Therefore, in the S_1/Z_2 orbifold, for each of the broken generators there is a massless scalar field, $A_5^{(0)}(x)$, in the 4D theory.

8.2 Model construction

Our model of comprehensive unification employs a $SO(18)$ bulk gauge symmetry and an $S_1/(Z_2 \times Z_2')$ orbifold. The fermion content includes a single **256** spinor that will unify all the SM families. As will be shown below, the motivation for this orbifold with two different parities is that it allows to obtain the appropriate chiral spectrum of fermions. Specifically, we consider a circular fifth dimension of radius $R = 2L/\pi$, with walls at $y = 0, L$ and a warped metric [251]:

$$ds^2 = e^{-2\sigma(y)}\eta_{\mu\nu}dx^\mu dx^\nu + dy^2\,, \tag{8.16}$$

with

$$\begin{aligned} \sigma(y) &= \sigma(y + 2L) = \sigma(-y) \\ \sigma(y) &= ky \;\text{ for }\; 0 \le y \le L\,. \end{aligned} \tag{8.17}$$

We define the equivalence relations [246]

$$\begin{aligned} &\mathbf{P_0} : y \sim -y\,, \\ &\mathbf{P_1} : y' \sim -y'\,. \end{aligned} \tag{8.18}$$

where $y' \equiv y + L$. Thus the second relation in Eq. (8.18) is equivalent to $y \sim y + 2L$. In the standard Randall-Sundrum terminology, we can say that

the bulk region, $0 < y < L$, is sandwiched between a Planck brane ($y = 0$) and a IR brane ($y = L$).

The action of these equivalences $\mathbf{P}_0$, $\mathbf{P}_1$ on matter fields is

$$\begin{aligned} \Phi(x, y) &= P_0^\Phi \Phi(x, -y)\,, \\ \Phi(x, y') &= P_1^\Phi \Phi(x, -y')\,, \end{aligned} \tag{8.19}$$

where P_0^Φ and P_1^Φ are matrices that represent the action of the Z_2 on the bulk fields. As in the simpler S_1/Z_2 case, we can classify fields by their (P_0^Φ, P_1^Φ) values. It will be convenient to write the orbifold conditions for gauge fields as:

$$\begin{pmatrix} A_\mu \\ A_y \end{pmatrix} (x, y_j - y) = P_j^A \begin{pmatrix} A_\mu \\ -A_y \end{pmatrix} (x, y_j + y)(P_j^A)^{-1}\,, \tag{8.20}$$

where $(y_0, y_1) \equiv (0, L)$. Thus

$$A_M(x, y + 2L) = U A_M(x, y) U^{-1}, \tag{8.21}$$

with $U = P_1^A P_0^A$.

We will choose the orbifold parities:

$$\begin{aligned} P_0^A &= \mathrm{diag}(\mathbb{I}_{10}, -\mathbb{I}_8)\,, \\ P_1^A &= \mathrm{diag}(\mathbb{I}_{18})\,. \end{aligned} \tag{8.22}$$

and the corresponding representation matrices for P_j^Φ. These boundary conditions reduce $SO(18) \to SO(10) \times SO(8)$ and allow a chiral fermion spectrum in 4 dimensions.

As before, we can decompose a generic five-dimensional field as:

$$\Phi(x, y) = \frac{1}{\sqrt{L}} \sum_{n=0}^{\infty} \phi^{(n)}(x) f_n(y)\,, \tag{8.23}$$

where $\phi^{(n)}$ are the Kaluza-Klein (KK) excitations and the KK eigenmodes, $f_n(y)$, in RS space obey:

$$\frac{1}{L} \int dy\, e^{(2-s)\sigma} f_m(y) f_n(y) = \delta_{mn}\,. \tag{8.24}$$

The index $s = 2, 4, 1$ depends on whether the field is a vector field, a scalar or a fermion, respectively. See [242] for details.

In more detail, according to Eq. (8.20), the $SO(18)$ gauge adjoint representation will split as

$$\mathbf{153} = (\mathbf{45}, \mathbf{1})^{++} + (\mathbf{1}, \mathbf{28})^{++} + (\mathbf{10}, \mathbf{8})^{-+}\,, \tag{8.25}$$

so, due to the action of P_0^A, only adjoint fields corresponding to $SO(10) \times SO(8)$ have zero modes. Because the fifth components, A_y, have opposite boundary condition, they have only Kaluza-Klein modes.

A left-handed fermion field will have a massless zero-mode only when it has Neumann (+) boundary conditions at both Planck and IR branes

$$\phi^{(++)}(x, y) = \frac{1}{\sqrt{L}}(\phi^{(0)}_{++}(x) f(y)^{(0)} + \text{higher modes})\,, \tag{8.26}$$

The same occurs with right-handed fields that have Dirichlet (−) boundary conditions at both branes, while fields with $(+, -)$ or $(-, +)$ do not have zero modes regardless of their chirality. The $\phi^{(0)}(x)$ zero mode is a massless field in four dimensions, while the $\phi^{(n)}(x)$ Kaluza-Klein modes have masses of order $\mathcal{O}(1/L)$, and do not appear in the low-energy spectrum of the theory.

The main motivation for considering the $S_1/(Z_2 \times Z_2')$ orbifold instead of the S_1/Z_2 can be easily understood when we study the fermion zero modes. As before, fermions that propagate in the bulk come in Dirac pairs with both chiralities. Therefore, the **256** spinor has a LH and a RH compontent. If we were to have the simplest S_1/Z_2:

$$\begin{aligned} \mathbf{256}_L(x^\mu, -y) &= P\,\mathbf{256}_L(x^\mu, y)\,, \\ \mathbf{256}_R(x^\mu, -y) &= -P\,\mathbf{256}_R(x^\mu, y)\,. \end{aligned} \tag{8.27}$$

If P does not break the $SO(18)$ gauge symmetry, that is $P = \text{diag}(\mathbb{I}_{18})$, then we have zero modes only for $\mathbf{256}_L$. On the other hand, if we consider $P = \text{diag}(\mathbb{I}_{10}, -\mathbb{I}_8)$, massless zero modes will appear for $(\mathbf{16}, \mathbf{8})_L$ and $(\overline{\mathbf{16}}, \mathbf{8}')_R$ (see Eq.(8.1)). In either case one does not improve the situation with respect to the standard 4D scenario [148]. The way out, and the novel part of this work, is to consider $S_1/(Z_2 \times Z_2')$. This orbifold allows us to obtain a chiral spectrum from the $SO(10)$ and Lorentz point of view. In other words, $P_1 = \text{diag}(\mathbb{I}_{18})$ removes the zero modes of $\mathbf{256}_R$ and $P_0 = \text{diag}(\mathbb{I}_{10}, -\mathbb{I}_8)$

breaks the initial $SO(18)$ gauge symmetry and, additionally, removes the zero modes of $(\overline{\mathbf{16}}, \mathbf{8}')_L$.

Focusing on the LH fermion spinor (the situation for the RH component changes accordingly) we have:

$$\mathbf{256} = (\mathbf{16}, \mathbf{8})^{++} + (\overline{\mathbf{16}}, \mathbf{8}')^{-+} . \tag{8.28}$$

Since only the first of these supports zero modes, the mirror families, together with $\mathbf{256}_R$, decouple from low-energy phenomenology.

Together with the bulk spinor and gauge fields, we will incorporate brane-localized scalars which implement spontaneous symmetry breaking by condensation (Higgs mechanism). Further breaking to the Standard Model might proceed through intermediate steps associated with either a Pati-Salam [252] or left-right symmetric [253] stage. However, here we assume just the simplest case of direct breaking (see section 5.3) by Higgs fields in the representations

$$(\mathbf{210}, \mathbf{1}) + (\mathbf{126}, \mathbf{1}) + (\mathbf{10}, \mathbf{1}) . \tag{8.29}$$

While the scalars $(\mathbf{210}, \mathbf{1})$ and $(\mathbf{126}, \mathbf{1})$ are localized at the Planck brane, the $(\mathbf{10}, \mathbf{1})$ is confined to the IR brane. As we will see, quantitative unification of couplings roughly supports this simplest choice *a posteriori*. The $(\mathbf{10}, \mathbf{1})$ lies at the TeV scale and drives electroweak breaking. Planck brane scalars naturally acquire large masses, thanks to the warp factor.

A special feature of $SO(8)$ is the existence of three different 8-dimensional representations: vector, spinor, and alternate spinor. They are equivalent to one another under a symmetric S_3 "triality" group of outer automorphisms. For our purposes, it may be simpler to regard the spinor $\mathbf{8}$ of our fermions as an equivalent vector, and break $SO(8) \to SO(5)$ by means of an adjoint, or three vectors. Alternatively, we might take the spinor as it comes, and note that it decomposes as $\mathbf{8} \to 2 \times \mathbf{1} + \mathbf{6}$ under the natural $SU(4)$ subgroup of $SO(8)$. We can break to that using a spinor. Then exploiting the isomorphism $SU(4) \to SO(6)$, we break down to $SO(5)$ using a vector of $SO(6)$. In either case, we have $\mathbf{8} \to 3 \times \mathbf{1} + \mathbf{5}$ under the breaking: $SO(8) \to SO(5)$. Assuming that this breaking occurs through $SO(10)$ singlet scalars, the details do not influence low energy phenomenology.

The upshot is that our chiral, low-energy fermions transforms as $3 \times (\mathbf{16}, \mathbf{1}) + (\mathbf{16}, \mathbf{5})$ under $SO(10) \times SO(5)$. Running of couplings down to low

energies suggests that the $SO(5)$ becomes strongly interacting at $\mathcal{O}(\text{TeV})$[2]. Thus the **5** will be confined, and at low energies we arrive at just three chiral spinor families of $SO(10)$, as desired. (The mechanism of "heavy color confinement" has a long history in this context, see Refs. [46, 148, 254]).

Proton decay is potentially very rapid, if the scale of the IR brane is low. The simplest solution is to make that scale large, e.g. associated with conventional unification or with gravitational physics. In this scenario, we are using the extra dimension to address chirality, rather than the hierarchy problem. Other solutions may be possible [255, 256].

8.3 Gauge coupling evolution

One can write the running of the gauge coupling constants in the four dimensional unified gauge theory

$$\alpha_i^{-1}(M_Z) = \alpha_{GUT}^{-1} + \frac{b_i}{2\pi} \log \frac{M_{GUT}}{M_Z} + \Delta_i \,, \tag{8.30}$$

where Δ_i denote threshold corrections. Within a five dimensional warped space-time one should take into account contributions from the Kaluza-Klein modes, as well. In [257] it was argued that warped extra dimensions, unlike flat extra dimensions, lead to logarithmic running of couplings. Indeed, an equation similar to Eq. (8.30) holds, with the b_i given as [255, 257]:

$$\begin{aligned} b_i^{RS} = \frac{1}{3}[-C_2(G)(11I^{1,0}(\Lambda) - \frac{1}{2}I^{1,i}(\Lambda)) + \\ + 2I^{1/2,0}(\Lambda)T_f(R) + I^{2,0}(\Lambda)T_s(R)] \,. \end{aligned} \tag{8.31}$$

We take the cut-off scale to be $\Lambda \sim k$, which implies the numerical values [257]:

$$\begin{aligned} I^{1,0} &= 1.024 \,, \\ I^{1,i} &= 0.147 \,, \\ I^{1/2,0} &= 1.009 \,, \\ I^{2,0} &= 1.005 \,. \end{aligned} \tag{8.32}$$

[2]Note that if confinement takes place above EW scale the only allowed condensate is formed by the SM singlet contained in the $(\mathbf{16}, \mathbf{5})$.

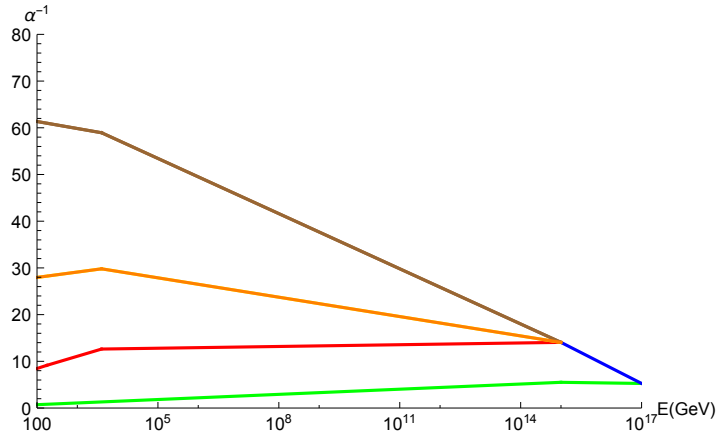

Figure 8.1: Running of gauge couplings (top-down approach): below the SO(10) scale we have the SO(5) gauge coupling (green line) in addition to the Standard Model couplings (red, orange and brown lines). See text.

For scalars localized on branes, we just change $I^{2,0}(\Lambda) \to 1$. In Fig. (8.1) we fix, for definiteness, the unification scale at 10^{15} GeV, and perform a first estimate of the electroweak mixing angle within a top-down approach. We find $\sin^2\theta_w \approx 0.215$, to be compared with the observed value 0.22. Given our neglect of (inherently uncertain) threshold corrections and higher order renormalization, this seems an acceptable result (see below).

Note that in this simplest case (see section 5.3) one breaks the $SO(10)$ directly to $SU(3)\times SU(2)\times U(1)$. One finds that the $SO(5)$ coupling reaches non-perturbative values at $\mathcal{O}$(TeV) (green curve). This fact is reflected into a kink in the evolution of the Standard Model couplings at this value. Thanks to the large number of "active" flavors (at energies above the $SO(5)$ confinement scale we have 8 families contributing to the beta functions) the evolution of g_3 is nearly flat all the way from few TeV up to the GUT scale (see red curve). Above the GUT scale α_{10} (blue curve) rises again due to the large Higgs boson multiplets.

In Fig. (8.2) we compare the bottom-up running at one loop compared with a similar Standard Model extrapolation. One sees that our simple unification scenario gives a marginal improvement with respect to the minimal Standard Model case. However, these results come from a rough estimate, taking renormalization group evolution to first order and neglecting threshold corrections.

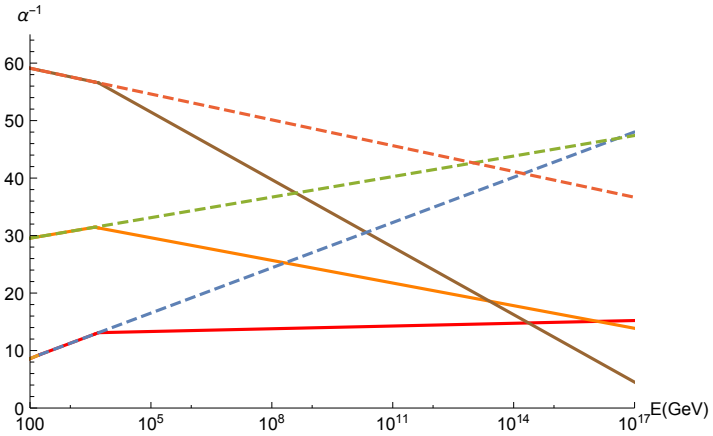

Figure 8.2: Running of gauge couplings below the SO(10) scale compared with the SM (dashed lines). Bottom-up approach.

Charged fermion masses arise from the $\langle(\mathbf{10},\mathbf{1})\rangle$ vacuum expectation value[3], while neutrino masses can be induced by the conventional (high scale) seesaw mechanism [44, 46, 47, 253, 258, 259]. The doublet-triplet splitting problem may be solved with a generalization of the Dimopoulos-Wilczek mechanism [260] for $SO(18)$, using a heavy bulk scalar that leaves the SU(2) doublet massless.

As a final comment we note that the breaking of the $SO(3)$ subgroup of $SO(8)$ will be important in connection with the flavor puzzle, and could lead to new ways of addressing details of the family mass hierarchy and mixing pattern. The implementation of specific mechanisms will be the main goal of the next chapter.

8.4 Hypercolor and hyperbaryons

The evolution of each of the SO(10) and SO(8) coupling constants can be computed imposing the initial unification condition

$$g_{10}(M_{18}) = g_8(M_{18})\,, \tag{8.33}$$

[3]The **10** scalar belongs to a **18** localized at the IR brane, where the SO(18) is not broken by boundary conditions. When orbifold breaking takes place this scalar splits as $\mathbf{18} \to \mathbf{10} + \mathbf{8}$, and the **8** can be decoupled using a generalized Dimopoulos-Wilczek mechanism.

at some scale $M_{18} \lesssim M_P$ where gauge couplings meet. (In our concrete estimates we set M_{18}, the scale which breaks $SO(8)$ to $SO(5)$, at $\approx 10^{17}$ GeV.) The value of $g_{10}(M_{18})$ can be inferred from the observed value of Standard Model couplings. The largest Standard Model coupling at low energies is the g_3 of strong $SU(3)$. Being a larger gauge symmetry, our $SO(5)$ is "more asymptotically free" than the QCD interaction, characterized by the group $SU(3)$, and we expect that its coupling becomes confining at a larger mass scale. This is confirmed by our numerical estimates. We infer a confinement scale around $\mathcal{O}$(TeV), in order of magnitude. We will refer to $SO(5)$ as hypercolor, and the $SO(5)$ vector fermions as hyperquarks.

$SO(5)$ supports a Z_2 conserved quantum number, which counts the number of vector indices [261]. It is analogous to quark number (or baryon number) in QCD, but of course the distinction between Z_2 and conventional, additive baryon number has major physical consequences. The lightest unconfined Z_2 odd ($SO(5)$ singlet) states are hyperbaryons. In quark model language, they are formed from 5 hyperquarks; in operator language, the lowest mass dimension operator that creates them involves the product of 5 hyperquark fields. Although they are highly stable individually, hyperbaryons can annihilate into ordinary matter in pairs. Conversely, they might be pair-produced in high energy collisions.

At high enough temperatures in the early universe, $T \gg 10$ TeV, hyperbaryons would be in thermal equilibrium and their number density will be comparable to the photon number density. As the temperature cools below their mass $M \sim 10$ TeV, their equilibrium abundance will diminish, until they become so rare that annihilation cannot keep up with the expansion of the universe, and a residual abundance freezes out. This scenario has a long history in cosmology and has been reviewed in chapter 4.

The ratio of the residual number density of hyperbaryons to photons is of order $\sim M/M_{\rm Planck}$, and the freezout temperature is parametrically less than M by a logarithmic factor, roughly $\ln M/M_{\rm Planck}$. A more careful calculation, following [132], gives

$$\Omega_\chi h^2 \approx 10^{-5}\Big(M/TeV\Big)^2 \tag{8.34}$$

Thus for $M \lesssim 10$ TeV the relic hyperbaryons contribute only a small fraction of the mass density of the universe. In consequence, though the current hyperbaryon relic abundance presents no obvious phenomenological catastrophe, the relic hyperbaryons might conceivably be detectable. One

may also envisage that the lightest hyperbaryon contributes to the dark matter density, as suggested in Ref. [262]. It is noteworthy that this cosmological mass bound ensures that if they exist at all, hyperbaryons are not far beyond the reach of high-energy accelerators currently under discussion (see [213]).

As a final remark, we note that if such a strong hypercolor interaction exists it may also have interesting implications for axion physics. The reason is that, since $SO(18)$ brings together QCD and hypercolor, in principle the instantons associated to the hypercolor interaction could induce a potentially large mass for the axion, as recently studied in [263, 264]. In this case one expects a mass relation for the axion:

$$m_a^2 f_a^2 \sim \Lambda_{QCD}^4 + \Lambda_{HC}^4 \approx \Lambda_{HC}^4 \,. \tag{8.35}$$

Where we have used that the confinement scale of hypercolor is much larger than the QCD scale. This scenario, however, deserves a detailed study that will be presented elsewhere.

8.5 Summary

In this chapter, based on reference [202], we have presented a model of comprehensive unification, bringing together both gauge and family structure, with several attractive features. Within this approach, the existence of multiple fermion families and the fact that they appear in spinor representations of $SO(10)$ are intimately connected. Thanks to a novel approach, combining orbifold projection, Higgs symmetry breaking, and hypercolor confinement in a reasonably simple way we can obtain just three chiral families, as is observed. As we have shown, an interesting consequence of this new framework is the emergence of highly stable hyperbaryons, with mass $\sim$ 10 TeV, protected by a discrete Z_2 symmetry associated with the $SO(5)$ hypercolor group. These particles provide an attractive target for accelerator and astrophysical searches.

Chapter 9

$SO(3)$ as a gauge family symmetry: the threefold way

Since the late '70s and beginning of the '80s many proposals have been made to explain family replication and the pattern of fermion masses and mixings. To this end, it seems appropriate to consider symmetry groups containing triplet representations. Many possibilities emerge. For example, one can use discrete symmetries like $\Delta(27)$ [265], A_4 [266] or T_7 [267] as flavor symmetries, since all of them contain triplet representations. However, only two options appear if one considers continuous symmetries: $SU(3)$ and $SO(3)$. Therefore, the requirement of a gauged theory of flavor reduces our possible choices considerably.

$SU(3)$ is an appealing possibility that has been studied in the past (see for example [268, 269]). This family symmetry is particularly interesting because one can use Higgses in sextet, **6**, representation. The **6** is an interesting representation to explain why the third family is much heavier than the second and first generations. A fermion mass term, in this case, must come from the VEV of a Higgs with $SU(3)$ charge

$$M_f \sim y_f \bar{f}_L \langle H \rangle f_R \,. \tag{9.1}$$

This possibility, however, requires a chiral assignment of flavor charge to fermions, $f_L \sim \mathbf{3}$ and $f_R \sim \mathbf{3}^*$, and is plagued by anomalies unless extra, exotic fermions are introduced to cancel them. Therefore one loses mini-

mality to generate the hierarchy among generations[1]. We will not consider this possibility further.

In this chapter, based on reference [271], we consider $SO(3)$ as a gauge family symmetry. The $SO(3)$ group is theoretically interesting because it is more easily compatible with the ideas of GUTs. In the usual $SU(5)$ and $SO(10)$ theories one embeds the Standard Model particle content in the chiral, anomaly free sets of representations: $3 \times (\bar{\mathbf{5}} + \mathbf{10})$ for $SU(5)$, and $3 \times \mathbf{16}$ for $SO(10)$. Assigning these representations as $SU(3)$ triplets would have lead to anomalies. For example, in a $SO(10) \times SU(3)$ theory the standard $(\mathbf{16}, \mathbf{3})$ combination has an $[SU(3)_F]^3$ anomaly. This is not the case for $SO(3)$ because it is automatically anomaly free. Therefore, it is interesting to consider, as a source of guidance, its possible deeper origin. This was explored in the previous chapter (based in [202]) where we revived the idea of Comprehensive Unification, merging gauge and family symmetry, that was unsuccessfully proposed in the '80s [148].

More specifically, the breaking scheme $SO(18) \to SO(10) \times SO(5) \times SO(3)$ [46] allows for the standard $SO(10)$ gauge unification together with a hypercolor $SO(5)$, which confines the 5 extra families (leaving 3), and an $SO(3)$ family symmetry group. This motivates consideration of $SO(3)$ as a family unification group. $SO(3)$ as a gauge family symmetry was first proposed in [33]. In their pioneer work, Wilczek and Zee proposed that in the same way the $SU(2)$ group relates up and down-type fermions a new interaction relating families in the *horizontal* direction could explain family replication. In addition, the authors also propose a particular symmetry breaking pattern as the origin of the fermion mass and mixing hierarchies.

The use of $SO(3)$ family symmetry was a successful, predictive scenario. First of all, in that framework quark mixing angles can be written, in first approximation, in terms of quark masses:

$$V_{CKM} \approx \begin{pmatrix} 1 & -\sqrt{\frac{m_d}{m_s}} + \sqrt{\frac{m_u}{m_c}} & \sqrt{\frac{m_u m_c}{m_t^2}} - \sqrt{\frac{m_d m_s}{m_b^2}} \\ \sqrt{\frac{m_d}{m_s}} - \sqrt{\frac{m_u}{m_c}} & 1 & 0 \\ -\sqrt{\frac{m_u m_c}{m_t^2}} + \sqrt{\frac{m_d m_s}{m_b^2}} & 0 & 1 \end{pmatrix}. \tag{9.2}$$

[1]Note that this requirement of anomaly cancellation is absent if the $SU(3)_F$ is a global symmetry. However, quantum gravity might require that all symmetries should be gauged [270].

Additionally, a relation between quark and lepton masses appears:

$$\frac{m_e m_\mu}{m_\tau^2} = \frac{m_d m_s}{m_b^2} = \frac{m_u m_c}{m_t^2} \,. \tag{9.3}$$

With this formula, Wilczek and Zee predicted a very light top quark:

$$m_t^{predicted} \approx 15 \; GeV. \tag{9.4}$$

It is important to remark that this idea was born 16 years before the top quark was discovered![2] In 1995 the top quark was discovered with a mass $m_t \sim 173$ GeV, ruling out the original proposal. Notice also that due to the predicted CKM matrix, the b quark - whose properties were not very well known by that time -, was expected to decay mainly to up quarks.

In this chapter, based on reference [271], we will explore a new approach to $SO(3)$ as a gauge family symmetry inspired by Comprehensive Unification. Within a reasonably economical model, several appealing features emerge:

- A Peccei-Quinn symmetry, leading to axions, which is both natural and crucial to ensure correct mass relations
- Extreme fine tuning is not required
- A characteristic "golden" formula relating quark and lepton masses, given in Eq. (9.14), (similar relations appear in other context [266, 267, 272])
- A successful explanatory framework for the CKM matrix, with two predictions, Eqs. (9.16) and (9.17)
- A conventional seesaw mechanism for neutrino mass generation at the PQ scale, supplemented by a connection between lepton number and PQ breaking, which relates the axion and neutrino mass scales, Eq. (9.22)

9.1 Model construction

We now develop a new, consistent flavor extension of the Standard Model in which the gauge symmetry is enlarged by adding the local $SO(3)_F$ fam-

[2] The author of this Thesis himself is few months older than the top quark.

ily symmetry. In addition to Standard Model particles, the model has an enlarged scalar sector and right handed neutrinos. This minimal extension is enough to accommodate fermion masses and mixings without fine tuning of parameters, and the other features mentioned earlier.

The field content of our model is displayed in Table 9.1. Especially noteworthy are the Peccei-Quinn charge assignments[3]. They arise from a transformation that commutes with $SO(10)$: all the fermion fields which occur in the $SO(10)$ spinor have the same PQ charge. It also commutes with $SO(3)_F$.

	q_L	u_R	d_R	l_L	e_R	ν_R	Φ^u	Φ^d	Ψ^u	Ψ^d	σ	ρ
$\mathrm{SU(3)_C}$	**3**	**3**	**3**	**1**	**1**	**1**	**1**	**1**	**1**	**1**	**1**	**1**
$\mathrm{SU(2)_L}$	**2**	**1**	**1**	**2**	**1**	**1**	**2**	**2**	**2**	**2**	**1**	**1**
$\mathrm{U(1)_Y}$	$\frac{1}{6}$	$\frac{2}{3}$	$-\frac{1}{3}$	$-\frac{1}{2}$	-1	0	$-\frac{1}{2}$	$\frac{1}{2}$	$-\frac{1}{2}$	$\frac{1}{2}$	0	0
$\mathrm{SO(3)_F}$	**3**	**3**	**3**	**3**	**3**	**3**	**5**	**5**	**3**	**3**	**5**	**1**
$\mathrm{U(1)_{PQ}}$	1	-1	-1	1	-1	-1	2	2	2	2	2	2

Table 9.1: Particle content and transformation properties under the SM and flavor $SO(3)$ gauge groups. The VEVs of SM singlets σ and ρ break $U(1)_{PQ}$ and lepton number, generating Majorana neutrino masses.

Symmetry breaking

In the model under consideration, symmetry breaking proceeds through the following set of scalar fields (see table 9.1 for the PQ charge assignment):

[3]Recently, an alternative framework with flavor-dependent Peccei-Quinn charges has been proposed in [273,274]. Our $U(1)_{PQ}$ symmetry is related to flavor in a rather different way, through the $SO(3)$ family symmetry.

$$
\begin{aligned}
&\Psi^u \sim (\mathbf{1}, \mathbf{2}, -1/2, \mathbf{3})\,, \\
&\Psi^d \sim (\mathbf{1}, \mathbf{2}, 1/2, \mathbf{3})\,, \\
&\Phi^u \sim (\mathbf{1}, \mathbf{2}, -1/2, \mathbf{5})\,, \\
&\Phi^d \sim (\mathbf{1}, \mathbf{2}, 1/2, \mathbf{5})\,, \\
&\sigma \sim (\mathbf{1}, \mathbf{1}, 0, \mathbf{5})\,, \\
&\rho \sim (\mathbf{1}, \mathbf{1}, 0, \mathbf{1})\,.
\end{aligned}
\tag{9.5}
$$

In addition to the EW doublets, there are two $\mathrm{SU(3)_c} \otimes \mathrm{SU(2)_L} \otimes \mathrm{U(1)_Y}$ singlet scalars, $\sigma \sim (\mathbf{1}, \mathbf{1}, 0, \mathbf{5})$ and $\rho \sim (\mathbf{1}, \mathbf{1}, 0, \mathbf{1})$. All of these fields will acquire nonzero vacuum expectation values.

Both $SO(3)$ singlet as well as the quintuplet, carry nontrivial PQ charges. Therefore, the spontaneous breaking of the Peccei-Quinn symmetry is triggered by their large vacuum expectation values (VEVs). On the other hand, the $SO(3)$ family symmetry breaking is associated to the VEV of the SM singlet scalar σ;

$$
\langle \sigma \rangle = v_\sigma \ \mathrm{diag}(0, 1, -1) \qquad \text{and} \qquad \langle \rho \rangle = v_\rho \ \mathrm{diag}(1, 1, 1) \tag{9.6}
$$

As we will see later, both VEVs play a key role in breaking lepton number, generating Majorana neutrino mass, and accounting for the large neutrino mixing angles observed in neutrino oscillations.

In order to break the electroweak symmetry we assume VEVs for the $\mathrm{SU(2)_L}$ scalar doublets, i.e. Φ^u and Φ^d, transforming as $SO(3)$ quintuplets, as well as Ψ^u and Ψ^d, transforming as $SO(3)$ triplets. We assume the following pattern for the VEVs:

$$
\begin{aligned}
\left\langle \Phi^{u,d} \right\rangle &= \begin{pmatrix} 0 & & \\ & -k^{u,d} & \epsilon_1^{u,d} \\ & \epsilon_1^{u,d} & k^{u,d} \end{pmatrix} \\
\left\langle \Psi^{u,d} \right\rangle &= \begin{pmatrix} v^{u,d} \\ 0 \\ \epsilon_2^{u,d} \end{pmatrix}\,,
\end{aligned}
\tag{9.7}
$$

where the small parameters parameters ϵ_i denote a perturbation with respect to the simplest alignments diag(0,-1,1) and (1,0,0). This symmetry

breaking pattern minimizes the Higgs potential [33], and provides a good description of the observed fermion mass hierarchy as we will see in the next section.

An important feature of the model is the existence of a spontaneously broken $U(1)$ global PQ symmetry. For definiteness, we fix the PQ quantum numbers as given in Table 9.1. The VEVs of SM singlets σ and ρ break $U(1)_{PQ}$ as well as lepton number. The alignment of the associated Nambu-Goldstone boson, G, is

$$G \approx \frac{1}{(v_\sigma^2 + v_\rho^2)^{1/2}} \left(v_\sigma \sigma^I + v_\rho \rho^I + \dots \right) \tag{9.8}$$

where ρ^I etc. denote the imaginary parts of scalars and $\dots$ denotes components along the isodoublet scalars $\Psi^{uI}, \Psi^{dI}, \Phi^{uI}, \Phi^{dI}$, weighted by their VEVs and times their PQ charges. Notice that, through these projections, G will couple directly to quarks and leptons at the tree level. These couplings are suppressed linearly by the PQ-breaking scale $(v_\sigma^2+v_\rho^2)^{1/2}$. Thus we arrive at a model of the DFSZ type [98] (see Chapter 3) including coupling to neutrinos.

9.2 "Golden formula" for quarks and lepton masses

Given the $SO(3)$ multiplication rules, $\mathbf{3}\times\mathbf{3} = \mathbf{1}+\mathbf{3}+\mathbf{5}$, one can use the vector (triplet) and the two-index symmetric traceless tensor (quintuplet) representations to build the following invariant Yukawa Lagrangian,

$$\mathcal{L} = \bar{q}_L(y_1\Psi^u + y_2\Phi^u)u_R + \bar{q}_L(y_3\Psi^d + y_4\Phi^d)d_R + \bar{l}_L(y_5\Psi^d + y_6\Phi^d)e_R + \text{h.c.} \tag{9.9}$$

Note that the "duplicated" scalar sector, with two scalar doublets selectively coupled to up-type/down-type fermions, does *not* imply an effective nonminimal low-energy Higgs sector, as we shall discuss further below.

After electroweak breaking, Eq. (9.9) leads to the quark mass matrices

$$M^u = \begin{pmatrix} 0 & y_1\epsilon_2^u & 0 \\ -y_1\epsilon_2^u & -y_2 k^u & y_1 v^u + y_2\epsilon_1^u \\ 0 & -y_1 v^u + y_2\epsilon_1^u & y_2 k^u \end{pmatrix} \tag{9.10}$$

$$M^d = \begin{pmatrix} 0 & y_3\epsilon_2^d & 0 \\ -y_3\epsilon_2^d & -y_4 k^d & y_3 v^d + y_4\epsilon_1^d \\ 0 & -y_3 v^d + y_4\epsilon_1^d & y_4 k^d \end{pmatrix}, \tag{9.11}$$

and for the charged leptons

$$M^e = \begin{pmatrix} 0 & y_5\epsilon_2^d & 0 \\ -y_5\epsilon_2^d & -y_6 k^d & y_5 v^d + y_6\epsilon_1^d \\ 0 & -y_5 v^d + y_6\epsilon_1^d & y_6 k^d \end{pmatrix}, \tag{9.12}$$

where we take into account the VEV alignment patterns of the $SO(3)$ triplet and quintuplet scalars, respectively.

These matrices allow a good description of the charged fermion masses. Indeed, neglecting the ϵ_i parameters, assumed small, which describe the departure from the simplest VEV alignment, the eigenvalues of the matrices are given as

$$\begin{aligned} m_{u,d,e} &= 0\,, \\ m_{c,s,\mu} &= |y_{2,4,6}k^{u,d} - y_{1,3,5}v^{u,d}|\,, \\ m_{t,b,\tau} &= |y_{2,4,6}k^{u,d} + y_{1,3,5}v^{u,d}|\,. \end{aligned} \tag{9.13}$$

When one takes into account the small perturbations, ϵ_i, one finds that an interesting connection between fermion masses

$$\frac{m_\tau}{\sqrt{m_e m_\mu}} \approx \frac{m_b}{\sqrt{m_d m_s}}\,. \tag{9.14}$$

This successful formula nicely relates down-type quark and charged lepton masses. On the other hand, the doubled Higgs structure forced by PQ symmetry allows us to avoid the unwanted top quark mass prediction $\frac{m_\tau}{\sqrt{m_e m_\mu}} \approx \frac{m_t}{\sqrt{m_u m_c}}$, present in [33]. Analogous relations between quark and lepton masses also emerge in other flavor symmetry schemes, such as the ones proposed in [266, 267, 272], but without connection to an underlying Peccei-Quinn symmetry.

9.3 Emergence of the CKM matrix

We now show that, in addition to Eq. (9.14), our $SO(3)$ family symmetry scheme provides a dynamical framework for the CKM matrix describing quark mixing and CP violation.

It is clear from Eqs. (9.10), (9.11) and (9.12) that, in the limit of vanishing ϵ_i, the charged fermions of the first family are massless. Moreover, when the perturbations $\epsilon_i \to 0$, the matrix that diagonalizes $M_{u,d}.M_{u,d}^{\dagger}$ is given by

$$\mathcal{U}_L^{u,d} = \begin{pmatrix} 1 & 0 & 0 \\ 0 & 1/\sqrt{2} & 1/\sqrt{2} \\ 0 & -1/\sqrt{2} & 1/\sqrt{2} \end{pmatrix} , \tag{9.15}$$

for up and down-type quarks, with eigenvalues given by Eq. (9.13). The CKM matrix, defined as $V_{\rm CKM} = \mathcal{U}_{uL}\mathcal{U}_{dL}^{\dagger}$, is naturally "aligned" to be just the identity matrix.

The perturbations of the eigenvectors of $M.M^{\dagger}$ which result from turning on the perturbations around the minima get translated into a small shift of the matrices in Eq. (9.15), which no longer coincide. Their mismatch is the CKM matrix. After turning on these perturbations, the electron and the up and down quarks, all get nonzero masses, while small quark mixing angles emerge naturally.

Thanks to the structured breaking of the $SO(3)$ family symmetry, one can predict mixing angles in terms of quark masses. We have the well-known Gatto-Sartori-Tonin [275] relation for the Cabibbo angle

$$\theta_C \approx \sqrt{\frac{m_d}{m_s}} - \sqrt{\frac{m_u}{m_c}} , \tag{9.16}$$

while for $|V_{ub}|$ we get

$$|V_{ub}| \approx \frac{\sqrt{m_d m_s}}{m_b} - \frac{\sqrt{m_u m_c}}{m_t} , \tag{9.17}$$

which extends a relation found in Ref. [33]. Finally, the doubling of scalar quintuplets $\left\langle \Phi^{u,d} \right\rangle$ plays a crucial role in generating $|V_{cb}|$, given as

$$|V_{cb}| = \frac{\epsilon_1^u}{2k^u} - \frac{\epsilon_1^d}{2k^d} . \tag{9.18}$$

In contrast to θ_C and $|V_{ub}|$, the $|V_{cb}|$ matrix element can only emerge from the duplicated set of quintuplets, i.e. from the fact that Φ^u and Φ^d are different fields. Otherwise, the b quark would decay predominantly to up quarks through the weak charged current. Thus, in the present framework, mass hierarchies and mixing angles arise as perturbations around the symmetry breaking minima of the scalar potential, rather than hierarchies in the Yukawa couplings. CP violation can be accommodated through nontrivial phases in the Yukawa couplings, but no useful prediction emerges.

9.4 Neutrino masses and mixings

Neutrino masses arise naturally in $SO(10)$ unification through a conventional (type-I) seesaw mechanism [44–48]. In order to capture this at our level of analysis we add right-handed neutrinos ν_R transforming under the Peccei-Quinn symmetry, as in Table 9.1.

The relevant Yukawa Lagrangian to generate neutrino masses is given by

$$\mathcal{L}_\nu = \bar{l}_L(y_D\Psi^u + \tilde{y}_D\Phi^u)\nu_R + \bar{\nu}^c_R(y_M\sigma + y'_M\rho)\nu_R\,, \tag{9.19}$$

The vacuum expectation values of ρ and σ break the Peccei-Quinn symmetry spontaneously, as well as lepton number. The last terms in Eq. (9.19) generate Majorana masses for ν_R after symmetry breaking. Notice also that $\langle\sigma\rangle$ breaks the SO(3) family symmetry.

To support a viable seesaw mechanism, both ρ and σ are necessary. If there were only the flavor singlet, neutrino mixing would be similar to that of quarks, hence small, and ruled out by the neutrino oscillation data [185]. Were there only the quintuplet, a two index traceless symmetric tensor, the seesaw would be singular, leaving four light neutrinos, instead of three. The symmetry breaking pattern obtained through the simultaneous presence of σ and ρ plays a key role in order to account for why neutrinos mix in such a different way from quarks.

In short, in our model the quark mixing and the mass hierarchies arise from departures from the simplest VEV alignment of the Higgs fields, $\epsilon_i \neq 0$ in Eq. (9.7), and are significantly constrained. In contrast, neutrino masses and (generically large) lepton mixing are directly associated with Peccei-Quinn breaking.

9.5 Higgs scalar spectrum

Our explicit implementation of $SO(3)$ flavor symmetry requires several scalar multiplets. In the context of renormalizable quantum field theory, without further constraints, there are many scalar coupling terms, and - given that most of the spectrum is lifted to a high mass scale - few observational handles on them. Thus a complete analysis is both impractical and pointless; but we do need to ensure that an acceptable low-energy sector can emerge.

Generically, all the fields other than the axion will acquire mass terms of order the flavor and PQ breaking scale, barring cancellations between bare and induced mass terms. For purposes of $SU(2) \times U(1)$ breaking, we require at least one much lighter doublet. Notoriously, that requires a conspiracy or fine-tuning among parameters. This is an aspect of the hierarchy problem, which we do not address here. The only slight good news is that the existence of more than one doublet would require additional fine tuning, so that the minimal one doublet structure, which so far is supported by experimental observations, is minimally unnatural.

To illustrate the mechanism whereby induced mass terms arise, consider the quartic operator $\Psi_u^\dagger \Psi_u \sigma^\dagger \rho$. Its contraction is unique and can be easily visualized in matrix form. If $\langle\sigma\rangle$ is aligned in the diagonal (recall it is symmetric and traceless) and ρ is an $SO(3)$ singlet we get, after $SO(3)$ breaking takes place,

$$\begin{aligned}\langle\rho\rangle\, \Psi_u^\dagger \left\langle\sigma^\dagger\right\rangle \Psi_u &= v_\rho \begin{pmatrix} \Psi_{1u}^\dagger & \Psi_{2u}^\dagger & \Psi_{3u}^\dagger \end{pmatrix} \begin{pmatrix} 0 & 0 & 0 \\ 0 & -v_\sigma & 0 \\ 0 & 0 & v_\sigma \end{pmatrix} \begin{pmatrix} \Psi_{1u} \\ \Psi_{2u} \\ \Psi_{3u} \end{pmatrix} \\ &= -v_\sigma v_\rho |\Psi_{2u}|^2 + v_\sigma v_\rho |\Psi_{3u}|^2 \,. \end{aligned} \tag{9.20}$$

One sees that the vacuum expectation value of the above operator generates a splitting of order the flavor/PQ breaking scale among the electroweak doublet components of Ψ_u, so that two of them can be made heavy, i.e. at the large symmetry breaking scale, leaving only one massless. This argument may be escalated to the full scalar potential, which contains many

relevant quartics, viz.

$$\begin{gathered}\Phi_u^\dagger\Phi_u\sigma^\dagger\sigma\,,\ \Phi_u^\dagger\Phi_u\sigma^\dagger\rho\,,\ \Phi_u^\dagger\Phi_u\rho^\dagger\rho\,,\ \Psi_u^\dagger\Psi_u\sigma^\dagger\sigma\,,\ \Psi_u^\dagger\Psi_u\sigma^\dagger\rho\,,\ \Psi_u^\dagger\Psi_u\rho^\dagger\rho\,,\\ \Phi_d^\dagger\Phi_d\sigma^\dagger\sigma\,,\ \Phi_d^\dagger\Phi_d\sigma^\dagger\rho\,,\ \Phi_d^\dagger\Phi_d\rho^\dagger\rho\,,\ \Psi_d^\dagger\Psi_d\sigma^\dagger\sigma\,,\ \Psi_d^\dagger\Psi_d\sigma^\dagger\rho\,,\ \Psi_d^\dagger\Psi_d\rho^\dagger\rho\,,\\ \Phi_u^\dagger\Psi_u\sigma^\dagger\sigma\,,\ \Phi_u^\dagger\Psi_u\sigma^\dagger\rho\,,\ \Phi_u^\dagger\Psi_u\sigma\rho^\dagger\,,\Phi_d\Psi_d^\dagger\sigma^\dagger\sigma\,,\ \Phi_d\Psi_d^\dagger\sigma^\dagger\rho\,,\ \Phi_d\Psi_d^\dagger\sigma\rho^\dagger\,,\\ \Phi_u\Phi_d\sigma^\dagger\sigma^\dagger\,,\ \Phi_u\Phi_d\sigma^\dagger\rho^\dagger\,,\ \Phi_u\Phi_d\rho^\dagger\rho^\dagger\,,\ \Psi_u^\dagger\Psi_d^\dagger\sigma\sigma\,,\ \Psi_u^\dagger\Psi_d^\dagger\sigma\rho\,,\ \Psi_u^\dagger\Psi_d^\dagger\rho\rho\,,\\ \Phi_d\Psi_u\sigma^\dagger\sigma^\dagger\,,\ \Phi_d\Psi_u\sigma^\dagger\rho^\dagger\,,\ \Phi_u^\dagger\Psi_d^\dagger\sigma\sigma\,,\ \Phi_u^\dagger\Psi_d^\dagger\sigma\rho \qquad (9.21)\end{gathered}$$

These operators can be obtained in a systematic way using the code in [276]. Most of the operators above have several, different contractions. One finds that, after breaking, the scalar mass^2 matrix typically contains suitable off-diagonal terms, ensuring that the light doublet is a linear combination of $\Psi^u, \Psi^d, \Phi^u, \Phi^d$ wherein each appears with a nonzero coefficient. This light doublet, responsible of EWSB, corresponds to the Higgs found at the LHC.

9.6 Discussion

Before closing, we comment briefly on several issues which deserve mention.

1. The PQ symmetry $U(1)_{PQ}$ is conserved at the classical level, and to all orders in perturbation theory, but violated nonperturbatively. One can visualize the breaking using QCD instantons, and infer its character by analyzing anomalies. In this way, one may discover that a nontrivial Z_N subgroup of $U(1)_{PQ}$ is valid even nonperturbatively. Our model, as it stands with doubly PQ-charged scalar fields, has $N = 12$. If scalar fields which are not Z_N singlets acquire VEVs, the possibility of domain walls arises. Such domain walls are very dangerous for early universe cosmology [165]. The most straightforward way to avoid this difficulty is to assume that the Z_N breaking is followed by a period of cosmic inflation, so that potential domain walls get pushed beyond the horizon. Another possibility is to arrange that $N = 1$. (We could also allow $N = 2$, since the PQ-breaking VEVs have PQ charge 2). This does not occur in our model as it stands, but it can be achieved by adding suitable colored fermions. In the absence of other motivations, however, that construction seems contrived. Another compelling solution could be the mechanism proposed in [105] by the author of this Thesis and A. Caputo.

2. The vacuum expectation values of the ρ and σ scalars are responsible both for Peccei-Quinn and lepton number symmetry breaking. This entails an interesting conceptual relation between the axion and neutrino mass scales, of the form

$$m_a \sim (\Lambda_{QCD} m_\pi / v^2) m_\nu \,, \tag{9.22}$$

where m_π is the pion mass and v is the electroweak scale. This relation, implies that the axion mass is parametrically smaller than the neutrino mass, according to the square of the ratio of QCD to electroweak scales. Since it assumes that the Yukawa couplings involving the neutrino field is of order unity, it should be applied using the heaviest of the light neutrinos. Of course, we cannot preclude the possibility that PQ symmetry breaks at a higher scale, through condensates which do not generate neutrino masses; this effect could drive the axion mass down further. Such light axions, $m_a \ll O(\mu)$eV, usually tend to overproduce DM through the misalignment mechanism. A compelling solution in which the axion field relaxes to its minimum during inflation, hence reducing its relic abundance, has been recently proposed [277, 278].

3. The presence of extra gauge bosons coupled to flavor will mediate $\Delta F = 2$ neutral flavor changing interactions at tree-level. The most sensitive probe appears to be $K^0 - \bar{K}^0$ mixing [279]. From this we estimate

$$\frac{g^2}{M_F^2} \lesssim \frac{1}{[10^4\,\text{TeV}]^2} \,, \tag{9.23}$$

where the gauge boson mass is $M_F \sim g f_a$. This constrains the Peccei-Quinn breaking scale to be $f_a \gtrsim 10^7$ GeV, a much weaker bound than the one from astrophysical constraints (see Chapter 3).

4. It is tempting to imagine that the small departures from the vacuum alignment in Eq.(9.7), ϵ_i, are generated through quantum corrections. This possibility has been very recently explored by Weinberg in [280] using a different family gauge group, $SO(3)_L \times SO(3)_R$. Interestingly enough, the radiative corrections do not disappear in the limit of large gauge boson mass, $M_G \to \infty$. The fact that these quantum corrections do not disappear does not contradict the decoupling theorem of quantum field theories. When M_G is large, it implies that the family group breaks at a large scale and, from an EFT point of view, the low-energy

theory is symmetric only under the EW group, $SU(2) \times U(1)$. This ensures that in the case ϵ_i are generated through quantum corrections, they will remain finite in the limit of large gauge boson masses[4]. This allows to have sizeable quantum effects and being consistent with the $\Delta F = 2$ bounds mentioned above. The application of this mechanism for our $SO(3)$ scenario will be considered in a near future.

9.7 Summary

Motivated by ideas arising in comprehensive unification based on spinors (see chapter 8), the goal of this chapter, based on reference [271], has been to consider the consequences of supplementing the SM gauge symmetry with commuting $SO(3)$ flavor and PQ symmetries in a way consistent with $SO(10)$ embedding. Proceeding in a bottom-up way, we have analyzed a novel, minimal $SO(3)_F \times U(1)_{PQ}$ extension of the SM unifying together the three families of matter. Fairly simple choices of multiplet structure and symmetry breaking pattern allowed us to accommodate the known phenomenology of quark and lepton masses and mixings, and to make several nontrivial connections among them. The PQ symmetry is a crucial ingredient, and of course it continues to serve its familiar roles in ensuring accurate strong T symmetry and in providing, in axions, a good dark matter candidate.

[4] I thank S. Weinberg for raising this point during an interesting email correspondence.

Part IV

Final Remarks

Final Thoughts and Conclusions

If you are reading this, you made it! You managed to go through the Thesis and now you are probably wondering what are the conclusions. There is no definite conclusion, though. In this Thesis, I have shown you what is my personal vision of BSM physics. Another reason why there are no concrete conclusions is because I find satisfaction in learning about different things. I am strongly convinced that only learning and studying the many faces and aspects of Nature we will obtain a better understanding of our world. This is the main reason why, during the different parts of the Thesis, I have always tried to connect different open questions in fundamental physics.

In the first part I have done my best to motivate the reader about the need of going beyond the Standard Model of particle physics. Despite it is an incredibly successful theory and predicts many phenomena very accurately, we have several compelling indications that point in the direction of a more fundamental theory. Since the list of open questions is excessively long for any PhD Thesis (see 1.3), I have restricted myself to neutrino masses, dark matter, flavor and GUTs, with particular emphasis in their possible links.

On the other hand, parts II and III are based on research articles that I have completed during my PhD. Here, in this section, I summarize the main results and findings of each chapter.

Spontaneous breaking of lepton number and dark matter

In chapter 6 we have discussed the possibility of having a $U(1)_L$ lepton number symmetry spontaneously broken after inflation, and examined whether relatively light majorons can form the cosmological dark matter.

The spontaneous violation of the $\mathrm{U}(1)_L$ symmetry results in the formation of cosmic strings. We assume that the majoron has a nonzero mass, which explicitly breaks the $\mathrm{U}(1)_L$ symmetry at low energies. This breaking effect leads to the formation of domain walls attaching cosmic strings, when the Hubble parameter decreases to the majoron mass scale, m_J. These topological defects shrink to a point because of the tension of the domain walls and subsequently decay into non-relativistic majorons. In this thesis we have determined the parameter region where the total amount of majorons is consistent with the observed amount of dark matter. In particular, we have found that a majoron with $m_J \lesssim \mathcal{O}(1)\,\mathrm{eV}$ or even lighter is a viable dark matter candidate with lifetime, in some cases, a few orders of magnitude longer than the age of the Universe. The decay of such a light and *short lived*[5] majoron leads to an observable neutrino signal to the PTOLEMY experiment [162, 163]. A small fraction of relativistic majorons can also be produced thermally which, due to their small mass $m_J \leq \mathcal{O}(1)$ eV, contributes to the energy density of the Universe as dark radiation. This would be indirectly observed by the future observation of CMB anisotropies, like CMB-S4 [181, 182].

Non-relativistic majorons have large density perturbations because they are produced from the decay of topological defects. Overdense regions condense forming boson stars after the matter-radiation equality. We have discussed for the first time the properties of these majoron stars, including their size and mass. Moreover, we have shown that the neutrino production rate from a boson star may be drastically suppressed by the Pauli statistics at its surface. However, a precise determination of the amount of majorons that condense in these boson stars requires a more careful quantitative analysis.

Colored dark matter and radiative neutrino masses

In the standard scenario, DM candidates are usually asssumed to be electrically neutral and without color charge. Nevertheless, under certain circumstances colored particles can also constitute the dominant part of cosmological DM. This is precisely the case that has been studied in chapter 7, where DM is a bound state of a new colored fermion.

In this chapter we have considered a fermion transforming as $\mathcal{Q} \sim (8, 1, 0)$. The hadronic state, $\mathcal{Q}\mathcal{Q}$, is able to describe the observed DM

[5]Short here means comparable to the age of the Universe.

relic abundance if the fermion mass is [201]:

$$M_{\mathcal{Q}} = 12.5 \pm 1 \text{ TeV}\,. \tag{9.24}$$

In this thesis we have explicitly shown that such an exotic fermion can also be the neutrino mass messenger under certain circumstances. We have considered two models where we have Dirac and Majorana neutrino masses. In the first case, for Dirac neutrinos, the DM stability plays a crucial role to forbid the Majorana mass terms at the Lagrangian level. Additionally, the same symmetry that explains DM longevity, together with a discrete Z_2 symmetry, forbids the tree-level Dirac neutrino mass. In the case of Majorana neutrinos, DM stability and the fact that the DM particle carries color charge forbid the tree-level Dirac mass terms for neutrinos. In close analogy to the Dirac case, only radiative Majorana mass terms are allowed. Both variants slightly differ in their particle content, as we can see in tables: 7.1 and 7.2.

Regarding the phenomenology, both models have aspects in common such as the LFV process $\mu \to e\gamma$ studied in section 7.4. This process constrains the scalar masses to be:

$$\left| \sum_a h_\mu^a h_e^{a*} \left(\frac{50\,\text{TeV}}{M_{\eta_a^+}} \right)^2 \right| \lesssim 1.5. \tag{9.25}$$

Another implication which does not depend on the nature of the neutrino mass is the production of colored fermions, $\mathcal{Q}$, at hadron colliders. Due to their color charge, one expects that these particles are coupiously produced at colliders, given enough energy, in processes such as $q_i\bar{q}_i \to \mathcal{Q}\bar{\mathcal{Q}}$ and $gg \to \mathcal{Q}\bar{\mathcal{Q}}$. From LHC data, we know that $M_{\mathcal{Q}} > 2$ TeV. Despite this limit is still far from the colored DM prediction, $M_{\mathcal{Q}} = 12.5$ TeV, the relevant parameter space of these models will be fully tested once we combine direct DM detection limits (see Fig.7.1) and data from future hadron colliders.

A process which only appears in the case of Majorana neutrinos is neutrinoless double beta decay. Despite the process is not specific of this model, we have considered this possibility in section 7.3, comparing the preditions to the experimental limits and future sensitivities.

Comprehensive unification using spinors

As we have seen in part I, despite the SM describes a vast range of phenomena precisely and very accurately, it contains a diversity of interactions and, when we come to the fermions, a plethora of independent elements. Theories based on the $SO(10)$ gauge group beautifully unify fundamental interactions and all the particles of a given family. Indeed, upon symmetry breaking down to the SM gauge group, the $SO(10)$ spinor representation splits as:

$$\mathbf{16} \to q_L + \bar{u}_R + \bar{d}_R + l_L + \bar{e}_R + \bar{\nu}_R \,. \tag{9.26}$$

In addition to the quantum numbers of a SM family, this spinor contains a representation with the quantum numbers of a right-handed neutrino.

The $SO(10)$ theory, however, offers no information about family replication, since the number of spinors, **16**, is just a free parameter. As we have reviewed in section 5.3, one can go beyond the minimal $SO(10)$ theory to explain family replication using spinors. This occurs thanks to the properties of spinors, which decompose repetitively. In particular, after symmetry breaking, a $SO(2n + 2m)$ spinor with dimension 2^{n+m-1} decomposes into 2^m copies of the $SO(2n)$ spinor.

It has been shown in the past [148] that the smallest group with spinor representations containing (at least) three SM families is the $SO(18)$ group. One can easily see that, in this case, the **256** spinor splits as

$$\mathbf{256} \to (\mathbf{16}, \mathbf{8}) \;+\; (\overline{\mathbf{16}}, \mathbf{8}') \,, \tag{9.27}$$

when the the $SO(18)$ gauge symmetry breaks down to $SO(10) \times SO(8)$. From the $SO(10)$ point of view, the spinor **256** contains 8 families and 8 mirror families with the wrong chirality. The problem of removing the mirror families and obtaining just 3 chiral families was unsolved since the '80s.

In chapter 8, in order to solve the problematic proliferation of fermions, we have considered a theory based on the $SO(18)$ gauge group in a completely new, extra-dimensional framework. The fundamental idea is to combine the mechanism of orbifold symmetry breaking together with hypercolor confinement. The mirror families disappear from the low-energy spectrum thanks to the orbifold symmetry breaking. On the other hand, the extra families are confined thanks to the hypercolor interaction, effectively leaving just three chiral SM families.

In more detail, we have employed a gauge theory in a 5-dimensional space-time. The boundary conditions on the $S_1/(Z_2 \times Z_2')$ orbifold break the initial gauge symmetry down to $SO(10) \times SO(8)$ and remove the fermionic zero modes of the $(\overline{\mathbf{16}}, \mathbf{8}')$ part.

The extra families, corresponding to the $(\mathbf{16}, \mathbf{8})$ part, are removed from the low-energy spectrum when the $SO(5)$ subgroup of $SO(8)$, which remains unbroken, becomes strongly coupled and confining at around the TeV scale. For historical reasons we refer to this interaction as hypercolor. When we consider the breaking $SO(10) \times SO(8) \to SO(10) \times SO(5)$, the representation splits as:

$$(\mathbf{16}, \mathbf{8}) \to 3 \times (\mathbf{16}, \mathbf{1}) + (\mathbf{16}, \mathbf{5})\,. \tag{9.28}$$

This means that the three observed SM families are precisely given by the hypercolor singlets, $3 \times (\mathbf{16}, \mathbf{1})$.

Similarly to the baryon number in the strong interaction, the $SO(5)$ interaction supports a conserved quantum number. Unlike baryon number, in the case of hypercolor, the conserved symmetry is a discrete Z_2 symmetry under which the hyperquarks, $(\mathbf{16}, \mathbf{5})$, are charged. Due to this exact symmetry, and because of group theoretic properties of $SO(5)$, the lightest unconfined state (Z_2 odd and $SO(5)$ neutral) are hyperbaryons composed of 5 hyperquarks. These particles are thermally produced in the early universe with a relic abundance today given by:

$$\Omega_\chi h^2 \approx 10^{-5} \Big(M/\mathrm{TeV} \Big)^2 , \tag{9.29}$$

with M the hyperbaryon mass. For $M \lesssim O(10)$ TeV, despite they are conceivably detectable at future colliders, the relic hyperbaryons contribute only a small fraction of the mass density of the universe.

$SO(3)$ as a gauge family symmetry

Since the late '70s and beginning of the '80s many proposals have been made to explain family replication and the pattern of fermion masses and mixings. To this end, it seems appropriate to consider symmetry groups containing triplet representations. In analogy to other fundamental interactions it seems compelling to relate the SM families with a gauge symmetry. In this case there are only two possibilities: $SU(3)$ and $SO(3)$. The $SU(3)$ option is challenged by gauge anomalies if one considers a minimal fermion content. On the other hand, the $SO(3)$ group is anomaly free. Additionally,

$SO(3)$ is a natural subgroup of $SO(18)$. Therefore it fits perfectly with the idea of comprehensive unification using spinors developed in chapter 8.

This sort of gauge family symmetries were studied by Wilczek and Zee at the end of the '70s [33]. In their work, in addition to other predictions, they obtained an interesting relation between fermion masses:

$$\frac{m_e m_\mu}{m_\tau^2} = \frac{m_d m_s}{m_b^2} = \frac{m_u m_c}{m_t^2} \,. \tag{9.30}$$

While the first relation is reasonably well satisfied, the second predicted a too light top quark: $m_t \approx 15$ GeV. When the top quark was discovered with a much larger mass (today we know that its mass is $m_t^{exp} = 172.9 \pm 0.4$ GeV), the minimal $SO(3)$ model was ruled out.

In this thesis, and in particular in chapter 9, we have determined the minimal requirements of a theory with a $SO(3)$ gauge family symmetry to be consistent with experimental data and, at the same time, keep the successful predictions. Specifically we have studied a theory with commuting $SO(3)$ family and PQ symmetries in a way consistent with $SO(18)$ comprehensive unification. Within a reasonably simple model, several appealing features appear:

- Thanks to the Peccei-Quinn symmetry, in addition to solving the strong CP problem, we obtain axion DM.

- We keep the successful, interesting connection between down-type quarks and charged lepton masses, $\frac{m_e m_\mu}{m_\tau^2} = \frac{m_d m_s}{m_b^2}$. At the same time, thanks to a duplicated Higgs sector (see table 9.1), the top quark mass becomes a free parameter.

- We explain the origin of the CKM matrix and obtain some of the quark mixing angles as a function of their mass. The Cabibbo angle is given by $\theta_C \approx \sqrt{\frac{m_d}{m_s}} - \sqrt{\frac{m_u}{m_c}}$. We also get a relation for the CKM matrix element: $|V_{ub}| \approx \frac{\sqrt{m_d m_s}}{m_b} - \frac{\sqrt{m_u m_c}}{m_t}$. Unlike in the original proposal, we obtain a small but non-zero $|V_{cb}|$ matrix element (see Eq.(9.18)).

- The smallness of the neutrino mass scale is explained thanks to the type-I seesaw mechanism and we obtain a conceptual relation between this scale and the axion mass: $m_a \sim (\Lambda_{QCD} m_\pi / v_{EW}^2) m_\nu$.

- The PQ and $SO(3)$ family symmetries are spontaneously broken at the same energy scale. Since $SO(3)$ gauge bosons contribute to $\Delta F = 2$

processes like $K^0 - \bar{K}^0$ mixing, we obtain a lower bound for axion decay constant: $f_a > 10^7$ GeV.

Looking for connections between different aspects of Nature has been incredible fruitful in the past. Despite there is no guarantee that it will remain useful in the future, as physicists we need to keep trying and continue looking for simple and predictive theories that can be tested. In the end, it is the experiment and not the beauty of our theories what will show us the path towards the understanding of Nature.

Resum de la Tesi

El tema principal d'aquesta Tesi és l'estudi de la física més enllà del Model Estàndard (ME). Aquest és, clarament, un camp tremendament ampli que recull molts aspectes de física fonamental, incloent-hi branques de la física de partícules i la cosmologia. Durant aquests anys he pogut gaudir de nombroses col·laboracions (vegeu llistat de publicacions) amb físics i físiques de renom, algunes de les quals he inclòs en aquesta tesi. Per motius obvis, durant la realització d'aquesta tesi m'he centrat en un nombre finit d'aspectes de la física més enllà del ME els quals inclouen la generació de les masses dels neutrins, la matèria fosca i les teories de gran unificació i del sabor.

Els continguts d'aquesta tesi es troben dividits en tres parts clarament diferenciades. En la primera, he introduït el ME i he enumerat els diferents motius, o indicis, que ens fan sospitar la necessitat de trobar una teoria més profunda, més fonamental. A més, en diferents capítols i amb relativa profunditat he descrit els temes principals sobre els quals he basat la meua investigació: la generació de la massa del neutrí (2), la matèria fosca (4) i les teories de gran unificació (5). En aquests capítols, corresponents a la primera part de la tesi, he intentat fer una revisió bibliogràfica dels temes en qüestió perquè el lector no expert puga adquirir el nivell adequat per a una comprensió plena de les parts 2 i 3, les quals estan basades en treballs d'investigació publicats en articles en revistes de nivell internacional.

La part 2 està basada en articles on he estudiat la possible connexió entre l'origen de la massa del neutrí i la naturalesa de la matèria fosca. D'altra banda, en la part 3 m'he centrat en determinades teories que permeten l'explicació de l'origen del *sabor* al ME i també dels números quàntics de les partícules fonamentals.

Per tal de simplificar la discussió, he dividit aquest resum en 3 parts, de manera que cadascuna resumeix una de les parts de la tesi.

El Model Estàndard i més enllà

Durant el segle XX, diferents avanços a nivell teòric i experimental van desencadenar el naixement del Model Estàndard, la teoria confirmada més precisa que disposem per una descripció de la Natura al nivell més profund. El ME és una teoria gauge de les interaccions fortes i electrofebles. Per tant, a més d'invariància sota transformacions del grup de Lorentz, el ME es basa en la invariància gauge, és a dir a nivell local, respecte del grup:

$$SU(3)_C \times SU(2)_L \times U(1)_Y \,. \tag{9.31}$$

EL ME conté els 8 gluons de la interacció forta, $SU(3)_C$, i els 4 bosons corresponents a la part electrofeble, $SU(2)_L \times U(1)_Y$. D'altra banda, els fermions del ME s'agrupen en diferents representacions del grup de gauge en funció a la seua quiralitat:

$$\begin{pmatrix} \nu_l \\ e \end{pmatrix}_L \,, \quad \begin{pmatrix} u \\ d \end{pmatrix}_L \,, \quad e_R \,, \quad u_R \,, \quad d_R \,. \tag{9.32}$$

Tal com veiem, els camps levogirs s'organitzen en doblets del grup $SU(2)_L$ mentre que els camps dextrogirs són singlets de $SU(2)_L$, violant la simetria de paritat al nivell més fonamental. Aquesta estructura és replicada tres vegades, donant-nos el que coneixem com les famílies del ME. Aquest és un dels misteris que s'han investigat en les parts de recerca d'aquesta tesi.

Si la simetria gauge 9.31 fos exacta, el món seria molt diferent del que coneixem. El motiu és que les partícules elementals no tindrien massa i, a més, la força nuclear feble tindria un abast infinit i una major intensitat. Per tant, resulta necessari trencar aquesta simetria. Aquesta ruptura ha de ser d'un tipus molt particular, el que coneixem com ruptura espontània de la simetria. El mecanisme de Higgs és el responsable d'aquest procés al ME. La idea principal de la ruptura espontània de simetries és que el Lagrangià preserva la simetria mentre que el buit, entés com a estat de mínima energia, la trenca. Aquesta idea simple i bonica és portada a terme al ME per un camp escalar complex, el que coneguem com a camp de Higgs, que es transforma com:

$$H = \begin{pmatrix} H^+ \\ H^0 \end{pmatrix} \,. \tag{9.33}$$

Al ME, l'estat de mínima energia s'assoleix quan el Higgs desenvolupa un valor d'expectació del buit:

$$\langle H \rangle = \frac{1}{\sqrt{2}} \begin{pmatrix} 0 \\ v \end{pmatrix} . \tag{9.34}$$

A causa de la interacció amb aquest condensat, el grup de gauge del ME (vegeu equació (9.31)) es trenca espontàniament, donant lloc a la interacció electromagnètica:

$$SU(2)_L \times U(1)_Y \to U(1)_{EM} . \tag{9.35}$$

Les masses dels fermions es generen quan els fermions interaccionen amb el buit del Higgs per mitjà de les interaccions de Yukawa (vegeu Eq. (1.26)). Aquesta interacció genera les matrius de massa dels fermions:

$$M^f_{ij} = Y^f_{ij} \frac{v}{\sqrt{2}} , \tag{9.36}$$

que es diagonalitzen per mitjà de rotacions de les components levogires i dextrogires:

$$f_{iL} = \mathcal{U}^f_{L\,ij} f'_{jL} , \quad f_{iL} = \mathcal{U}^f_{R\,ij} f'_{jR} . \tag{9.37}$$

En les equacions anteriors l'índex f indica el tipus de fermió: quarks de tipus up, quarks de tipus down i leptons carregats.

El fet de que els estats de massa i els estats de sabor no coincideixen, és a dir que les matrius de canvi de base $\mathcal{U}^f_{L\,ij} \neq \mathbb{I}$, i a més que les matrius corresponents als quarks tipus up i dels quarks tipus down són diferents, $\mathcal{U}^u_{L\,ij} \neq \mathcal{U}^d_{L\,ij}$, resulta en l'aparició de la matriu CKM, V_{CKM}. Aquesta matriu, ve donada per:

$$V_{CKM} = \mathcal{U}_{u\,L} \mathcal{U}^\dagger_{d\,L} = \begin{pmatrix} V_{ud} & V_{us} & V_{ub} \\ V_{cd} & V_{cs} & V_{cs} \\ V_{td} & V_{ts} & V_{tb} \end{pmatrix} , \tag{9.38}$$

i és la responsable de les transicions de sabor entre diferents famílies en el sector dels quarks. En el ME aquestes transicions estan mediades per el corrent carregat i connecten quarks de tipus *up* amb quarks de tipus *down*.

Un altre aspecte important del ME que està íntimament lligat a l'estructura en famílies és la violació de la simetria CP per la interacció feble. La raó és que aquest fenomen, en el sector dels quarks, solament és possible si existeixen almenys 3 famílies. A més, la violació de CP requereix que tots els angles de mescla de la matriu CKM siguen diferents de zero.

Una vegada hem resumit els aspectes clau del ME, cal recordar les diferents evidències i motivacions que tenim per a anar més enllà:

- **La generació de massa dels neutrins.** En el ME els neutrins no tenen massa. No obstant això, gràcies als experiments d'oscil·lacions de neutrins sabem que aquestes partícules tenen una massa no nul·la. A més, explicar que les seues masses estan a una escala ordres de magnitud més menuda que la dels fermions del ME ens fa sospitar que aquest mecanisme va més enllà del mecanisme de Higgs.

- **El problema del sabor.** És un fet remarcable que els fermions del ME s'organitzen en famílies i que aquestes estiguen replicades 3 vegades. A més, la jeràrquica distribució de les seues masses i el peculiar patró de mescles no està explicat en el ME.

- **La matèria fosca.** Les observacions astrofísiques i cosmològiques indiquen que n'hi ha aproximadament 5 vegades més matèria de la que *vegem*. Les interaccions i la naturalesa d'aquesta *matèria fosca* són actualment desconegudes.

- **La unificació de les forces.** La quantització de la càrrega elèctrica és un dels problemes més importants de la física. Amb el naixement del ME, aquesta pregunta ha sigut reescalada a explicar l'origen de les diferents interaccions i les seues intensitats relatives. Les teories de gran unificació responen aquestes preguntes gràcies a l'ús de grups de simetria gauge simples que, per baix d'una determinada energia, es trenquen espontàniament al grup del ME.

- **Asimetria matèria-antimatèria.** Resulta impossible explicar, en el marc de la teoria del Big Bang, perquè l'Univers conté matèria i no antimatèria. Per a explicar-ho cal anar més enllà del ME introduïnt ingredients que permitisquen realitzar les conegudes com a *condicions de Sakharov*.

- **Violació de la simetria CP en la interacció forta.** El fet que la interacció feble sí viola la simetria CP, és complicat explicar per què aquest fenomen no es dona en el sector de la interacció forta.

- **El problema de la jerarquia.** Explicar la diferència de magnitud entre l'escala de Planck i l'escala electrofeble, aproximadament un factor 10^{16}, és un dels problemes oberts que ha tractat d'explicar la física teòrica durant els últims 40 anys.

- **Inflació cosmològica.** Amb la finalitat de resoldre el problema de la planitud i el problema de l'horitzó de la teoria del Big Bang, l'univers inflacionari és la millor explicació que tenim actualment de les peculiars condicions inicials del nostre Univers. Es desconeix la duració i el moment en el qual va ocórrer aquesta fase de l'Univers primitiu, si és que va ocórrer.

- **La constant cosmològica i energia fosca.** De les observacions cosmològiques sabem que actualment l'Univers s'expandeix de forma accelerada. En aquest cas el problema radica en entendre perquè l'Univers pareix estar dominar per un *fluid*, anomenat energia fosca, que es comporta de forma semblant a una constant cosmològica amb una densitat d'energia $\rho_{vac} \sim (3 \text{ meV})^4$.

- **Gravetat quàntica.** Mentre que l'electromagnetisme i les forces nuclears forta i feble tenen una descripció quàntica satisfactòria, de moment no tenim una teoria quàntica de la gravitació. Probablement, el candidat més prometedor és la teoria de cordes en la qual u canvia la descripció de la Natura en termes de partícules per objectes tals com cordes i membranes.

Aquesta tesi recull els diferents avanços publicats en diferents articles sobre els primers quatre problemes.

L'origen de la massa del neutrí i la seua relació amb la matèria fosca

El descobriment de les oscil·lacions de neutrins va conduir a Takaaki Kajita i Arthur McDonald a guanyar el premi Nobel en física en 2015. Aquest fenomen mecanoquàntic és actualment una de les evidències més sòlides de la necessitat d'anar més enllà del ME. Aquestes oscil·lacions ocorren quan els autoestats de massa i autoestats de sabor no coincideixen. En aquest cas, existeix una probabilitat no nul·la que un neutrí produït amb sabor α

siga detectat com a neutrí de sabor β. Aquest procés només pot ocórrer si almenys dos neutrins tenen masses no degenerades.

Al contrari que la resta de fermions, els neutrins no tenen massa en el ME. No obstant això, cada vegada tenim més indicis que el ME és solament una teoria efectiva d'una realitat més fonamental. Per tant, podem prendre el ME com una teoria efectiva i afegir una col·lecció d'operadors amb dimensió $d > 4$:

$$\mathcal{L} = \mathcal{L}_{SM}^{(4)} + \sum_{i=4}^{\infty} \frac{C_i}{\Lambda^{i-4}} O_i \,. \tag{9.39}$$

Aquests operadors, O_i, han de respectar les simetries gauge del ME però no necessàriament les simetries globals tals com el número leptònic o bariònic. De fet, Weinberg va ser el primer a adonar-se que l'operador:

$$\mathcal{O}_5 \sim l_L l_L \phi\phi \,, \tag{9.40}$$

genera masses per als neutrins després de la ruptura espontània de la simetria electrofeble. En aquest cas, l'escala típica de la massa del neutrí ve donada per $m_\nu \sim \langle\phi\rangle^2 / \Lambda$ i és possible acomodar el valor experimental $m_\nu \sim O(0.1)$ eV si Λ és suficientment gran.

Existeixen diferents possibilitats per a obtenir l'operador de Weinberg (9.40) en el marc d'una teoria renormalitzable. D'una banda tenim els mecanismes de *seesaw* que el generen a nivell arbre i d'altra banda podem generar-lo a nivell radiatiu, és a dir degut a correccions quàntiques, habitualment conegudes amb el nom de *loops*. Com veurem a continuació, en aquesta tesi hem considerat les dues possibilitats i, a més, hem estudiat com aquests mecanismes poden relacionar-se amb la matèria fosca cosmològica.

La natura de la matèria fosca és una de les qüestions més urgents en física fonamental. Gràcies a diferents observacions, des de les corbes de rotació de les galàxies al fons còsmic de microones, actualment tenim evidència sòlida que existeix aproximadament 5 vegades més matèria no relativista que de matèria bariònica que observem en l'espectre electromagnètic. Aquesta matèria no relativista addicional és allò que anomenem matèria fosca i la seua composició és un dels misteris més profunds de l'Univers.

En funció del mecanisme de producció, la seua estabilitat i la detectabilitat, existeixen diferents tipus de matèria fosca. La idea fonamental és que aquesta component s'ha de comportar com a matèria no relativista i ha de ser produïda de forma controlada a l'univers primitiu. A més, la interacció amb el sector del ME ha de ser suficientment feble per tal d'evitar els límits experimentals (vegeu secció 4.2). Exemples de candidats a matèria

fosca inclouen els *WIMPS*, és a dir, partícules massives que interaccionen feblement amb el ME, i els *axions* i altres bosons lleugers.

La part 2 d'aquesta tesi inclou les dues possibilitats. Mentre que en un cas la matèria fosca presenta un comportament molt semblant a un *WIMP*, també s'ha considerat la possibilitat de que la matèria fosca estiga formada per un bosó extremadament lleuger. En ambdós casos la matèria fosca juga un paper clau en la generació de massa per als neutrins.

Matèria fosca amb color i masses de neutrins radiatives

En el cas estàndard, la matèria fosca és una partícula sense càrrega elèctrica ni color. No obstant això, sota determinades circumstàncies, és possible que la matèria fosca siga un estat hadrònic compost per partícules amb color. Aquest és el cas que s'ha estudiat al capítol 7, en el qual un nou fermió més enllà del ME forma estats hadrònics amb un comportament molt semblant a un *WIMP*.

En aquest capítol s'ha considerat un fermió Q que es transforma baix els números quàntics del ME com:

$$\mathcal{Q} \sim (8, 1, 0)\,. \tag{9.41}$$

Aquest estat hadrònic, $\mathcal{Q}\mathcal{Q}$, és capaç de descriure l'abundància actual de matèria fosca quan la massa de $\mathcal{Q}$ és:

$$M_{\mathcal{Q}} = 12.5 \pm 1 \text{ TeV}\,. \tag{9.42}$$

A més, gràcies a tècniques de teories de camp efectives, podem estimar la seua secció eficaç en experiments de detecció directa com

$$\sigma_{\text{SI}} \approx 2 \times 10^{-45} \text{ cm}^2 \left(\frac{20 \text{ TeV}}{M_{\mathcal{Q}\mathcal{Q}}}\right)^6 \frac{\Omega_{\mathcal{Q}\mathcal{Q}}}{\Omega_{\text{Planck}}}\,. \tag{9.43}$$

En aquest capítol, a més, s'ha demostrat com el fermió $\mathcal{Q}$ no solament compon la matèria fosca sinó que a més és l'ingredient clau en la generació de la massa dels neutrins per a dues variants: neutrins de Dirac i neutrins de Majorana. En el primer cas, per a neutrins de Dirac, l'estabilitat de la matèria fosca juga un paper clau en prohibir els termes de massa de Majorana a tots els ordres en teoria de pertorbació i, a més, fer que la massa de Dirac aparega únicament a nivell radiatiu. Per al cas de neutrins

de Majorana, l'estabilitat de la matèria fosca és la responsable de que els termes de massa de Dirac no apareguen a nivell arbre i que únicament tinguem aquests termes de majorana a nivell radiatiu. Ambdues variants difereixen en el seu contingut de partícules com vegem en les taules 7.1 i 7.2.

Respecte a la fenomenologia associada a les dues variants, n'hi ha aspectes comuns i altres que depenen de si els neutrins tenen masses de Dirac o de Majorana. Per exemple, en les dues variants u espera tindre desintegracions exòtiques dels muons del tipus $\mu \to e\gamma$. Aquests processos es coneixen genèricament com a processos de violació del sabor leptònic i, en els casos que hem considerat, es deuen a la presència d'escalars amb càrrega elèctrica que inevitablement acompanyen als escalars responsables de la generació de masses dels neutrins. Aquest procés restringeix l'espai de paràmetres dels escalars:

$$\left| \sum_a h_\mu^a h_e^{a*} \left(\frac{50\,\text{TeV}}{M_{\eta_a^+}} \right)^2 \right| \lesssim 1.5. \tag{9.44}$$

Una altra implicació fenomenològica que no depén de la naturalesa del neutrí és la producció dels fermions $\mathcal{Q}$ a acceleradors de partícules. Com que són partícules amb càrrega de color, u espera que els fermions que componen la matèria fosca en aquest cas siguen produïts copiosament en col·lisionadors d'hadrons com el LHC. A partir de processos com $q_i\bar{q}_i \to \mathcal{Q}\bar{\mathcal{Q}}$ i $gg \to \mathcal{Q}\bar{\mathcal{Q}}$, actualment sabem que la massa d'aquest fermió deu ser $M_\mathcal{Q} > 2$ TeV. Malgrat que encara està lluny de la predicció del model $M_\mathcal{Q} = 12.5$ TeV, aquestos valors seran posats a prova a futurs acceleradors tals com FCC.

Finalment, cal mencionar que hi ha altres implicacions fenomenològiques que sí depenen de la natura de la massa del neutrí. Com és ben sabut, l'observació d'una doble desintegració β sense neutrins és un senyal inequívoc que els neutrins són partícules de Majorana. Encara que no és un fenomen exclusiu del model que hem estudiat, aquesta possibilitat s'ha estudiat en la secció 7.3.

Ruptura espontània del número leptònic i matèria fosca

En el capítol 6 hem estudiat les implicacions a nivell cosmològic de la violació espontània del número leptònic. L'idea principal és que quan la simetria associada al número leptònic es trenca espontàniament, degut al teorema de Goldstone, un bosó sense massa apareix a la teoria: el majoron.

No obstant això, per tal de ser un bon candidat a matèria fosca, el majoron ha de tindre una massa $m_J \lesssim O(1)$ KeV. Al llarg del capítol s'ha considerat la possibilitat que efectes (de moment) desconeguts indueixen operadors efectius que trenquen la simetria de número leptònic de forma explícita i, per tant, el majoron obté una massa menuda. Al llarg del capítol hem estudiat l'evolució cosmològica i també els diferents mecanismes de producció de majorons, tèrmics i no tèrmics, a l'univers primitiu. S'ha demostrat explícitament que quan el majoron és lleuger, els mecanismes no tèrmics tals com oscil·lacions coherents al voltant del mínim de potencial i la desintegració de defectes topològics, dominen la producció d'aquesta partícula.

Respecte a les implicacions fenomenològiques associades a la cosmologia del model del majoron, cal destacar la possibilitat de detecció d'aquesta partícula a experiments de detecció de neutrins còsmics tals com Ptolemy. En aquest cas, hem demostrat explícitament que si Ptolemy detectara un majoron, aquests majorons necessàriament provenen de la desintegració d'un defecte topològic associat a la ruptura del número leptònic, $U(1)_L$.

Finalment, també hem estudiat la possibilitat que els majorons formen estats gravitatòriament lligats, també coneguts com a estrelles de bosons. Les propietats d'aquestes poden ser estudiades qualitativament emprant els mètodes descrits en la secció 6.4, els quals es basen a estudiar l'equilibri entre diferents contribucions a l'energia de l'estrella. En funció de quina és la contribució dominant: l'energia potencial gravitatòria, l'energia cinètica dels majorons o l'energia degut a l'autointeracció d'aquests bosons, distingim dos règims qualitativament diferents. Al primer, corresponent al règim diluït, l'energia potencial gravitatòria és compensada per l'energia cinètica dels majorons, que impedeix el col·lapse. D'aquest equilibri obtenim el radi crític

$$R_c \sim \frac{\sqrt{\lambda_4} M_P}{m_J^2}\,, \tag{9.45}$$

que determina el radi per davall del qual l'autointeracció dels majorons s'esdevé important. A mesura que la massa total augmenta, el radi decreix i arribem a R_c, i entrem en el règim dens de l'estrella, en el qual la massa total pot augmentar mentre que el radi roman constant $R \sim R_c$. L'estabilitat d'aquest règim dens depèn del tipus d'autointeracció dels bosons. Si l'autointeracció és atractiva, l'estrella col·lapsara, possiblement formant el que es coneix com a *bosenova*. D'altra banda, si l'autointeracció és repulsiva, aquesta branca s'espera que siga estable a escales de temps cosmològiques i podria tindre implicacions molt interessants.

En aquest capítol hem estimat que la desintegració dels defectes topològics pot donar lloc a estrelles molt més massives d'allò que s'obté al considerar altres mecanismes de producció de bosons tals com les oscil·lacions coherents. Si a més, la autointeracció dels majorons és repulsiva, aquest mecanisme de producció podria donar lloc a estrelles de bosons supermassives amb implicacions interessants per a la formació d'estructures a l'univers primitiu i, fins i tot, l'explicació de l'origen dels forats negres super massius que es creu existeixen al centre de totes les galàxies.

Gran Unificació i física del sabor

Des del naixement de la teoria quàntica, els físics i físiques han intentat demostrar l'existència de la unitat de càrrega elèctrica elemental. En altres paraules, han intentat demostrar que la càrrega elèctrica està quantitzada. Paul Dirac va ser el primer a demostrar que l'existència de monopols magnètics automàticament implicaria la quantització de la càrrega elèctrica. Durant quasi cent anys, diferents experiments han intentat, sense èxit, trobar aquests elusius monopols magnètics. Hui en dia, més de 80 anys després del treball de Paul Dirac i gràcies al descobriment de les teories gauge com a descripció de les interaccions fonamentals, la majoria de físics i físiques estan convençuts que els diferents números quàntics de les partícules del ME tenen el seu origen a una teoria unificada que descriu la Natura mitjançant una única interacció. En llenguatge modern, parlem de teories de gran unificació com aquelles teories gauge que unifiquen les interaccions fonamentals del ME a energies molt elevades, al voltant de $M_{GUT} \sim 10^{16}$ GeV. La forma d'aconseguir-ho és mitjançant un grup de simetria simple que, després d'un procés de ruptura espontània molt semblant a la ruptura de la simetria electrofeble, ens dona el grup de gauge del ME a baixes energies. Per tant, aquestes teories unificades, a més d'explicar perquè les partícules del ME tenen els números quàntics que tenen, també expliquen la raó de l'existència de les múltiples interaccions i les seues respectives intensitats.

D'altra banda, i com hem mencionat abans, un dels problemes oberts en física és el problema del sabor. Aquest es basa en la dificultat d'explicar les diferents masses dels diferents fermions del ME i la seua particular mescla. El problema del sabor, radica en una qüestió encara més fonamental: l'estructura en famílies del ME. Cadascuna de les partícules elementals està replicada 3 vegades, amb masses cada vegada més grans. Per exemple, a més de l'electró tenim els leptons: muó i tau, que són partícules amb els

mateixos números quàntics però amb una massa creixent. Mentre que el muó té una massa que és 200 vegades més gran que la massa de l'electró, el tau és aproximadament 17 vegades més pesat que el muó. El mateix ocorre en el sector dels quarks on, per exemple, el quark top és aproximadament 10^5 vegades més pesat que el quark up.

La part 3 de la tesi ha estat dedicada a l'estudi del problema de les famílies del ME. Primerament, en el capítol 8 hem explorat la possibilitat d'unificar no solament les diferents interaccions del ME sinó també les diferents famílies en única representació d'un grup de gauge simple. D'altra banda, al capítol 9, des d'un punt de vista de baixes energies hem considerat la possibilitat de que una nova interacció gauge relacione les diferents famílies del ME. Com veurem, les dues formes d'abordar el problema de les famílies estàn relacionades, ja que el grup de gauge que considerem en el capítol 9, $SO(3)_F$, és un subgrup del grup en el qual es basa la teoria unificada del capítol 8.

Unificació de les famílies del ME amb $SO(18)$

Com hem dit abans, malgrat que el ME descriu una immensitat de fenpmens amb una precisió remarcable, existeixen una sèrie de propietats sobre les quals no ofereix cap informació. Entre ells estan la diversitat d'interaccions i números quàntics que tenen les partícules elementals. Les teories de gran unificació, i en concret les teories basades en el grup gauge $SO(10)$, aconsegueixen unificar les interaccions fonamentals i també resulten exitoses unificant les diferents partícules corresponents a cada família. Per posar un exemple, la representació espinorial del grup $SO(10)$, representada per **16**, conté els números quàntics apropiats per a descriure una família del ME:

$$\mathbf{16} \to q_L + \bar{u}_R + \bar{d}_R + l_L + \bar{e}_R + \bar{\nu}_R \,. \tag{9.46}$$

Aquest espinor, a més, conté un camp amb els números quàntics corresponent a un neutrí dextrogir i, per tant, conté els ingredients mínims per a generar masses per als neutrins.

Malgrat que la teoria $SO(10)$ explica les diferents interaccions i números quàntics, és una teoria que no aporta informació sobre el sabor de les partícules. En altres paraules, el número de famílies i les seues masses característiques són paràmetres lliures. Aquesta és la principal motivació per a anar més enllà i considerar teories que, a més d'unificar les diferents interaccions, aconseguisquen explicar l'estructura de famílies del ME. Com s'ha

demostrat al capítol 8, les teories de gran unificació basades en representacions espinorials resulten particularment apropiades. El motiu és que, com hem vist a la secció 5.3, els espinors es descomponen de forma repetitiva. En concret, un espinor del grup $SO(2n+2m)$, el qual té dimensió 2^{n+m-1}, es descompon com 2^m copies del seu subgrup $SO(2n)$. Aquesta propietat resulta particularment suggerent per a acomodar la repetitiva estructura en famílies del ME.

Altre avantatge de les teories de gran unificació basades en grups del tipus $SO(N)$ és que tots (amb excepció de $SO(6)$, el qual és isomòrfic a $SU(4)$) estan lliures d'anomalies. A més, els grups corresponents a la sèrie $SO(4n+2)$ tenen representacions complexes. Per tant, els grups d'aquesta sèrie resulten particularment apropiats per a descriure el ME, el qual es basa en l'ús de representacions quirals. Òbviament, el cas $n=2$ correspon a la teoria de gran unificació basada en $SO(10)$.

Tenint en compte aquestes consideracions, el grup més menut capaç de descriure 3 famílies quirals és el grup de gauge $SO(18)$. Per a veure-ho, resulta convenient considerar el procés de ruptura de simetria $SO(18) \to SO(10) \times SO(8)$. En aquest cas, l'espinor de $SO(18)$, el qual té dimensió 256 es descomposa com:

$$\mathbf{256} \to (\mathbf{16}, \mathbf{8}) \; + \; (\overline{\mathbf{16}}, \mathbf{8}') \, . \tag{9.47}$$

Per tant, des del punt de vista de $SO(10)$, el espinor **256** conté 8 famílies i 8 antifamílies (les quals tenen els números quàntics de les famílies usuals però amb la quiralitat oposada). Aquest problema va fer que en el període de temps des dels anys 80 fins a hui les teories d'unificació de famílies basades en $SO(18)$ no es consideraren massa seriosament.

En el capítol 8 hem reconsiderat la possibilitat d'emprar la representació espinorial de $SO(18)$ des d'un punt de vista completament nou. L'idea bàsica és que combinant el mecanisme de ruptura de simetria basat en *orbifolds* junt amb el confinament d'una interacció forta nova, anomenada *hipercolor*, aconseguim que l'espectre de baixes energies continga únicament les 3 famílies del ME.

En més detall, hem emprat una teoria gauge 5-dimensional que permet eliminar els modes zero corresponents a les antifamílies. Açò ocorre gràcies al fet que la dimensió addicional està plegada amb una topologia semblant a un cercle, l'anomenat *orbifold*. Gràcies a unes condicions de contorn no trivials en el *orbifold*, la part corresponent a $(\overline{\mathbf{16}}, \mathbf{8}')$ no apareix a baixes energies i, així, eliminem el problema de les antifamílies del espinor de $SO(18)$.

No obstant això, encara tenim massa famílies, ja que la representació corresponent a $(\mathbf{16}, \mathbf{8})$ és equivalent a 8 famílies del ME. Per tal d'eliminar la resta de famílies de l'espectre, hem suposat que el grup $SO(8)$ experimenta un procés de ruptura espontània en direcció al grup $SO(5)$. A més, hem demostrat que aquest grup resultant, que anomenem *hipercolor*, aconsegueix confinar a energies properes a l'escala del TeV. En altres paraules, després de considerar el procés de ruptura de simetria, el grup de simetria gauge ve donat per $SO(10) \times SO(5)$ i la representació es descompon com:

$$(\mathbf{16}, \mathbf{8}) \to 3 \times (\mathbf{16}, \mathbf{1}) + (\mathbf{16}, \mathbf{5})\,. \tag{9.48}$$

La part $3 \times (\mathbf{16}, \mathbf{1})$ correspon a les famílies del ME i els fermions continguts a $(\mathbf{16}, \mathbf{5})$ són confinats gràcies a l'*hipercolor*, $SO(5)$.

De forma semblant al número bariònic de la interacció forta, la interacció *hipercolor* basada en $SO(5)$ conté una simetria conservada. En aquest cas és una simetria discreta del tipus Z_2. Cadascun dels *hiperquarks* tenen càrrega (-1) sota aquesta simetria, de forma que existeix un estat anomenat *hiperbarió* el qual és estable gràcies a la conservació de Z_2. Aquests hiperbarions, compostos per 5 hiperquarks, poden produir-se en l'univers primitiu. L'abundància d'aquests pot estimar-se com:

$$\Omega_\chi h^2 \approx 10^{-5}\Big(M/TeV\Big)^2\,, \tag{9.49}$$

on M és la massa de l'hiperbarió. Per tant, per a $M \lesssim O(10)$ TeV, els hiperbarions contribueixen d'una forma subdominant a la densitat d'energia de l'Univers. No obstant això, si $M \sim$ TeV aquests podrien detectar-se a acceleradors de partícules i, possiblement, altres experiments de detecció directa de matèria fosca.

La simetria $SO(3)$ com a simetria gauge entre famílies

Des de finals dels anys 70 i principis dels anys 80, s'han proposat multitud de teories amb la intenció d'explicar la replicació de les famílies i la particular distribució de masses dels fermions i la seua mescla. La majoria de les propostes contenen algun grup de simetria que relaciona les diferents famílies i, únicament quan aquesta simetria es trenca, expliquem per que els fermions tenen unes masses distribuïdes de forma tan jeràrquica.

Mentre que existeixen vàries possibilitats per a descriure 3 famílies emprant grups de simetria discrets, únicament existeixen 2 grups continus amb

representacions de triplets. Aquests són els grups $SU(3)$ i $SO(3)$. El problema de $SU(3)$ és que si u considera únicament el contingut fermiònic del ME, aquest grup generalment presenta anomalies. En canvi, $SO(3)$ és un grup de simetria que conté triplets i, a més, no pateix d'aquest problema. Per tant, una interacció gauge basada en el grup $SO(3)$ és l'elecció mínima per a descriure 3 famílies amb un contingut de fermions fidel al ME. A més, $SO(3)$ és un subgrup de $SO(18)$. Per tant, si u considera que, a molt altes energies la Natura ve descrita per una teoria unificada basada en $SO(18)$, és natural esperar que a energies intermitjes puga aparèixer una simetria gauge $SO(3)$ que relaciona les diferents famílies del ME. Aquestes raons fan el grup $SO(3)$ particularment interesant.

Aquest tipus de teoria va ser considerat, en primer lloc, per F. Wilczek i A. Zee a finals dels 70. En un treball pioner, van estudiar com aquesta simetria gauge és capaç d'oferir prediccions de les masses i mescles dels fermions del ME. Després d'un mecanisme de ruptura de la simetria $SO(3)$, els fermions del ME obtenen massa i apareix una relació entre les masses de quarks i leptons:

$$\frac{m_e m_\mu}{m_\tau^2} = \frac{m_d m_s}{m_b^2} = \frac{m_u m_c}{m_t^2} \,. \tag{9.50}$$

A pesar de que la primera igualtat es satisfà amb una precisió raonable, la segona està en contradicció amb l'experiment, ja que prediu un quark top amb una massa de $m_t \approx 15$ GeV. Cal mencionar que aquesta teoria va ser proposada quasi 20 anys abans del descobriment del top, que hui en dia sabem que té una massa de $m_t^{exp} = 172.9 \pm 0.4$ GeV.

En el capítol 9 hem estudiat quina és l'extensió mínima que tenim que fer de la teoria original per tal d'evitar la predicció errònia de la massa del quark top. Inspirats en la teoria de gran unificació basada en $SO(18)$, hem considerat la teoria gauge de famílies basada en $SO(3)$ i l'hem extès afegint la simetria de Peccei-Quinn, $U(1)_{PQ}$. Aquesta simetria és responsable de resoltre el problema de la violació de la simetria CP per la interacció forta. Amb un model relativament senzill, obtenim vàries característiques atractives:

- Degut a la simetria de Peccei-Quinn, obtenim l'axió, partícula que a més de resoldre el problema de la violació de la simetria CP per la interacció forta és un bon candidat a matèria fosca (vegeu capítol 4).

- Obtenim un relació interessant entre masses de quarks tipus down i leptons carregats: $\frac{m_e m_\mu}{m_\tau^2} = \frac{m_d m_s}{m_b^2}$.

- Expliquem l'origen de la matriu CKM i relacionem la mescla dels diferents quarks amb la seua massa. Per a l'angle de Cabibbo obtenim $\theta_C \approx \sqrt{\frac{m_d}{m_s}} - \sqrt{\frac{m_u}{m_c}}$. Per a l'element de la matriu CKM obteim la predicció: $|V_{ub}| \approx \frac{\sqrt{m_d m_s}}{m_b} - \frac{\sqrt{m_u m_c}}{m_t}$.
- Explicació de l'origen de la massa del neutrí per mitjà del mecanisme de seesaw a la escala d'energia de la ruptura de la simetria de Peccei-Quinn. Per tant, obtenim una relació entre la massa del axió i la massa del neutrí: $m_a \sim (\Lambda_{QCD} m_\pi / v^2) m_\nu$.

A més, cal afegir que els bosons de gauge corresponents a $SO(3)$ són responsables de processos d'oscil·lació de mesons tals com les oscil·lacions $K^0 - \bar{K}^0$. Per tant, podem posar un limit inferior a la massa d'aquestos bosons, relacionat amb l'escala de ruptura del grup de simetria, donat per:

$$\frac{g^2}{M_F^2} \lesssim \frac{1}{[10^4\ \mathrm{TeV}]^2}\,. \tag{9.51}$$

En el model que hem estudiat, $M_F = g f_a$, i així obtenim un limit inferior a constant de desintegració del axió, $f_a > 10^7$ GeV.

Bibliography

[1] S. Weinberg, "A model of leptons," *Phys. Rev. Lett.* **19** (1967) 1264–1266. [Cited on pages 3 and 5.]

[2] S. L. Glashow, "Partial symmetries of weak interactions," *Nucl. Phys.* **22** (1961) 579–588. [Cited on pages 3 and 5.]

[3] A. Salam, "Weak and electromagnetic interactions,". Originally printed in Proceedings Of The Nobel Symposium, Sweden, Stockholm 1968, Elementary Particle Theory, Ed. Svartholm, pp 367-377. [Cited on pages 3 and 5.]

[4] S. Tomonaga, "On a relativistically invariant formulation of the quantum theory of wave fields," *Prog. Theor. Phys.* **1** (1946) 27–42. [Cited on page 3.]

[5] J. S. Schwinger, "On Quantum electrodynamics and the magnetic moment of the electron," *Phys. Rev.* **73** (1948) 416–417. [Cited on page 3.]

[6] R. P. Feynman, "Space-time approach to nonrelativistic quantum mechanics," *Rev. Mod. Phys.* **20** (1948) 367–387. [Cited on page 3.]

[7] R. P. Feynman, "Mathematical formulation of the quantum theory of electromagnetic interaction," *Phys. Rev.* **80** (1950) 440–457. [Cited on page 3.]

[8] T. D. Lee and C.-N. Yang, "Question of Parity Conservation in Weak Interactions," *Phys. Rev.* **104** (1956) 254–258. [Cited on page 3.]

[9] C. S. Wu, E. Ambler, R. W. Hayward, D. D. Hoppes, and R. P. Hudson, "Experimental Test of Parity Conservation in Beta Decay," *Phys. Rev.* **105** (1957) 1413–1414. [Cited on page 4.]

[10] C.-N. Yang and R. L. Mills, "Conservation of Isotopic Spin and Isotopic Gauge Invariance," *Phys. Rev.* **96** (1954) 191–195. [Cited on page 4.]

[11] M. Gell-Mann, "A Schematic Model of Baryons and Mesons," *Phys. Lett.* **8** (1964) 214–215. [Cited on page 4.]

[12] G. Zweig, "An SU(3) model for strong interaction symmetry and its breaking. Version 1,". [Cited on page 4.]

[13] **Particle Data Group** Collaboration, P. A. Zyla *et al.*, "Review of Particle Physics," *PTEP* **2020** no. 8, (2020) 083C01. [Cited on pages 4, 10, 16, and 17.]

[14] R. P. Feynman, "The behavior of hadron collisions at extreme energies," *Conf. Proc. C* **690905** (1969) 237–258. [Cited on page 4.]

[15] J. D. Bjorken and E. A. Paschos, "Inelastic Electron Proton and gamma Proton Scattering, and the Structure of the Nucleon," *Phys. Rev.* **185** (1969) 1975–1982. [Cited on page 5.]

[16] P. W. Higgs, "Broken Symmetries and the Masses of Gauge Bosons," *Phys.Rev.Lett.* **13** (1964) 508–509. [Cited on pages 5 and 10.]

[17] F. Englert and R. Brout, "Broken Symmetry and the Mass of Gauge Vector Mesons," *Phys.Rev.Lett.* **13** (1964) 321–323. [Cited on pages 5 and 10.]

[18] G. Guralnik, C. Hagen, and T. Kibble, "Global Conservation Laws and Massless Particles," *Phys.Rev.Lett.* **13** (1964) 585–587. [Cited on pages 5 and 10.]

[19] G. 't Hooft and M. J. G. Veltman, "Regularization and Renormalization of Gauge Fields," *Nucl. Phys.* **B44** (1972) 189–213. [Cited on page 5.]

[20] C. G. Bollini and J. J. Giambiagi, "Dimensional Renormalization: The Number of Dimensions as a Regularizing Parameter," *Nuovo Cim.* **B12** (1972) 20–26. [Cited on page 5.]

[21] D. J. Gross and F. Wilczek, "Ultraviolet Behavior of Nonabelian Gauge Theories," *Phys. Rev. Lett.* **30** (1973) 1343–1346. [Cited on pages 5, 65, and 66.]

[22] H. D. Politzer, "Reliable Perturbative Results for Strong Interactions?," *Phys. Rev. Lett.* **30** (1973) 1346–1349. [Cited on pages 5, 65, and 66.]

[23] D. J. Gross and F. Wilczek, "Asymptotically Free Gauge Theories. 1," *Phys. Rev.* **D8** (1973) 3633–3652. [Cited on page 5.]

[24] D. J. Gross and F. Wilczek, "Asymptotically Free Gauge Theories. 2.," *Phys. Rev.* **D9** (1974) 980–993. [Cited on page 5.]

[25] C. Quigg and R. Shrock, "Gedanken Worlds without Higgs: QCD-Induced Electroweak Symmetry Breaking," *Phys. Rev. D* **79** (2009) 096002, arXiv:0901.3958 [hep-ph]. [Cited on page 9.]

[26] J. Bardeen, L. N. Cooper, and J. R. Schrieffer, "Theory of superconductivity," *Phys. Rev.* **108** (Dec, 1957) 1175–1204. https://link.aps.org/doi/10.1103/PhysRev.108.1175. [Cited on page 10.]

[27] **Particle Data Group** Collaboration, C. Patrignani *et al.*, "Review of Particle Physics," *Chin. Phys.* **C40** no. 10, (2016) 100001. [Cited on page 12.]

[28] K. S. Babu, "TASI Lectures on Flavor Physics," in *Theoretical Advanced Study Institute in Elementary Particle Physics: The Dawn of the LHC Era*, pp. 49–123. 2010. arXiv:0910.2948 [hep-ph]. [Cited on page 14.]

[29] O. Gedalia and G. Perez, "Flavor Physics," in *Theoretical Advanced Study Institute in Elementary Particle Physics: Physics of the Large and the Small*, pp. 309–382. 2011. arXiv:1005.3106 [hep-ph]. [Cited on page 14.]

[30] Y. Grossman, "Introduction to flavor physics," in *2009 European School of High-Energy Physics*. 6, 2010. arXiv:1006.3534 [hep-ph]. [Cited on page 14.]

[31] C. Jarlskog, "Commutator of the Quark Mass Matrices in the Standard Electroweak Model and a Measure of Maximal CP Violation," *Phys.Rev.Lett.* **55** (1985) 1039. [Cited on pages 14 and 17.]

[32] M. Pospelov and A. Ritz, "Electric dipole moments as probes of new physics," *Annals Phys.* **318** (2005) 119–169, arXiv:hep-ph/0504231 [hep-ph]. [Cited on page 14.]

[33] F. Wilczek and A. Zee, "Horizontal Interaction and Weak Mixing Angles," *Phys. Rev. Lett.* **42** (1979) 421. [Cited on pages 18, 132, 136, 137, 138, and 152.]

[34] A. H. Guth, "The Inflationary Universe: A Possible Solution to the Horizon and Flatness Problems," *Phys. Rev.* **D23** (1981) 347–356. [Adv. Ser. Astrophys. Cosmol.3,139(1987)]. [Cited on pages 19 and 50.]

[35] **Supernova Search Team** Collaboration, A. G. Riess *et al.*, "Observational evidence from supernovae for an accelerating universe and a cosmological constant," *Astron. J.* **116** (1998) 1009–1038, arXiv:astro-ph/9805201. [Cited on page 19.]

[36] **Supernova Cosmology Project** Collaboration, S. Perlmutter *et al.*, "Measurements of Ω and Λ from 42 high redshift supernovae," *Astrophys. J.* **517** (1999) 565–586, arXiv:astro-ph/9812133. [Cited on page 19.]

[37] S. Weinberg, "The cosmological constant problem," *Rev. Mod. Phys.* **61** (Jan, 1989) 1–23. https://link.aps.org/doi/10.1103/RevModPhys.61.1. [Cited on page 19.]

[38] **Planck** Collaboration, N. Aghanim *et al.*, "Planck 2018 results. VI. Cosmological parameters," arXiv:1807.06209 [astro-ph.CO]. [Cited on pages 19, 26, 48, 50, 87, and 103.]

[39] R. P. Feynman, "Quantum theory of gravitation," *Acta Phys. Polon.* **24** (1963) 697–722. [Cited on page 20.]

[40] P. Svrcek and E. Witten, "Axions In String Theory," *JHEP* **06** (2006) 051, arXiv:hep-th/0605206. [Cited on page 20.]

[41] T. Kajita, "Nobel lecture: Discovery of atmospheric neutrino oscillations," *Rev. Mod. Phys.* **88** (Jul, 2016) 030501. https://link.aps.org/doi/10.1103/RevModPhys.88.030501. [Cited on pages 21 and 22.]

[42] A. B. McDonald, "Nobel lecture: The sudbury neutrino observatory: Observation of flavor change for solar neutrinos," *Rev. Mod. Phys.* **88** (Jul, 2016) 030502. https://link.aps.org/doi/10.1103/RevModPhys.88.030502. [Cited on pages 21 and 22.]

[43] S. Weinberg, "Baryon and lepton nonconserving processes," *Phys. Rev. Lett.* **43** (1979) 1566–1570. [Cited on pages 21 and 28.]

[44] J. Schechter and J. W. F. Valle, "Neutrino Masses in SU(2) x U(1) Theories," *Phys.Rev.* **D22** (1980) 2227. [Cited on pages 21, 22, 28, 29, 104, 111, 128, and 139.]

[45] P. Minkowski, "mu -> e gamma at a rate of one out of 1-billion muon decays?," *Phys. Lett.* **B67** (1977) 421. [Cited on pages 21, 28, 29, and 139.]

[46] M. Gell-Mann, P. Ramond, and R. Slansky, "Complex Spinors and Unified Theories," *Conf. Proc.* **C790927** (1979) 315–321, arXiv:1306.4669 [hep-th]. [Cited on pages 21, 28, 29, 126, 128, 132, and 139.]

[47] T. Yanagida, "Horizontal symmetry and masses of neutrinos," *Conf. Proc.* **C7902131** (1979) 95–99. [Cited on pages 21, 28, 29, 128, and 139.]

[48] R. N. Mohapatra and G. Senjanovic, "Neutrino Mass and Spontaneous Parity Violation," *Phys. Rev. Lett.* **44** (1980) 912. [Cited on pages 21, 28, 29, and 139.]

[49] E. Ma, "Verifiable radiative seesaw mechanism of neutrino mass and dark matter," *Phys.Rev.* **D73** (2006) 077301, arXiv:hep-ph/0601225 [hep-ph]. [Cited on pages 21, 29, 31, 34, 38, and 101.]

[50] J. W. Valle and J. C. Romao, *Neutrinos in high energy and astroparticle physics*. Wiley-VCH, Berlin, 1st edition ed., 2015. [Cited on page 21.]

[51] J. Schechter and J. W. F. Valle, "Neutrino oscillation thought experiment," *Phys. Rev.* **D23** (1981) 1666. [Cited on pages 22 and 27.]

[52] **Super-Kamiokande collaboration** Collaboration, Y. Fukuda *et al.*, "Evidence for oscillation of atmospheric neutrinos," *Phys. Rev. Lett.* **81** (1998) 1562–1567, hep-ex/9807003. [Cited on page 22.]

[53] **SNO collaboration** Collaboration, Q. R. Ahmad *et al.*, "Direct evidence for neutrino flavor transformation from neutral-current interactions in the Sudbury Neutrino Observatory," *Phys. Rev. Lett.* **89** (2002) 011301, nucl-ex/0204008. [Cited on page 22.]

[54] P. F. de Salas, D. V. Forero, S. Gariazzo, P. Martínez-Miravé, O. Mena, C. A. Ternes, M. Tórtola, and J. W. F. Valle, "2020 global reassessment of the neutrino oscillation picture," *JHEP* **02** (2021) 071, arXiv:2006.11237 [hep-ph]. [Cited on pages 25, 26, 27, and 104.]

[55] I. Esteban, M. C. Gonzalez-Garcia, M. Maltoni, T. Schwetz, and A. Zhou, "The fate of hints: updated global analysis of three-flavor neutrino oscillations," *JHEP* **09** (2020) 178, arXiv:2007.14792 [hep-ph]. [Cited on page 26.]

[56] F. Capozzi, E. Di Valentino, E. Lisi, A. Marrone, A. Melchiorri, and A. Palazzo, "Global constraints on absolute neutrino masses and their ordering," *Phys. Rev. D* **95** no. 9, (2017) 096014, arXiv:2003.08511 [hep-ph]. [Addendum: Phys.Rev.D 101, 116013 (2020)]. [Cited on page 26.]

[57] M. Aker *et al.*, "First direct neutrino-mass measurement with sub-eV sensitivity," arXiv:2105.08533 [hep-ex]. [Cited on page 26.]

[58] M. Hirsch, R. Srivastava, and J. W. F. Valle, "Can one ever prove that neutrinos are Dirac particles?," *Phys.Lett.* **B781** (2018) 302–305, arXiv:1711.06181 [hep-ph]. [Cited on page 26.]

[59] J. Schechter and J. Valle, "Neutrinoless Double beta Decay in SU(2) x U(1) Theories," *Phys.Rev.* **D25** (1982) 2951. [Cited on pages 26 and 28.]

[60] W. Rodejohann and J. W. F. Valle, "Symmetrical Parametrizations of the Lepton Mixing Matrix," *Phys.Rev.* **D84** (2011) 073011, arXiv:1108.3484 [hep-ph]. [Cited on pages 27 and 110.]

[61] S. Weinberg, "Universal Neutrino Degeneracy," *Phys. Rev.* **128** (1962) 1457–1473. [Cited on page 27.]

[62] **PTOLEMY** Collaboration, M. G. Betti *et al.*, "Neutrino physics with the PTOLEMY project: active neutrino properties and the light sterile case," *JCAP* **07** (2019) 047, arXiv:1902.05508 [astro-ph.CO]. [Cited on page 27.]

[63] R. N. Mohapatra and G. Senjanovic, "Neutrino masses and mixings in gauge models with spontaneous parity violation," *Phys. Rev.* **D23** (1981) 165. [Cited on page 28.]

[64] R. Foot, H. Lew, X. G. He, and G. C. Joshi, "Seesaw neutrino masses induced by a triplet of leptons," *Z. Phys.* **C44** (1989) 441. [Cited on page 29.]

[65] Y. Farzan, S. Pascoli, and M. A. Schmidt, "Recipes and Ingredients for Neutrino Mass at Loop Level," *JHEP* **03** (2013) 107, arXiv:1208.2732 [hep-ph]. [Cited on page 29.]

[66] Y. Cai, J. Herrero-García, M. A. Schmidt, A. Vicente, and R. R. Volkas, "From the trees to the forest: a review of radiative neutrino mass models," *Front. in Phys.* **5** (2017) 63, arXiv:1706.08524 [hep-ph]. [Cited on page 29.]

[67] A. Zee, "A theory of lepton number violation, neutrino majorana mass, and oscillation," *Phys. Lett.* **B93** (1980) 389. [Cited on page 29.]

[68] X.-G. He, "Is the Zee model neutrino mass matrix ruled out?," *Eur. Phys. J. C* **34** (2004) 371–376, arXiv:hep-ph/0307172. [Cited on page 29.]

[69] C. Boehm, Y. Farzan, T. Hambye, S. Palomares-Ruiz, and S. Pascoli, "Is it possible to explain neutrino masses with scalar dark matter?," *Phys. Rev. D* **77** (2008) 043516, arXiv:hep-ph/0612228. [Cited on page 29.]

[70] E. Ma and O. Popov, "Pathways to Naturally Small Dirac Neutrino Masses," *Phys. Lett. B* **764** (2017) 142–144, arXiv:1609.02538 [hep-ph]. [Cited on page 29.]

[71] S. Centelles Chuliá, R. Srivastava, and J. W. F. Valle, "Seesaw roadmap to neutrino mass and dark matter," *Phys. Lett. B* **781** (2018) 122–128, arXiv:1802.05722 [hep-ph]. [Cited on page 29.]

[72] E. Ma, N. Pollard, R. Srivastava, and M. Zakeri, "Gauge $B - L$ Model with Residual Z_3 Symmetry," *Phys. Lett. B* **750** (2015) 135–138, arXiv:1507.03943 [hep-ph]. [Cited on page 29.]

[73] M. Reig, J. W. F. Valle, and C. A. Vaquera-Araujo, "Realistic $\mathrm{SU(3)_c} \otimes \mathrm{SU(3)_L} \otimes \mathrm{U(1)_X}$ model with a type II Dirac neutrino

seesaw mechanism," *Phys. Rev.* **D94** no. 3, (2016) 033012, arXiv:1606.08499 [hep-ph]. [Cited on page 29.]

[74] A. Aranda, C. Bonilla, S. Morisi, E. Peinado, and J. W. F. Valle, "Dirac neutrinos from flavor symmetry," *Phys. Rev. D* **89** no. 3, (2014) 033001, arXiv:1307.3553 [hep-ph]. [Cited on page 29.]

[75] S. Centelles Chuliá, E. Ma, R. Srivastava, and J. W. F. Valle, "Dirac Neutrinos and Dark Matter Stability from Lepton Quarticity," *Phys. Lett. B* **767** (2017) 209–213, arXiv:1606.04543 [hep-ph]. [Cited on page 29.]

[76] E. Peinado, M. Reig, R. Srivastava, and J. W. F. Valle, "Dirac neutrinos from Peccei–Quinn symmetry: A fresh look at the axion," *Mod. Phys. Lett. A* **35** no. 21, (2020) 2050176, arXiv:1910.02961 [hep-ph]. [Cited on page 29.]

[77] P. Escribano, M. Reig, and A. Vicente, "Generalizing the Scotogenic model," *JHEP* **07** (2020) 097, arXiv:2004.05172 [hep-ph]. [Cited on pages 29, 31, and 33.]

[78] J. Schechter and J. W. F. Valle, "Neutrino Decay and Spontaneous Violation of Lepton Number," *Phys. Rev.* **D25** (1982) 774. [Cited on pages 30, 31, 55, 60, 77, 79, and 84.]

[79] Y. Chikashige, R. N. Mohapatra, and R. D. Peccei, "Are There Real Goldstone Bosons Associated with Broken Lepton Number?," *Phys. Lett.* **98B** (1981) 265–268. [Cited on pages 31, 55, 77, 79, and 84.]

[80] Y. Farzan, "A Framework to Simultaneously Explain Tiny Neutrino Mass and Huge Missing Mass Problem of the Universe," *Mod. Phys. Lett. A* **25** (2010) 2111–2120, arXiv:1009.1234 [hep-ph]. [Cited on page 31.]

[81] Y. Farzan, "Strategies to link tiny neutrino masses with huge missing mass of the Universe," *Int. J. Mod. Phys. A* **26** (2011) 2461–2485, arXiv:1106.2948 [hep-ph]. [Cited on page 31.]

[82] Y. Farzan, S. Pascoli, and M. A. Schmidt, "AMEND: A model explaining neutrino masses and dark matter testable at the LHC and MEG," *JHEP* **10** (2010) 111, arXiv:1005.5323 [hep-ph]. [Cited on page 31.]

[83] I. M. Ávila, V. De Romeri, L. Duarte, and J. W. F. Valle, "Phenomenology of scotogenic scalar dark matter," *Eur. Phys. J. C* **80** no. 10, (2020) 908, arXiv:1910.08422 [hep-ph]. [Cited on page 31.]

[84] G. 't Hooft, "Naturalness, chiral symmetry, and spontaneous chiral symmetry breaking," *NATO Sci. Ser. B* **59** (1980) 135–157. [Cited on pages 34 and 108.]

[85] G. Passarino and M. J. G. Veltman, "One loop corrections for e^+e^- annihilation into $\mu^+\mu^-$ in the Weinberg model," *Nucl. Phys.* **B160** (1979) 151. [Cited on page 35.]

[86] C. Baker *et al.*, "An Improved experimental limit on the electric dipole moment of the neutron," *Phys. Rev. Lett.* **97** (2006) 131801, arXiv:hep-ex/0602020. [Cited on page 39.]

[87] J. M. Pendlebury *et al.*, "Revised experimental upper limit on the electric dipole moment of the neutron," *Phys. Rev. D* **92** no. 9, (2015) 092003, arXiv:1509.04411 [hep-ex]. [Cited on page 39.]

[88] T. Banks, M. Dine, and E. Gorbatov, "Is there a string theory landscape?," *JHEP* **08** (2004) 058, arXiv:hep-th/0309170. [Cited on page 39.]

[89] J. F. Donoghue, "Dynamics of M theory vacua," *Phys. Rev. D* **69** (2004) 106012, arXiv:hep-th/0310203. [Erratum: Phys.Rev.D 69, 129901 (2004)]. [Cited on page 39.]

[90] R. D. Peccei and H. R. Quinn, "CP Conservation in the Presence of Instantons," *Phys. Rev. Lett.* **38** (1977) 1440–1443. [,328(1977)]. [Cited on pages 39, 40, 41, and 55.]

[91] F. Wilczek, "Problem of Strong P and T Invariance in the Presence of Instantons," *Phys. Rev. Lett.* **40** (1978) 279–282. [Cited on pages 39, 40, 41, and 55.]

[92] S. Weinberg, "A New Light Boson?," *Phys. Rev. Lett.* **40** (1978) 223–226. [Cited on pages 39, 40, 41, and 55.]

[93] A. Hook, "TASI Lectures on the Strong CP Problem and Axions," *PoS* **TASI2018** (2019) 004, arXiv:1812.02669 [hep-ph]. [Cited on pages 40 and 57.]

[94] L. Di Luzio, M. Giannotti, E. Nardi, and L. Visinelli, "The landscape of QCD axion models," arXiv:2003.01100 [hep-ph]. [Cited on pages 40 and 43.]

[95] G. Grilli di Cortona, E. Hardy, J. Pardo Vega, and G. Villadoro, "The QCD axion, precisely," *JHEP* **01** (2016) 034, arXiv:1511.02867 [hep-ph]. [Cited on pages 40, 41, and 57.]

[96] C. Vafa and E. Witten, "Parity Conservation in QCD," *Phys. Rev. Lett.* **53** (1984) 535. [Cited on page 40.]

[97] T. W. Donnelly, S. J. Freedman, R. S. Lytel, R. D. Peccei, and M. Schwartz, "Do axions exist?," *Phys. Rev. D* **18** (Sep, 1978) 1607–1620. https://link.aps.org/doi/10.1103/PhysRevD.18.1607. [Cited on pages 41 and 42.]

[98] M. Dine, W. Fischler, and M. Srednicki, "A Simple Solution to the Strong CP Problem with a Harmless Axion," *Phys. Lett.* **104B** (1981) 199–202. [Cited on pages 42 and 136.]

[99] A. R. Zhitnitsky, "On Possible Suppression of the Axion Hadron Interactions. (In Russian)," *Sov. J. Nucl. Phys.* **31** (1980) 260. [Yad. Fiz.31,497(1980)]. [Cited on page 42.]

[100] P. Sikivie, "Of Axions, Domain Walls and the Early Universe," *Phys. Rev. Lett.* **48** (1982) 1156–1159. [Cited on page 42.]

[101] A. Vilenkin, "Cosmic Strings and Domain Walls," *Phys. Rept.* **121** (1985) 263–315. [Cited on pages 42 and 78.]

[102] G. Lazarides and Q. Shafi, "Axion Models with No Domain Wall Problem," *Phys. Lett.* **115B** (1982) 21–25. [Cited on pages 42 and 81.]

[103] S. M. Barr and J. E. Kim, "New Confining Force Solution of the QCD Axion Domain-Wall Problem," *Phys. Rev. Lett.* **113** no. 24, (2014) 241301, arXiv:1407.4311 [hep-ph]. [Cited on pages 42 and 81.]

[104] M. Reig, "Dynamical Peccei-Quinn symmetry breaking and the instanton interference effect: axion models without domain wall problem," arXiv:1901.00203 [hep-ph]. [Cited on pages 42 and 81.]

[105] A. Caputo and M. Reig, "Cosmic implications of a low-scale solution to the axion domain wall problem," *Phys. Rev. D* **100** no. 6, (2019) 063530, arXiv:1905.13116 [hep-ph]. [Cited on pages 42 and 141.]

[106] M. Srednicki, "Axion Couplings to Matter. 1. CP Conserving Parts," *Nucl. Phys.* **B260** (1985) 689–700. [Cited on pages 42 and 43.]

[107] J. E. Kim, "Weak Interaction Singlet and Strong CP Invariance," *Phys. Rev. Lett.* **43** (1979) 103. [Cited on page 43.]

[108] M. A. Shifman, A. I. Vainshtein, and V. I. Zakharov, "Can Confinement Ensure Natural CP Invariance of Strong Interactions?," *Nucl. Phys.* **B166** (1980) 493–506. [Cited on page 43.]

[109] I. G. Irastorza and J. Redondo, "New experimental approaches in the search for axion-like particles," *Prog. Part. Nucl. Phys.* **102** (2018) 89–159, arXiv:1801.08127 [hep-ph]. [Cited on page 43.]

[110] F. Wilczek, "Axions and Family Symmetry Breaking," *Phys. Rev. Lett.* **49** (1982) 1549–1552. [Cited on pages 43 and 55.]

[111] **CAST** Collaboration, V. Anastassopoulos *et al.*, "New CAST Limit on the Axion-Photon Interaction," *Nature Phys.* **13** (2017) 584–590, arXiv:1705.02290 [hep-ex]. [Cited on page 44.]

[112] E. Armengaud *et al.*, "Conceptual Design of the International Axion Observatory (IAXO)," *JINST* **9** (2014) T05002, arXiv:1401.3233 [physics.ins-det]. [Cited on page 44.]

[113] S. J. Asztalos, G. Carosi, C. Hagmann, D. Kinion, K. van Bibber, M. Hotz, L. J. Rosenberg, G. Rybka, J. Hoskins, J. Hwang, P. Sikivie, D. B. Tanner, R. Bradley, and J. Clarke, "Squid-based microwave cavity search for dark-matter axions," *Phys. Rev. Lett.* **104** (Jan, 2010) 041301. https://link.aps.org/doi/10.1103/PhysRevLett.104.041301. [Cited on page 44.]

[114] M. Betz, F. Caspers, M. Gasior, M. Thumm, and S. W. Rieger, "First results of the CERN Resonant Weakly Interacting sub-eV Particle Search (CROWS)," *Phys. Rev. D* **88** no. 7, (2013) 075014, arXiv:1310.8098 [physics.ins-det]. [Cited on page 44.]

[115] K. Ehret *et al.*, "New ALPS Results on Hidden-Sector Lightweights," *Phys. Lett. B* **689** (2010) 149–155, arXiv:1004.1313 [hep-ex]. [Cited on page 44.]

[116] **OSQAR** Collaboration, R. Ballou *et al.*, "New exclusion limits on scalar and pseudoscalar axionlike particles from light shining through a wall," *Phys. Rev. D* **92** no. 9, (2015) 092002, arXiv:1506.08082 [hep-ex]. [Cited on page 44.]

[117] R. Bähre *et al.*, "Any light particle search II —Technical Design Report," *JINST* **8** (2013) T09001, arXiv:1302.5647 [physics.ins-det]. [Cited on page 44.]

[118] L. Capparelli, G. Cavoto, J. Ferretti, F. Giazotto, A. D. Polosa, and P. Spagnolo, "Axion-like particle searches with sub-THz photons," *Phys. Dark Univ.* **12** (2016) 37–44, arXiv:1510.06892 [hep-ph]. [Cited on page 44.]

[119] G. G. Raffelt, "Astrophysical axion bounds," *Lect. Notes Phys.* **741** (2008) 51–71, arXiv:hep-ph/0611350 [hep-ph]. [,51(2006)]. [Cited on page 44.]

[120] A. Arvanitaki, S. Dimopoulos, S. Dubovsky, N. Kaloper, and J. March-Russell, "String Axiverse," *Phys. Rev.* **D81** (2010) 123530, arXiv:0905.4720 [hep-th]. [Cited on page 44.]

[121] A. Arvanitaki and S. Dubovsky, "Exploring the String Axiverse with Precision Black Hole Physics," *Phys. Rev. D* **83** (2011) 044026, arXiv:1004.3558 [hep-th]. [Cited on page 44.]

[122] A. Arvanitaki, M. Baryakhtar, and X. Huang, "Discovering the QCD Axion with Black Holes and Gravitational Waves," *Phys. Rev. D* **91** no. 8, (2015) 084011, arXiv:1411.2263 [hep-ph]. [Cited on page 45.]

[123] M. Baryakhtar, M. Galanis, R. Lasenby, and O. Simon, "Black hole superradiance of self-interacting scalar fields," arXiv:2011.11646 [hep-ph]. [Cited on page 45.]

[124] V. M. Mehta, M. Demirtas, C. Long, D. J. E. Marsh, L. McAllister, and M. J. Stott, "Superradiance in String Theory," arXiv:2103.06812 [hep-th]. [Cited on page 45.]

[125] C. O'HARE, "cajohare/axionlimits: Axionlimits," July, 2020. https://doi.org/10.5281/zenodo.3932430. [Cited on pages 45 and 46.]

[126] G. Bertone and D. Hooper, "History of dark matter," *Rev. Mod. Phys.* **90** no. 4, (2018) 045002, arXiv:1605.04909 [astro-ph.CO]. [Cited on page 47.]

[127] A. D. Linde, "A New Inflationary Universe Scenario: A Possible Solution of the Horizon, Flatness, Homogeneity, Isotropy and Primordial Monopole Problems," *Phys. Lett.* **108B** (1982) 389–393. [Adv. Ser. Astrophys. Cosmol.3,149(1987)]. [Cited on page 50.]

[128] A. Albrecht and P. J. Steinhardt, "Cosmology for Grand Unified Theories with Radiatively Induced Symmetry Breaking," *Phys. Rev. Lett.* **48** (1982) 1220–1223. [Adv. Ser. Astrophys. Cosmol.3,158(1987)]. [Cited on page 50.]

[129] E. W. Kolb and M. S. Turner, "The Early Universe," *Front. Phys.* **69** (1990) 1–547. [Cited on page 51.]

[130] D. Baumann, *Cosmology. Part III Mathematical Tripos.* [Cited on page 52.]

[131] L. J. Hall, K. Jedamzik, J. March-Russell, and S. M. West, "Freeze-In Production of FIMP Dark Matter," *JHEP* **03** (2010) 080, arXiv:0911.1120 [hep-ph]. [Cited on page 53.]

[132] K. Griest and M. Kamionkowski, "Unitarity Limits on the Mass and Radius of Dark Matter Particles," *Phys. Rev. Lett.* **64** (1990) 615. [Cited on pages 55, 118, and 129.]

[133] J. Preskill, M. B. Wise, and F. Wilczek, "Cosmology of the Invisible Axion," *Phys. Lett.* **120B** (1983) 127–132. [Cited on page 55.]

[134] L. F. Abbott and P. Sikivie, "A Cosmological Bound on the Invisible Axion," *Phys. Lett.* **B120** (1983) 133–136. [,URL(1982)]. [Cited on page 55.]

[135] M. Dine and W. Fischler, "The Not So Harmless Axion," *Phys. Lett.* **120B** (1983) 137–141. [Cited on page 55.]

[136] A. Arvanitaki, S. Dimopoulos, M. Galanis, L. Lehner, J. O. Thompson, and K. Van Tilburg, "The Large-Misalignment Mechanism for the Formation of Compact Axion Structures:

Signatures from the QCD Axion to Fuzzy Dark Matter," arXiv:1909.11665 [astro-ph.CO]. [Cited on page 56.]

[137] J. Huang, A. Madden, D. Racco, and M. Reig, "Maximal axion misalignment from a minimal model," *JHEP* **10** (2020) 143, arXiv:2006.07379 [hep-ph]. [Cited on page 56.]

[138] M. Reig, "The Stochastic Axiverse," arXiv:2104.09923 [hep-ph]. [Cited on page 56.]

[139] L. Hui, J. P. Ostriker, S. Tremaine, and E. Witten, "Ultralight scalars as cosmological dark matter," *Phys. Rev.* **D95** no. 4, (2017) 043541, arXiv:1610.08297 [astro-ph.CO]. [Cited on page 57.]

[140] M. Schumann, "Direct Detection of WIMP Dark Matter: Concepts and Status," *J. Phys. G* **46** no. 10, (2019) 103003, arXiv:1903.03026 [astro-ph.CO]. [Cited on pages 58 and 59.]

[141] M. W. Goodman and E. Witten, "Detectability of Certain Dark Matter Candidates," *Phys. Rev. D* **31** (1985) 3059. [Cited on page 58.]

[142] T. R. Slatyer, "Indirect Detection of Dark Matter," in *Theoretical Advanced Study Institute in Elementary Particle Physics: Anticipating the Next Discoveries in Particle Physics*, pp. 297–353. 2018. arXiv:1710.05137 [hep-ph]. [Cited on pages 60 and 61.]

[143] **ATLAS** Collaboration, "Dark matter summary plots for s-channel mediators,". [Cited on page 62.]

[144] S. Dimopoulos, S. Raby, and F. Wilczek, "Supersymmetry and the Scale of Unification," *Phys. Rev. D* **24** (1981) 1681–1683. [Cited on page 66.]

[145] H. Georgi and S. L. Glashow, "Unity of All Elementary Particle Forces," *Phys. Rev. Lett.* **32** (1974) 438–441. [Cited on pages 67 and 117.]

[146] **Super-Kamiokande** Collaboration, K. Abe *et al.*, "Search for proton decay via $p \to e^+\pi^0$ and $p \to \mu^+\pi^0$ in 0.31 megaton·years exposure of the Super-Kamiokande water Cherenkov detector," *Phys. Rev. D* **95** no. 1, (2017) 012004, arXiv:1610.03597 [hep-ex]. [Cited on page 70.]

[147] H. Georgi, "Towards a Grand Unified Theory of Flavor," *Nucl.Phys.* **B156** (1979) 126. [Cited on page 71.]

[148] F. Wilczek and A. Zee, "Families from Spinors," *Phys. Rev.* **D25** (1982) 553. [Cited on pages 71, 117, 124, 126, 132, and 150.]

[149] H. Fritzsch and P. Minkowski, "Unified Interactions of Leptons and Hadrons," *Annals Phys.* **93** (1975) 193–266. [Cited on page 72.]

[150] H. Georgi, "The State of the Art—Gauge Theories," *AIP Conf. Proc.* **23** (1975) 575–582. [Cited on page 72.]

[151] T. Gonzalo Velasco, *Model Building and Phenomenology in Grand Unified Theories*. PhD thesis, University Coll. London, 2015. [Cited on page 73.]

[152] D. Croon, T. E. Gonzalo, L. Graf, N. Košnik, and G. White, "GUT Physics in the era of the LHC," *Front. in Phys.* **7** (2019) 76, arXiv:1903.04977 [hep-ph]. [Cited on page 73.]

[153] M. Reig, J. W. F. Valle, and M. Yamada, "Light majoron cold dark matter from topological defects and the formation of boson stars," *JCAP* **09** (2019) 029, arXiv:1905.01287 [hep-ph]. [Cited on pages 77 and 99.]

[154] C. Bonilla and J. W. F. Valle, "Naturally light neutrinos in *Diracon* model," *Phys. Lett. B* **762** (2016) 162–165, arXiv:1605.08362 [hep-ph]. [Cited on page 77.]

[155] V. Berezinsky and J. Valle, "The KeV majoron as a dark matter particle," *Phys.Lett.* **B318** (1993) 360–366, arXiv:hep-ph/9309214 [hep-ph]. [Cited on pages 77, 78, and 93.]

[156] F. Bazzocchi, M. Lattanzi, S. Riemer-Sorensen, and J. W. Valle, "X-ray photons from late-decaying majoron dark matter," *JCAP* **0808** (2008) 013, arXiv:0805.2372 [astro-ph]. * Brief entry *. [Cited on pages 77, 84, and 93.]

[157] M. Lattanzi *et al.*, "Updated CMB, X- and gamma-ray constraints on Majoron dark matter," *Phys.Rev.* **D88** (2013) 063528, arXiv:1303.4685 [astro-ph.HE]. [Cited on pages 77, 84, and 93.]

[158] M. Lattanzi, R. A. Lineros, and M. Taoso, "Connecting neutrino physics with dark matter," *New J.Phys.* **16** (2014) 125012, arXiv:1406.0004 [hep-ph]. [Cited on pages 77, 84, and 93.]

[159] J.-L. Kuo *et al.*, "Decaying warm dark matter and structure formation," arXiv:1803.05650 [astro-ph.CO]. [Cited on pages 77, 78, 84, 86, and 93.]

[160] T. W. B. Kibble, "Topology of Cosmic Domains and Strings," *J. Phys.* **A9** (1976) 1387–1398. [Cited on page 78.]

[161] M. Lattanzi and J. Valle, "Decaying warm dark matter and neutrino masses," *Phys.Rev.Lett.* **99** (2007) 121301, arXiv:0705.2406 [astro-ph]. * Brief entry *. [Cited on pages 78, 84, and 93.]

[162] D. McKeen, "Cosmic neutrino background search experiments as decaying dark matter detectors," arXiv:1812.08178 [hep-ph]. [Cited on pages 78, 93, and 148.]

[163] Z. Chacko, P. Du, and M. Geller, "Detecting a Secondary Cosmic Neutrino Background from Majoron Decays in Neutrino Capture Experiments," arXiv:1812.11154 [hep-ph]. [Cited on pages 78, 93, and 148.]

[164] S. R. Coleman, "Why There Is Nothing Rather Than Something: A Theory of the Cosmological Constant," *Nucl. Phys.* **B310** (1988) 643. [Cited on page 79.]

[165] Ya. B. Zeldovich, I. Yu. Kobzarev, and L. B. Okun, "Cosmological Consequences of the Spontaneous Breakdown of Discrete Symmetry," *Zh. Eksp. Teor. Fiz.* **67** (1974) 3–11. [Sov. Phys. JETP40,1(1974)]. [Cited on pages 81 and 141.]

[166] A. Vilenkin, "Gravitational Field of Vacuum Domain Walls and Strings," *Phys. Rev.* **D23** (1981) 852–857. [Cited on pages 81 and 92.]

[167] G. Lazarides, M. Reig, Q. Shafi, R. Srivastava, and J. W. F. Valle, "Spontaneous Breaking of Lepton Number and Cosmological Domain Wall Problem," arXiv:1806.11198 [hep-ph]. [Cited on page 81.]

[168] R. Sato, F. Takahashi, and M. Yamada, "Unified Origin of Axion and Monopole Dark Matter, and Solution to the Domain-wall Problem," *Phys. Rev.* **D98** no. 4, (2018) 043535, arXiv:1805.10533 [hep-ph]. [Cited on page 81.]

[169] B. Audren, J. Lesgourgues, G. Mangano, P. D. Serpico, and T. Tram, "Strongest model-independent bound on the lifetime of Dark Matter," *JCAP* **1412** no. 12, (2014) 028, arXiv:1407.2418 [astro-ph.CO]. [Cited on page 83.]

[170] M. Kachelriess, R. Tomas, and J. W. F. Valle, "Supernova bounds on Majoron-emitting decays of light neutrinos," *Phys. Rev.* **D62** (2000) 023004, hep-ph/0001039. [Cited on page 84.]

[171] Y. Farzan, "Bounds on the coupling of the Majoron to light neutrinos from supernova cooling," *Phys. Rev. D* **67** (2003) 073015, arXiv:hep-ph/0211375. [Cited on page 84.]

[172] L. Heurtier and Y. Zhang, "Supernova Constraints on Massive (Pseudo)Scalar Coupling to Neutrinos," *JCAP* **1702** no. 02, (2017) 042, arXiv:1609.05882 [hep-ph]. [Cited on page 84.]

[173] C. Garcia-Cely and J. Heeck, "Neutrino Lines from Majoron Dark Matter," *JHEP* **05** (2017) 102, arXiv:1701.07209 [hep-ph]. [Cited on page 84.]

[174] J. Heeck and D. Teresi, "Cold keV dark matter from decays and scatterings," *Phys. Rev.* **D96** no. 3, (2017) 035018, arXiv:1706.09909 [hep-ph]. [Cited on page 86.]

[175] V. Iršič *et al.*, "New Constraints on the free-streaming of warm dark matter from intermediate and small scale Lyman-α forest data," *Phys. Rev.* **D96** no. 2, (2017) 023522, arXiv:1702.01764 [astro-ph.CO]. [Cited on page 87.]

[176] K. Nakayama, F. Takahashi, and T. T. Yanagida, "A theory of extra radiation in the Universe," *Phys. Lett.* **B697** (2011) 275–279, arXiv:1010.5693 [hep-ph]. [Cited on page 87.]

[177] S. Weinberg, "Goldstone Bosons as Fractional Cosmic Neutrinos," *Phys. Rev. Lett.* **110** no. 24, (2013) 241301, arXiv:1305.1971 [astro-ph.CO]. [Cited on page 87.]

[178] C. Pitrou, A. Coc, J.-P. Uzan, and E. Vangioni, "Precision big bang nucleosynthesis with improved Helium-4 predictions," *Phys. Rept.* **754** (2018) 1–66, arXiv:1801.08023 [astro-ph.CO]. [Cited on page 87.]

[179] B. D. Fields, K. A. Olive, T.-H. Yeh, and C. Young, "Big-Bang Nucleosynthesis after Planck," *JCAP* **03** (2020) 010, arXiv:1912.01132 [astro-ph.CO]. [Erratum: JCAP 11, E02 (2020)]. [Cited on page 87.]

[180] G. Mangano, G. Miele, S. Pastor, T. Pinto, O. Pisanti, and P. D. Serpico, "Relic neutrino decoupling including flavor oscillations," *Nucl. Phys.* **B729** (2005) 221–234, arXiv:hep-ph/0506164 [hep-ph]. [Cited on page 87.]

[181] W. L. K. Wu, J. Errard, C. Dvorkin, C. L. Kuo, A. T. Lee, P. McDonald, A. Slosar, and O. Zahn, "A Guide to Designing Future Ground-based Cosmic Microwave Background Experiments," *Astrophys. J.* **788** (2014) 138, arXiv:1402.4108 [astro-ph.CO]. [Cited on pages 87 and 148.]

[182] **CMB-S4** Collaboration, K. N. Abazajian *et al.*, "CMB-S4 Science Book, First Edition," arXiv:1610.02743 [astro-ph.CO]. [Cited on pages 87 and 148.]

[183] M. Kawasaki, K. Saikawa, and T. Sekiguchi, "Axion dark matter from topological defects," *Phys. Rev.* **D91** no. 6, (2015) 065014, arXiv:1412.0789 [hep-ph]. [Cited on page 90.]

[184] F. S. Queiroz and K. Sinha, "The Poker Face of the Majoron Dark Matter Model: LUX to keV Line," *Phys.Lett.* **B735** (2014) 69–74, arXiv:1404.1400 [hep-ph]. [Cited on page 93.]

[185] P. F. de Salas *et al.*, "Status of neutrino oscillations 2018: first hint for normal mass ordering and improved CP sensitivity," arXiv:1708.01186 [hep-ph]. [Cited on pages 93, 104, 111, 112, and 139.]

[186] **Majorana** Collaboration, S. I. Alvis *et al.*, "A Search for Neutrinoless Double-Beta Decay in ^{76}Ge with 26 kg-yr of Exposure from the MAJORANA DEMONSTRATOR," arXiv:1902.02299 [nucl-ex]. [Cited on page 93.]

[187] Z. G. Berezhiani, A. Y. Smirnov, and J. W. F. Valle, "Observable Majoron emission in neutrinoless double beta decay," *Phys. Lett.* **B291** (1992) 99, hep-ph/9207209. [Cited on page 93.]

[188] E. Braaten and H. Zhang, "Axion Stars," arXiv:1810.11473 [hep-ph]. [Cited on page 94.]

[189] E. Braaten, A. Mohapatra, and H. Zhang, "Nonrelativistic Effective Field Theory for Axions," *Phys. Rev.* **D94** no. 7, (2016) 076004, arXiv:1604.00669 [hep-ph]. [Cited on page 94.]

[190] K. Mukaida, M. Takimoto, and M. Yamada, "On Longevity of I-ball/Oscillon," *JHEP* **03** (2017) 122, arXiv:1612.07750 [hep-ph]. [Cited on pages 94 and 97.]

[191] J. Eby, P. Suranyi, and L. C. R. Wijewardhana, "Expansion in Higher Harmonics of Boson Stars using a Generalized Ruffini-Bonazzola Approach, Part 1: Bound States," *JCAP* **1804** no. 04, (2018) 038, arXiv:1712.04941 [hep-ph]. [Cited on page 94.]

[192] M. H. Namjoo, A. H. Guth, and D. I. Kaiser, "Relativistic Corrections to Nonrelativistic Effective Field Theories," *Phys. Rev.* **D98** no. 1, (2018) 016011, arXiv:1712.00445 [hep-ph]. [Cited on page 94.]

[193] J. Eby, K. Mukaida, M. Takimoto, L. C. R. Wijewardhana, and M. Yamada, "Classical Nonrelativistic Effective Field Theory and the Role of Gravitational Interactions," arXiv:1807.09795 [hep-ph]. [Cited on pages 94 and 97.]

[194] E. Braaten, A. Mohapatra, and H. Zhang, "Classical Nonrelativistic Effective Field Theories for a Real Scalar Field," arXiv:1806.01898 [hep-ph]. [Cited on page 94.]

[195] A. H. Guth, M. P. Hertzberg, and C. Prescod-Weinstein, "Do Dark Matter Axions Form a Condensate with Long-Range Correlation?," *Phys. Rev.* **D92** no. 10, (2015) 103513, arXiv:1412.5930 [astro-ph.CO]. [Cited on page 96.]

[196] E. W. Kolb and I. I. Tkachev, "Axion miniclusters and Bose stars," *Phys. Rev. Lett.* **71** (1993) 3051–3054, arXiv:hep-ph/9303313 [hep-ph]. [Cited on page 96.]

[197] E. Braaten, A. Mohapatra, and H. Zhang, "Emission of Photons and Relativistic Axions from Axion Stars," *Phys. Rev.* **D96** no. 3, (2017) 031901, arXiv:1609.05182 [hep-ph]. [Cited on page 97.]

[198] L. Visinelli, S. Baum, J. Redondo, K. Freese, and F. Wilczek, "Dilute and dense axion stars," *Phys. Lett.* **B777** (2018) 64–72, arXiv:1710.08910 [astro-ph.CO]. [Cited on page 97.]

[199] A. G. Cohen, S. R. Coleman, H. Georgi, and A. Manohar, "The Evaporation of Q Balls," *Nucl. Phys.* **B272** (1986) 301–321. [Cited on page 97.]

[200] M. Kawasaki and M. Yamada, "Q ball Decay Rates into Gravitinos and Quarks," *Phys. Rev.* **D87** no. 2, (2013) 023517, arXiv:1209.5781 [hep-ph]. [Cited on page 97.]

[201] V. De Luca, A. Mitridate, M. Redi, J. Smirnov, and A. Strumia, "Colored Dark Matter," *Phys. Rev.* **D97** no. 11, (2018) 115024, arXiv:1801.01135 [hep-ph]. [Cited on pages 101, 102, 114, and 149.]

[202] M. Reig, J. W. F. Valle, C. A. Vaquera-Araujo, and F. Wilczek, "A Model of Comprehensive Unification," *Phys. Lett.* **B774** (2017) 667–670, arXiv:1706.03116 [hep-ph]. [Cited on pages 101, 118, 130, and 132.]

[203] M. Reig, D. Restrepo, J. W. F. Valle, and O. Zapata, "Bound-state dark matter and Dirac neutrino masses," *Phys. Rev.* **D97** no. 11, (2018) 115032, arXiv:1803.08528 [hep-ph]. [Cited on pages 101 and 114.]

[204] M. Reig, D. Restrepo, J. W. F. Valle, and O. Zapata, "Bound-state dark matter with Majorana neutrinos," arXiv:1806.09977 [hep-ph]. [Cited on pages 101 and 114.]

[205] R. H. Cyburt, B. D. Fields, V. Pavlidou, and B. D. Wandelt, "Constraining strong baryon dark matter interactions with primordial nucleosynthesis and cosmic rays," *Phys. Rev. D* **65** (2002) 123503, arXiv:astro-ph/0203240. [Cited on page 102.]

[206] **XENON** Collaboration, E. Aprile *et al.*, "Dark Matter Search Results from a One Tonne×Year Exposure of XENON1T," arXiv:1805.12562 [astro-ph.CO]. [Cited on page 103.]

[207] **XENON** Collaboration, E. Aprile *et al.*, "Physics reach of the XENON1T dark matter experiment," *JCAP* **1604** no. 04, (2016) 027, arXiv:1512.07501 [physics.ins-det]. [Cited on page 103.]

[208] **LUX-ZEPLIN** Collaboration, D. S. Akerib *et al.*, "Projected WIMP sensitivity of the LUX-ZEPLIN (LZ) dark matter experiment," arXiv:1802.06039 [astro-ph.IM]. [Cited on page 103.]

[209] **DARWIN** Collaboration, J. Aalbers *et al.*, "DARWIN: towards the ultimate dark matter detector," *JCAP* **1611** (2016) 017, arXiv:1606.07001 [astro-ph.IM]. [Cited on page 103.]

[210] **CMS** Collaboration, C. Collaboration, "Search for heavy stable charged particles with 12.9 fb^{-1} of 2016 data,". [Cited on pages 103 and 113.]

[211] **ATLAS** Collaboration, T. A. collaboration, "Reinterpretation of searches for supersymmetry in models with variable R-parity-violating coupling strength and long-lived R-hadrons,". [Cited on page 103.]

[212] S. Centelles Chuliá, "Dirac neutrinos, dark matter stability and flavour predictions from Lepton Quarticity," 2017. arXiv:1711.10719 [hep-ph]. [Cited on page 104.]

[213] **FCC** Collaboration, A. Abada *et al.*, "FCC Physics Opportunities: Future Circular Collider Conceptual Design Report Volume 1," *Eur. Phys. J. C* **79** no. 6, (2019) 474. [Cited on pages 104 and 130.]

[214] Y. Farzan and E. Ma, "Dirac neutrino mass generation from dark matter," *Phys. Rev.* **D86** (2012) 033007, arXiv:1204.4890 [hep-ph]. [Cited on page 105.]

[215] A. V. Manohar and M. B. Wise, "Flavor changing neutral currents, an extended scalar sector, and the Higgs production rate at the CERN LHC," *Phys. Rev.* **D74** (2006) 035009, arXiv:hep-ph/0606172 [hep-ph]. [Cited on page 105.]

[216] S. I. Bityukov and N. V. Krasnikov, "The Search for new physics by the measurement of the four jet cross-section at LHC and FNAL," *Mod. Phys. Lett.* **A12** (1997) 2011–2028, arXiv:hep-ph/9705338 [hep-ph]. [Cited on page 105.]

[217] Y. Bai and B. A. Dobrescu, "Collider Tests of the Renormalizable Coloron Model," arXiv:1802.03005 [hep-ph]. [Cited on page 105.]

[218] D. Hehn and A. Ibarra, "A radiative model with a naturally mild neutrino mass hierarchy," *Phys. Lett.* **B718** (2013) 988–991, arXiv:1208.3162 [hep-ph]. [Cited on page 107.]

[219] Valencia-Globalfit-website. http://globalfit.astroparticles.es/, 2018. [Cited on pages 111 and 112.]

[220] M. Hirsch *et al.*, "Predicting neutrinoless double beta decay," *Phys. Rev.* **D72** (2005) 091301. [Cited on page 111.]

[221] L. Dorame, D. Meloni, S. Morisi, E. Peinado, and J. W. F. Valle, "Constraining Neutrinoless Double Beta Decay," *Nucl.Phys.* **B861** (2012) 259–270, arXiv:1111.5614 [hep-ph]. [Cited on page 111.]

[222] L. Dorame, S. Morisi, E. Peinado, J. W. F. Valle, and A. D. Rojas, "A new neutrino mass sum rule from inverse seesaw," *Phys.Rev.* **D86** (2012) 056001, arXiv:1203.0155 [hep-ph]. [Cited on page 111.]

[223] **CUORE** Collaboration, C. Alduino *et al.*, "First Results from CUORE: A Search for Lepton Number Violation via $0\nu\beta\beta$ Decay of ^{130}Te," *Phys. Rev. Lett.* **120** no. 13, (2018) 132501, arXiv:1710.07988 [nucl-ex]. [Cited on page 111.]

[224] **EXO** Collaboration, J. B. Albert *et al.*, "Search for Neutrinoless Double-Beta Decay with the Upgraded EXO-200 Detector," *Phys. Rev. Lett.* **120** no. 7, (2018) 072701, arXiv:1707.08707 [hep-ex]. [Cited on page 111.]

[225] **GERDA** Collaboration, M. Agostini *et al.*, "Improved Limit on Neutrinoless Double-β Decay of ^{76}Ge from GERDA Phase II," *Phys. Rev. Lett.* **120** no. 13, (2018) 132503, arXiv:1803.11100 [nucl-ex]. [Cited on page 111.]

[226] **KamLAND-Zen** Collaboration, A. Gando *et al.*, "Search for Majorana Neutrinos near the Inverted Mass Hierarchy Region with KamLAND-Zen," *Phys. Rev. Lett.* **117** no. 8, (2016) 082503, arXiv:1605.02889 [hep-ex]. [Addendum: Phys. Rev. Lett.117,no.10,109903(2016)]. [Cited on page 111.]

[227] **nEXO** Collaboration, J. B. Albert *et al.*, "Sensitivity and Discovery Potential of nEXO to Neutrinoless Double Beta Decay," arXiv:1710.05075 [nucl-ex]. [Cited on page 111.]

[228] **SNO+** Collaboration, S. Andringa *et al.*, "Current Status and Future Prospects of the SNO+ Experiment," *Adv. High Energy Phys.* **2016** (2016) 6194250, arXiv:1508.05759 [physics.ins-det]. [Cited on page 111.]

[229] **LEGEND** Collaboration, N. Abgrall *et al.*, "The Large Enriched Germanium Experiment for Neutrinoless Double Beta Decay (LEGEND)," *AIP Conf. Proc.* **1894** no. 1, (2017) 020027, arXiv:1709.01980 [physics.ins-det]. [Cited on page 111.]

[230] L. Lavoura, "General formulae for f1 –> f2 gamma," *Eur. Phys. J.* **C29** (2003) 191–195, arXiv:hep-ph/0302221. [Cited on page 112.]

[231] **MEG** Collaboration, A. M. Baldini *et al.*, "Search for the lepton flavour violating decay $\mu^+ \to e^+\gamma$ with the full dataset of the MEG experiment," *Eur. Phys. J. C* **76** no. 8, (2016) 434, arXiv:1605.05081 [hep-ex]. [Cited on page 113.]

[232] G. Grilli di Cortona, E. Hardy, and A. J. Powell, "Dirac vs Majorana gauginos at a 100 TeV collider," *JHEP* **08** (2016) 014, arXiv:1606.07090 [hep-ph]. [Cited on page 114.]

[233] A. Hayreter and G. Valencia, "LHC constraints on color octet scalars," *Phys. Rev.* **D96** no. 3, (2017) 035004, arXiv:1703.04164 [hep-ph]. [Cited on page 114.]

[234] V. Miralles and A. Pich, "LHC bounds on colored scalars," *Phys. Rev. D* **100** no. 11, (2019) 115042, arXiv:1910.07947 [hep-ph]. [Cited on page 114.]

[235] R. Slansky, "Group Theory for Unified Model Building," *Phys.Rept.* **79** (1981) 1–128. [Cited on page 117.]

[236] J. Bagger and S. Dimopoulos, "O(18) Revived: Splitting the Spinor," *Nucl. Phys. B* **244** (1984) 247–261. [Cited on page 118.]

[237] J. Bagger, S. Dimopoulos, E. Masso, and M. H. Reno, "A Realistic Theory of Family Unification," *Nucl. Phys. B* **258** (1985) 565–600. [Cited on page 118.]

[238] K. S. Babu, S. M. Barr, and B. Kyae, "Family unification in five-dimensions and six-dimensions," *Phys. Rev.* **D65** (2002) 115008, arXiv:hep-ph/0202178 [hep-ph]. [Cited on page 118.]

[239] S. M. Barr, "e^-8 Family Unification, Mirror Fermions, and New Low-energy Physics," *Phys. Rev.* **D37** (1988) 204. [Cited on page 118.]

[240] Y. BenTov and A. Zee, "Origin of families and $SO(18)$ grand unification," *Phys. Rev.* **D93** no. 6, (2016) 065036, arXiv:1505.04312 [hep-th]. [Cited on page 118.]

[241] Y. Kawamura, "Gauge symmetry breaking from extra space S**1 / Z(2)," *Prog. Theor. Phys.* **103** (2000) 613–619, arXiv:hep-ph/9902423. [Cited on pages 118 and 122.]

[242] T. Gherghetta and A. Pomarol, "Bulk fields and supersymmetry in a slice of AdS," *Nucl. Phys. B* **586** (2000) 141–162, arXiv:hep-ph/0003129. [Cited on pages 118 and 124.]

[243] R. Barbieri, L. J. Hall, and Y. Nomura, "A Constrained standard model from a compact extra dimension," *Phys. Rev. D* **63** (2001) 105007, arXiv:hep-ph/0011311. [Cited on page 118.]

[244] G. Altarelli and F. Feruglio, "SU(5) grand unification in extra dimensions and proton decay," *Phys. Lett. B* **511** (2001) 257–264, arXiv:hep-ph/0102301. [Cited on page 118.]

[245] L. J. Hall and Y. Nomura, "Gauge unification in higher dimensions," *Phys. Rev. D* **64** (2001) 055003, arXiv:hep-ph/0103125. [Cited on page 118.]

[246] A. Hebecker and J. March-Russell, "A Minimal S**1 / (Z(2) x Z-prime (2)) orbifold GUT," *Nucl. Phys. B* **613** (2001) 3–16, arXiv:hep-ph/0106166. [Cited on pages 118 and 122.]

[247] P. R. Archer, "The Fermion Mass Hierarchy in Models with Warped Extra Dimensions and a Bulk Higgs," *JHEP* **09** (2012) 095, arXiv:1204.4730 [hep-ph]. [Cited on page 118.]

[248] P. Chen *et al.*, "Warped flavor symmetry predictions for neutrino physics," *JHEP* **01** (2016) 007, arXiv:1509.06683 [hep-ph]. [Cited on page 118.]

[249] Y. Grossman and M. Neubert, "Neutrino masses and mixings in nonfactorizable geometry," *Phys. Lett. B* **474** (2000) 361–371, arXiv:hep-ph/9912408. [Cited on page 118.]

[250] A. Ahmed, A. Carmona, J. Castellano Ruiz, Y. Chung, and M. Neubert, "Dynamical origin of fermion bulk masses in a warped

extra dimension," *JHEP* **08** (2019) 045, arXiv:1905.09833 [hep-ph]. [Cited on page 121.]

[251] L. Randall and R. Sundrum, "A Large mass hierarchy from a small extra dimension," *Phys. Rev. Lett.* **83** (1999) 3370–3373, arXiv:hep-ph/9905221 [hep-ph]. [Cited on page 122.]

[252] J. C. Pati and A. Salam, "Lepton number as the fourth color," *Phys. Rev.* **D10** (1974) 275–289. [Cited on page 125.]

[253] R. N. Mohapatra and G. Senjanovic, "Neutrino masses and mixings in gauge models with spontaneous parity violation," *Phys. Rev.* **D23** (1981) 165. [Cited on pages 125 and 128.]

[254] G. F. Giudice and S. Raby, "A New paradigm for the revival of technicolor theories," *Nucl. Phys.* **B368** (1992) 221–247. [Cited on page 126.]

[255] A. Pomarol, "Grand unified theories without the desert," *Phys. Rev. Lett.* **85** (2000) 4004–4007, arXiv:hep-ph/0005293 [hep-ph]. [Cited on page 126.]

[256] M. Bando, T. Kugo, T. Noguchi, and K. Yoshioka, "Brane fluctuation and suppression of Kaluza-Klein mode couplings," *Phys. Rev. Lett.* **83** (1999) 3601–3604, arXiv:hep-ph/9906549 [hep-ph]. [Cited on page 126.]

[257] L. Randall and M. D. Schwartz, "Unification and the hierarchy from AdS5," *Phys. Rev. Lett.* **88** (2002) 081801, arXiv:hep-th/0108115 [hep-th]. [Cited on page 126.]

[258] S. Glashow, "The future of elementary particle physics," *Proceedings of the 1979 Cargese Summer Institute on Quarks and Leptons J.-L. Basdevant, D. Speiser, J. Weyers, R. Gastmans, and M. Jacob, eds.), Plenum Press, New York* **687** . [Cited on page 128.]

[259] G. Lazarides, Q. Shafi, and C. Wetterich, "Proton lifetime and fermion masses in an SO(10) model," *Nucl. Phys.* **B181** 287. [Cited on page 128.]

[260] S. Dimopoulos and F. Wilczek, "Incomplete Multiplets in Supersymmetric Unified Models.," *Report. No. NSF-ITP-82-07* (1982) . [Cited on page 128.]

[261] O. Antipin, M. Redi, A. Strumia, and E. Vigiani, "Accidental Composite Dark Matter," *JHEP* **07** (2015) 039, arXiv:1503.08749 [hep-ph]. [Cited on page 129.]

[262] A. Mitridate, M. Redi, J. Smirnov, and A. Strumia, "Dark Matter as a weakly coupled Dark Baryon," arXiv:1707.05380 [hep-ph]. [Cited on page 130.]

[263] T. Gherghetta, N. Nagata, and M. Shifman, "A Visible QCD Axion from an Enlarged Color Group," *Phys. Rev.* **D93** no. 11, (2016) 115010, arXiv:1604.01127 [hep-ph]. [Cited on page 130.]

[264] S. Dimopoulos, A. Hook, J. Huang, and G. Marques-Tavares, "A collider observable QCD axion," *JHEP* **11** (2016) 052, arXiv:1606.03097 [hep-ph]. [Cited on page 130.]

[265] I. de Medeiros Varzielas, G. G. Ross, and J. Talbert, "A Unified Model of Quarks and Leptons with a Universal Texture Zero," arXiv:1710.01741 [hep-ph]. [Cited on page 131.]

[266] S. Morisi, E. Peinado, Y. Shimizu, and J. W. F. Valle, "Relating quarks and leptons without grand-unification," *Phys. Rev.* **D84** (2011) 036003, arXiv:1104.1633 [hep-ph]. [Cited on pages 131, 133, and 137.]

[267] C. Bonilla, S. Morisi, E. Peinado, and J. W. F. Valle, "Relating quarks and leptons with the T_7 flavour group," *Phys. Lett.* **B742** (2015) 99–106, arXiv:1411.4883 [hep-ph]. [Cited on pages 131, 133, and 137.]

[268] Z. G. Berezhiani and M. Y. Khlopov, "Cosmology of Spontaneously Broken Gauge Family Symmetry," *Z. Phys. C* **49** (1991) 73–78. [Cited on page 131.]

[269] I. de Medeiros Varzielas and G. G. Ross, "SU(3) family symmetry and neutrino bi-tri-maximal mixing," *Nucl. Phys. B* **733** (2006) 31–47, arXiv:hep-ph/0507176. [Cited on page 131.]

[270] L. M. Krauss and F. Wilczek, "Discrete Gauge Symmetry in Continuum Theories," *Phys. Rev. Lett.* **62** (1989) 1221. [Cited on page 132.]

[271] M. Reig, J. W. F. Valle, and F. Wilczek, "SO(3) family symmetry and axions," *Phys. Rev.* **D98** no. 9, (2018) 095008, arXiv:1805.08048 [hep-ph]. [Cited on pages 132, 133, and 143.]

[272] S. Morisi, M. Nebot, K. M. Patel, E. Peinado, and J. Valle, "Quark-Lepton Mass Relation and CKM mixing in an A4 Extension of the Minimal Supersymmetric Standard Model," *Phys.Rev.* **D88** (2013) 036001, arXiv:1303.4394 [hep-ph]. [Cited on pages 133 and 137.]

[273] Y. Ema, K. Hamaguchi, T. Moroi, and K. Nakayama, "Flaxion: a minimal extension to solve puzzles in the standard model," *JHEP* **01** (2017) 096, arXiv:1612.05492 [hep-ph]. [Cited on page 134.]

[274] L. Calibbi, F. Goertz, D. Redigolo, R. Ziegler, and J. Zupan, "Minimal axion model from flavor," *Phys. Rev.* **D95** no. 9, (2017) 095009, arXiv:1612.08040 [hep-ph]. [Cited on page 134.]

[275] R. Gatto, G. Sartori, and M. Tonin, "Weak Selfmasses, Cabibbo Angle, and Broken SU(2) x SU(2)," *Phys. Lett.* **B28** 128–130. [Cited on page 138.]

[276] R. M. Fonseca, "The Sym2Int program: going from symmetries to interactions," *J. Phys. Conf. Ser.* **873** no. 1, (2017) 012045, arXiv:1703.05221 [hep-ph]. [Cited on page 141.]

[277] P. W. Graham and A. Scherlis, "Stochastic axion scenario," *Phys. Rev. D* **98** no. 3, (2018) 035017, arXiv:1805.07362 [hep-ph]. [Cited on page 142.]

[278] F. Takahashi, W. Yin, and A. H. Guth, "QCD axion window and low-scale inflation," *Phys. Rev. D* **98** no. 1, (2018) 015042, arXiv:1805.08763 [hep-ph]. [Cited on page 142.]

[279] **Particle Data Group** Collaboration, C. Patrignani *et al.*, "Review of Particle Physics," *Chin. Phys.* **C40** no. 10, (2016) 100001. [Cited on page 142.]

[280] S. Weinberg, "Models of Lepton and Quark Masses," *Phys. Rev. D* **101** no. 3, (2020) 035020, arXiv:2001.06582 [hep-th]. [Cited on page 142.]